G E U S

Report file no.

18386

Offshore Volcanic Rocks in Baffin Bay
A seismic interpretation of the structures and development of the Palaeogene offshore volcanic rocks in central West Greenland and on the Baffin Island margin, eastern Canada; PhD thesis

Skaarup, N.

GEUS; Københavns Universitet
Copenhagen
03-12-2001

DANMARKS OG GRØNLANDS GEOLOGISKE UNDERSØGELSE RAPPORT 2001/117

Offshore Volcanic Rocks in Baffin Bay

A seismic interpretation of the structures and development of the Palaeogene offshore volcanic rocks in central West Greenland and on the Baffin Island margin eastern Canada

PhD thesis 2001

Nina Skaarup

UNIVERSITY OF COPENHAGEN
GEOLOGICAL MUSEUM

GEOLOGICAL SURVEY OF DENMARK AND GREENLAND
MINISTRY OF THE ENVIRONMENT

GEUS

OFFSHORE VOLCANIC ROCKS IN BAFFIN BAY

A seismic interpretation of the structures and development of the Palaeogene offshore volcanic rocks in central West Greenland and on the Baffin Island margin, eastern Canada

Contents:

Introduction

Data
- seismic data
- gravity data
- magnetic data
- wells and rock samples

Methods
- seismic interpretation
- gravity modelling
- AVO analysis of a bright spot

Results
- Structures, stratigraphy and thickness of the offshore volcanic rocks in West Greenland
- Dating of the offshore volcanic rocks
- AVO analysis
- Mapping volcanic and basement structures on the Baffin Island margin

Conclusion

References

Acknowledgements

Introduction

The Palaeogene volcanic province in central West Greenland extends 550 km in a north–south direction and 200 km east–west (Henderson, 1973; Henderson et al. 1981, Whittaker, 1996) with an altitude variation from 2 km above sea-level for the highest onshore exposures to depths of 9 km offshore for the lowest interpreted volcanic rocks. In 1992 and following years extensive seeps of crude oil were discovered in Cretaceous sediments and Palaeogene volcanic rocks onshore Nuussuaq (Christiansen, 1993; Christiansen et al., 1994; Christiansen et al., 1995; Christiansen et al., 1996; Christiansen et al., 1998). Analysis of the oils have shown that they were derived from source rocks in the underlying Cretaceous and lower Paleocene sediments (Bojesen-Koefoed et al., 1999). This has resulted in increased interest in the structure and development of the area, including the volcanic rocks offshore. Whittaker (1995) used reflection seismic data to make a preliminary interpretation of the area offshore Disko and Nuussuaq. The offshore volcanic rocks crop out at seabed in the near-shore area, where they dip west. Further west they are covered by a wedge of Eocene and younger sediments. Whittaker (1995) described a number of large rotated fault-blocks containing structural closures at top volcanic level that could indicate leads capable of trapping hydrocarbons.

Whittaker's (1995) work combined with the discovery of oil in the basalts onshore, led the Geological Survey of Denmark and Greenland (GEUS) to acquire 1960 km of new multi-channel 2D seismic data in the area between 68°N and 71°N in 1995. These data were the primary data source for this Ph.D. project, and the main goal for the project was to map the extent and structure, and to determine the thickness and seismic stratigraphy of the volcanic rocks in the area between 68°N and 71°N, offshore west of Disko.

The 1995 seismic data were integrated with the older seismic data interpreted by Whittaker (1995), and a detailed interpretation of the top volcanic surface and structures was carried out. During this work a bright spot was discovered above a structural high at the top of the volcanic rocks. The bright spot and 5 structural closures were mapped and described in paper 1: Skaarup, N. & Chalmers, J. A. (1998): A possible new hydrocarbon play, offshore West Greenland.

To test the bright spot further, the seismic attributes were studied using Amplitude Variation versus Offset (AVO) analysis. The AVO processing was carried out by Dave White, Robertson Research International, and I did the interpretation in cooperation with James Chalmers. This work was presented in paper 2: Skaarup, N., Chalmers, J. A. and White, D. (2000): An AVO study of a possible new hydrocarbon play, offshore central West Greenland.

To map every single feature of the volcanic section has no purpose, so the first step of the mapping task was to divide the section into a small number of seismic units bounded above and below by disconformities, each containing several seismic facies. The number and definition of the units went through several revisions, based on tentative local mappings. The final version, which was mapped throughout the area, was based on a division into five seismic units. A determination of the total thickness of the offshore volcanic rocks has not been possible from the seismic data alone, because of the uncertainty in interpreting the base of the volcanic section. To give an estimate of the thickness of the volcanic section, models based on both the seismic lines and gravity data have been created. The models were tied to the ends of the gravity profiles modelled by Chalmers (1998) in the onshore and fjord area. All of this work is presented in paper 3 in this thesis (Skaarup, N.: Seismic stratigraphy and structure of Palaeogene volcanic rocks, offshore central West Greenland).

During my Ph.D. study, I spent half a year at The Geological Survey of Canada, Atlantic (GSCA) in Dartmouth, Nova Scotia. Their archives contain 80,000 km of reflection 2D seismic data acquired by the oil industry during the 1970s and 1980s on the Baffin Island margin, to which I had access. I used 30,000 km of the data to interpret the volcanic and basement structures in the area between

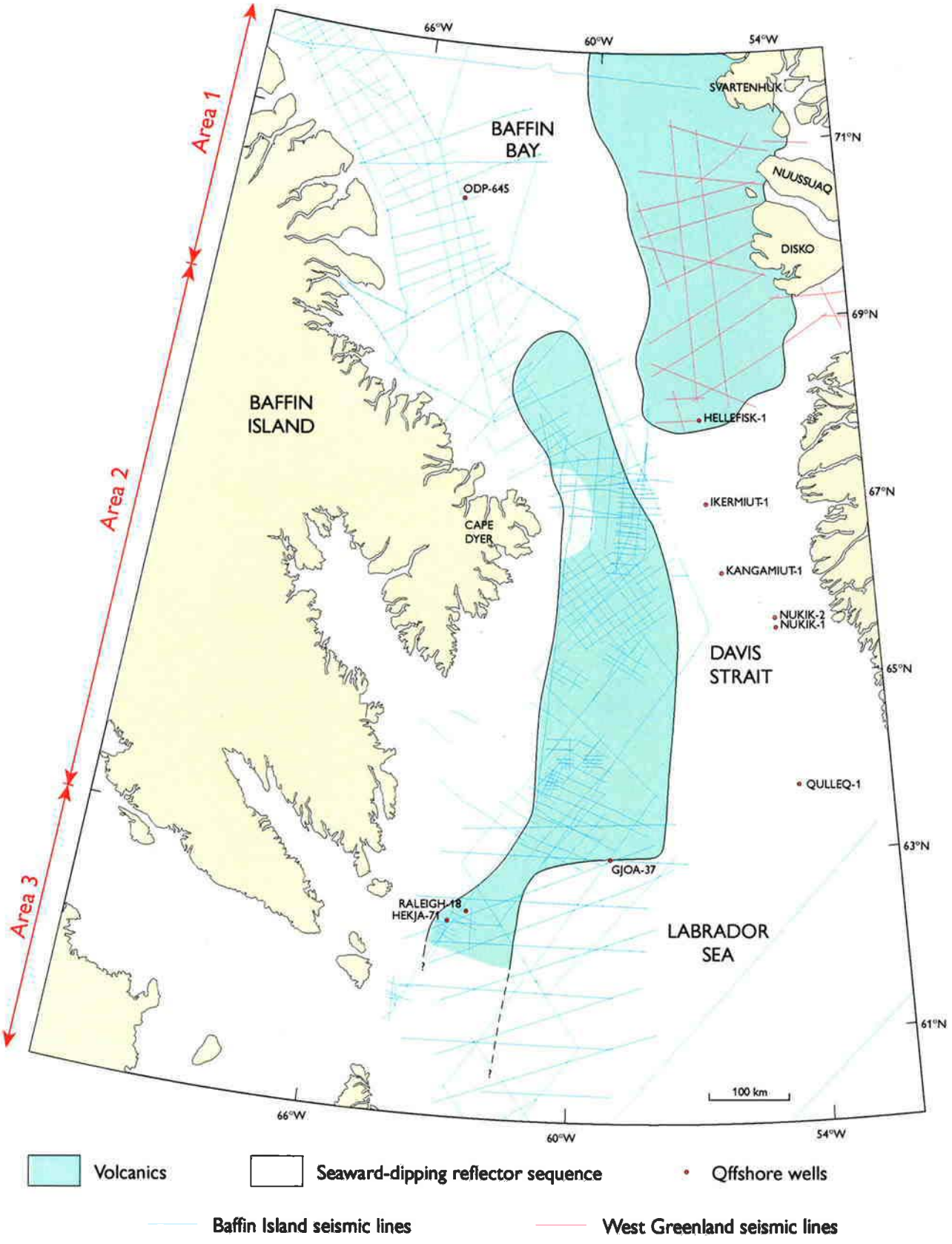

Fig. 1: Seismic lines used on the Greenland and Baffin Island margins. Also the offshore wells; six on the Greenlandic margin and four on the Baffin Island margin are shown. The Baffin Island margin has been divided into three areas, Area 1, 2 and 3, displayed in red on the left side of the figure, and the area where the seaward-dipping reflector sequence has been interpreted is shown
(GB01.07-052-nsk)

60° and 72°N along the margin. The interpretation of the seismic data was combined with newly compiled magnetic and gravity data. The primary results of the study were to divide the margin into volcanic and non-volcanic areas, and to make a new estimate of the location of the continent-ocean boundary. The new estimate of the continent-ocean boundary in the Davis Strait was used together with earlier and new determinations of the continent-ocean boundary on the Greenland side to make a preliminary reconstruction of the plates in the Davis Strait/Baffin Bay region in early Cenozoic time. This work is presented in paper 4, included in this thesis (Skaarup, N., Jackson, H.R. & Oakey, G.: A seismic reflection and potential field study of Baffin Bay/Davis Strait, eastern Canada: implications for tectonic evolution).

Data

Seismic data

On the Greenland margin, digital 2D data from 1990 and 1995 were used. The data set consists of 23 multi-channel reflection seismic lines with a total length of 2760 km. Four seismic lines were acquired by the Geological Survey of Greenland (GGU) in 1990, using a 3616 cu. in. bolt airgun, a 3000 m-long analogue streamer with 120 channels, and 60-fold processing; 19 seismic lines were acquired in 1995 by GEUS using a 4100 cu. in. sleeve air gun, a 4500 m-long digital streamer with 360 channels, and 90-fold processing. The spacing of the grid of seismic lines varies between 30 km and 50 km (Fig. 1). Additionally a single, short, 15-fold seismic reflection line was recorded by GGU in 1994 on the south-coast of Nuussuaq.

On the Baffin Island margin, 2D seismic data on paper records from the 1970s and 1980s were used. The data set consists of 30,000 km of seismic reflection data from 13 different surveys, using airgun arrays with a total volume of 1200 cu. in. at a pressure of 1800 psi, a 2200-2400 m long analogue streamer, and 24-fold processing.

Gravity data

The gravity data used for the modelling offshore West Greenland were acquired during the GEUS 1995 seismic cruise, using a La Coste and Romberg gravity meter and processed by the National Survey and Cadastre-Denmark (KMS) to yield free-air data. Additional onshore data from KMS and GGU have been terrain corrected and converted to Bouguer anomalies and combined with the free-air anomaly data offshore to form a single data set.

The gravity data used for the Davis Strait area were a compilation gridded at 5 km resolution. Data sources included marine ship observations, aerogravity over Greenland, and station data over Baffin Island. Bouguer anomalies for land data were reduced by the Geological Survey of Canada (GSC) and KMS, and marine data were presented as free air anomalies.

Magnetic data

The magnetic data used in both the central West Greenland and Davis Strait areas were compiled from various marine surveys, aeromagnetic surveys, and gridded sources, and were finally gridded with a resolution of 2 km. Onshore Greenland, the regional survey data were collected by the American Naval Research Lab with a 10 km track spacing. A detailed coastal survey (64°N-69°N) and a regional survey (south of 68°N) had been compiled by GEUS. The data around Disko came from the DNAG magnetic grid (Verhoef et al., 1996).

Wells and rock samples

Five exploration wells were drilled offshore West Greenland in the mid-1970s (Rolle, 1985), and one in the summer of 2000 (Christiansen et al., 2001), all south of the area studied (Fig. 1). The northernmost well (Hellefisk-1) terminated in volcanic rocks and has been used to control the interpretation of the volcanic rocks. The well GRO#3 was drilled onshore on the south coast of

Nuussuaq in 1996 and penetrated 2700 m of Paleocene and Upper Cretaceous sediments below 303 m of Paleocene hyaloclastites (Christiansen et al., 1999).

On the Northeastern Baffin Shelf four wells were drilled in the late1970s and mid-1980s (Fig. 1). Two of the wells (Hekja-71 and Gjoa-37) terminated in volcanic rocks (Klose et al., 1982) and have been used to improve control of the interpretation of the volcanic surface on the seismic data in this area. Besides the wells, 73 samples are available of rocks from the seabed along the Baffin Island shelf (MacLean, 1978; MacLean and Falconer, 1979; MacLean and Williams, 1983).

Methods

Seismic interpretation

The seismic data from the West Greenland margin has been interpreted on a Sun work-station using Landmark SeisWorks-2D® software. Apart from the seabed reflection, the reflection from the top of the volcanic rocks is the most prominent reflection on the seismic data. It is normally seen as a single, sharp positive reflection, in most places as distinct volcanic mounds overlain by onlapping sediments (Fig. 2, sp. 13,800-14,000).

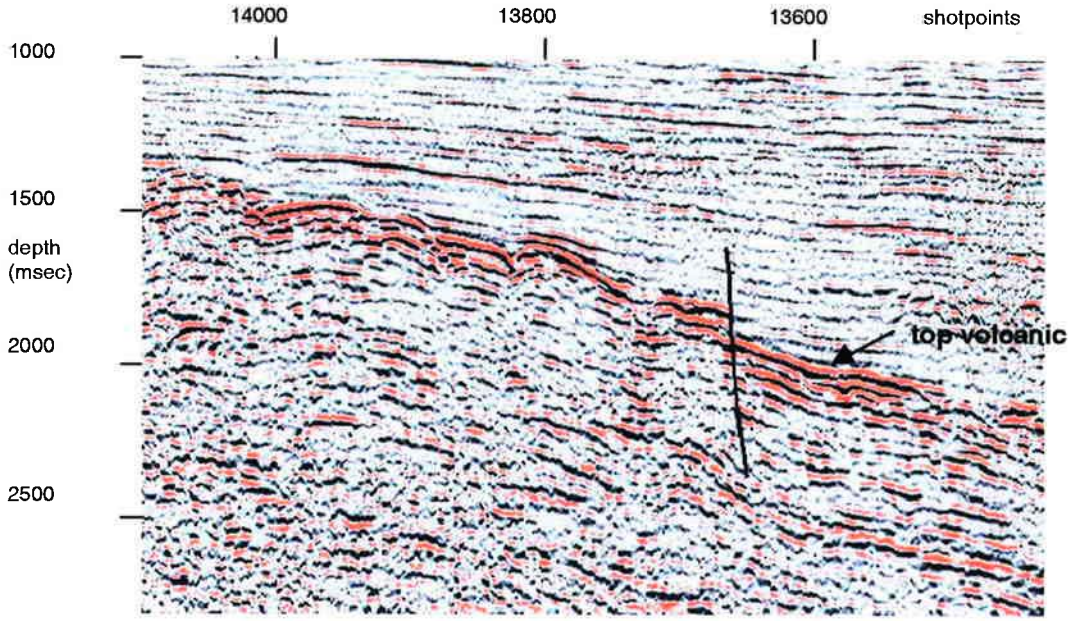

Fig. 2: Part of seismic line GGU/95-12 on which the top volcanic reflection is normally seen as a single, sharp positive reflection (to the right), but often shows a more irregular surface with several generations of lava flows.

The predominant seismic facies pattern within the volcanic rocks is parallel to sub-parallel, with various degrees of downlapping features and different degrees of reflectivity. These parallel-bedded units pass through more downlapping units of both oblique and sigmoidal outline to almost chaotic hummocky clinoforms. In most places it is only possible to interpret the internal features within the volcanic rocks in the uppermost part of the volcanic section, because the signal fades deeper into the section. The layering seen on the seismic data can be real reflections and a direct equivalent to the onshore volcanic rocks, which expose a marked layering and prograding facies

onshore Nuussuaq (e.g. Pedersen et al. 1993). The layering can arise from the impedance contrast between the interbedding of sediments and tuffs, or between the flows themselves and their vesicular upper parts (Planke, 1994; Planke & Eldholm, 1994). Another explanation for the layered appearance on the seismic data of the submarine lava successions could be a complex interference pattern between thin, closely spaced volcanic flows (Barton & White, 1997).

The minimum vertical size of features interpreted on the seismic records are of the order of one wavelength, i.e. 50 m, which is much less than the maximum height of the hyaloclastite foresets seen onshore (700 m), so it is possible that individual prograding volcanic facies can be interpreted on the seismic data.

The lack of reflections from the deeper parts of volcanic rocks has been explained by large energy transmission losses due to the large impedance contrasts of interbedded sediments and basalts (Pujol et al., 1989), and loss of continuity in the seismic signal may be caused by lateral variations in flow thickness, alteration, dykes and interbedded sediments (Planke & Eldholm, 1994). However, poor reflections from depth is also seen in the thick volcanic section, where no interbedded sediments are seen. The fading seen on these seismic data has made it impossible to interpret the base of the volcanic rocks with any kind of certainty. In the northwestern part of the studied area, a highly-reflective southeasterly dipping reflection can be seen on two intersecting seismic lines (Fig. 3). This dipping reflection could be interpreted as the base of the volcanic rocks from the seismic data alone, but it could also be a long dike or fault plane, or an S-reflector at the base of the crust, as recognized on other volcanic margins (Chian et al,1995).

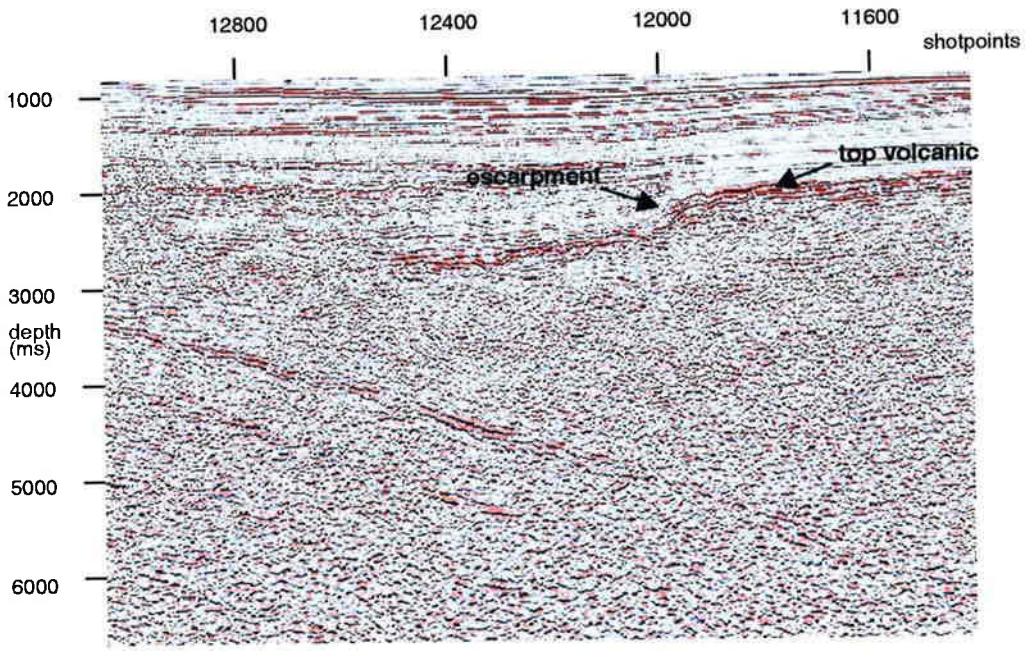

Fig. 3: Part of seismic line GGU/95-12 where a strongly dipping highly-reflective reflection can be seen below the top volcanic surface. Also an escarpment at sp. 12.000 can be seen

Because of the transmission loss mentioned above, no base to the volcanic rocks has been interpreted from the seismic data alone. Rather, the lowest seismic unit is defined as that occurring between the lowermost interpretable volcanic marker horizon and the base of the volcanic rocks interpreted from modelling of gravity data.

The most obvious first division of the volcanic section would be one of defining the seismic units by separating horizontal, downlapping and opaque seismic facies. The direct and most apparent onshore analogy, however, consists of horizontal, subaerial volcanic rocks that pass laterally into downlapping subaqueous hyaloclastites. Thus a division has been devised based on highly-reflective surfaces onto which there are clear downlapping reflections , and each separate seismic unit contains horizontal, downlapping and sometimes opaque facies.

Six different seismic units have been interpreted. The uppermost unit corresponds to the post-volcanic sedimentary section. Below this, five seismic units have been interpreted within the volcanic rocks (Fig. 4), and their distributions can be seen in Fig. 5 (the division of the seismic units and their distribution is described in detail in paper 3).

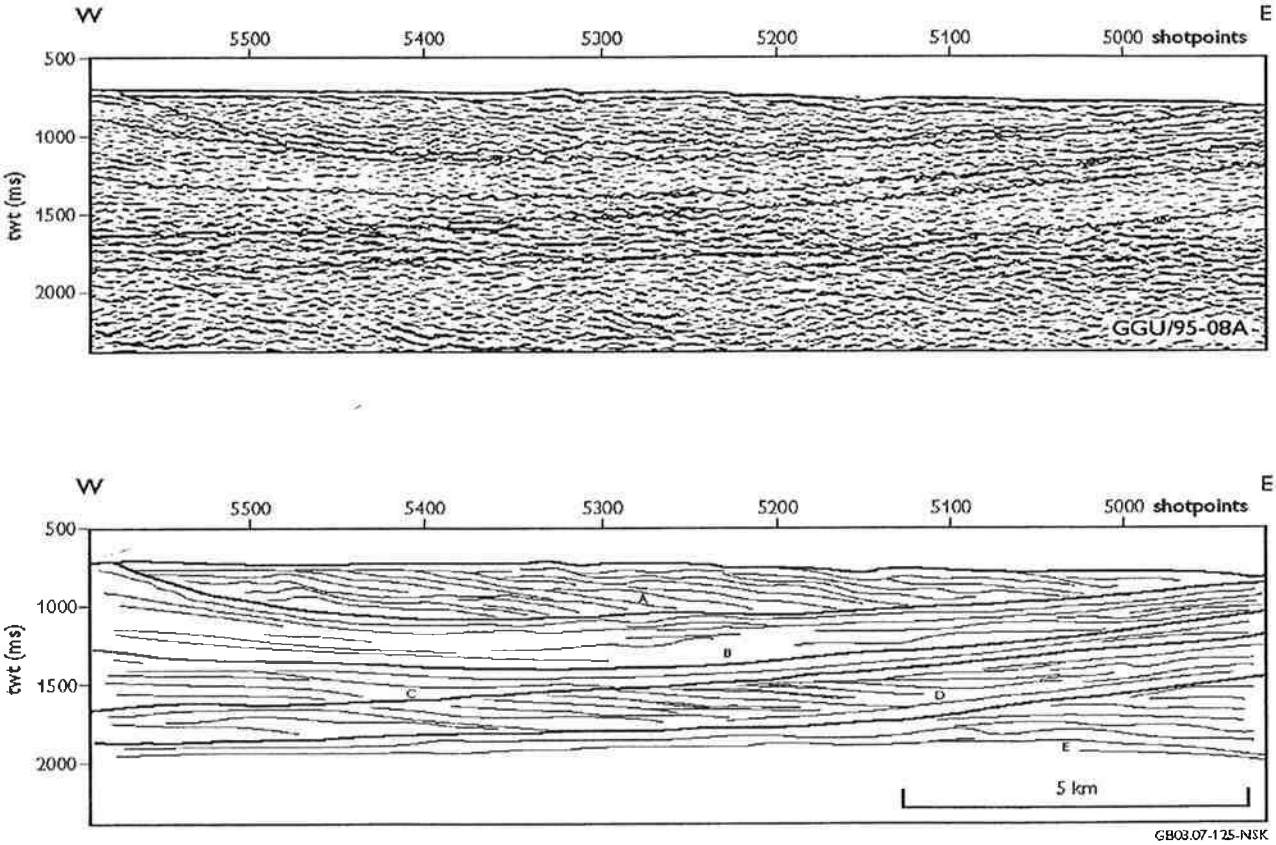

Fig. 4: Part of seismic line GGU/95-08A where the division into the five different volcanic units A-E can be seen. The uppermost, Unit A, is here seen to contain a strongly downlapping appearance where the top reflection is seen to pass into eastwards-prograding facies, where the apparent dip decreases from west to east, from 11.3°-3.7°. The height of the downlapping units in this offshore basin is 700-800 m, which is a direct equivalent to what is seen onshore in a 700 m deep basins observed in the Vaigat Formation on the south coast of Nuussuaq (Pedersen et al. 1993) (figure from paper 3)

On the Canadian margin, the seismic records are from the 1970s and 1980s and of much poorer quality due to the recording techniques used at that time. The strong interest from the industry at that time resulted in a denser net of seismic data than in Greenland, where the lines are between

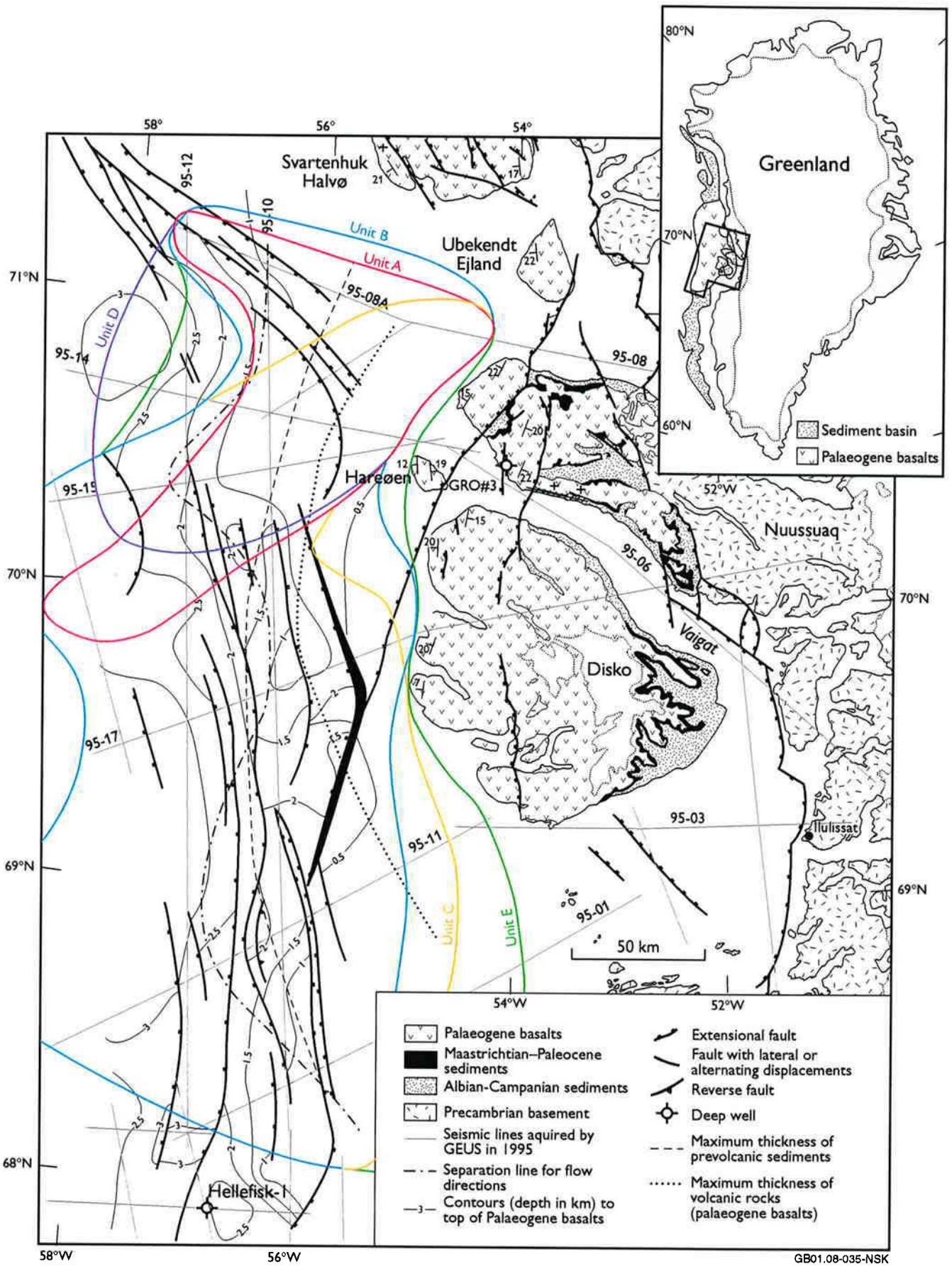

Fig. 5: The extension of the five different volcanic units (coloured solid lines labelled Unit A - Unit E). Also shown: maximum thickness of the volcanic rocks (black dotted line) and maximum thickness of the pre-volcanic sediments (black dashed line). The two lines have almost the same curved outline around Disko, but the line for the pre-volcanic sediments is displaced by 20-50 km towards west. Further to the west the separation line for flow directions (black dash-dotted line) indicates the location of the apparent eruption zone interpreted from the seismic data. Finally, the four nearshore seismic lines are shown, which Chalmers (1998) extended onshore to get basement control for his gravity modelling of the onshore area (gray solid lines, from south to north labelled 95-03, 95-17, 95-06 and 95-08). Additional features, described in the legend, are shown for reference purposes
(GB01.08-035-nsk)

30 km and 50 km apart. On the Canadian margin, the spacing is of the order of 15-30 km (Fig. 1). The seismic data is available only as paper records and the interpretation was done using coloured pencils. Because of the limited time and data quality, the seismic interpretation was concentrated on basement and volcanic structures. On most of the seismic lines, the basement reflection is seen as the strongest reflection except for the seabed. In some places the basement surface is rough, and in others smooth, often draped by high-amplitude sedimentary horizons (Fig. 6). The reflections from volcanic rocks are of relatively high amplitude with little energy penetrating the horizon. In areas where volcanic rocks are exposed at the seabed they obscure deeper signals preventing the interpretation of the basement surface. This interpretation is described in detail in paper 4.

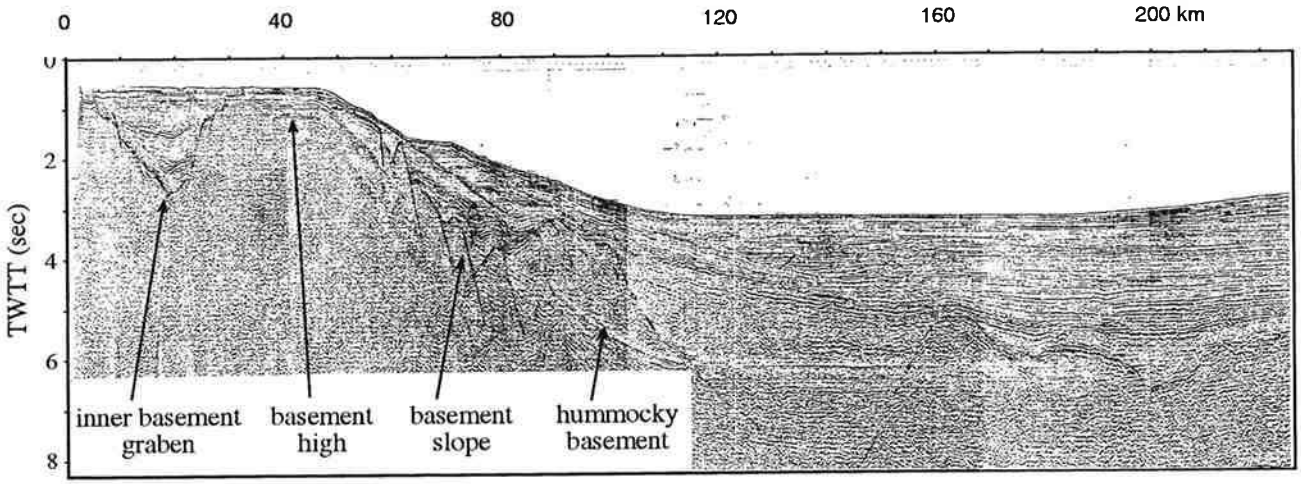

Fig. 6: Part of seismic line BE-74-51 across the non-volcanic margin on the northeastern Baffin Island margin where several coast-parallel basement highs can be seen. The basement graben at 10-25 km can be followed for a long distance along the Baffin Island shelf

Gravity modelling

Seismic reflections from deep below the top of the volcanic rocks are obscured in most places because of the large difference in seismic impedance between the overlying water or sediments, and the volcanic rocks. However, in places distinct reflections can be seen at even great depths below thick sections of volcanic rocks (e.g. Fig. 3), whereas in other places internal features cannot be interpreted even in the very uppermost volcanic rocks. Modelling the section by combining knowledge from the seismic records with gravity data collected along the lines at the same time was used to give an indication of the thickness of the volcanic rocks.

The gravity modelling was done using 'Gravmag', an interactive 2.5D gravity modelling program from the British Geological Survey (Pedley et al., 1993) and is described in further details in paper 3. The model was constructed as a six layer model; From above: water, post-volcanic sediments, volcanic rocks interpreted from the seismic data + possible deeper volcanic rocks, pre-volcanic sediments, crust, and mantle. The data for the upper three layers, the seabed, the top volcanic reflector and the lowermost interpreted volcanic unit used as the base of interpreted volcanic rocks, are taken from the interpretation of the seismic data and were assumed to be known and fixed parameters in the model. The boundaries between the lower three layers; the pre-volcanic sediments, the crust and the mantle were treated as variable parameters. The densities used for the model (see figure caption for Appendix 1) were partly derived from Chalmers et al. (1999), except for the densities for the post-volcanic sediments which were derived from density logs from the six offshore wells further south (Bate, 1995; Christiansen et al., 2001).

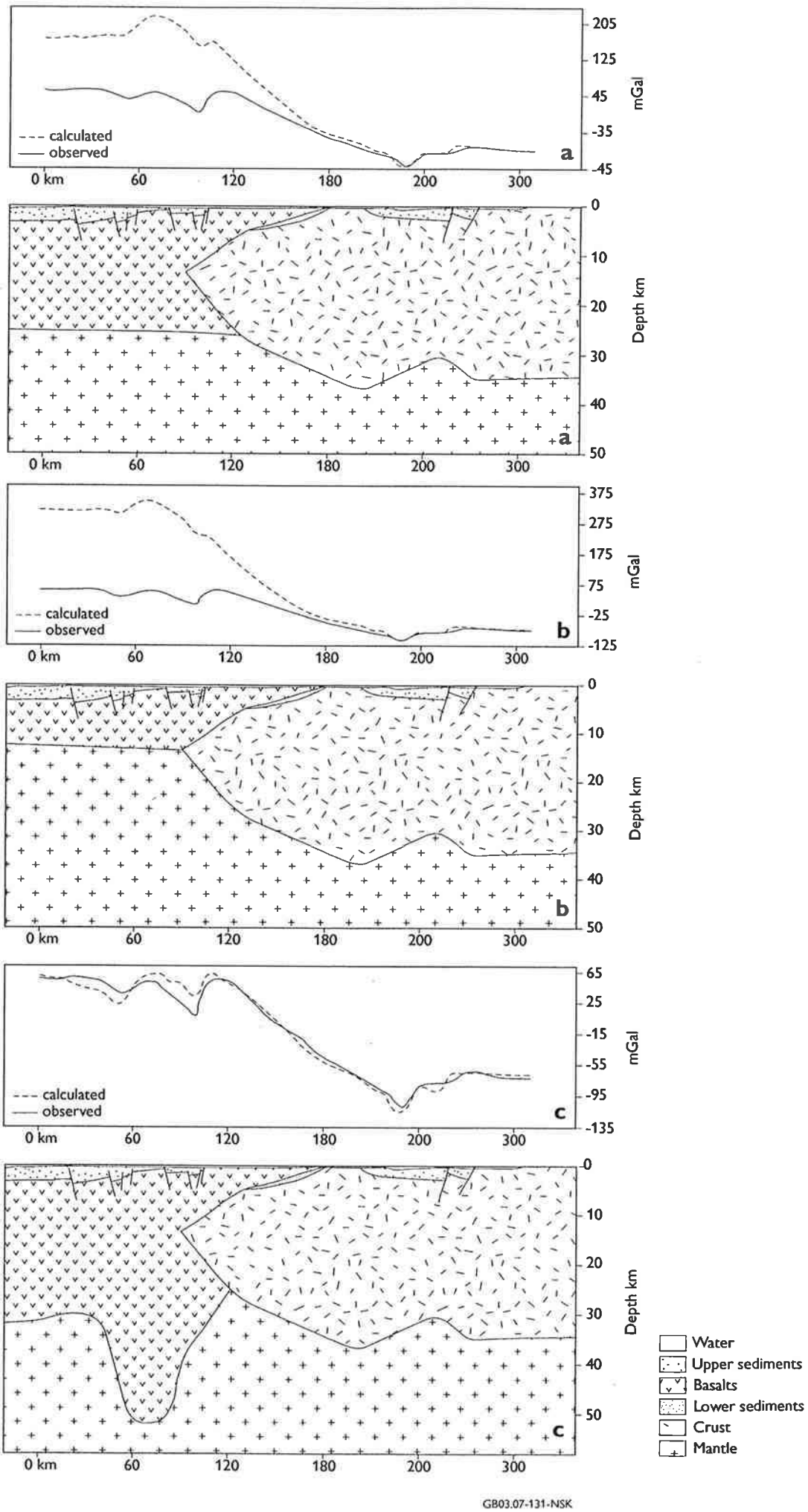
205
125
45
-35
-45
mGal
calculated
observed
a
0 km
60
120
180
200
300
0
10
20
30
40
50
Depth km
375
275
175
75
-25
-125
b
65
25
-15
-55
-95
-135
c
Water
Upper sediments
Basalts
Lower sediments
Crust
Mantle
GB03.07-131-NSK

Fig. 7

Before modelling the upper part of the geological section, the background gravity signal from the mantle and lower crust had to be subtracted from the data. This was done by constructing a reference model consisting of two components, crust and mantle, extending 10,000 km in both directions. A model with the crust 30 km thick was assumed to be in isostatic equilibrium (Chalmers, 1998) and all modelling was carried out with reference to this assumption. This reference model generated an anomaly of -625 mGal which was then added to the observed data. The next step was to move the boundary between the crust and mantle to fit the data locally. Attempts are made to keep the crust/mantle boundary as smooth and straight as possible.

Chalmers (1998) generated gravity profiles along four nearshore seismic lines in the Nuussuaq basin by extending them onshore to basement outcrop (Fig. 5). These lines have been used as the starting points for modelling the 6 east-west offshore lines in this project (Appendix 1-6). Two north-south lines have been modelled to tie between the east-west lines (Appendix 7-8).

Geoffroy *et al.* (1998, 2001) proposed that the monoclinal flexure of the basaltic series onshore West Disko represents onshore exposure of a seaward-dipping reflector sequences derived from a plume-related plate break-up, and infer that the ocean-continent boundary must lie close to the west coast of Disko.

To test their hypothesis, a model of "Icelandic warm oceanic crust" (Fig. 7a) was constructed along an onshore line crossing Disko, where basement control can be achieved from the Disko gneiss ridge (Chalmers 1998), and extended westwards where control of top basalt is obtained from the offshore seismic line GGU/95-17. Moho offshore is assumed to be at a depth of 25 km, and the continental crust has been terminated a short distance offshore. This model gives a difference between the calculated and measured gravity data of 120–160 mGal in the area of assumed oceanic crust.

An additional model for "ordinary cool oceanic crust" (Fig. 7b) has been calculated, where the Moho is assumed to be at a depth of 12-13 km. This model shows a difference between calculated and measured gravity data of 250–300 mGal.

It might be that the assumptions made about depth to Moho were badly wrong in the model shown in Fig. 7a. To test this, a model was constructed where the depth to Moho was modelled to fit a 'thick oceanic crust' model to the measured gravity data. The results are shown in Fig. 7c. It is felt that incorporating a "bulge" of the Moho to over 50 km depth is unrealistic, and White (1992) shows that heavily intruded or underplated crust does not reach deeper than 27 km at the Hatton Bank volcanic margin. The most likely way of reducing the excess mass shown in models 7a to 7c is by incorporating a layer of sediment and further modelling was done assuming continental crust in the offshore area and sediments between the volcanic rocks and the continental basement.

A first result of the modelling is that there is no obvious single solution, but a lot of different solutions which all have a good fit between the observed and calculated data, and which all could display a part of the real geology. The overall result of the modelling is a thickening of the volcanic section off the coast (Fig. 8), curving around Disko and Nuussuaq, with the maximum thickness around 56°W-56°15´W (Fig. 5). The line of maximum thickness for the pre-volcanic sedimentary section below the volcanic rocks displays almost the same curved outline as the volcanic rocks (Fig. 5).

The pronounced high-amplitude southeast-dipping reflection (Fig. 3) which can be seen on two intersecting seismic lines in the northern part of the studied area, can be seen to coincide very well with the boundary between the volcanic rocks and the underlying sediments on the modelling case of line 14 (Appendix 5).

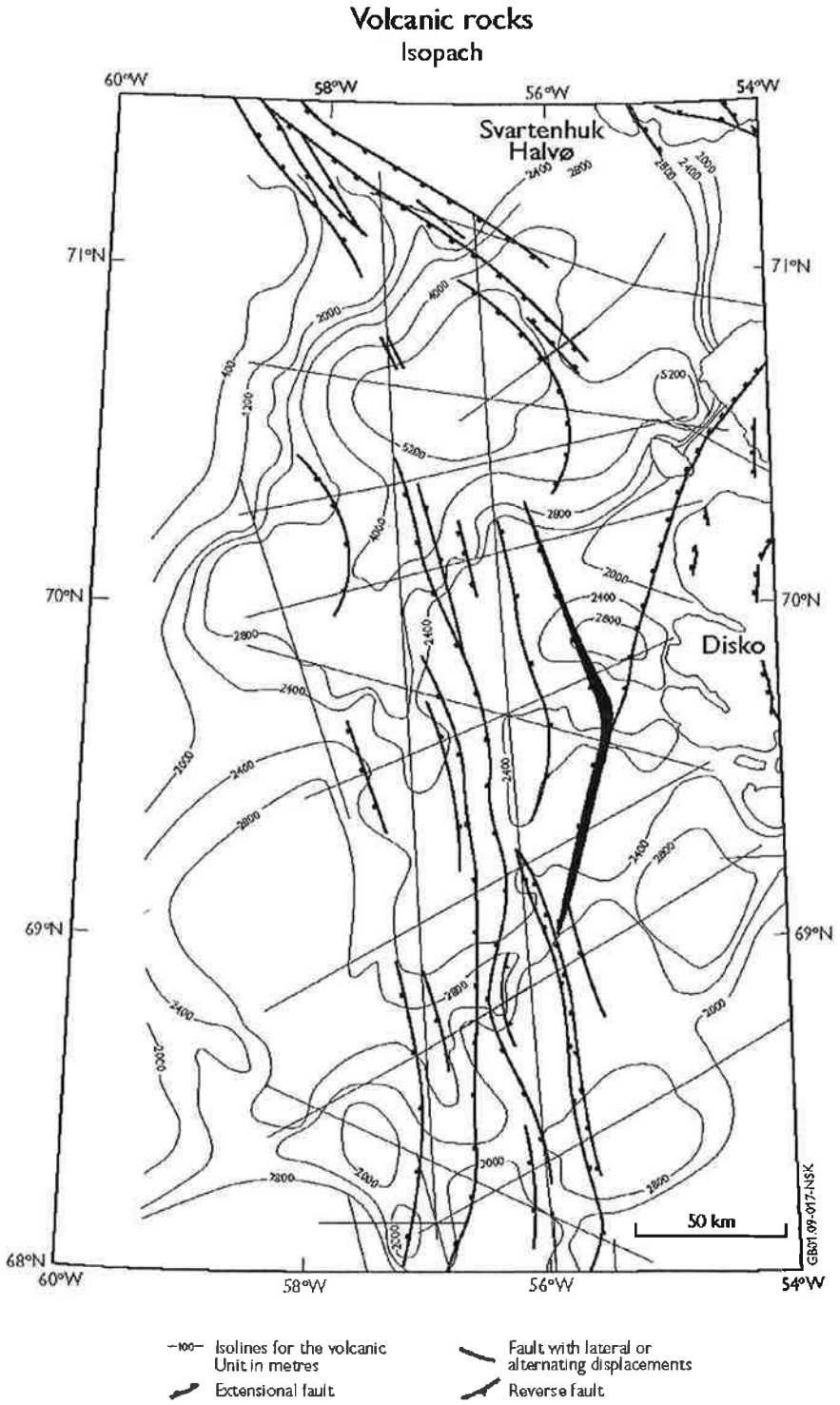

Fig. 8: Isopach map of the volcanic section, based on the results of the gravity modelling. The thickness of the volcanic section shows a curved outline around Disko and Nuussuaq, with the maximum curve at 56°W in the north and 55°30´W in the south, with a local maximum just west of Hareøen at 5–5.5 km

AVO analysis of a bright spot

Bright spots on seismic data can be indicative of the presence of gas in clastic sediments, and when a bright spot was discovered above a structural high at top volcanic level west of Disko, it was considered that it might be a direct indicator of hydrocarbons. This was the main reason for the detailed AVO-based investigation described in paper 2. Amplitude Variation versus Offset (AVO) is the examination of the variation of amplitude and phase of seismic reflections at different distances between shot and receiver (offset) (Fig. 9). The technique has been found to be useful in the direct detection of hydrocarbons on seismic data.

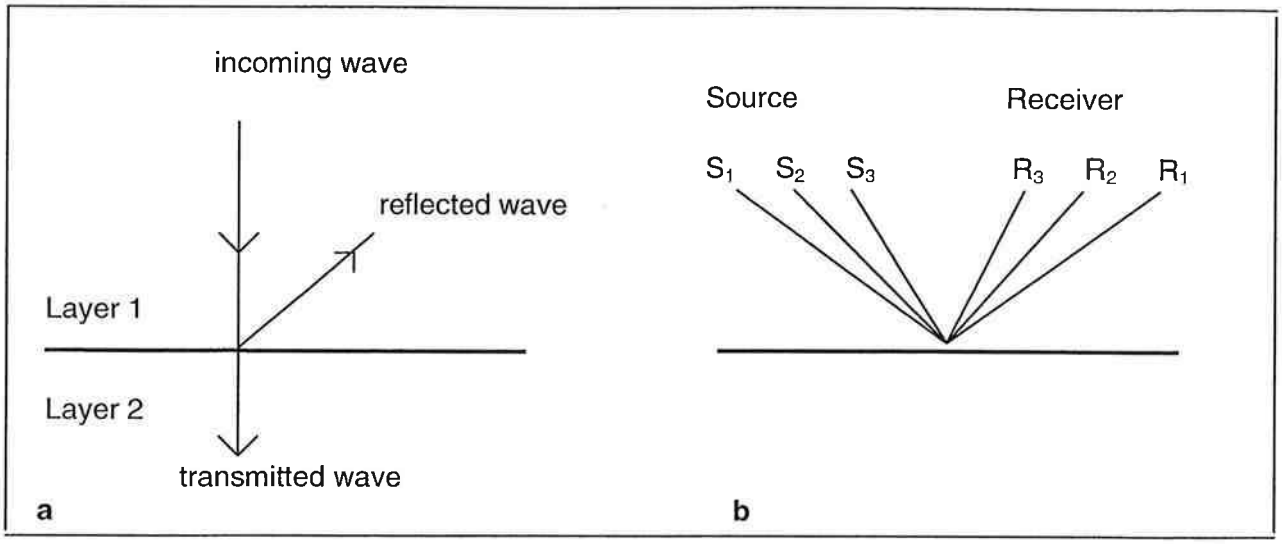

Fig. 9: a) When a vertically travelling seismic wave encounter a subsurface interface between two intervals of different acoustic impedance, some energy is reflected and some transmitted. The proportion of reflected energy, and therefore the amplitude of the reflected wave, depends on the contrast in acoustic impedance, which is a product of the density and P-wave velocity within the interval. b) The source-receiver distance is called the offset, and the AVO analyses is the examination of the variation of the amplitude and phase of the reflected wave at different offsets

When vertically-travelling seismic waves meet a sub-surface interface between two intervals of different acoustic impedance, some of the energy is reflected and some transmitted (Fig. 9). The proportion of reflected energy, and therefore the amplitude of the reflected wave, depends on the contrast in acoustic impedance (Fig. 10). When the seismic waves meet a large acoustic contrast, the amplitude of the reflected seismic energy can be anomalously strong and appear as a 'bright spot' on the seismic section. The acoustic impedance can be altered by the presence of hydrocarbons, but also coal or an igneous sill in a clastic environment can produce a bright spot on the seismic data. To distinguish between such possibilities, additional techniques of analysis, such as the variation of reflection amplitude with offset between the seismic source and receiver, can be used.

$$\text{Reflection coefficient} = \frac{Z_2 - Z_1}{Z_2 + Z_1}$$

$$\text{Acoustic impedance} = Z = \text{density} \cdot \text{velocity}$$

Fig. 10: The relationship between the reflection coefficient and the acoustic impedance. The presence of hydrocarbons, particularly gas, can alter the acoustic impedance of an interval, and the amplitude of seismic energy reflected from the hydrocarbon-bearing interval can be anomalously strong, a so-called bright spot

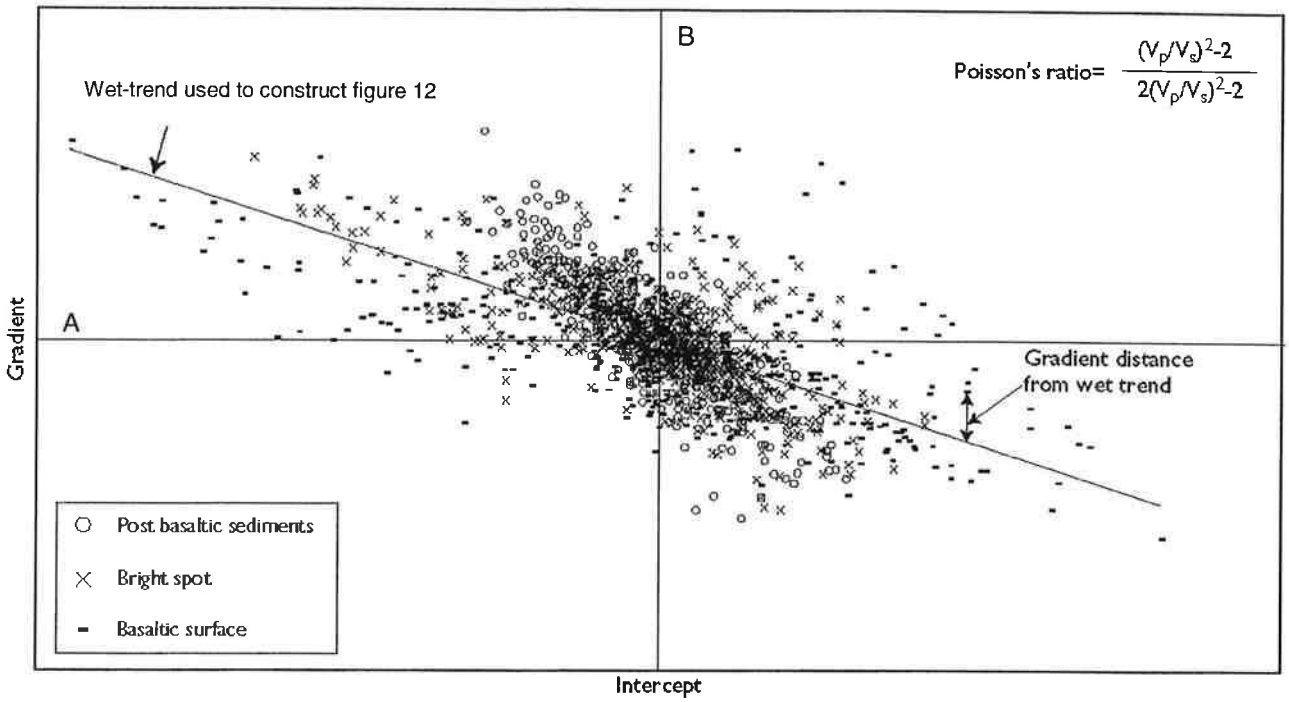

Fig. 11: Amplitude versus gradient crossplot from the seismic line GGU/95-17, sp. 2745.5-2755. The wet-trend line used to construct Fig. 12 is shown and how the distance from the wet-trend was measured is also indicated. A plot of distance from the wet-trend for line GGU/95-17 across the prospect is shown in Fig. 12 (figure from paper 2)

From a plot of reflection amplitude against $\sin^2\theta$, the amplitude at zero-offset (A) and the gradient (B) can be derived (Fig. 11). The gradient (B) of the $\sin^2\theta$ term contains Poisson's ratio as a factor. This latter variation gives an anomalous AVO response when the Poisson's ratio contrast is anomalous, and may occur when free gas is present in the pore space. It is commonly found that in brine saturated rocks there is a linear relationship between A and B that may pass through the origin, 'the wet trend' (Castagna and Swan, 1997). Deviations from this trend on a cross-plot of A and B may indicate the presence of hydrocarbons (Fig. 12).

By grouping the AVO responses, a classification of the impedance contrast against the reflection coefficient can be found, and thereby classifying the possibility for gas sands. In paper 2 a detailed examination of the bright spot recognized west of Disko has been described.

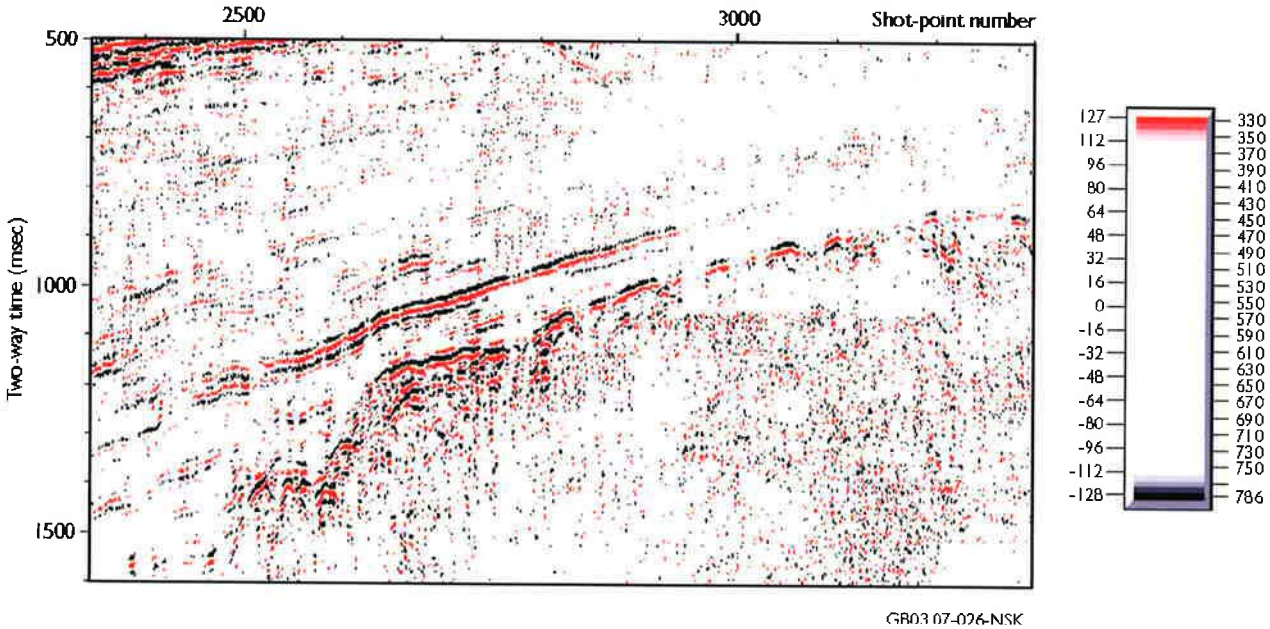

Fig. 12: The gradient distance from the wet-trend plot of line GGU/95-17 (Fig. 11). A general wet-trend was defined that applies at all shotpoints, and for every sample point at that shotpoint the gradient distance between the point and the trend was calculated, either above or below the trend (as shown on Fig. 11). Gradient distance from the wet-trend is shown by colour, and the colour scheme was chosen to emphasize the AVO anomaly points that lie farthest from the wet-trend. The points that are farthest from the background trend clearly lie just above the top of the volcanic rocks and the bright spot about 100 ms above the top volcanic reflection (figure from paper 2)

Results

Structures, stratigraphy and thickness of the offshore volcanic rocks in West Greenland

In the central West Greenland volcanic province, the top volcanic surface has been mapped in the area between 68°N and 71°N. The top volcanic surface crops out close to the coast of Nuussuaq and Disko, around 55°W-55°30'W, and dips towards west below sediments of Eocene age and younger. The volcanic rocks are not limited to within this area, but seem to continue west of 58°30'W, which is the western limit of the data.

Structures at top volcanic level have been interpreted and mapped. The fault pattern is dominated by elongate, steep, normal faults, trending N-S, curving towards the NNW north of 70°30'N. The faults define horsts, rotated blocks, and grabens with complex minor faulting within (described in details in papers 1 and 3).

The volcanic section has been divided into five seismic units. The predominant seismic facies in the volcanic rocks is parallel to subparallel, with various degrees of downlap. These parallel-bedded units pass into downlapping units of both oblique and sigmoidal to almost chaotic hummocky clinoforms. The seismic units contain both horizontally layered facies and downlapping facies, as a direct equivalent to the onshore exposures, where horizontally subaerial volcanic rocks pass into downlapping subaqueous hyaloclastites. In Figure 5 the extent of the five seismic volcanic facies has been plotted, and in appendices 9–13 an isopach map for each of the seismic units is shown.

On several seismic lines, volcanic foresets in the uppermost volcanic unit show eastward directions east of an irregular line around 56W°-57°W, and westward directions west of this line (Fig. 5). This indicates a roughly north-south trending eruption zone almost in the middle of the studied area.

Gravity modelling
It has not been possible to interpret the base of the volcanic rocks from the seismic data alone, mainly because of the transmission loss within the volcanic rocks, but a modelling of the thickness of the volcanic rocks by combining gravity data and the seismic interpretation has been tried. The most significant result of the gravity modelling is the testing of the presence of different kind of crust in the offshore volcanic area. The modelling showed that the presence of oceanic crust in the studied area is inconsistent with observations, whereas continental crust and sediments present below the volcanic rocks fit the models.

The modelling of the offshore area was tied to the onshore basement by using the end results of Chalmers (1998), which gave control of the level of continental crust at the eastern end of the modelling. The modelling showed a thickening of the volcanic rocks off the coast towards west, curving around Disko, with its maximum thickness of 4 km–5.5 km lying around 56°W-56°15'W (Fig. 8). From the gravity modelling the thickness of the pre-volcanic sediments has also been interpreted. It shows a steeply thickening westwards off the coast, a curved outline as the volcanic rocks, with a maximum thickness of 7 km–9 km around 56°30'W (Fig. 5), a bit more westerly than the volcanic rocks.

Dating of the offshore volcanic rocks
By combining Ar/Ar and K/Ar age determination and geomagnetic polarity determination from onshore exposures on Disko and Nuussuaq with an Ar/Ar age determination from the offshore well Hellefisk-1, and the seismic interpretation of the volcanic units in the offshore area, an estimate of the age of the offshore volcanic rocks can be given (described in further details in paper 3).

Onshore, most of the exposed volcanic rocks were erupted in two phases, the first between 60.7 Ma and 59.4 Ma and the second between 54.8 Ma to 53.6 Ma, or 52.5 Ma (Storey et al., 1998; Riisager & Abrahamsen 1999). Offshore, the uppermost interpreted seismic unit, seismic unit A, which is normally magnetised, and could overlie the offshore extension of the Kanísut Member, the uppermost of the onshore volcanic rocks, which is reverse magnetized. Therefore seismic unit A could have been erupted during C24n, but also during C26n and C25n. Seismic Unit B is interpreted to reach the Hellefisk-1 well, where the dating shows an age of C25, and therefore seismic unit B should have been erupted during C25 at the latest, and more probably during C26. The date from Hellefisk-1, at the C26n/C25r boundary (Williamson et al., 2001) is in the break between the onshore exposures. Thus the clear dividing of the onshore volcanic rocks into two separate episodes of eruptions can not be confirmed from the offshore volcanic rocks. The direct correlation between the onshore and offshore volcanic rocks in the western part of Vaigat, and the complexity and unknown thickness of the lowermost interpreted volcanic unit are two very large uncertainties in this estimate. Also the presence, just west of Disko, of intrusive rocks that have been dated some 25 Ma younger than the volcanic rocks of the Vaigat and Maligât Formations onshore Nuussuaq and Disko, provides another source of uncertainty in this estimate of the eruption periods.

AVO analysis
The AVO analysis indicated the presence of two bright spot anomalies, one 100 msec above the top volcanic level, and one immediately above the top volcanic reflection. A crossplot of the reflection amplitude against the amplitude at zero-offset suggests that both AVO anomalies should be classified as class IV (Castagna and Swan, 1997), which could indicate a presence of a tight zone in a sealing layer above a hydrocarbon sand. There is evidence that the upper bright spot, about 100 msec above the top basalts, lies immediately above an unconformity. Fairly strong reflections below the unconformity that show no AVO anomaly are truncated by the unconformity surface (Fig. 13) that can be traced immediately below the upper bright spot event. The bright spot event could indicate the presence of any of a number of sand types; for example turbidite/mass movement sands within a channel fill in a low-stand systems tract or a coast/shelf sand within a transgressive systems tract (described in details in paper 2).

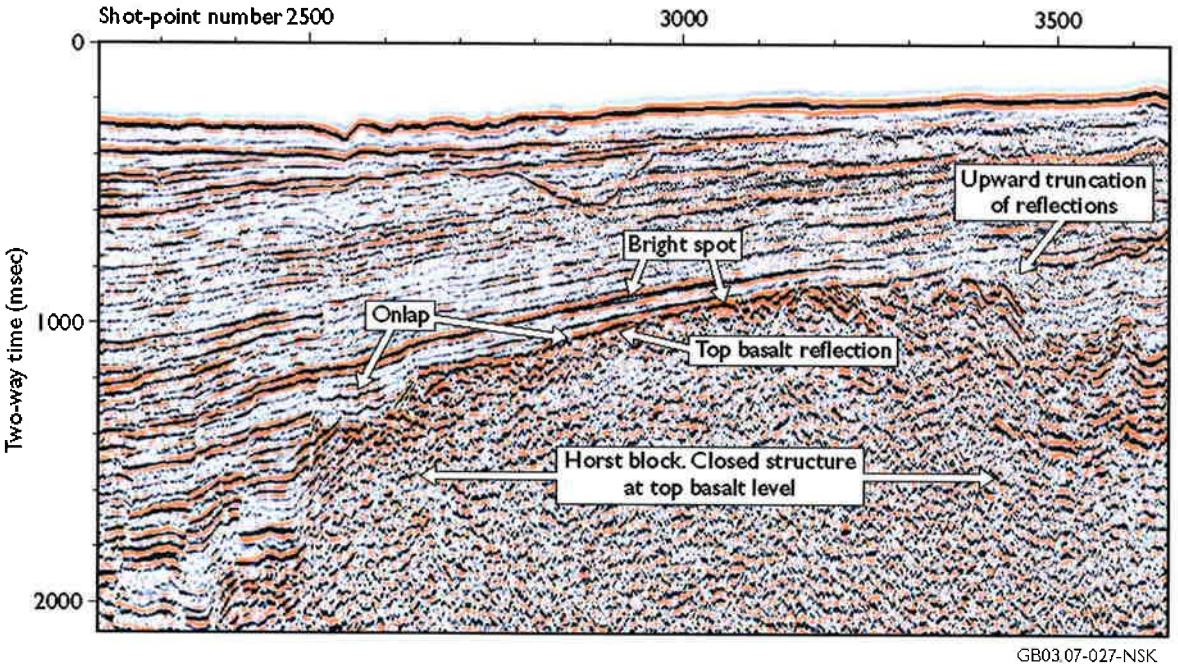

Fig. 13: Part of seismic line GGU/95-17, running southwest-northeast, showing the closed structure above which the bright spot were recognized. The horst block at top volcanic level is bounded by faults to its east and west. Above the structure the bright spot is indicated (figure from paper 2)

Mapping volcanic and basement structures on the Baffin Island margin

The continental margin of Baffin Island has been divided into three distinct areas (Fig. 1). In these areas basement and volcanic structures have been interpreted from seismic reflection data, and combined with newly compiled maps of gravity and magnetic data (described in paper 4). Area 1, northeastern Baffin Shelf, with its coast-parallel grabens and continental basement highs, and seaward deepening basement has been interpreted as a non-volcanic margin. In area 2, off Cape Dyer where onshore volcanic rocks are exposed, a seaward dipping reflector sequence was recognized (Fig. 14), and extensive volcanic rocks were interpreted at and below seabed. This part of the margin was interpreted as volcanic. In area 3, the southernmost area, the depth to basement drops rapidly offshore, and thick prograding sedimentary wedges producing high-amplitude gravity anomalies are interpreted. This part of the margin is interpreted to be non-volcanic.

Based on the interpretation of the seismic data and the gravity and magnetic data, a new determination of the continent-ocean boundary was made for the North American plate in the Davis Strait. This new boundary was used in a plate reconstruction for C33 and C27 time, because both have been suggested as the time of the initial opening of the Labrador Sea, Davis Strait and Baffin Bay (Roest and Srivastava, 1989; Chalmers and Laursen, 1995). At C33 time, a slight gap is left in the southernmost area, but there is extensive overlap to the north between the two plates. At C27 time, the boundaries in the central and northern areas are adjacent and the volcanic rocks on both sides of Davis Strait overlap, but there is a significant gap in the southernmost area. These results strongly suggest that there needs to be a refinement of the poles of rotation.

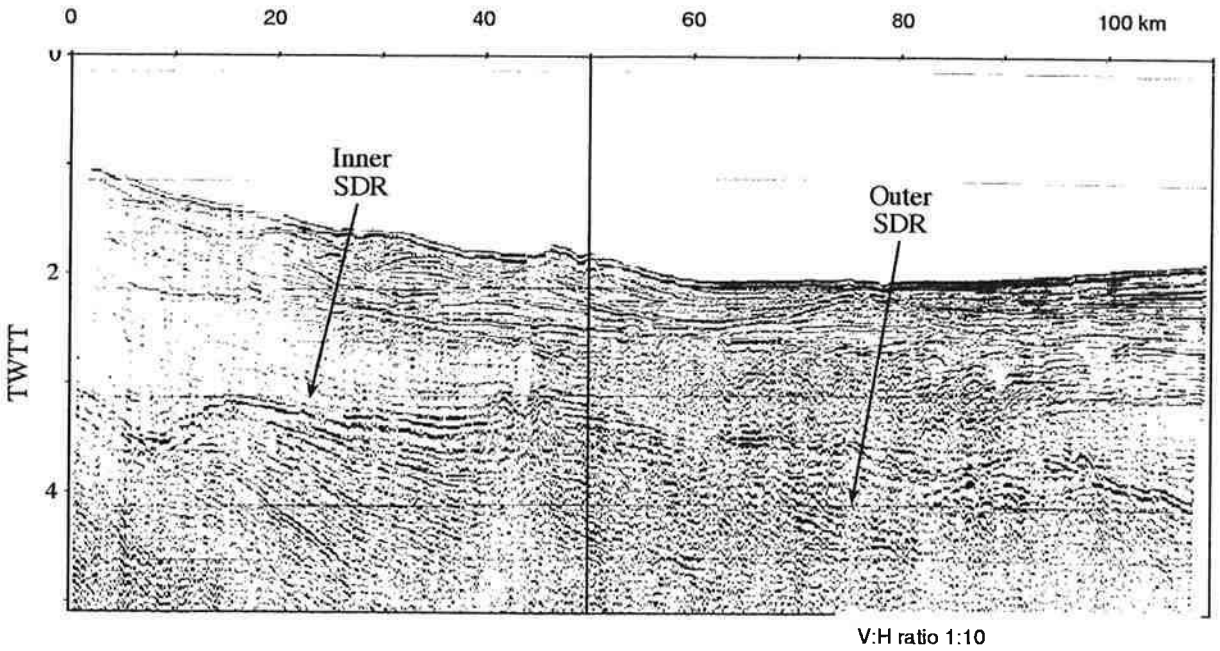

Fig. 14: Part of seismic line 200/75 on the southeastern Baffin shelf where two sets of seaward-dipping reflectors can be seen

Conclusion

A mapping of the structures and seismic stratigraphy of the offshore volcanic rocks in the area between 68°N and 71°N on the central West Greenland margin has been carried out, and the fault pattern and features at top volcanic level have been described in detail. The thickness of the volcanic rocks has been estimated by modelling of gravity data. Only modelling where sediments are present below the volcanic section gives geologically realistic results. The volcanic rocks range in thickness from around 2 km in the eastern part directly off the coast, to a maximum of 5.5 km before thinning towards west. The pre-volcanic sediments display maximum thicknesses of 7 km–9 km, but displaced c. 50 km west compared to the maximum thicknesses of the volcanic rocks. An eruption zone has been identified trending almost N-S through the studied area.

It is not possible to correlate datings of the volcanic rocks directly from the onshore to the offshore area, thus the results of the combination of the Ar/Ar datings and geomagnetic polarity determination is that the clear division onshore into two separate periods of eruptions cannot be confirmed from the offshore section, and that the uppermost volcanic rocks in the offshore area, seem to be younger than the uppermost dated onshore volcanic rocks.

An evaluation of two bright spot anomalies, one 100 msec above the top volcanic level, and one immediately above has been carried out using AVO analysis. Both could be classified as a hydrocarbon sand, overlain by a tight sealing layer.

On the Baffin Island margin, the structures at basement level have been mapped, and by combining the seismic interpretation with newly compiled gravity and magnetic maps, a new continent-ocean boundary has been interpreted. The extent of the volcanic covered area has been enlarged compared to earlier studies. A preliminary plate reconstruction for the Davis Strait/Baffin Bay has been calculated for the initiation of seafloor spreading at C33 and C27-time, both showing gaps and overlaps in different regions between the Greenland and North American plates.

References

Barton, A. J. & White, R. S. 1997. Volcanism on the Rockall continental margin. Journal of the Geological Society of London, 154, 531-536.

Bate, K. J. 1995. Pressure indicators from the sedimentary basins of West Greenland. Grønlands Geologiske Undersøgelse, Open file series, 95/13, 1-40.

Bojesen-Koefoed, J. A., Christiansen, F. G., Nytoft, H. P. & Pedersen, A. K. 1999. Oil seepage onshore West Greenland: evidence of multiple source rocks and oil mixing. In: Spencer, A. M. (ed.) Petroleum Geology of Northwest Europe: Proceedings of the 5th Conference. Geological Society, London, 305-314.

Castagna, J. P. & Swan, H.W. 1997. Principles of AVO crossplotting. The Leading Edge, 4, 337-342.

Chalmers, J. A. 1998. Gravity models in the Disko-Nuussuaq area of central West Greenland Geological Survey of Denmark and Greenland, Report, 1998/21, 1-55.

Chalmers, J. A. and Laursen, K. H. (1995) Labrador Sea: the extent of continental and oceanic crust and the timing of the onset of seafloor spreading, Marine and Petroleum Geology 12 205-217.

Chalmers, J. A., Pulvertaft, T. C. R., Marcussen, C. & Pedersen, A. K. 1999. New insight into the structure of the Nuussuaq Basin, central West Greenland. Marine and Petroleum Geology, 16, 197-224.

Chian, D., Keen, C., Reid, I. and Louden, K. E. 1995. Evolution of the nonvolcanic rifted margins: new results from the conjugate margins of the Labrador Sea Geology 23 589-592

Christiansen, F. G. 1993. Disko Bugt Project 1992, West Greenland. Rapport Grønlands Geologiske Undersøgelse, 159, 47-52.

Christiansen, F. G., Bate, K. J., Dam, G., Marcussen, C. & Pulvertaft, T. C. R. 1996. Continued geophysical and petroleum geological activities in West Greenland in 1995 and the start of onshore exploration. Bulletin Grønlands Geologiske Undersøgelse, 172, 15-21.

Christiansen, F. G., Boesen, A., Bojesen-Koefoed, J., Dalhoff, F., Dam, G., Neuhoff, P. S., Pedersen, A. K., Pedersen, G. K., Stannius, L. S. & Zinck-Jørgensen, K.1998. Petroleum geological activities onshore West Greenland in 1997. Review of Greenland Activities, Bulletin, 1-9.

Christiansen, F. G., Boesen, A., Bojesen-Koefoed, J. A., Chalmers, J. A., Dalhoff, F., Dam, G., Hjortkjær, B. F., Kristensen, L., Larsen, L. M., Marcussen, C., Mathiesen, A., Nøhr-Hansen, H., Pedersen, A. K., Pedersen, G. K., Pulvertaft, T. C. R., Skaarup, N. & Sønderholm, M. 1999. Petroleum geological activities in West Greenland in 1998. Geology of Greenland Survey Bulletin, 183, 44-56.

Christiansen, F. G., Bojesen-Koefoed, J. A., Chalmers, J. A., Dalhoff, F., Mathiesen, A., Sønderholm, M., Dam, G., Gregersen, U., Marcussen, C., Nøhr-Hansen, H., Piasecki, S., Preuss, T., Pulvertaft, T. C. R., Rasmussen, J. A. and Sheldon, E. (2001) Petroleum geological activities in West Greenland in 2000. Geology of Greenland Survey Bulletin **189**.

Christiansen, F. G., Dam, G. & Pedersen, A. K. 1994. Discovery of live oil at Marraat, Nuussuaq: field work, drilling and logging. Rapport Grønlands Geologiske Undersøgelse, 160, 57-63.

Christiansen, F. G., Marcussen, C. & Chalmers, J. A. 1995. Geophysical and petroleum geological activities in the Nuussuaq-Svartenhuk Halvø area 1994: promising results for an onshore exploration potential. Rapport Grønlands Geologiske Undersøgelse, 165, 32-41.

Geoffroy, L., Gelard, J. P., Lepvrier, C. & Olivier, P. 1998. The coastal flexure of Disko (West Greenland), onshore expression of the 'oblique reflectors'. *Journal of Geological Society of London, **155***, 463-473.

Geoffroy, L., Callot, J.-P., Scaillet, S., Skuce, A., Gélard, J. P., Ravilly, M., Angelier, J., Bonin, B., Cayet, C., Perrot, K. and Lepvrier, C. 2001. Southeast Baffin volcanic margin and the North American-Greenland plate separation. *Tectonics*, **20**, 566-584.

Henderson, G. 1973. The geological setting of the West Greenland basin in the Baffin Bay region. Geological Survey of Canada Paper, 71-23, 521-544.

Henderson, G., Schiener, E. J., Risum, J. B., Croxton, C. A. & Andersen, B. B. 1981. The West Greenland Basin. In: Kerr, J. W. & Fergusson, A. J. (eds) Geology of the North Atlantic Borderlands. Canadian Society of Petroleum Geologists, Memoirs, 7, 399-428.
Klose, G. W., Malterre, E., McMillan, N. J. & Zinkan, C. G. 1982. Petroleum exploration offshore southern Baffin Island, Northern Labrador Sea, Canada, in: Arctic geology and geophysics (Eds. Embry, A. F. & Balkwill, H. R.) Canadian Society of Petroleum Geologists Memoir 8 233-244
Larsen, L. M. & Pedersen, A. K. 1992. Volcanic marker horizons in the upper part of the Maligât Formation on eastern Disko and Nuussuaq, Tertiary of West Greenland: syn- to post-volcanic basin movements. Rapport Grønlands Geologiske Undersøgelse, 155, 85-93
MacLean, B. (1978) Marine geological-geophysical investigations in 1977 of the Scott inlet and Cape Dyer - Frobisher Bay areas of the Baffin Island continental shelf Current Research, Part B, Geological Survey of Canada 78-1B 13-20
MacLean, B. & Falconer, R. H. K. (1979) Geological/geophysical studies in Baffin Bay and Scott Inlet-Buchanan Gulf and Cape Dyer-Cumberland Sound areas of the Baffin Island shelf, in: Current Research, Part B, Geological Survey of Canada 79-1B 231-244
MacLean, B. and Williams, G. L. (1983) Geological investigations of the Baffin Island shelf in 1982, in: Current Research, Part B, Geological Survey of Canada 83-1B 309-315
Pedersen, A. K., Larsen, L. M. & Dueholm, K. S. 1993. Geological section along the south coast of Nuussuaq, central West Greenland. 1: 20 000. Coloured geological sheet. Copenhagen, Denmark, Grønlands Geologiske Undersøgelse.
Pedley, R. C., Busby, J. P. & Dabek, Z. K. 1993. Gravmag vl. 5 user manual - Interactive 2.5D gravity and magnetic modelling. Technical Report WK/93/26/R. Regional Geophysics Series, British Geological Survey, 73 p.
Planke, S. 1994. Geophysical response of flood basalts from analysis of wire line logs: Ocean Drilling Program Site 642, Vøring volcanic margin. Journal of Geophysical Research, 99, 9279-9296.
Planke, S. & Eldholm, O.1994. Seismic response and construction of seaward dipping wedges of flood basalts: Vøring volcanic margin. Journal of Geophysical Research, 99, 9263-9278.
Pujol, J., Fuller, B. N. & Smithson, S. B. 1989. Interpretation of a vertical seismic profile conducted in the Columbia Plateau basalts. Geophysics, 54, 1258-1266.
Riisager, P. & Abrahamsen, N. 1999. Magnetostratigraphy of Paleocene basalts from the Vaigat Formation of West Greenland. Geophysical Journal International, 137, 774-782.
Roest, W. R. and Srivastava, S. P. 1989 Sea-floor spreading in the Labrador Sea: A new reconstruction, Geology 17 1000-1003
Rolle, F. 1985. Late Cretaceous (Tertiary sediments offshore central West Greenland: lithostratigraphy, sedimentary evolution, and petroleum potential. Canadian Journal of Earth Sciences, 22, 1001-1019.
Skaarup, N. (paper 3, included in this thesis) Seismic stratigraphy of Palaeogene volcanic rocks, offshore central West Greenland (submitted to Journal of the Geological Society)
Skaarup, N. & Chalmers, J. A. 1998. A possible new hydrocarbon play, offshore West Greenland. Geology of Greenland Survey Bulletin, 180, 28-30
Skaarup, N., Chalmers, J. A. and White, D. 2000. An AVO study of a possible new hydrocarbon play, offshore central West Greenland. AAPG Bulletin, 84, No 2, 174-182
Skaarup, N., Jackson, H. R. & Oakey, G. (paper 4, included in this thesis) A seismic reflection and potential field study of Baffin Bay / Davis Strait, eastern Canada: implications for tectonic evolution
Storey, M., Duncan, R. A., Pedersen, A. K., Larsen, L. M. & Larsen, H. C. 1998. 40Ar/39Ar geochronology of the West Greenland Tertiary volcanic province. Earth and Planetary Science Letters, 160, 569-586.
Verhoef, J., Roest, W. R, Macnab, R. Arkhani-Hamed, J., and Members of the Project Team (1996) Magnetic anomalies of the Arctic and North Atlantic Oceans and adjacent Land Areas Geological Survey of Canada open file report 3151, CD-Rom.
White, R. S. 1992. Magmatism during and after continental break-up. *In*: Storey, B. C., Alabaster, T. & Pankhurst, R. J. (eds) *Magmatism and the causes of Continental Break-up*, Geological Society Special Publication, **68**, 1-16.

Whittaker, R. C. 1995. A preliminary assessment of the structure, basin development and petroleum potential offshore central West Greenland. Grønlands Geologiske Undersøgelse Open File Series, 95/9, 1-43.
Whittaker, R. C. 1996. A preliminary seismic interpretation of an area with extensive Tertiary basalts offshore central West Greenland. Bulletin Grønlands Geologiske Undersøgelse, 172, 28-31.
Williamson, M.-C., Villeneuve, M. E., Larsen, L. M., Jackson, H. R., Oakey, G. N. & MacLean, B. 2001. Age and petrology of offshore basalts from the Southeast Baffin Shelf, Davis Strait, and western Greenland continental margin. St. John's 2001, Abstract Volume 26, 162.

Acknowledgements

At the end of a long-term project a large number of people always deserve thanks and acknowledgement for their contributions. I try to list all of them below, although Murphy's law ensures that I have probably forgotten a few. So first of all, I want to thank those few: although not explicitly mentioned here, your contributions are highly appreciated!

Next in line are my two supervisors Jim Chalmers and Asger Ken Pedersen; Jim has always been a rewarding discussion partner during our years of co-operation in the fields of Greenland margin and Davis Strait/Baffin Bay problematics. Also, his comments on different versions of my manuscripts have always resulted in large improvements, scientifically and linguistically. Asger, introduced me to the onshore volcanic geology on Disko and Nuussuaq, and commented on various versions of my manuscripts and, perhaps most importantly, organized a very inspiring field trip in July of 1998 in the search of oil in the volcanic rocks onshore West Greenland.

Anders Boesen showed me a lot of the secrets of structural geology during a great field season, June of 1998 in the Nuussuaq and Disko area.

Chris Pulvertaft has been a great inspiration, and carried out miracles when helping me turning a hopeless first draft of the manuscript about volcanic stratigraphy into a decent and meaningful paper.

Jette Halskov has been very helpful, drawing most of the figures, and re-drawing as corrections became necessary. Her quick and careful craftsmanship is one of the reasons why I managed to get this work finished on schedule.

Talking about figures, Claus Brandt Jacobsen worked hard on many late night shifts to get the nice isopach maps from my interpretation of the volcanic successions.

The Geophysical Department at GEUS has been (and still is) a wonderful place to work.

Ruth Jackson has been a great help organizing my stay in Nova Scotia. She has also been a very inspiring partner in the work on the Baffin Island margin.

Gordi Oakey carried out a great job when organizing the production of the maps of gravity, magnetics and physiography of the Davis Strait/Baffin Bay region. These maps were important tools in the interpretation of the structures on the Baffin Island margin.

The Marine Regional Geoscience Department at GSCA, Nova Scotia showed great hospitality, not just by letting me carry out my work there, but also by providing office space and much inspiration for my husband during our stay.

My husband, Thomas has been a major support all the way. The process, and especially the trip to Nova Scotia, would never have been such a fun and fruitful experience if not for someone to share it with.

Finally, little Linus showed up half way through the work, and changed my life totally and deeply: More dirty nappies, more sleepless nights and much more fun than ever before!

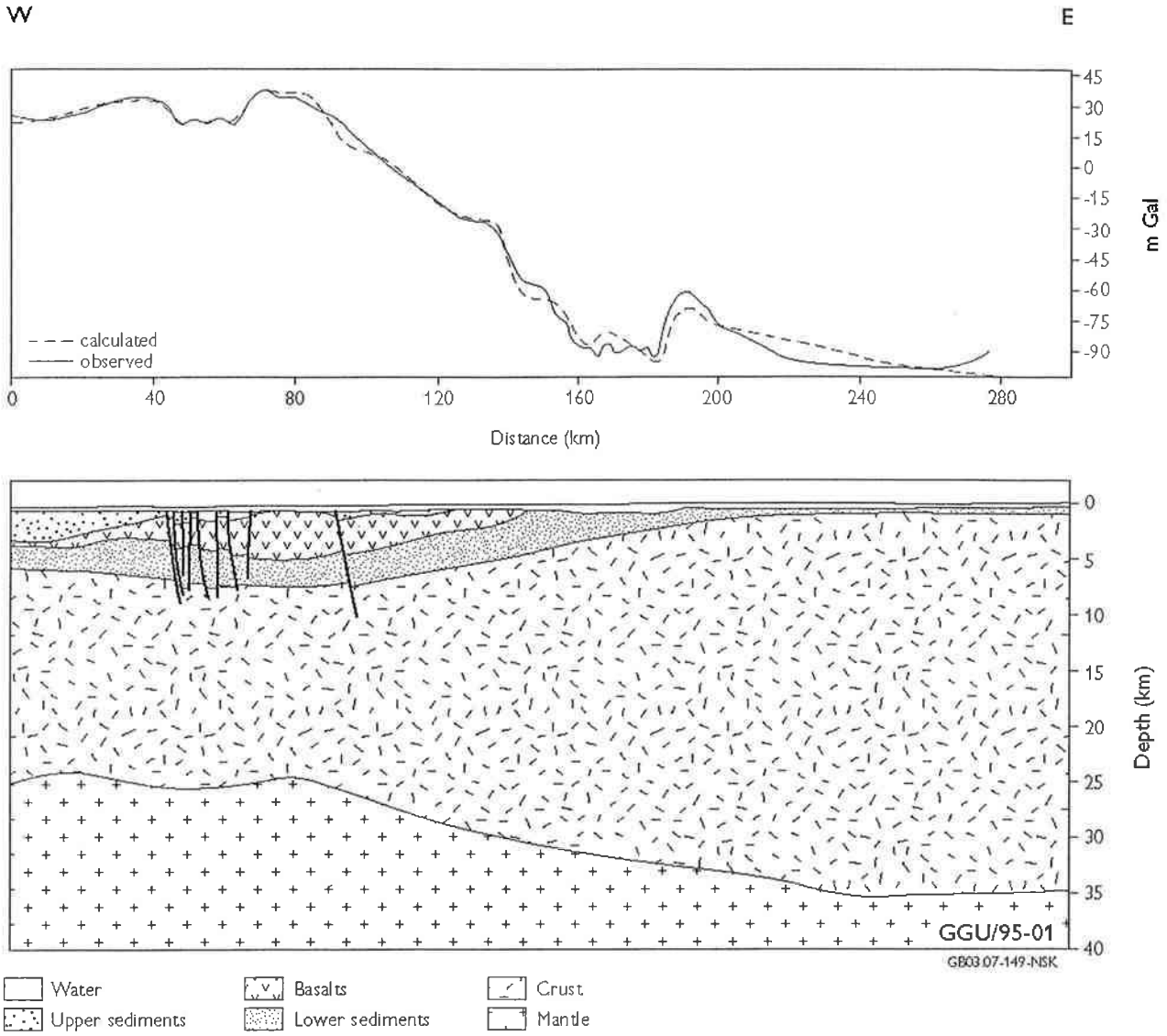

Appendix 1: Line GGU/95-01, an east-west line in the southernmost part of the studied area, with an interpreted geological section derived from the gravity modelling. The local minimum in the gravity values seen at 45-65 km, is compensated by faulting at top volcanic level. The volcanic rocks display thicknesses from 2 km to a maximum of 5 km, with thinning westwards to 1/2-1 km. The prevolcanic sediments display a rather homogenous thickness of about 4 km, before thinning westwards. The densities used for the gravity modelling were: water 1.0 Mg/m^3, post-volcanic sediments 2.2 Mg/m^3, volcanic rocks 3.0 Mg/m^3, pre-volcanic sediments 2.55 Mg/m^3, crust 2.8 Mg/m^3, mantle 3.3 Mg/m^3, background 3.3 Mg/m^3

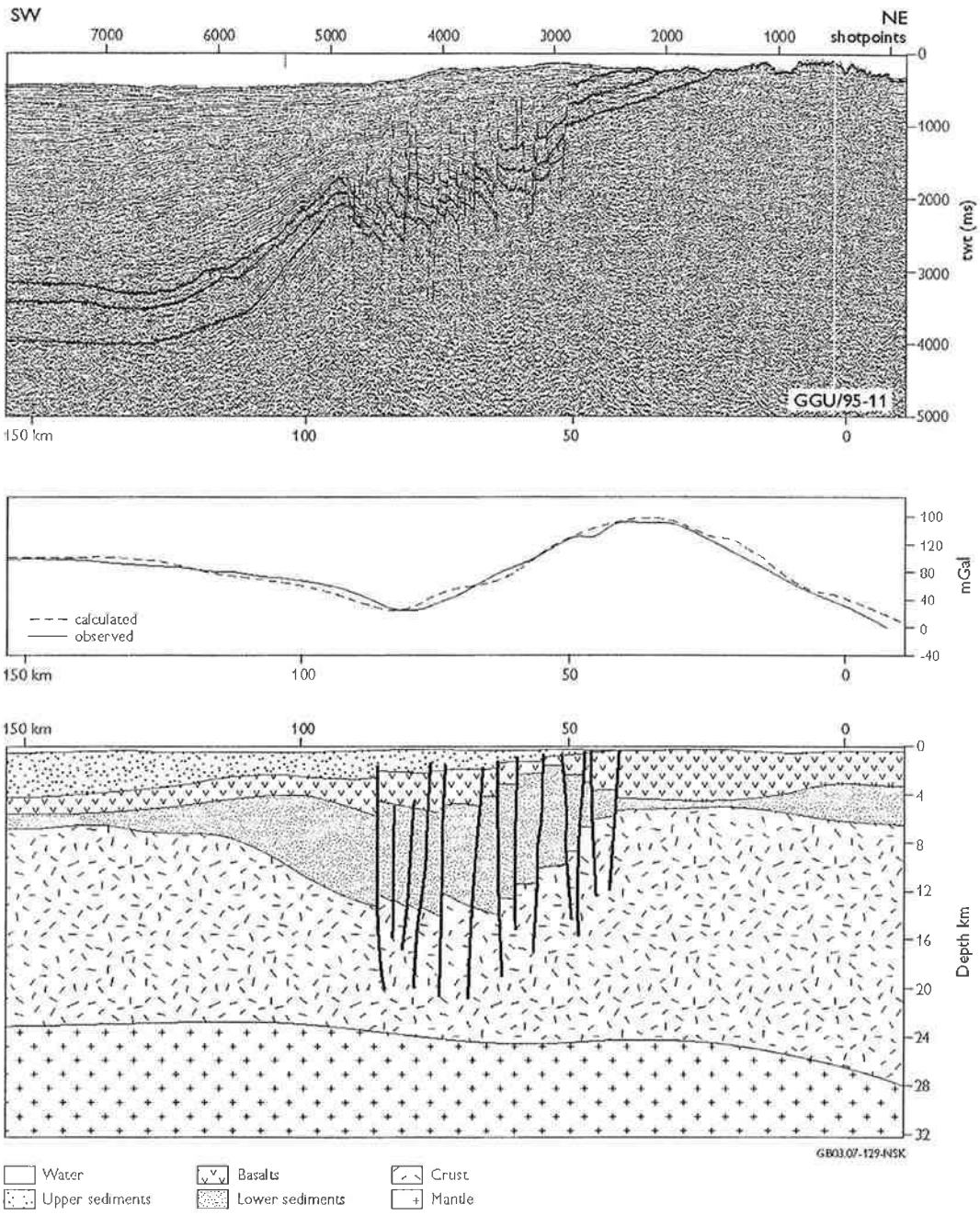

Appendix 2: Line GGU/95-11, an east-west line in the southern part of the studied area, with the interpreted geological section from the gravity modelling shown together with the seismic section. The intense faulted area (sp. 3000-5000) with straight, almost vertical, mostly normal faults is interpreted as a pull-apart basin in the geological model. The volcanic rocks display thicknesses to a maximum of 4 km, whereas the pre-volcanic sediments are modelled to be 7–7.5 km thick within the fault blocks at 50–80 km

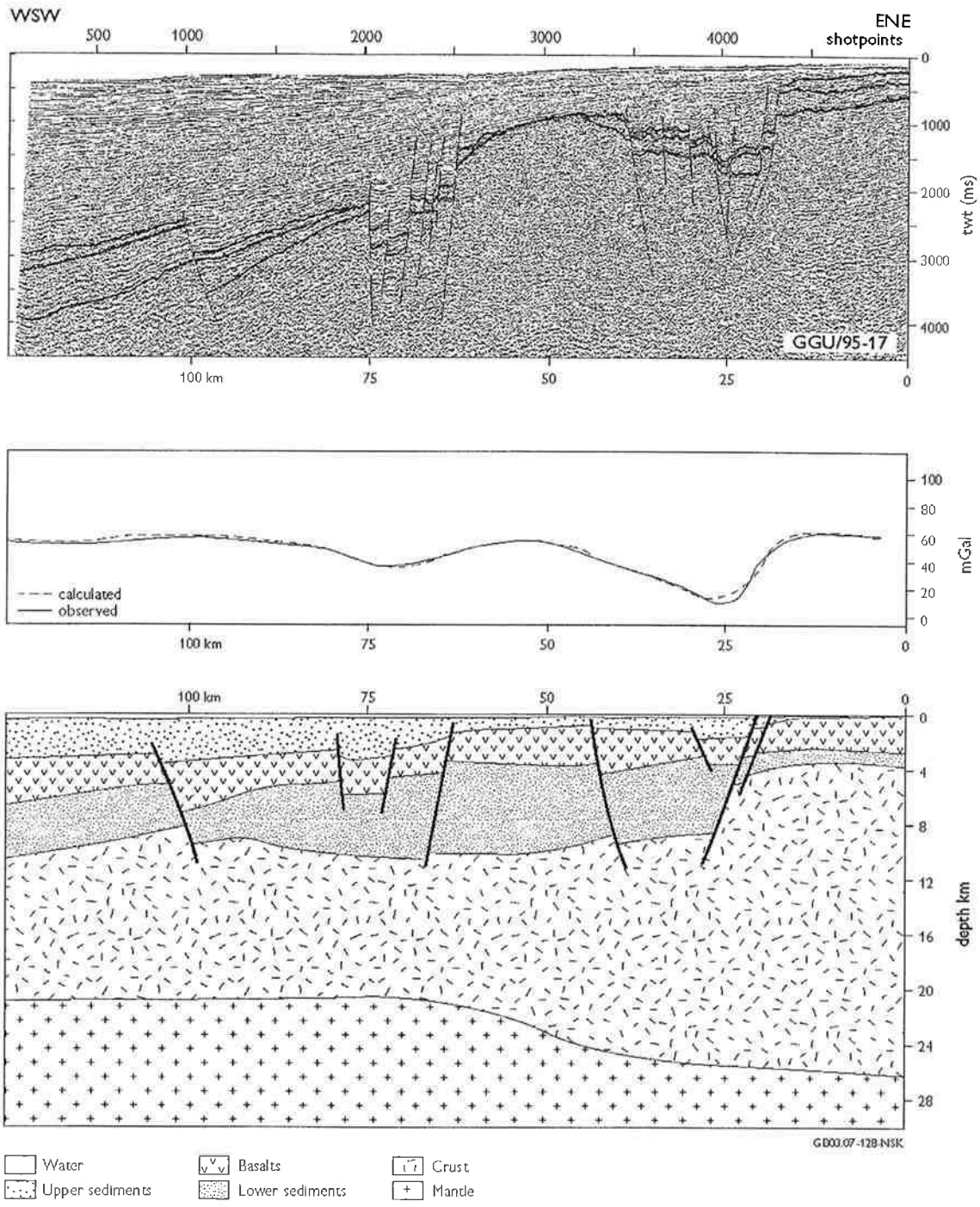

Appendix 3: Line GGU/95-17, an east–west line in the middle of the studied area, with the interpreted geological section from the gravity modelling shown together with the seismic section. The volcanic section display thicknesses of 2.5-4 km, whereas the pre-volcanic sediments were modelled to be up to 6.5 km thick in the central area at 40–75 km. The abrupt fall in the gravity anomaly at 25 km, is partly compensated by the topography of the volcanic surface and by an abrupt increase in the thickness of the pre-volcanic sediments

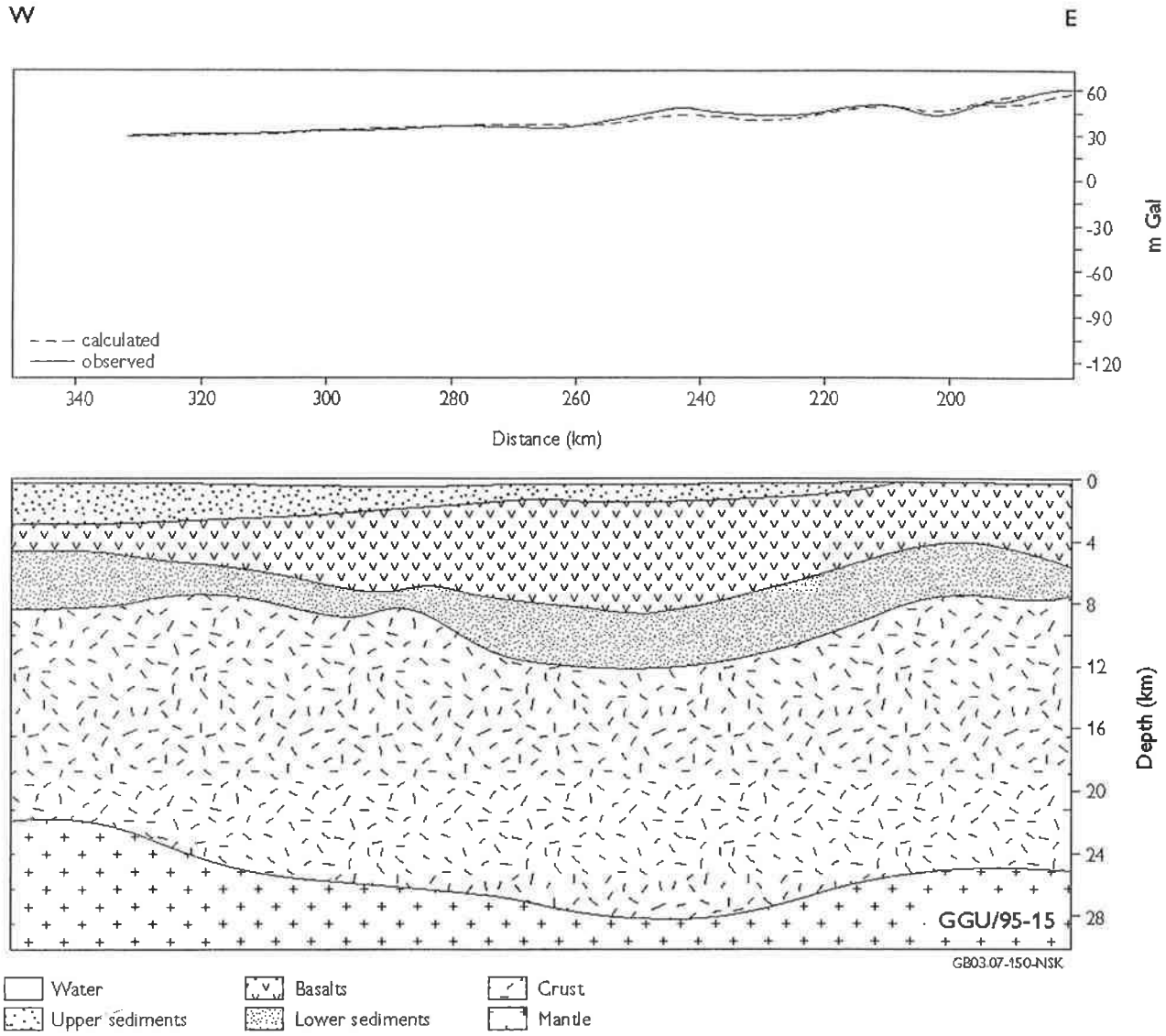

Appendix 4: Line GGU/95-15, an east-west line with the interpreted geological section from the gravity modelling. The volcanic section display thicknesses of 4-6.5 km in the centre of the line, whereas the prevolcanic sediments were modelled to be around 2-4 km thick for almost the entire length of the line

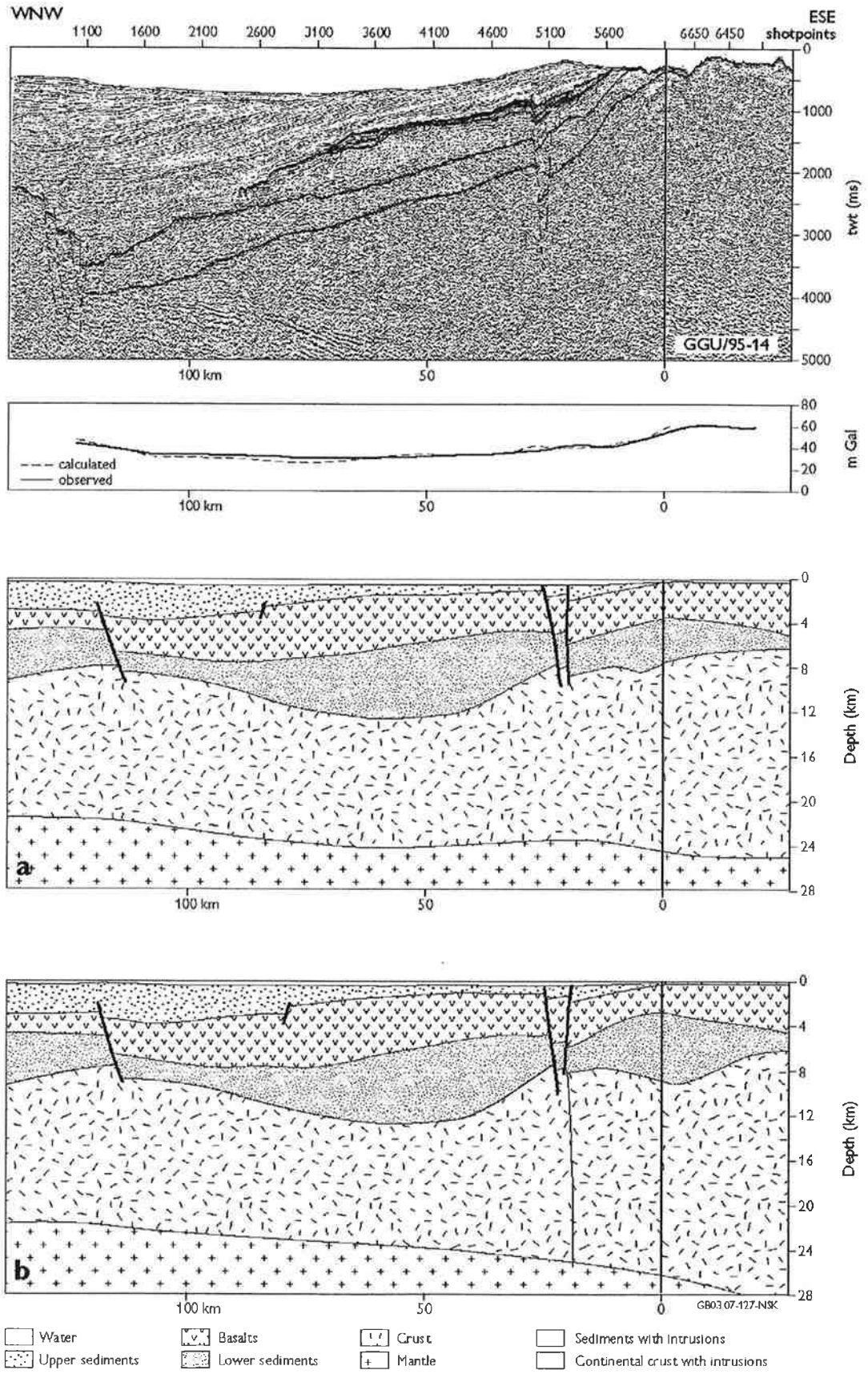
WNW
ESE
1100 1600 2100 2600 3100 3600 4100 4600 5100 5600 6650 6450 shotpoints
0
1000
2000
3000
4000
5000
twt (ms)
GGU/95-14
100 km
50
0
80
60
40
20
0
m Gal
calculated
observed
100 km
50
0
0
4
8
12
16
20
24
28
Depth (km)
a
100 km
50
0
b
GB03 07-127-NSK
Water
Upper sediments
Basalts
Lower sediments
Crust
Mantle
Sediments with intrusions
Continental crust with intrusions

Appendix 5: Line GGU/95-14, an east-west line in the northern part of the studied area with the interpreted geological section from the gravity modelling shown together with the seismic section. In version a the volcanic section display thicknesses of 3-5 km without any abrupt changes in outline, whereas the pre-volcanic sediments were modelled to be up to 7 km thick at their thickest in the central area at 50 km. In version b intrusions have been introduced into the pre-volcanic sediments and the crust in the nearshore area thereby raising the density, but that makes little significant difference in the modelling. At the intersection between the two lines, at 0 km, the volcanic rocks decrease from 3.5 km to 2.5 km thickness, the pre-volcanic sediments increase from 4 km to 6 km, and the crust/mantle boundary lowers 2 km, from 25 km to 27 km

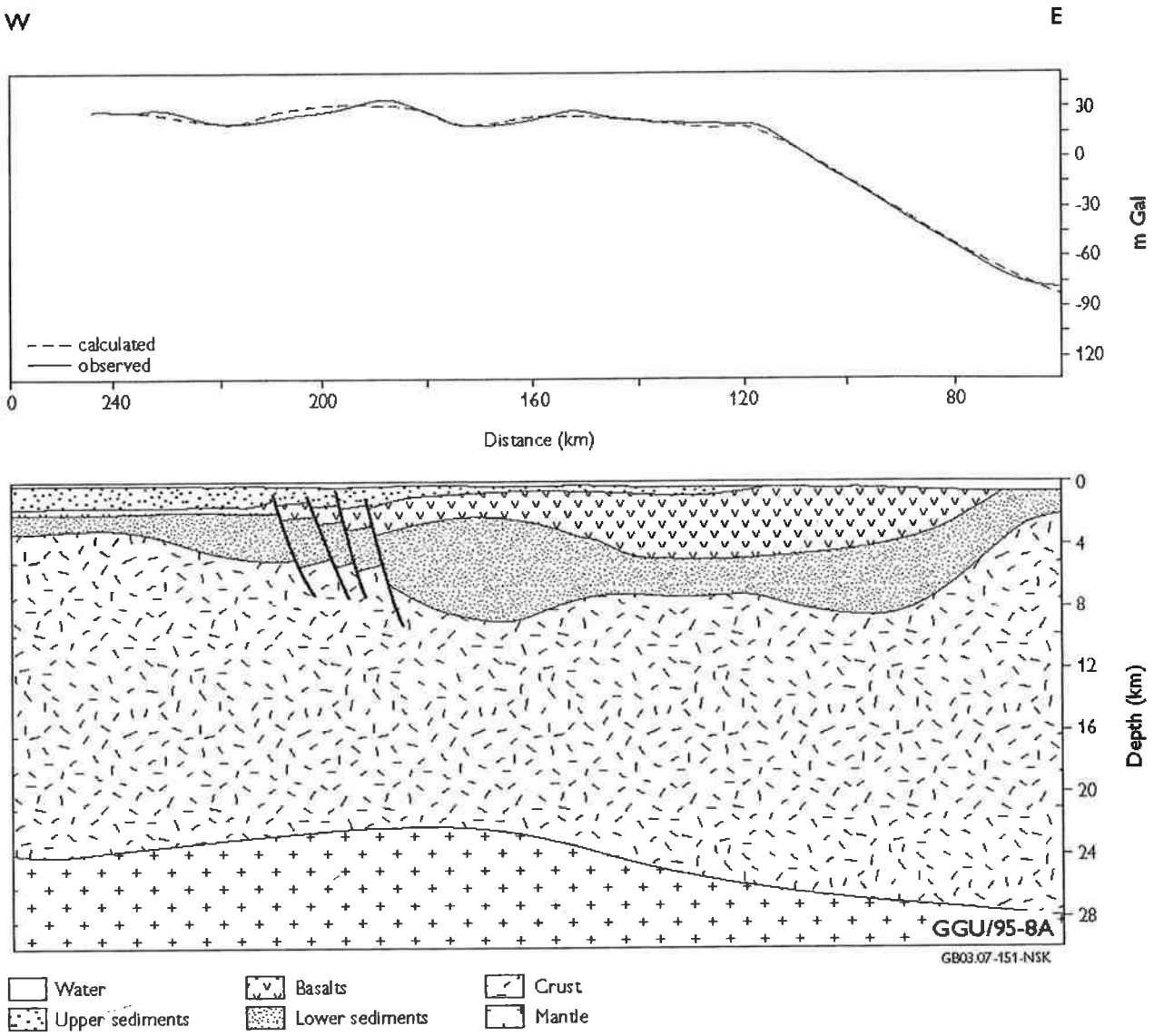

Appendix 6: Line GGU/95-08A, an east-west line in the northernmost part of the studied area with the interpreted geological section from the gravity modelling. The volcanic section displays maximum thicknesses of 5 km at around 100-140 km, whereas the pre-volcanic sediments were modelled to have a maximum thickness of about 6 km at 160–180 km

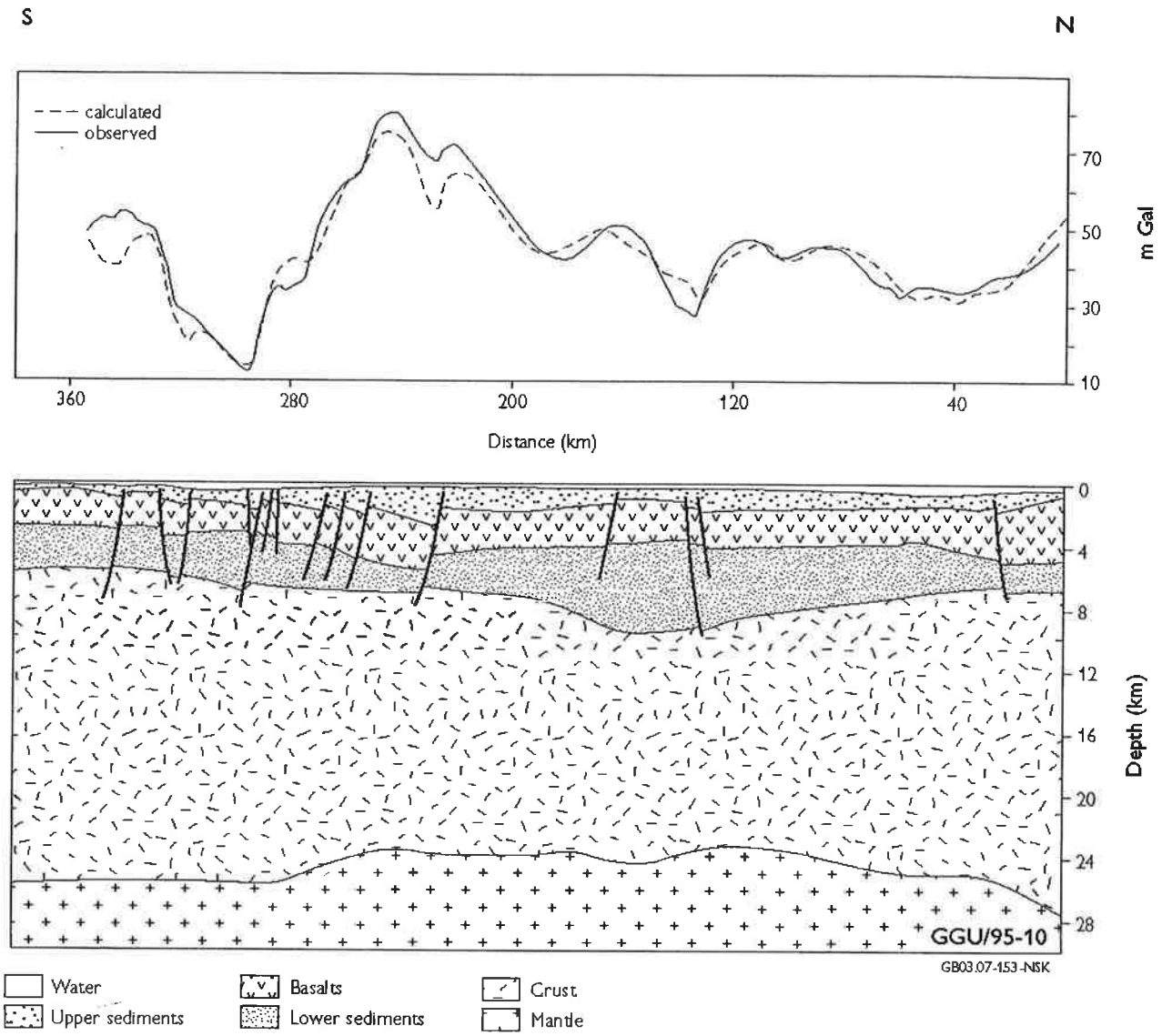

Appendix 7: Line GGU/95-10, a north-south line in the eastern part of the studied area with the interpreted geological section from the gravity modelling. The volcanic section is intersected by numerous faults, especially in the southern part, and the level of the top volcanic surface compensate for most of the fluctuations in the gravity data. The volcanic section displays thicknesses of 3-4 km on most of the line, whereas the pre-volcanic sediments were modelled to be a maximum of 6 km thick at 120-180 km

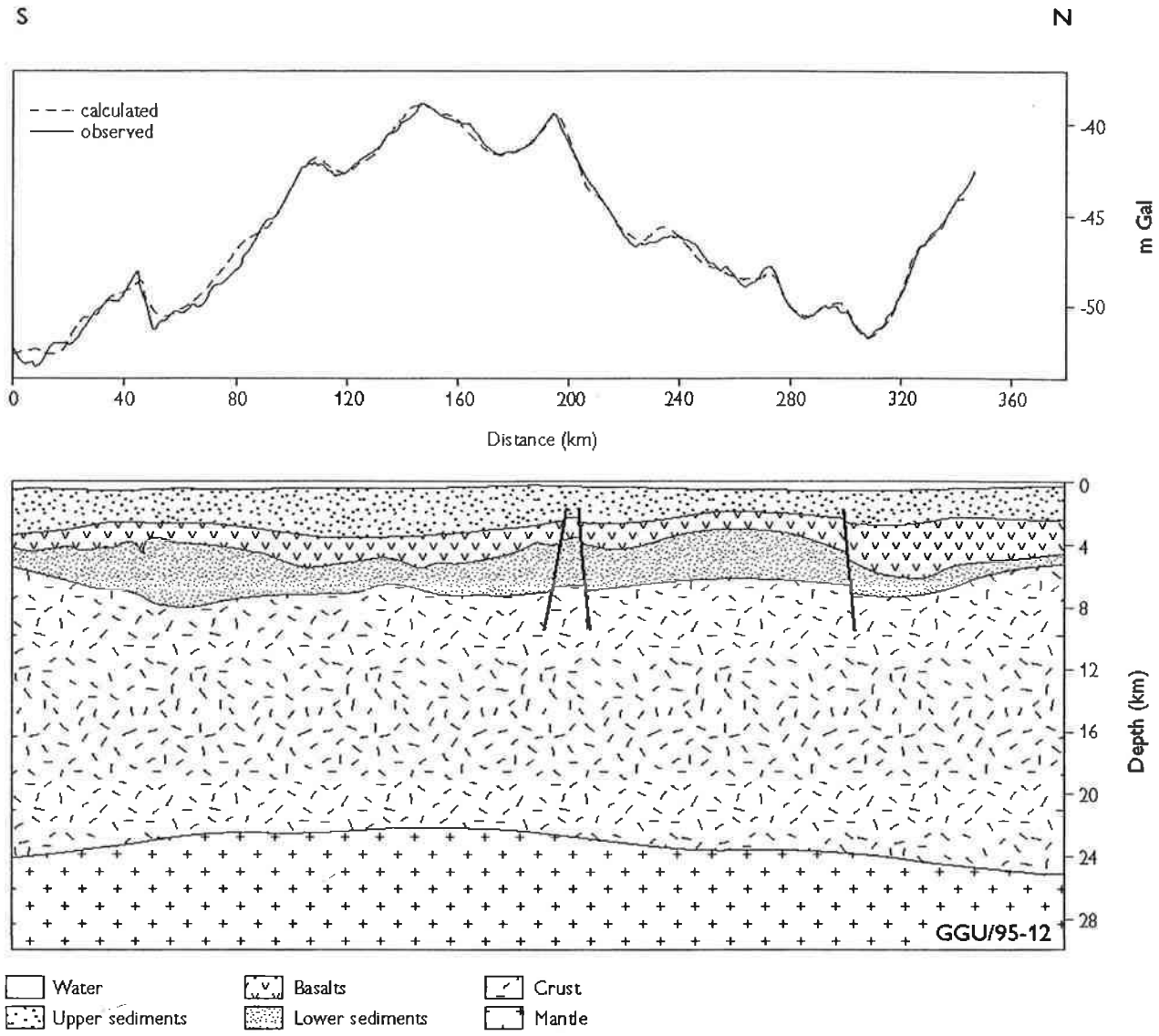

Appendix 8: Line GGU/95-12, a north-south line in the middle of the studied area with the interpreted geological section from the gravity modelling. The volcanic surface is less intersected by faults than that on line GGU/95-10 (Appendix 7), and both the volcanic rocks and the pre-volcanic section is thinner. The volcanic rocks display a thickness of 3.5 km in the northernmost part, otherwise they are around 2 km at most. The pre-volcanic section was modelled to have two maximum thicknesses of 3.5-4 km at 240-280 km and 40-80 km

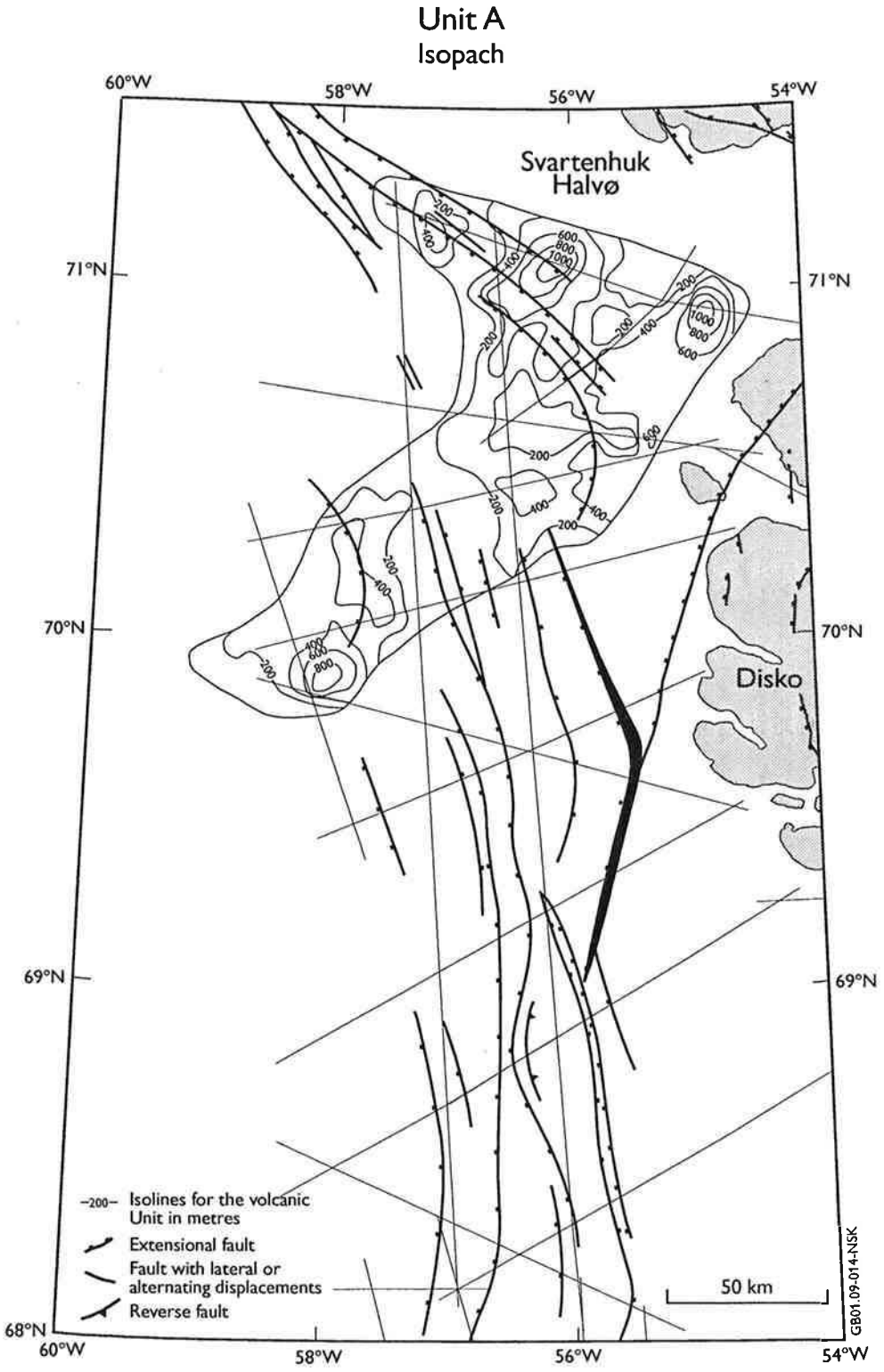

Appendix 9: Isopach map of seismic unit A. Unit A has a limited distribution to the northernmost part of the studied area, and occurs in a thin layer of 100–570 m.

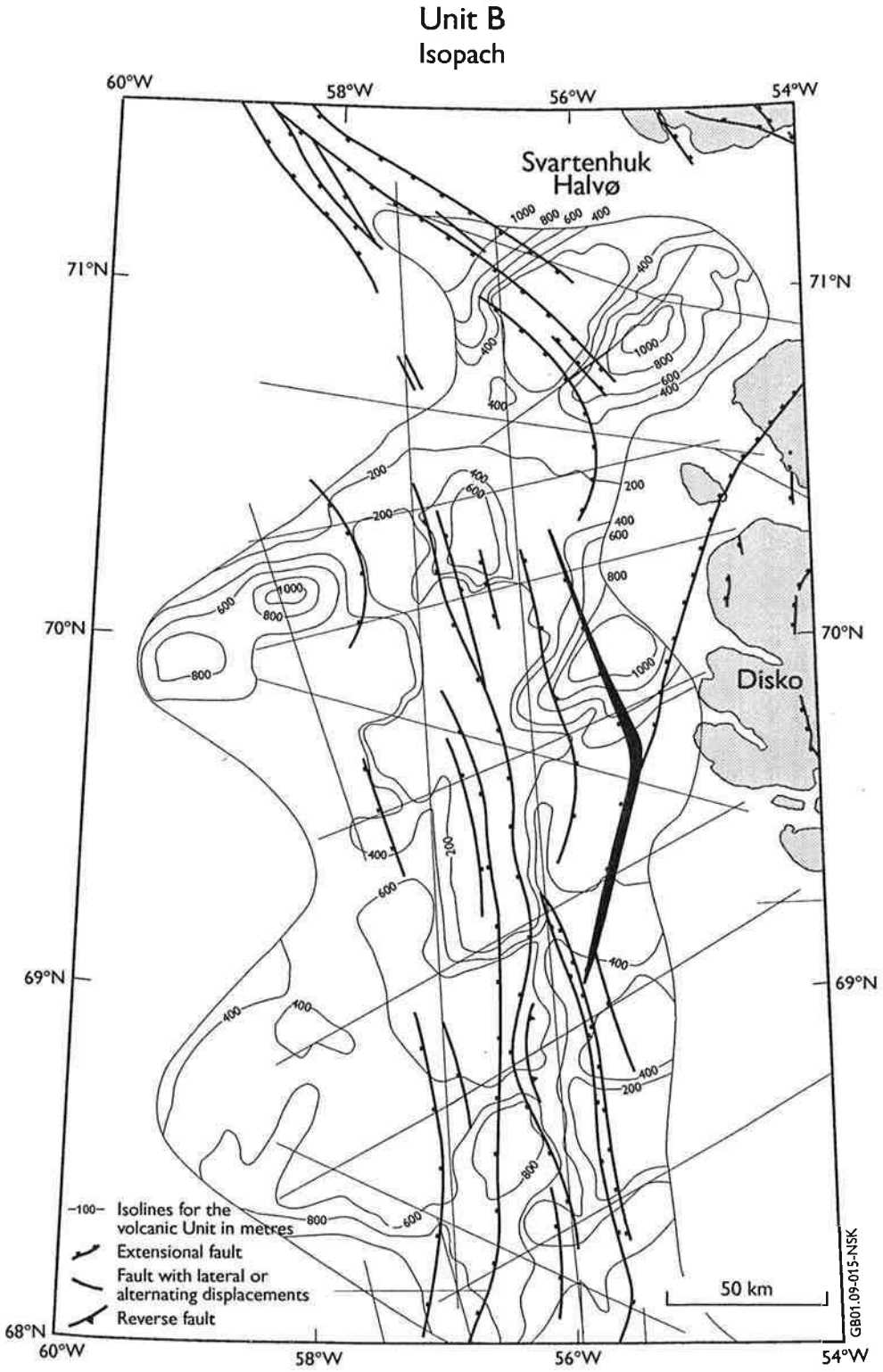

Appendix 10: Isopach map of seismic unit B. Unit B is interpreted in most of the studied area, and varies in thickness from 130–1000 m.

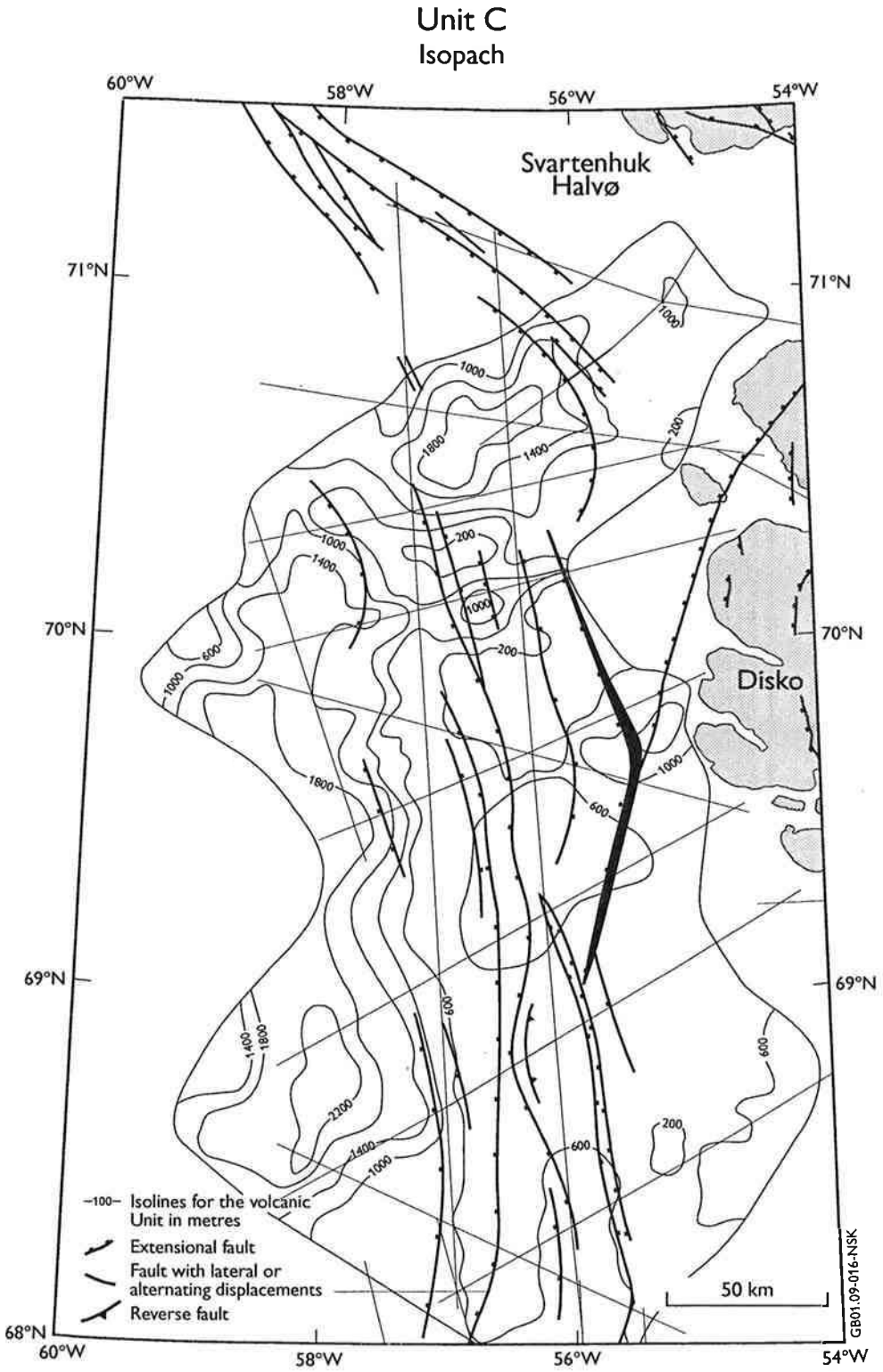

Appendix 11: Isopach map of seismic unit C. Unit C is interpreted in most of the studied area, and occurs in a layer of 260–1040 m.

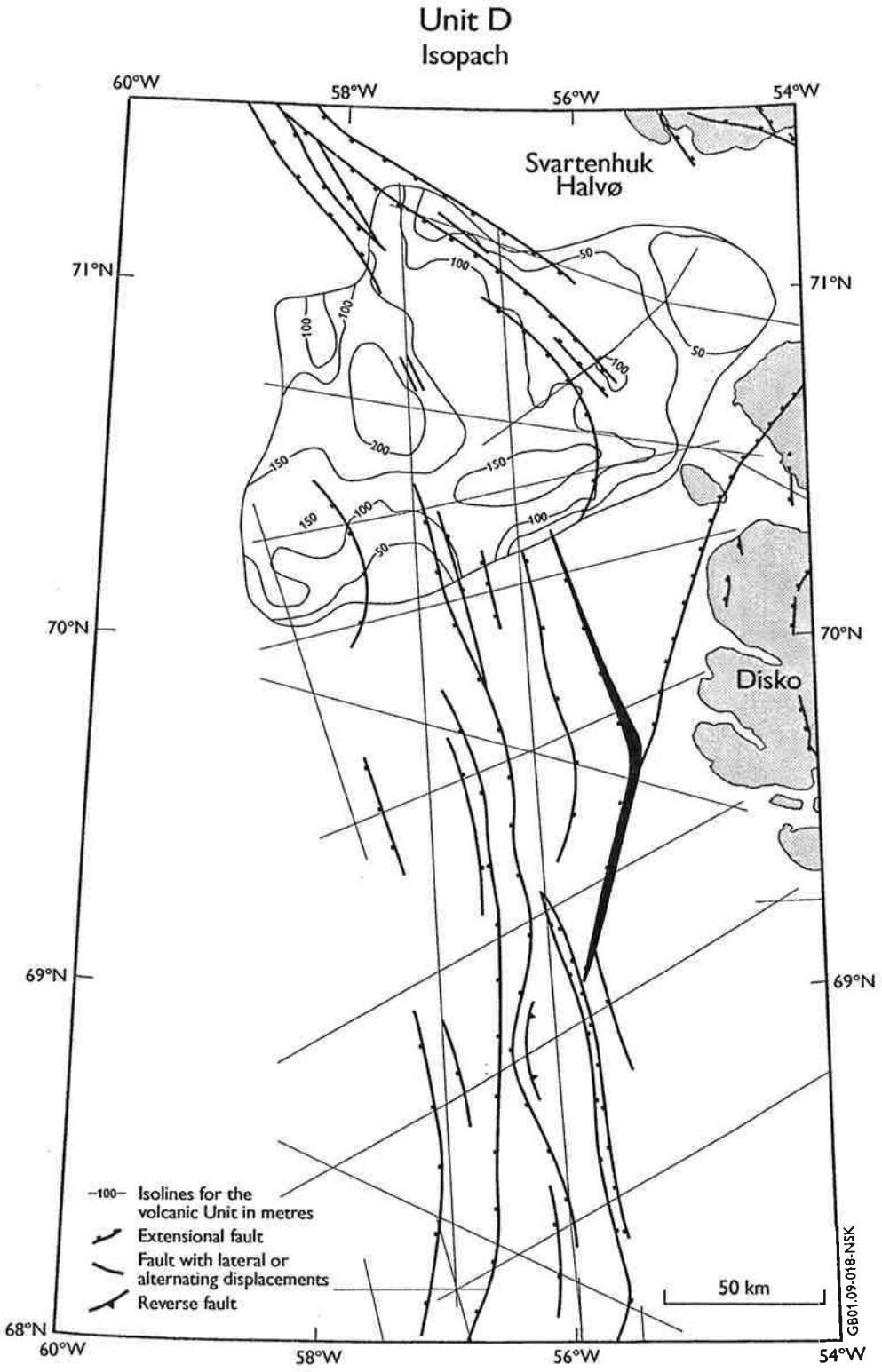

Appendix 12: Isopach map of seismic unit D. Unit D is restricted to the northernmost part of the studied area, and occurs in a layer of 310–1430 m.

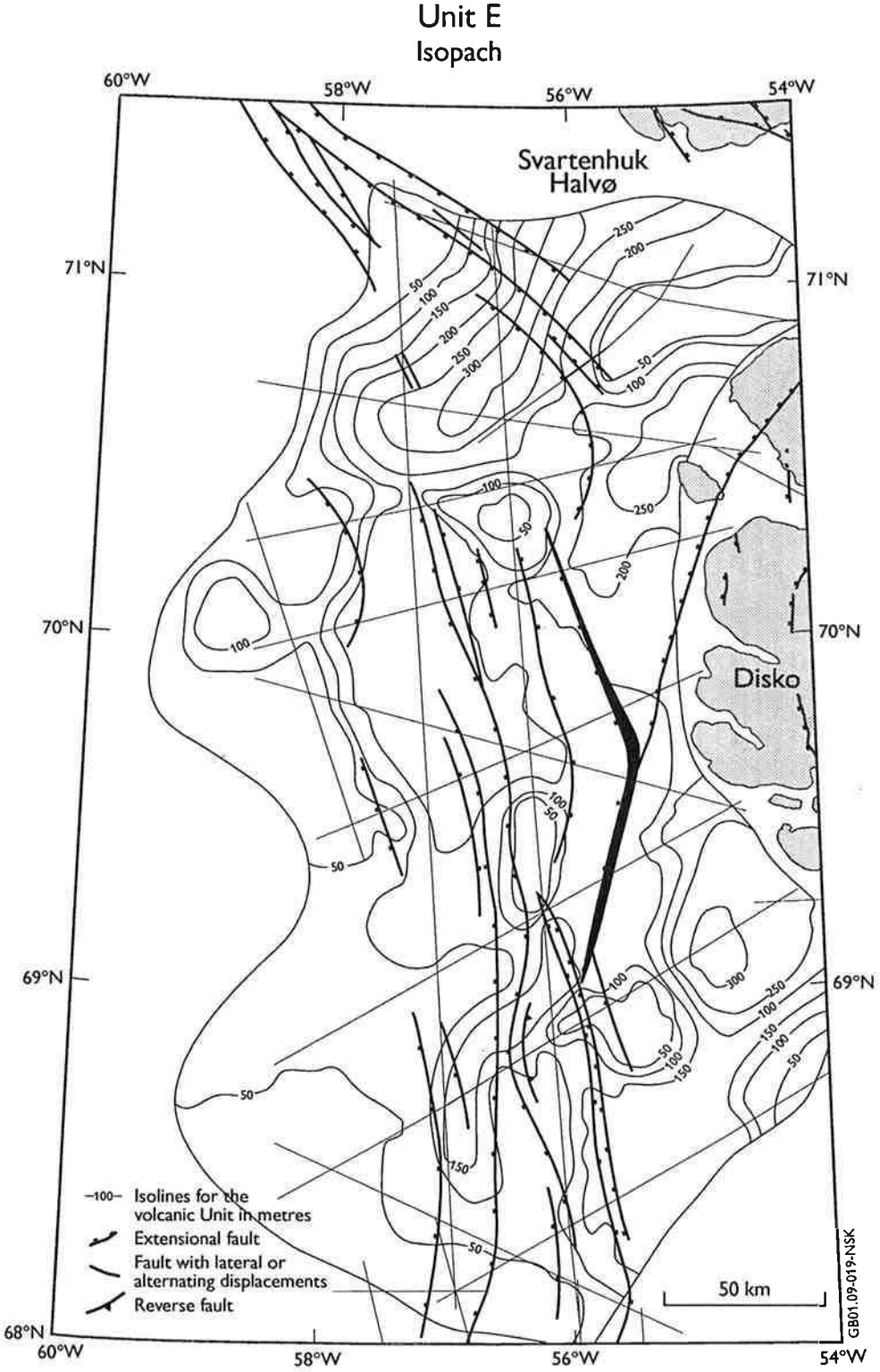

Appendix 13: Isopach map of seismic unit E. Unit E is interpreted in most of the studied area, and occurs in af layer of 250–4800 m. The base of Unit E is derived from the gravity modelling.

Paper 1

A possible new hydrocarbon play, offshore West Greenland

Geology of Greenland Survey Bulletin, 180, 28-30

Nina Skaarup & James A. Chalmers

A possible new hydrocarbon play, offshore central West Greenland

Nina Skaarup and James A. Chalmers

The discovery of extensive seeps of crude oil onshore central West Greenland (Christiansen *et al.* 1992, 1994, 1995, 1996, 1997, 1998, this volume; Christiansen 1993) means that the central West Greenland area is now prospective for hydrocarbons in its own right. Analysis of the oils (Bojesen-Koefoed *et al.* in press) shows that their source rocks are probably nearby and, because the oils are found within the Lower Tertiary basalts, the source rocks must be below the basalts. It is therefore possible that in the offshore area oil could have migrated through the basalts and be trapped in overlying sediments.

In the offshore area to the west of Disko and Nuussuaq (Fig. 1), Whittaker (1995, 1996) interpreted a few multichannel seismic lines acquired in 1990, together with some seismic data acquired by industry in the 1970s. He described a number of large rotated fault-blocks containing structural closures at top basalt level that could indicate leads capable of trapping hydrocarbons. In order to investigate Whittaker's (1995, 1996) interpretation, in 1995 the Geological Survey of Greenland acquired 1960 km new multichannel seismic data (Fig. 1) using funds provided by the Government of Greenland, Minerals Office (*now* Bureau of Minerals and Petroleum) and the Danish State through the Mineral Resources Administration for Greenland. The data were acquired using the Danish Naval vessel *Thetis* which had been adapted to accommodate seismic equipment.

The data acquired in 1995 have been integrated with the older data and an interpretation has been carried out of the structure of the top basalt reflection. This work shows a fault pattern in general agreement with that of

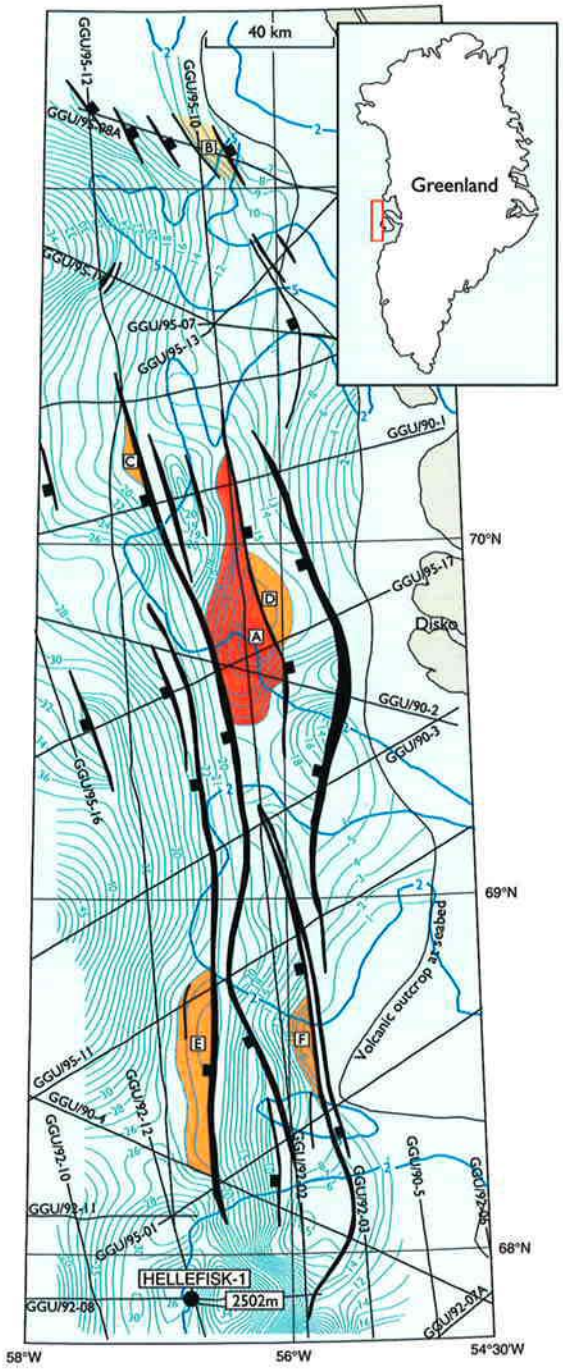

Fig. 1. Location map of the studied area showing the seismic lines, the five structural closures (structures A and C–F) and an additional lead (structure B), with structure A as the most prominent. Water depth shown by blue lines (only 200 and 500 m) and depth to top of the basalts by green lines (in hundreds of metres). The depth to the top of the Tertiary basalts at the Hellefisk-1 well is marked. Ticks on downthrow side of faults.

Geology of Greenland Survey Bulletin 180, 28–30 (1998)

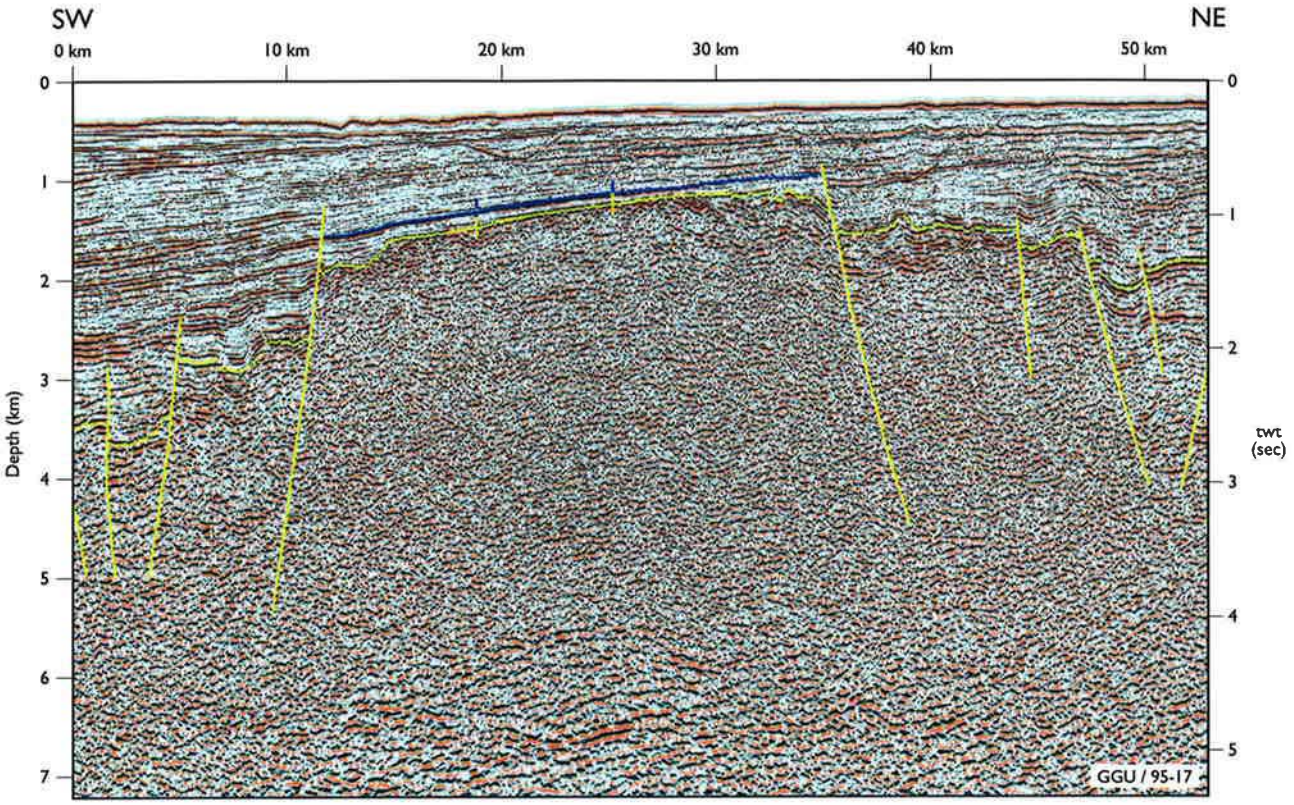

Fig. 2. Seismic section GGU/95-17 showing structure A as the horst block at top basalt level (yellow marker) bounded by faults to its east and west. Above the structure the 'bright spot' (blue marker) is shown. The post-basaltic sediments are seen to onlap structure A, indicating that deposition was controlled by topography. Below the centre of the structure some reflections are seen which are interpreted to be the base of the basaltic section. At depths of 5.5 km and 6.5 km strong reflections are seen which are tentatively interpreted to be from pre-basaltic sediments.

Whittaker (1995, 1996), although there are differences in detail. In particular the largest structural closure reported by Whittaker (1995) has not been confirmed. Furthermore, one of Whittaker's (1995) smaller leads seems to be larger than he had interpreted and may be associated with a DHI (direct hydrocarbon indicator) in the form of a 'bright spot'.

Interpretation

The seismic data used in this study were interpreted on a Sun work-station using Landmark SeisWorks-2D software.

The succession has been divided into intervals of different seismic character. The uppermost interval is present in most of the studied area, except east of 55°W where stratigraphically lower units crop out at seabed (Fig. 1). The uppermost unit is interpreted as sediments that can be tied to the Tertiary sediments in the Hellefisk-1 well (Rolle 1985). Throughout the study area the sediments lap onto top basalt level and indicate that the sedimentation was controlled by topographic structures (Fig. 2).

The top of the basalt unit is, except for the seabed, the most prominent reflector in the study area, and can also be tied to the Hellefisk-1 well (Rolle 1985). In many places reflections are visible from below the top of the basalts probably indicating that there are different seismic facies within the basalts and that sedimentary units may be found below the basalts. Work is continuing to determine the geological significance of the deeper, pre-top basalt reflections as well as the position of the base of the basalts.

Structure of the top basalt reflection

Whittaker (1995, 1996) showed that the top of the basalts is dissected by a complex system of steep, roughly N–S trending faults between 55°30′W and 57°W, south of 70°30′N. He suggested that this fault system consists of strike-slip faults related to oblique sea-floor spreading in Baffin Bay. The new data confirm Whittaker's (1995, 1996) interpretation in general terms. Steep faults with throws in places in excess of 1 km can be followed from seismic line to seismic line throughout most of the area

(Fig. 1). The faults define rotated blocks, and grabens have developed between the major faults. Complex minor faulting is commonly found within the grabens.

Farther north, the fault system shows a more NW–SE trend (Fig. 1). The coverage by 1990s data is very sparse in this area, but the older data used by Whittaker (1995, 1996) clearly shows this trend.

Prospectivity

Several structural closures at the top basalt level are shown on Figure 1 (structures A and C–F) and an additional lead (structure B) is indicated on the seismic lines.

The most promising structure, structure A, is situated west of Disko (Fig. 1). Structure A is bounded by faults to its east and west and closed by structural dip to the north and south. Figure 2 shows part of seismic line GGU/95-17 on which structure A can be seen as the horst block at top basalt level. Structural closure is mapped at about 1500 m depth and the shallowest part of the horst is at less than 1000 m depth. The structure is covered by 800–1300 m of sediments and approximately 200 m of water.

Above structure A a horizon within the sediments exhibits increased reflectivity (a 'bright spot'; Fig. 2) that approximately coincides with the structural closure mapped at top basalt level. The bright spot is seen on four seismic lines (Fig. 1) and is situated at a depth between 1000 and 1300 m below sea level, dipping from east to west. The bright spot has an extent of approximately 55 km in the N–S direction and from 7 to 23 km in the E–W direction, which gives an area of approximately 1000 km^2, so it could indicate the presence of large quantities of hydrocarbon. Preliminary results from an AVO (Amplitude Versus Offset) study on the bright spot on two seismic lines indicate that it is a Type 3 AVO anomaly in the sense of Castagna & Swan (1997), a typical gas-sand overlain by shale.

Several other small closures have been mapped and are shown and labelled on Figure 1. Whittaker (1995, 1996) mapped a large closure around the location of structure C in an area of sparse data coverage. Unfortunately the new data do not confirm Whittaker's (1995, 1996) mapping. Structure B can be seen on two seismic lines. However the structure is at the northern limit of seismic coverage, and there are no data to define its limits to the north. It is therefore unclear whether structure B is closed. All of these structures apart from B, are on the downthrown sides of faults, so their trapping potential is uncertain.

References

Bojesen-Koefoed, J.A., Christiansen, F.G., Nytoft, H.P. & Pedersen, A.K. in press: Oil seepage onshore West Greenland: evidence of multiple source rocks and oil mixing. In: Fleet, A.S. & Boldy, S. (eds): Petroleum geology of Northwest Europe. Proceedings of the 5th conference. London: Geological Society.

Castagna, J.P. & Swan, H.W. 1997: Principles of AVO crossplotting. Leading Edge **16**, 337–342.

Christiansen, F.G. 1993: Disko Bugt Project 1992, West Greenland. Rapport Grønlands Geologiske Undersøgelse **159**, 47–52.

Christiansen, F.G., Dam, G., McIntyre, D.J., Nøhr-Hansen, H., Pedersen, G.K. & Sønderholm, M. 1992: Renewed petroleum geological studies onshore West Greenland. Rapport Grønlands Geologiske Undersøgelse **155**, 31–35.

Christiansen, F.G., Dam, G. & Pedersen, A.K. 1994: Discovery of live oil at Marraat, Nuussuaq: field work, drilling and logging. Rapport Grønlands Geologiske Undersøgelse **160**, 57–63.

Christiansen, F.G., Marcussen, C. & Chalmers, J.A. 1995: Geophysical and petroleum geological activities in the Nuussuaq – Svartenhuk Halvø area 1994: promising results for an onshore exploration potential. Rapport Grønlands Geologiske Undersøgelse **165**, 32–41.

Christiansen, F.G., Bate, K.J., Dam, G., Marcussen, C. & Pulvertaft, T.C.R. 1996: Continued geophysical and petroleum geological activities in West Greenland in 1995 and the start of onshore exploration. Bulletin Grønlands Geologiske Undersøgelse **172**, 15–21.

Christiansen, F.G., Boesen, A., Dalhoff, F., Pedersen, A.K., Pedersen, G.K., Riisager, P. & Zinck-Jørgensen, K. 1997: Petroleum geological activities onshore West Greenland in 1996, and drilling of a deep exploration well. Geology of Greenland Survey Bulletin **176**, 17–23.

Christiansen, F.G., Boesen, A., Bojesen-Koefoed, J.A., Dalhoff, F., Dam, G., Neuhoff, P.S., Pedersen, A.K., Pedersen, G.K., Stannius, L.S. & Zinck-Jørgensen, K. 1998: Petroleum geological activities onshore West Greenland in 1997. Geology of Greenland Survey Bulletin **180**, 10–17 (this volume).

Rolle, F. 1985: Late Cretaceous – Tertiary sediments offshore central West Greenland: lithostratigraphy, sedimentary evolution and petroleum potential. Canadian Journal of Earth Sciences **22**, 1001–1019.

Whittaker, R.C. 1995: A preliminary assessment of the structure, basin development and petroleum potential offshore central West Greenland. Open File Series Grønlands Geologiske Undersøgelse **95/9**, 33 pp.

Whittaker, R.C. 1996: A preliminary seismic interpretation of an area with extensive Tertiary basalts offshore central West Greenland. Bulletin Grønlands Geologiske Undersøgelse **172**, 28–31.

Authors' address:

Geological Survey of Denmark and Greenland, Thoravej 8, DK-2400 Copenhagen NV, Denmark.

Paper 2

An AVO study of a possible new hydrocarbon play, offshore central West Greenland

AAPG Bulletin, 84, 174-182

Nina Skaarup, James A. Chalmers & Dave J. White

An AVO Study of a Possible New Hydrocarbon Play, Offshore Central West Greenland[1]

Nina Skaarup,[2] James A. Chalmers,[2] and Dave White[3]

ABSTRACT

Since 1992, extensive oil seeps have been discovered in Cretaceous sediment and Paleogene basalt onshore central West Greenland. Offshore, the basalts are buried under younger sediments. Interpretation of seismic data offshore has shown the presence of a closed structure at top basalt level. Within the sediments above the closed structure can be seen bright reflections that have strong AVO (amplitude variation with offset) anomalies. These features may indicate the presence of hydrocarbons that have migrated through the basalts from deeper source rocks and been trapped in the sediments above the basalts.

INTRODUCTION

The discovery of extensive crude oil seeps in Paleogene basalts and Cretaceous sediments onshore central West Greenland (Christiansen, 1993; Christiansen et al., 1992, 1994, 1995, 1996, 1997, 1998) means that the central West Greenland area may contain hydrocarbons. Analysis of the oils (Bojesen-Koefoed et al., 1999) shows that they come from at least five source rocks that are probably situated near the seeps. The source rocks are probably of Mesozoic and possibly earliest Paleogene age and must be situated below the basalts; therefore, in the offshore area to the west, oil may have been generated in source rocks below the basalts and may have migrated through the basalts to be trapped in overlying sediments.

Whittaker (1995, 1996) made a preliminary interpretation of the area offshore west of Disko and Nuussuaq (Figure 1), using four multichannel seismic lines acquired by the Geological Survey of Greenland (GGU) in 1990 and poorer quality seismic data acquired by industry in the 1970s. Whittaker (1995, 1996) described several large rotated fault blocks containing structural closures at top basalt level that could indicate leads capable of trapping hydrocarbons.

To investigate Whittaker's (1995, 1996) interpretation, 1960 km of new multichannel seismic data was acquired in 1995 by the new Geological Survey of Denmark and Greenland (GEUS), using the Danish Naval vessel *Thetis* (Christiansen et al., 1996).

The structure of the top basalt reflection has been interpreted using the 1995 lines integrated with the older data (Skaarup and Chalmers, 1998). The results show a fault pattern in general agreement with Whittaker (1995, 1996), although some of the larger structural closures suggested by Whittaker (1995) have not been confirmed; however, one of Whittaker's (1995) smaller leads is now interpreted to have a large area. The lead also appears to be associated with a direct hydrocarbon indicator (DHI) in the form of a bright spot, which shows a strong anomalous AVO (amplitude variation with offset) effect, probably indicating the presence of hydrocarbons.

REGIONAL GEOLOGY

The most extensive outcrops of Mesozoic-Tertiary rocks in the entire Labrador Sea-Davis Strait-Baffin Bay region occur in the Disko-Nuussuaq-Svartenhuk area of central West Greenland. The exposed rocks are fluvio-deltaic and marine sediments of Albian-early Paleocene age that are overlain by extensive middle-late Paleocene hyaloclastic breccias and continental flood basalts. The Mesozoic-Paleocene depositional area onshore is referred to as the Nuussuaq basin. This basin belongs to a complex of sedimentary basins, which were established in the Early Cretaceous, if not earlier, and extend from Melville Bay in the north (Whittaker et al., 1997) to

[1]Manuscript received July 29, 1998; revised manuscript received March 12, 1999; final acceptance July 9, 1999.

[2]Geological Survey of Denmark and Greenland, Thoravej 8, DK-2800 Copenhagen NV, Denmark; e-mail: nsk@geus.dk

[3]Robertson Research International Ltd., Horizon House, Azalea Drive, Swanley, Kent BR8 8JR, England.

Funds for acquisition and processing of the seismic data were provided in 1990 by the Mineral Resources Administration for Greenland and in 1995 by the Government of Greenland, Bureau of Minerals and Petroleum and the Danish State through the Mineral Resources Administration for Greenland. The Mineral Resources Administration for Greenland also provided funding for the AVO study. This paper is published with permission of the Geological Survey of Denmark and Greenland.

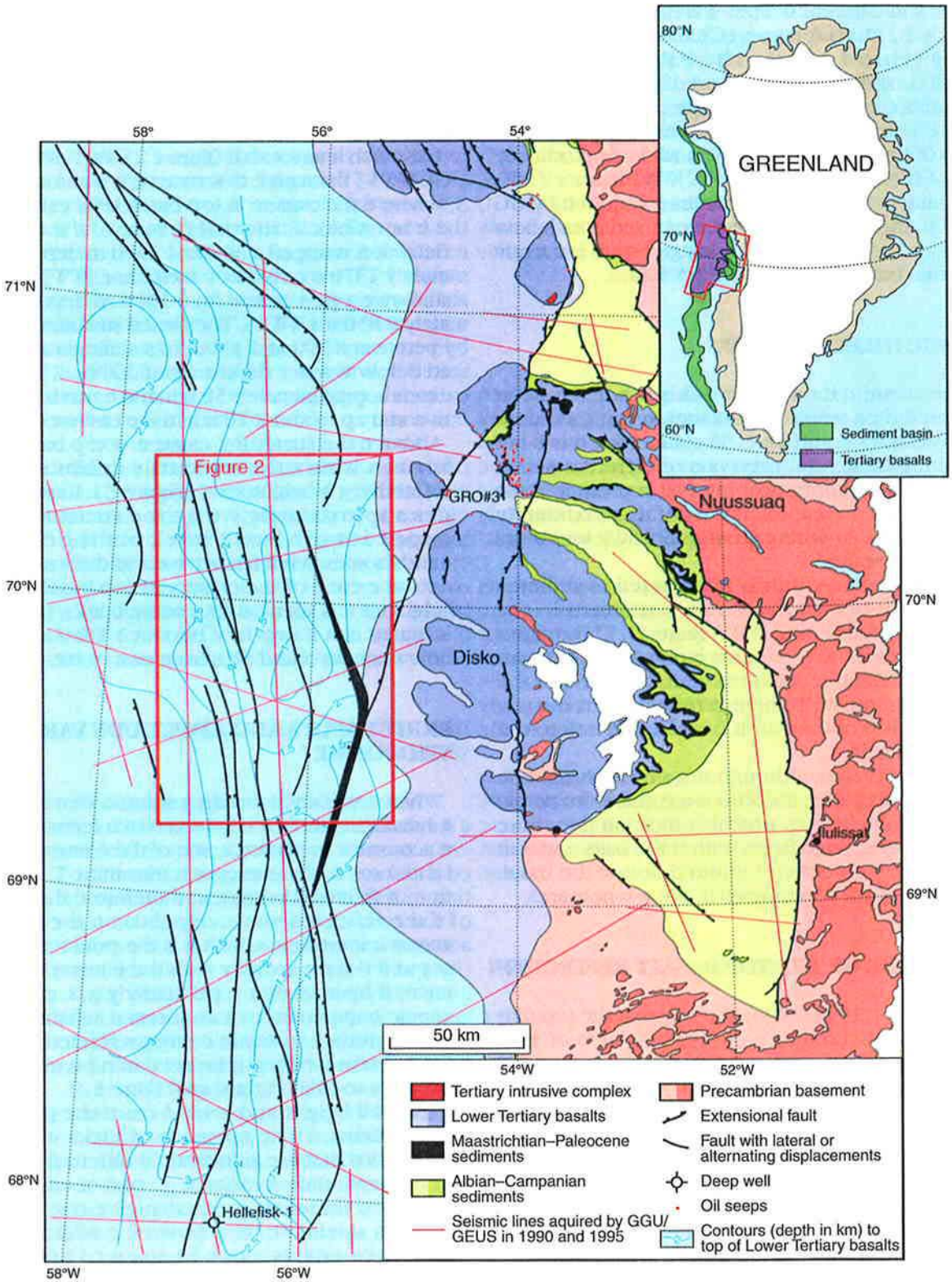

Figure 1—Central West Greenland, showing outcrop geology east of approximately 55°W and depth in kilometers to the top of the Paleogene basalts west of approximately 55°W. The seismic lines acquired by GGU/GEUS in 1990 and 1995, the Hellefisk-1 and GRO#3 wells, and oil seeps onshore are also marked. The inset map shows the location of the main map with respect to the Paleogene basalts and deep sedimentary basins offshore and onshore West Greenland.

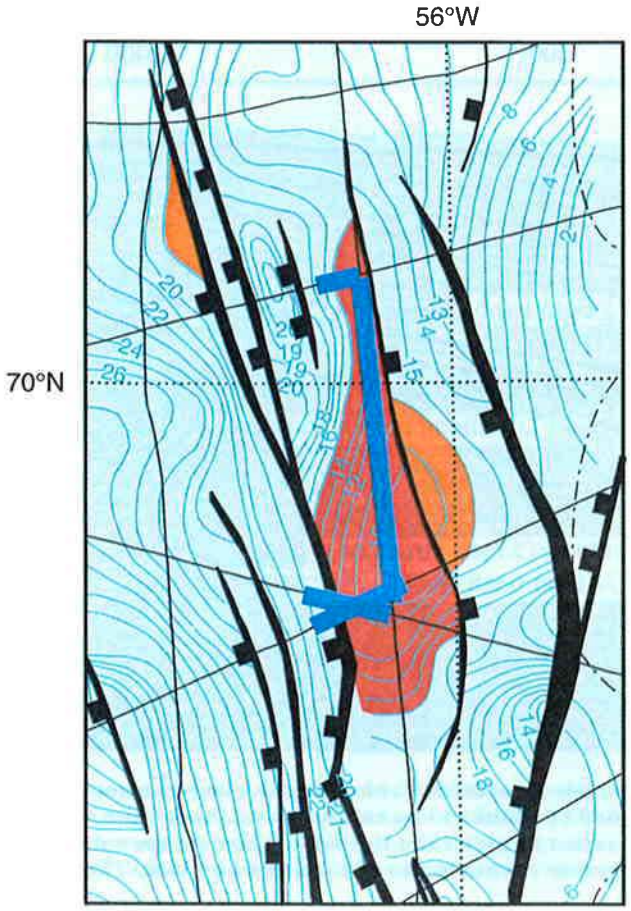

Figure 2—Detailed map of depths in hundreds of meters to the top of the Paleogene basalts. The major closed structure shown in Figures 3, 5, 6, and 7 is highlighted in red and other smaller closures are indicated in orange. The extent along the seismic lines of the bright spot/AVO anomaly discussed in the text is shown in dark blue.

between shot and receiver (offset). The technique has been found to be useful in the direct detection of hydrocarbons on seismic data.

At a subsurface interface between two intervals with different acoustic impedances, the reflection coefficient for impinging seismic waves varies as the square of the sine of the angle of incidence for small angles of incidence and small variation in seismic impedance (Shuey, 1985). The gradient (B) of the $\sin^2\theta$ term contains the Poisson's ratio contrast as a factor. This latter variation gives an anomalous AVO response when the Poisson's ratio contrast is anomalous, as may occur when free gas is present in the pore space. From a plot of reflection amplitude against $\sin^2\theta$, the amplitude at zero offset (A) (which is ideally equivalent to the true zero-offset data that would be recorded for a given common depth point if it were possible to have a coincident source and receiver) and the gradient (B) can be derived. In data from brine-saturated rocks, there is commonly a linear relationship between A and B that may pass through the origin (Castagna and Swan, 1997). Deviations from this trend on a crossplot of A and B may indicate the presence of hydrocarbons.

Rutherford and Williams (1989) grouped the AVO response from clastic sediments into three classes. Castagna and Swan (1997) enlarged the classification to four groups by separating Rutherford and Williams's (1989) class III into two classes, class III and class IV. Each class is defined by where in the A vs. B plot the points fall.

- Class I has positive A and negative B, indicating a relatively high impedance interval whose reflection coefficient decreases with offset, which is common behavior for a clean water-wet sand in shales of lower acoustic impedance.
- Class II has a near-zero A and near-zero or negative B, indicating a unit whose acoustic impedance is similar to the surrounding units, but (if B is strongly negative) whose Poisson ratio is different, a possible indication of hydrocarbons.
- Class III has negative A and B, indicating a low impedance unit with a decreasing (i.e., increasing negative) reflection coefficient with offset, commonly a characteristic of gas sands.
- Class IV has a low A but positive B, indicating a low impedance sand with an increasing (i.e., decreasing negative) magnitude of the reflection coefficient with offset.

AVO RESPONSE OF THE BRIGHT SPOT WEST OF DISKO

We have made an AVO study of the bright spot shown in Figure 3. An example of an AVO crossplot from line GGU/95-17 (shot points SP 2745.5–2755) is shown in Figure 4. Different symbols are used to show the points derived from the three intervals 852–952 ms for the postbasaltic sediments, 952–1052 ms for the bright-spot interval, and 1052–1152 ms for the top basalt surface. A least-squares fit through the points from the postbasalt sediments should give the water-wet clastic rocks trend (Castagna and Swan, 1997). The bright-spot interval plots partly in the upper left and partly in the upper and lower right quadrants of Figure 4, which suggests that the bright spot can be classified as a class IV AVO anomaly. Class IV indicates a low-impedance unit whose reflection coefficient becomes less negative with increasing angle of incidence. The top basalt surface interval also plots in the upper left and upper right quadrant of the diagram. The basalts should have a higher P-wave velocity and a higher acoustic impedance than the overlying sediments, so the top basalt should plot in the lower right quadrant and not in the upper left as

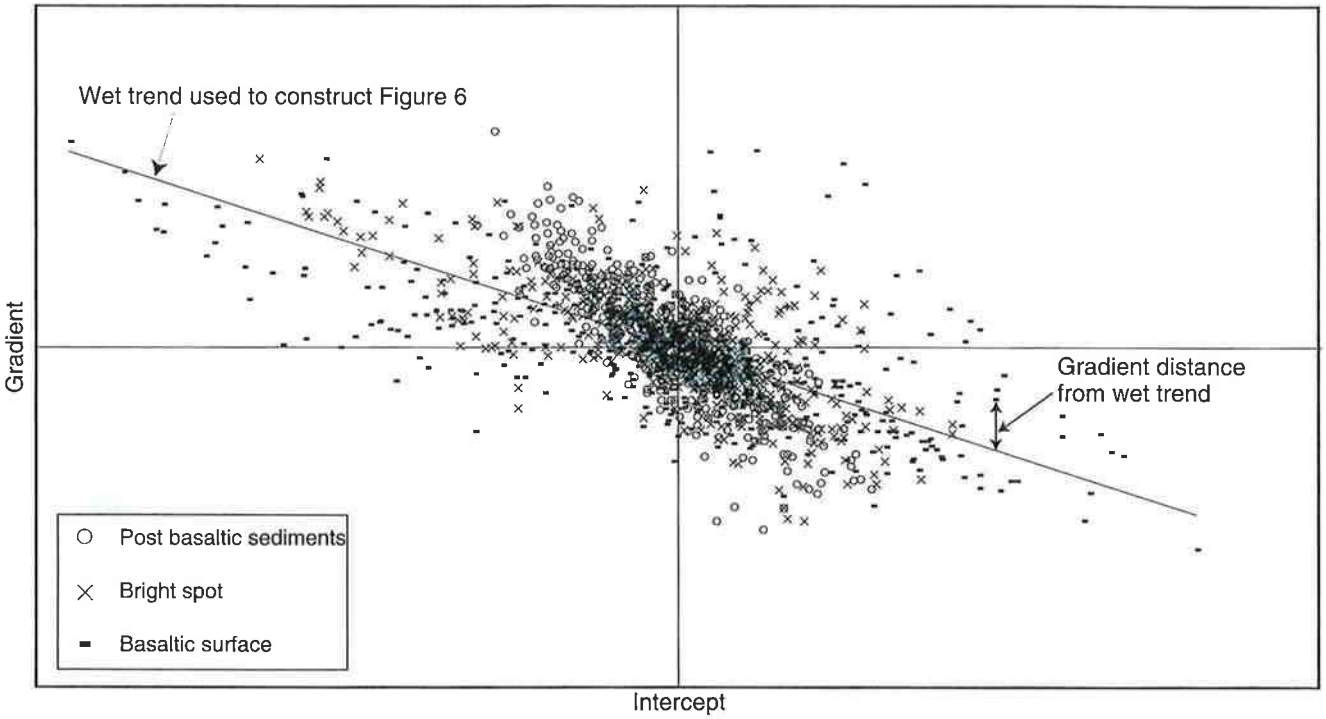

Figure 4—Amplitude vs. gradient crossplot from seismic line GGU/95-17, shot points 2745.5–2755. The wet-trend line used to construct Figure 6 is shown and also indicated is how the distance from the wet trend was measured. A plot of distance from the wet trend for line GGU/95-17 across the prospect is shown in Figure 6.

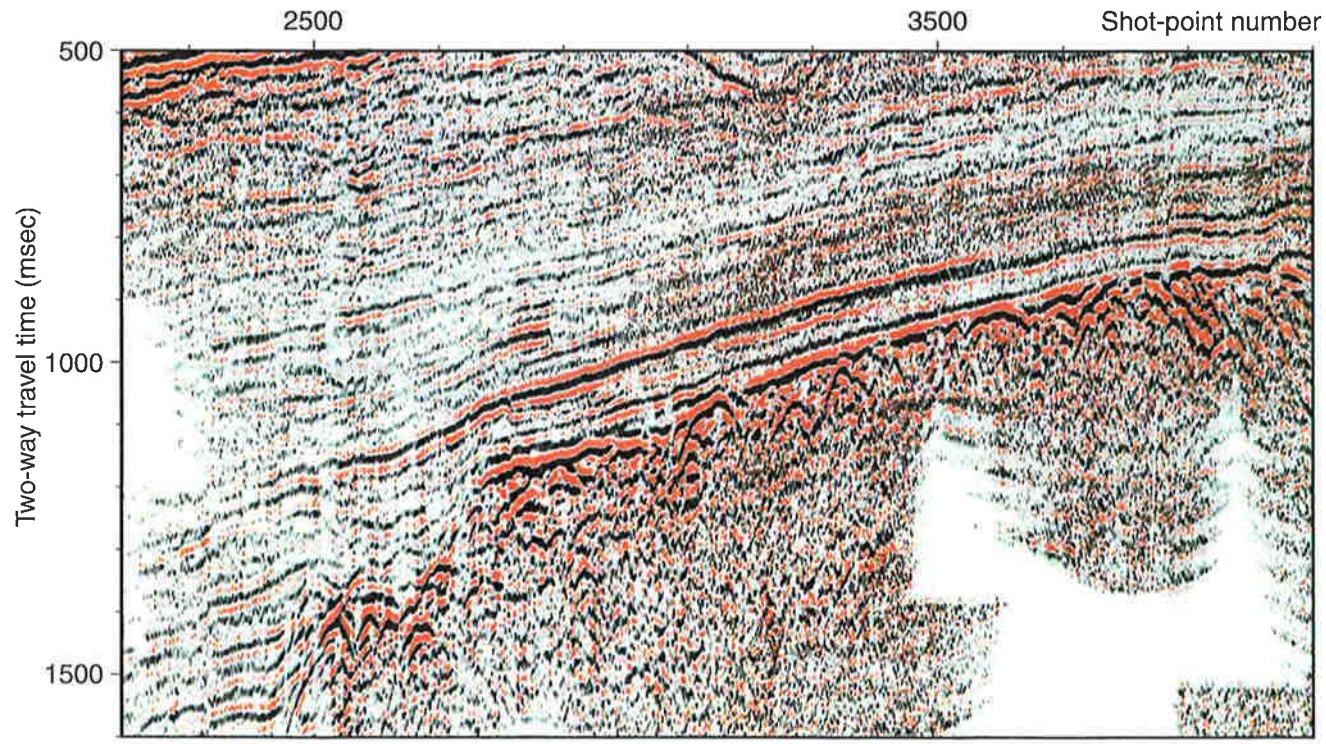

Figure 5—Stacked version of seismic line GGU/95-17 using only energy with angles of incidence greater than 27°. See text for discussion.

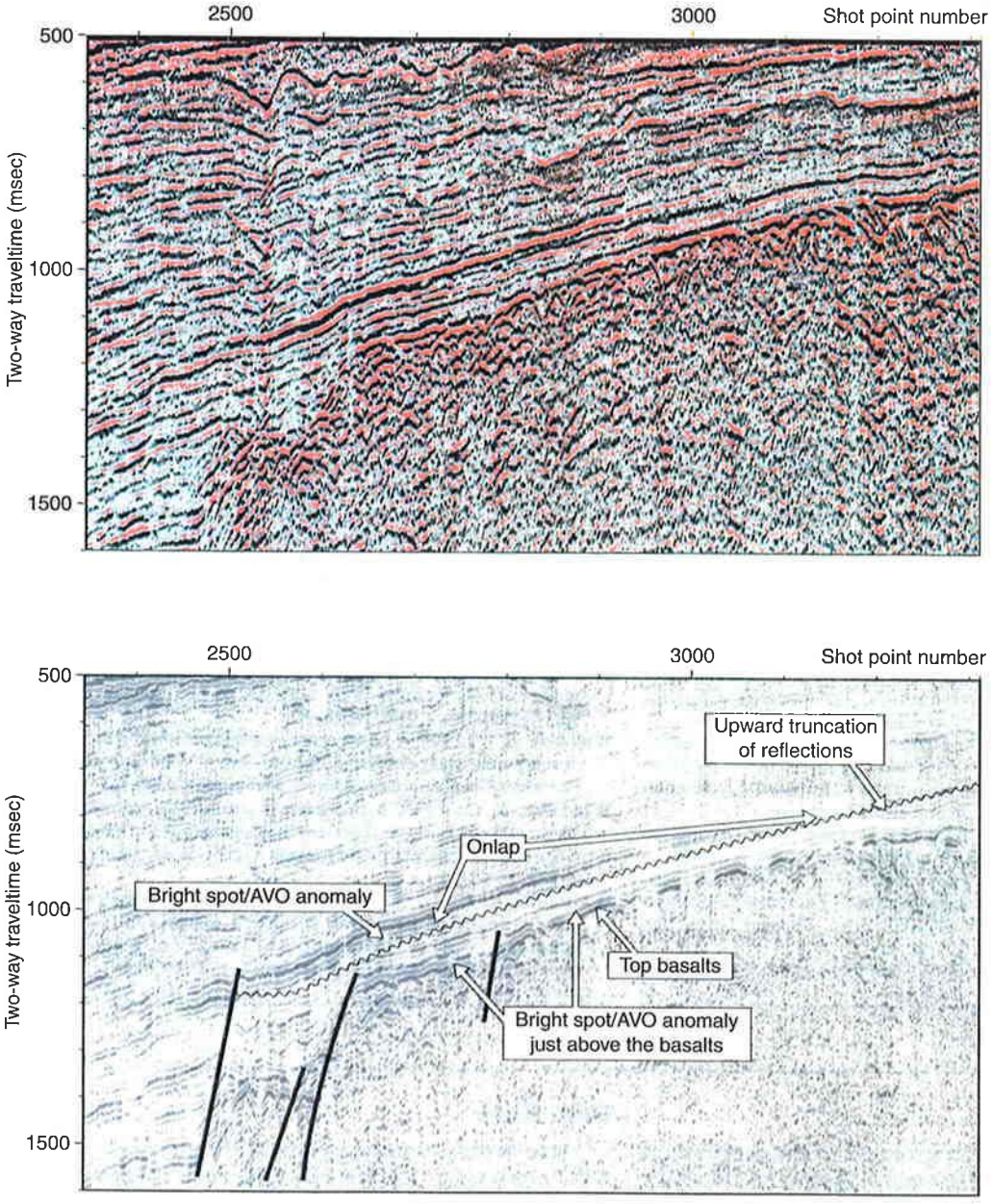

Figure 7—Zero offset stack version of seismic line GGU/95-17 showing uninterpreted and interpreted versions of the line. We interpret that the upper bright spot/AVO anomaly lies just above an unconformity that truncates underlying reflections. The lower AVO anomaly is the much smoother reflection immediately above the rougher reflection character from the basalts.

in the area offshore west of the oil seeps, oil or gas or both may have been generated in prebasaltic source rocks, migrated through the basalts, and are trapped in the sediments above the basalts. The bright spots and AVO anomalies discussed indicate strongly that this process may have occurred in at least one structure.

The sparse seismic coverage (seismic lines are typically 30–50 km apart) in the area make any quantitative estimates of hydrocarbons in place tentative. Conservative estimates for the areas of the two bright spots/AVO anomalies suggest that each might cover an area of 500 km^2. Each reflection also seems to come from a sand that is less than one wavelength in thickness, so reservoir thicknesses of between 12.5 m (minimum) and 50 m (maximum) are not unreasonable. Guesses of 50% for net reservoir rock to gross rock volume and 20% for porosity lead to total pore volume estimates on the order of 1.25 to 5 billion m^3. If the entire pore space were filled with oil and the water saturation were 30%, this would indicate oil-in-place figures as large as 5–30 billion bbl. If the entire pore space were filled with gas, corresponding figures would be 3 to 15 tcf.

The numbers quoted in the previous paragraph should be regarded as order of magnitude estimates only; however, even if the structure is much less continuous than the present data indicate and are only one-tenth the amount of hydrocarbons in place, the data presented here indicate the presence of an attractive hydrocarbon accumulation.

Paper 3

Seismic stratigraphy of Palaeogene volcanic rocks, offshore central West Greenland

To be submitted to Journal of the Geological Society

Nina Skaarup

Seismic stratigraphy and structure of Palaeogene volcanic rocks, offshore central West Greenland

NINA SKAARUP
Geological Survey of Denmark and Greenland
Thoravej 8, DK-2400 Copenhagen NV, Denmark

To be submitted to Journal of the Geological Society, London

Abstract: The Palaeogene volcanic province in central West Greenland extends 550 km in a north-south direction and 200 km east-west. From onshore exposure at 2 km above sea level to depths of 9 km for the deepest interpreted volcanic rocks offshore. The volcanic rocks offshore crop out at seabed in the nearshore area, from where they dip west and are covered by a wedge of Eocene and younger sediments. The structure at top volcanic level is dominated by elongate, steep N–S trending normal faults, which define horsts and grabens containing complex minor faulting. By combining the interpretation of the seismic data and modelling of gravity data, the possibility of the presence of oceanic crust in the volcanic offshore area has been tested and found to be inconsistent with the observed gravity field, whereas the presence of continental crust, where sediments are present below the volcanic section has been seen to fit the modelling. In the uppermost part of the offshore volcanic rocks, flow directions can be interpreted and appear to diverge to the east and west along a curved N–S trending line, indicating the presence of an eruption zone in the offshore area. A correlation between onshore datings of volcanic rocks, a new date from an offshore well, and the interpretation of seismic units, suggests that the main part of the volcanic rocks in the offshore area were erupted during C26r and earlier. A continent-ocean boundary, recognized by such diagnostic features as seaward-dipping reflector sequences cannot be interpreted directly from the seismic data. The margin west of Disko is thought to be a transform margin, which could account for the lack of seaward-dipping reflector sequences that have been interpreted mostly from extensional margins.

Keywords: West Greenland, volcanic rocks, seismic interpretation, gravity modelling, continent-ocean boundary.

The central West Greenland volcanic province extends 550 km in a north–south direction and 200 km east–west, covering 110 000 km^2 (Fig. 1, inset) (Henderson 1973; Henderson 1981; Whittaker 1996). The volcanic rocks offshore crop out at seabed in the near-shore area, from where they dip west; farther west they are covered by a wedge of Eocene and younger sediments. Whittaker (1995) used seismic reflection data to make a preliminary interpretation of the area offshore Disko and Nuussuaq (Fig. 1).

In 1992, crude oil was discovered in vesicles, vugs and fractures in the lower part of the volcanic succession over a wide area onshore (Christiansen 1993; Christiansen *et al.* 1994; Christiansen *et al.* 1995; Christiansen *et al.* 1996; Christiansen *et al.* 1998). Analyses of the oils show that these were derived from source rocks in the underlying Cretaceous and lower Paleocene sediments (Bojesen-Koefoed *et al.* 1999).

In 1995, the Geological Survey of Denmark and Greenland (GEUS) acquired 1960 km of new multi-channel seismic data to investigate the possibilities for oil exploration offshore. Skaarup *et al.* (2000) integrated these data with the older data interpreted by Whittaker, and carried out an interpretation of the structure at the top volcanic level (Fig. 1). This interpretation indicated a fault pattern in general agreement with Whittaker's preliminary pattern, although some differences were discovered.

Geoffroy *et al.* (1998) proposed that the coastal flexure of the basalt succession observed onshore Disko represents onshore exposure of seaward-dipping reflector sequences. In the discussion on this paper (Chalmers *et al.* 1999b) Geoffroy and his colleagues suggested that the continent-ocean boundary west of Disko is a major continent-ward-dipping fault and that the coastal flexure onshore Disko dips into another continent-ward-dipping listric fault lying closer to the coast. According to Geoffroy *et al.* (1998) the basalts form syntectonic fans dipping into these faults. Geoffroy *et al.* (2001) propose that seaward-dipping reflector sequences have not hitherto been recognized in the offshore section because the reflection from the top of the basalts is too strong. These propositions will be examined in discussion in the present paper.

Data

The main part of this work has been carried out on 23 multi-channel reflection seismic lines from two different surveys (Table 1): 4 seismic lines acquired by the Geological Survey of

Greenland (GGU) in 1990 and 19 seismic lines acquired in 1995 by the Geological Survey of Denmark and Greenland (GEUS). The spacing of the grid of seismic lines varies between 20 km and 50 km. To the north, older seismic data from the 1970's have been used to control interpretation of the top volcanic structures, and to the south, seismic data from the 1970's and 1992 have been used to establish a tie to the Hellefisk-1 well to improve control of the volcanic surface and the top volcanic structures.

Gravity data were acquired during the GEUS 1995 seismic cruise using a La Coste and Romberg gravity meter and processed to yield free-air data by the Danish National Survey and Cadastre (KMS). Additional onshore data from KMS and GGU have been terrain-corrected and converted to Bouguer anomalies and amalgamated with the free-air anomaly data offshore to form a single data set.

The magnetic data were compiled from various marine and aeromagnetic surveys by the Geological Survey of Canada and gridded to a final grid resolution of 2 km (Oakey *et al.* in press).

Summary of the offshore and onshore geology of the West Greenland volcanic province

The regional setting of the Davis Strait area is the consequence of the separation of the North American and Greenland plates. The separation may have started in Early Cretaceous with an initial period of stretching. There was a second period of tectonism in the latest Cretaceous and early Paleocene, prior to the onset of sea-floor spreading in the mid-Paleocene (Chalmers & Pulvertaft in press). During early sea-floor spreading, extensive volcanism occurred in the Davis Strait region, that is exposed in central West Greenland to the east and on Baffin Island to the west (Clarke & Pedersen 1976; Clarke & Upton 1971). Along the southern West Greenland and Labrador margins, south of the volcanic area, a transition zone consisting of highly-stretched continental crust and serpentinized peridotite, is interpreted to separate continental and oceanic crust, whereas along the southeast Baffin Island margin the continent-ocean boundary seems to be a complex transform zone which developed during sea-floor spreading in the late Paleocene and early Eocene (Chalmers & Pulvertaft in press). The ca. N–S faults seen offshore in the West Greenland volcanic province (Fig. 1) may be the northwards continuation or splays from this transform zone (Chalmers *et al.* 1993; Chalmers *et al.* 1999a). The offshore volcanic rocks in West Greenland reach south to 67°50´N and to about 59°W in the west before pinching

out, and are overlain by a succession of upper Palaeogene, Neogene and Quaternary sediments (Rolle 1985).

Onshore in the Disko–Nuussuaq area, extensive outcrops of Mesozoic-Palaeogene rocks occur. The rocks exposed are marine and non-marine sediments of Albian to early Paleocene age (Dam & Sønderholm 1994; Pedersen & Pulvertaft 1992) overlain by middle Paleocene and Eocene volcanic rocks (Clarke & Pedersen 1976; Storey *et al*, 1998). From an onshore reflection seismic line along the south coast of Nuussuaq (Fig. 1) it is known that the total thickness of sediments below the basalts is at least 6 km, 2700 m of which were penetrated by the GRO#3 exploration well (Chalmers *et al.* 1999a). The sediments belong to a complex of sedimentary basins extending from Melville Bay in the north (Whittaker *et al.* 1997) to around 62°N in the south (Chalmers *et al.* 1993) (Fig. 1, inset). The onshore volcanic rocks cover an area from 69°N in the south to 73°N in the north and from the coast in the west to the margin of the Inland Ice to the northwest where they lap onto the Precambrian basement.

The volcanic rocks onshore Nuussuaq and Disko are divided into the older Vaigat Formation and the younger Maligât Formation (Hald & Pedersen 1975; Pedersen 1985) (Fig. 2).

The Vaigat Formation is dominated by grey, olivine-rich, primitive rocks, but minor members consist of brownish-weathering aphyric or feldspar-phyric rocks, which are enriched in silica and may contain more or less digested sediment xenoliths (Pedersen 1979; Pedersen *et al.* 1996). The volcanism of the Vaigat Formation started from eruption centres in western Nuussuaq and consists of subaqueous mounds of pillow breccia and hyaloclastite and thin subaerial lava flows. Huge eastwards-prograding hyaloclastite fans with foreset heights up to 700 m and foreset dips of 15–27° were deposited in three separate cycles (Larsen & Pedersen 1988; Pedersen *et al.* 1993). The thickness of the Vaigat Formation varies between 0 and 1.5–2 km on Disko, 0–1.5 km on Nuussuaq, between 0 and >3 km on Svartenhuk, and more than 5 km on Ubekendt Ejland (Hald & Pedersen 1975).

The overlying Maligât Formation consists primarily of feldspar-phyric plateau basalts of subaerial origin. The formation is at least 1400 m thick and consists mainly of thick (10–100 m) massive lava flows of rather uniform appearance. Some of the distinctly subaerial lavas show red oxidised flow tops and are locally separated by up to 1 m reddish lateritized scoria (Larsen & Pedersen 1992).

At five coast localities on Disko, a detailed structural analysis of the Maligât Formation was described by Geoffroy *et al.* (1998). Tectonic analysis shows that NW–SE to N–S trending strike-slip and oblique-slip faults dip preferentially eastwards in relation to the westward dip of strata. The dominant strike-slip faulting episode predates the coastal flexure (Henderson 1973), and the eastward-dipping normal faults in the flexured areas are interpreted to have formed by tilting of an older set of initially-vertical strike-slip faults. The flexure is contemporaneous with dyke injection parallel to the axis of flexure and to an increase in the amount of extension across the area during the Paleocene, and Geoffroy *et al.* (1998) suggest that the coastal flexure is of both syn-magmatic and tectonic origin.

On Svartenhuk Halvø (Larsen & Pulvertaft 2000), the volcanic rocks are divided into the older Vaigat and the younger Svartenhuk Formations. The earliest eruptions on Svartenhuk happened in a water-filled basin with foreset heights of 250 m, but both subaerial lava flows and subaqueous hyaloclastites are present. The thickness of the Vaigat Formation increases from north to south in the range of 950 to 1100 m. The rocks of the Svartenhuk Formation are the stratigraphic equivalent of the rocks of the Maligât Formation on Nuussuaq and Disko and have a thickness of 2800 m as a minimum. In most places, the Svartenhuk Formation overlies the Vaigat Formation conformably without any obvious unconformity, but in a few places an angular unconformity can be seen between the two formations (Larsen & Pulvertaft 2000).

West of the Itilli fault on Nuussuaq, volcanic rocks of the Kanísut Member are found (Hald 1977). The member consists of 10–20 m thick tholeiitic lavas, with a few inter-basaltic sediment horizons, and has an exposed thickness of 2000 m. The Kanísut Member lavas dip 15–20° to between west and northwest (Henderson 1973) (Fig. 1).

Nine samples of the volcanic succession have been dated by Storey *et al.* (1998) using $^{40}Ar/^{39}Ar$ methods (Fig. 2). They found ages ranging from 60.4±0.5 Ma to 60.7±0.5 Ma for the Vaigat Formation, 60.5±0.4 Ma to 59.4±0.5 Ma for the Maligât Formation, 54.8 ±0.4 Ma for a dike and sill system on Nuussuaq, 53.6 ±0.3 Ma for West Disko dikes, and 52.5±0.2 Ma for the Kanísut Member on Nuussuaq. Geoffroy *et al.* (2001) dated five basaltic dikes on the south coast of Svartenhuk Halvø as 54.6 ±0.6 Ma. Riisager & Abrahamsen (1999) recorded the magnetic polarity transition C27n/C26r within the Vaigat Formation (Fig. 2), and Riisager *et al.* (1999) measured samples from the Kanísut Member to be reversely magnetized. According to the geomagnetic time-scale of Cande & Kent (1995), the sample of the Kanísut Member belongs to

the very lowermost part of the C23r period (Fig. 2). Besides the samples from the Vaigat and Maligât Formations and the dikes, two samples from intrusive rocks were dated. North of Nuussuaq on Ubekendt Ejland a lamprophyre dike was dated as 34.1±0.2 Ma, and west of Disko, an alkali basalt from a group of small skerries believed to be the remnant of volcanic necks, was dated as 27.4±0.6 Ma (Storey *et al.* 1998).

Seismic characteristics of the volcanic succession offshore

The reflection from the top of the volcanic rocks is the most prominent reflection on the seismic data, apart from the seabed reflection. The top volcanic reflection is normally seen as a single, sharp positive reflection, either as a flat surface or as an uneven surface over what may be small hyaloclastite mounds (Fig. 3). In places within the volcanic rocks, very distinct, parallel-bedded features can be seen (Fig. 4, sp. 7800–8000), which are abruptly interrupted by transparent areas that almost hide the seismic pattern. In Fig. 4, sections of very distinct prograding facies can be seen just below the top reflection.

A layered appearance is commonly seen in seismic profiles of subaerial lava successions. The impedance contrast required to produce strong reflections on the seismic data can be produced from the inter-bedding of basalts with sediments and tuffs, together with impedance contrasts within the flows themselves, and between the flows and their scoriaceous or vesicular upper parts (Planke 1994; Planke & Eldholm 1994). Another explanation for the layered appearance of subaerial lava successions could be a complex interference pattern between thin, closely-spaced volcanic flows (Barton & White 1997). Onshore central West Greenland, interbedded sediments and basalts, as well as alteration horizons on top of the volcanic flows are known (Larsen & Pedersen 1992), thus the layering observed in the basalts on the offshore seismic lines could easily be the offshore equivalent to the onshore layering. The minimum thickness of the features interpreted on the seismic records are of the order of one wavelength, i.e. 50 m, which is much less than the maximum height of the hyaloclastite foresets seen onshore, so we can expect that individual prograding volcanic facies can be interpreted on the seismic data. Fading of reflectivity of the deeper parts of the volcanic succession is a normal feature, and has been explained by large energy transmission losses due to the large impedance contrast between interbedded sediments and basalts (Pujol *et al.* 1989), and loss of continuity in the seismic signal may be caused by lateral variations in flow thickness, alteration, dykes and

interbedded sediments (Planke & Eldholm 1994). However, fading of reflection strength with depth is also seen in thick volcanic sections where no interbedded sediments are seen.

Because of the seismic properties of the volcanic rocks, most of the seismic energy is scattered or absorbed in the uppermost parts of the volcanic succession, which makes it almost impossible to interpret the deeper parts of the volcanic succession from the seismic data alone. In the present work an attempt to solve this problem has been made by combining the seismic data with gravity data in an integrated interpretation.

Seismic units

Six different seismic units can be recognized on the seismic records. The uppermost seismic unit corresponds with the post-volcanic sedimentary section, with clear parallel reflections and obvious channel features in places (Fig. 5, shot point (sp.) 4550). Below this, five seismic units have been interpreted as volcanic (Table 2). These are arranged in stratigraphic order from unit A, the uppermost, to unit E, the deepest, so that the description of the seismic units is also a description of stratigraphic units from the uppermost, the most distinct, to the deepest and least distinct.

In most places, the top surface of the volcanic section shows distinct mounds (Fig. 3, sp. 13800–14000) overlain by onlapping sediments, whereas in other places the top volcanic surface is clearly eroded (Fig. 4, sp. 8000–8400, and Fig. 6, sp. 12200–12600). The predominant seismic facies in the volcanic rocks is parallel to sub-parallel, with various degrees of downlap features and different degrees of reflectivity. These parallel-bedded units pass into more downlapping facies of both oblique and sigmoidal outline to almost chaotic hummocky clinoforms. Because of the transmission loss mentioned above, no base to the volcanic rocks can be interpreted from the seismic data alone. Rather, the lowermost seismic unit (unit E) is defined as that occurring between the lowermost interpretable volcanic marker horizon and the base of the volcanic rocks interpreted from the gravity modelling. The division of the volcanic rocks into seismic units is based on an interpretation of a combination of units of thick volcanic flows and 'interference' units formed by inter-fingering of smaller volcanic units with interbedded sediments and alteration horizons.

Seismic unit A. This is characterized by a very strong top reflection and a well-defined base with downlap surfaces (Fig. 7, sp. 800–1000). The internal pattern consists mostly of high-amplitude parallel to sub-parallel reflections with an individual spacing of 100–125 m. Seismic unit A is restricted to the northeastern part of the studied area (Fig. 8) and occurs in a rather thin layer of 100–400 m in most of the area.

The overall parallel-bedded pattern of seismic unit A with very strong reflections suggests a unit comparable with the flat-lying subaerial lava flows seen onshore. In the onshore Maligât Formation distinctly subaerial lavas show red oxidized flow tops and are separated by layers of laterite (Larsen & Pedersen 1992) which could give rise to the distinct layering seen in the offshore unit A.

Seismic unit B. This unit is characterized by a moderately strong top reflection (Fig. 7) when underlying unit A, but where it underlies sediments, the reflection from the top is very strong. In places the base is well-defined, with onlap surfaces (Fig. 9, sp. 4900-5100), while in other places the base just fades into the underlying unit. The internal facies pattern consists of low-amplitude to almost transparent, parallel to sub-parallel reflections. Seismic unit B has been interpreted over a large part of the studied area, except for the northwesternmost part (Fig. 10), and has a thickness ranging between 130–1000 m.

Unit B has an overall parallel to sub-parallel bedded pattern on the seismic lines similar to seismic unit A, but the reflections are weaker, and the very distinct layering that characterizes unit A is not seen. The onshore equivalent could be flat-lying subaerial lavas, without marked boundaries and laterite layers between the individual flows.

Seismic unit C. This unit is characterized by a very strong reflection from its top (Fig. 6), and in places its base is defined by downlap surfaces (Fig. 11, sp. 1200–1500). The internal facies pattern consists mostly of high-amplitude parallel to sub-parallel reflections, which in places pass into hummocky clinoforms. Unit C has been interpreted over a large part of the studied area, except for the northwestern part of the studied area (Fig. 12). It occurs in a layer 200–2200 m thick.

Besides a parallel-bedded pattern similar to that in the two overlying units, unit C also shows a transition from horizontal reflections into a clearly sigmoidal pattern in places. This could be a

transition from subaerial lava flows into subaqueous prograding hyaloclastites similar to those seen onshore along the south coast of Nuussuaq (Pedersen *et al.* 1993), formed by a single eruption. On the offshore section, the apparent dip of the foresets is 4–11°, whereas the foreset dips onshore Nuussuaq are somewhat steeper, 15–21°, but smaller dips are also seen.

Seismic unit D. This unit is characterized by a moderately strong to weak top reflection (Figs 3 and 6) when underlying one of the other volcanic units, whereas when underlying sediments the top reflection is very strong. The base is only sporadically defined by downlap surfaces. The internal facies pattern varies very much. In some places high-amplitude parallel to sub-parallel reflections pass into a clearly sigmoidal pattern (Fig. 4), whereas in other places the internal pattern consists of low-amplitude sub-parallel reflections, with smaller segments of downlapping events (Fig. 7). Seismic unit D is restricted to the northernmost part of the studied area (Fig. 13), and has a thickness ranging between 500-1500 m.

The alternating high and low-amplitude reflection pattern could be an effect of the considerable depth at which most of unit D is present. The transition from parallel-bedded to downlapping events has obvious onshore equivalents, as in unit C. The individual layers of both unit C and D (Fig. 6) have a thickness of 100 to 125 m per layer, which is comparable only with the thickest volcanic flows recognized onshore Nuussuaq. This indicates that the layering observed on the seismic data could be a seismic interference pattern rather than real reflections from thick lava flows.

Seismic unit E. This unit is characterized by a moderately strong top reflection when underlying other volcanic units (Figs 3 and 6), whereas when unit E underlies sediments (Fig. 4) the reflection from the top is very strong. The base of the unit is defined from modelling of gravity data. In Fig. 6, a very sharp, downlapping reflection can be seen to correspond to the base of the volcanic succession as defined by gravity modelling, but in most of the area nothing on the seismic data suggests a base to the volcanic rocks. The internal pattern of unit E consists mostly of a chaotic reflection pattern and is often indeterminable, but in some areas high-amplitude parallel to sub-parallel reflections can be seen (Fig. 6). Seismic unit E is present throughout the area (Fig. 14), and has a thickness ranging between 250–3000 m.

This seismic volcanic unit may show the difficulties that arise from poor penetration of seismic energy through the volcanic rocks, as illustrated by the chaotic low-amplitude reflection pattern

seen in most places. However, the chaotic pattern could also arise from submarine hyaloclastites erupted at the seafloor. Where better penetration is present the high-amplitude parallel to sub-parallel pattern, also recognized in the other units, could be interpreted as arising from subaerial lava flows.

Structures at top volcanic level

The volcanic area offshore is dominated by steep, N–S-striking, extensional faults with throws up to more than 1 km (Fig. 15). These faults can be followed throughout most of the area, with a more northwesterly trend in the northern part of the area (Fig. 1). The faults outline rotated fault blocks, and graben and horst structures have developed between the major faults. Complex minor faulting is commonly found within the grabens. This structural system, may be associated with transform strike-slip faults arising from sea-floor spreading in Labrador Sea and Baffin Bay (Chalmers *et al.* 1993). If so, it has the character of a typical transtensional area (Chalmers and Pulvertaft in press). This details of the pattern, with almost linear faults continuing for >100 km, could possibly arise from the fact that the seismic grid is very wide, and a tighter grid could quite likely reveal a more complex pattern.

Apart from the major large-scale structural features, several complex minor structures are recognized in the volcanic rocks. Eruption sites and basin infill structures are seen onshore in a variety of places and are features that could possibly be recognized on the offshore seismic data, but which could just as well be missed between the widely spaced grid.

South of 69°N and east of 56°W the area is dominated by steep, mainly extensional faults with large rotated fault blocks (Fig. 5). The throws have a magnitude of 100–700 m, and displacements reach far into the overlying sediments. The internal structures in the fault blocks are mostly dominated by parallel-bedded facies, indicating post-eruption tectonics. The existence of both normal and reverse faults (Fig. 16) could show that both transtensional and transpressional regimes have existed in the area, which supports the general model of major strike-slip movements in this area (Chalmers & Pulvertaft in press).

In the central area, west of Disko, several horst and graben structures can be followed north–south for 100 km. They are best developed in the central area, but die out to both north and south. 50 km west of Disko, a pronounced horst can be seen at top volcanic level. Seismic

reflections can be seen in the volcanic rocks in the fault blocks on the flanks of the structure, but within the horst itself nothing can be seen. The horst structures have their largest magnitude in the eastern part with throws as much as 1 km (Fig. 15), whereas the influence of the tectonic movements diminishes towards the west. Where internal patterns can be seen in the faulted blocks, they are mostly parallel to subparallel, indicating post-eruption movements. Both transtensional and transpressional forces could have been active in this area too.

South of 69°N the faulted blocks are rotated with minor drag of the volcanic rocks on the hanging walls of the faults in the eastern area, whereas to the west the volcanic rocks are only a little downfaulted with no drag on the faults (Fig. 16). This could indicate a fault system active for a longer period in the eastern part compared to the western part. Also here the internal pattern is mostly parallel-bedded, indicating post-eruption movements.

Northeast of 70°15´N, 56°30´W, a seaward-facing escarpment can be seen (Fig. 6). The escarpment can be traced for a distance of 120 km on four seismic lines (line GGU/95–10, –12, –14, and –15) and there is a fall of the top volcanic surface of 250–500 m. On both the N–S lines and the E–W line, seismic unit C is the uppermost volcanic unit with high-amplitude parallel-bedded reflections (Fig. 6). Immediately at the top of the escarpment, the top surface of the volcanic rocks shows some irregularities besides the small-scale mounded appearance. At the escarpment the reflections bend down and disappear. Seismic unit D, with its downlapping facies, continues below the escarpment.

An escarpment can define the border between former land and sea (e.g. Smythe *et al.* 1983), where one volcanic layer is erupted upon another, but with no tectonic influence deeper down. The Vøring escarpment is proposed to have developed after or during the emplacement of the volcanic flows on the landwards side of the escarpment (Berndt *et al.* 2001), while the seaward side submerged under sea level. On the East Greenland margin, escarpment features are interpreted to consist of inter-fingering sediments and volcanic rocks and are not necessarily of deep crustal nature either (Larsen 1990). However, some of the observed escarpment structures on the East Greenland shelf show a close relationship to the inferred ocean-to-continent transition. At the onshore outcrops on Nuussuaq, parallel-bedded subaerial volcanic units are seen to transform into downlapping subaqueous hyaloclastites (Pedersen *et al.* 1993), while at the offshore escarpment the parallel-bedded facies of seismic unit C clearly stop at the escarpment, while the downlapping facies of unit D continue separately below the escarpment.

The escarpment structure here could have been formed during rising sea level, where the different generations of volcanic flows can be seen as parallel-bedded reflections.

In the northern part of the area, several intra-basaltic basin infill structures can be seen (Fig. 1). Seismic unit A with its parallel-bedded facies is seen to pass into eastward-downlapping facies (Fig. 9). The apparent dip of the downlapping facies decreases from west to east, from 11.3° to 3.7°, and the height of the downlapping units in this 15 km broad offshore basin is 700–800 m. The height and dip of foresets in this basin could indicate that it might be a direct equivalent to the Vaigat Formation on the south coast of Nuussuaq (Pedersen *et al.* 1993), where subaerial volcanic rocks pass into dipping hyaloclastites fans with foreset heights of up to 700 m and foreset dips between up to 15–27°. The dips measured at the offshore lines are apparent dips, and are seen to be much smaller than the onshore dips, but smaller dips of 7–11° can also be observed onshore.

West of 58°W on line GGU/95-14, an extensional structure is seen (Fig. 11). This is a suite of SE-dipping, slightly listric extensional faults and an antithetic extensional fault at sp. 1135. On the southeastern side of the structure, the volcanic surface ends at a depth of 3.5 sec, but at the northwestern side the seismic signature is quite different. The small downfaulted part in the middle of the structure, at sp. 1500, has the form of a small pull-apart basin.

From the onshore exposures of the Vaigat Formation on Nuussuaq the volcanic rocks are known to have been flowing eastward (Pedersen *et al.* 1993). On the seismic data, volcanic foresets in the uppermost volcanic rocks show eastwards directions east of an irregular line around 56°–57°W, and westwards directions west of this line (Figs 4 and 17 inset). This indicates that there was a roughly north–south oriented eruption zone almost in the middle of the studied area.
The eruption is shown as a continuous line, but more likely it is dissected into several segments en echelon as seen in Iceland.

Gravity modelling of the volcanic section

The gravity modelling has been done using Gravmag, an interactive 2.5D gravity modelling program from British Geological Survey (Pedley *et al.* 1993). The models were constructed as a six layer model (from above): water, upper sediments, volcanic rocks interpreted from the

seismic data + possible lower volcanic rocks, lower sediments (where present), crust and mantle. The data for the upper three horizons; the seabed, the top of the volcanic rocks and the deepest interpreted volcanic unit, are taken from the interpretation of the seismic data and are held as known and fixed parameters in the models. The boundaries between the lower layers; the lower sediments (where present), the crust and the mantle are chosen as variable parameters. The densities used for the model (Table 3) are derived partly from Chalmers *et al.* (1999a), except the density for the upper sediments which is taken from density logs from the six offshore wells further south (Bate, 1995; Christiansen *et al.* in press).

Before modelling the upper part of the geological section, the background gravity signal from the mantle and lower crust has to be subtracted from the data. This was done by constructing a reference model consisting of two components, crust and mantle, and extending this 10 000 km in both directions. The reference model assumes Airy isostacy with 30 km thick crust. After entering the data derived from the interpretation from the seismic sections, a best fit of the calculated data for the whole area is found by moving the boundary between the crust and mantle so data fits the local level. It has been attempted to keep the crust/mantle boundary as smooth and straight as possible.

Chalmers *et al.* (1998) extended four nearshore seismic lines in the Nuussuaq Basin onshore to basement outcrop (Fig. 17). Their models at the offshore, western end of these lines have been used as starting points for modelling the 6 east–west offshore lines in this project. Three north–south lines have been modelled to tie between the east–west lines.

Geoffroy *et al.* (1998, 2001) proposed that the monoclinal flexure of the basaltic series onshore West Disko represents onshore exposure of a seaward-dipping reflector sequences derived from a plume-related plate break-up, and infer that the ocean-continent boundary must lie close to the west coast of Disko.

To test their hypothesis, a model of "Icelandic warm oceanic crust" (Fig. 18a) was constructed along an onshore line crossing Disko, where basement control can be achieved from the Disko gneiss ridge (Chalmers 1998), and extended westwards where control of top basalt is obtained from the offshore seismic line GGU/95-17. Moho offshore is assumed to be at a depth of 25 km, and the continental crust has been terminated a short distance offshore. This model gives a

difference between the calculated and measured gravity data of 120–160 mGal in the area of assumed oceanic crust.

An additional model for "ordinary cool oceanic crust" (Fig. 18b) has been calculated, where the Moho is assumed to be at a depth of 12-13 km. This model shows a difference between calculated and measured gravity data of 250–300 mGal.

It might be that the assumptions made about depth to Moho were badly wrong in the model shown in Fig. 18a. To test this, a model was constructed where the depth to Moho was modelled to fit a 'thick oceanic crust' model to the measured gravity data. The results are shown in Fig. 18c. It is felt that incorporating a "bulge" of the Moho to over 50 km depth is unrealistic, and White (1992) shows that heavily intruded or underplated crust does not reach deeper than 27 km at the Hatton Bank volcanic margin. The most likely way of reducing the excess mass shown in models 18a to 18c is by incorporating a layer of sediment and further modelling was done assuming continental crust in the offshore area and sediments between the volcanic rocks and the continental basement.

Some data from onshore have been used to control the models. Chalmers *et al.* (1999a) used Storey *et al.*'s (1998) observation of the presence of Eocene volcanic rocks in western Nuussuaq to estimate that there must be 3 km of the Maligât Formation and some 1-2 km of the Vaigat Formation under western Nuussuaq. At the south coast of Nuussuaq, the well GRO#3 (Christiansen *et al.* 1999) penetrated 2700 m of sediments below the volcanic rocks (Fig. 19), and 15 km to the east of the well a single, short, 15-fold onshore seismic line, recorded in 1994, shows at least 4.5–6, maybe 7–8 km of sediments below the volcanic section (Chalmers *et al.* 1999a). The presence of sedimentary xenoliths and metallic iron in many volcanic rocks in West Disko (Pedersen 1981), strongly indicate the presence of pre-volcanic sediments west of the Disko gneiss ridge.

There is, of course, no unique solution, but a range of different solutions all of which have a good fit between the observed and calculated data, and all of which could display a part of the real geology. All models, however, share similar features. The volcanic section thickens westward from the coast, curving around Disko and Nuussuaq, with the maximum thickness around 56°–56°15´W (Figs 17 and 20). The sedimentary section below the volcanic rocks displays more or less the same curved outline as the volcanic rocks (Fig. 17). The sedimentary

basin deepens very rapidly off the coast to a maximum depth to basement at 7–9 km around 56°30´W, somewhat more westerly than the position of the maximum thickness of the volcanic rocks.

In the southern part of the studied area, at line GGU/95-11 (Fig. 21) a suite of almost vertical faults (40–60 km west of Disko) can be seen to match a basin in the modelling, corresponding to a decreased thickness of the volcanic rocks and increased thickness of the lower sediments. Gravity highs require maximum thicknesses of the volcanic rocks of 4 km at 30 km west of Disko, and 3 km at 90–125 km west of Disko. The lower sedimentary section is modelled as a deep basin of 7–7.5 km thickness at its maximum (60–110 km west of Disko) to match the gravity low. The crust/mantle boundary shallows slightly from east to west from 28 km to 21 km depth.

In the middle of the area at line GGU/95-17 (Fig. 22) the volcanic section can be seen to display a rather uniform thickness at 2.5 to 3.5 km also within the horst. The depression in the gravity signal at 25 km west of Disko is matched by a significant increase of the thickness of the lower sedimentary section, from 1.5 km east of the faults to almost 6 km west of them. The thickness of the volcanic rocks at the western end of the line is about 3 km (Fig. 20). The crust/mantle boundary shallows slightly from 26 km depth in the east to 22 km depth in the west (Fig. 22).

In the northern part of the area at line GGU/95-14 (Fig. 23a) the volcanic section displays thicknesses about 3.5 km in the eastern part, increasing slightly to a maximum of 5.5 km at 65–70 km west of Disko. The lower sedimentary section displays a maximum thickness of 7 km at 50 km west of Disko. An attempt to put more mass from the volcanic rocks into the sediments and crust in the easternmost part of the line, by putting intrusions into the lower sediments and crust, and thereby raising the density, made no significant difference in the modelling (Fig. 23b). The difference between the two models is shown by a decrease in the thickness of the volcanic rocks from 3.5 to 2.5 km, an increase in the thickness of the lower sediments from 4 to 6 km, and a deepening of the crust/mantle boundary from 25 km to 27 km.

At the intersection of line GGU/95-14 (Fig. 23) and GGU/95-12 (Fig. 6) in the northern part of the area, a pronounced high-amplitude southeast-dipping reflection can be seen on the seismic data. On both of the models based on line GGU/95-14 (Fig. 23a and b) the dipping reflection

coincides very well with the boundary between the volcanic rocks and the lower sediments, so here the volcanic/sediment boundary can be seen very clearly.

Dating of the offshore volcanic succession

Storey *et al.*'s (1998) dating means that the Kanísut Member (Riisager *et al.*, 1999) (Fig. 2) from the westernmost part of Nuussuaq was emplaced during the earliest part of the C23 reverse period. The dates of the West Disko dikes and the Tartunaq dike and sill system on Nuussuaq, are 53.6 Ma and 54.8 Ma respectively (Storey *et al.* 1998) and the dikes on Svartenhuk Halvø gave a date of 54.6 Ma (Geoffroy *et al.* 2001), which places them all in the upper part of C24r. The presence of three datings showing almost the same age (53.6, 54.6 and 54.8 Ma) compared to one single dating of the Kanísut Member at 52.5 Ma, makes it reasonable to use the dates for the dikes and sills as the youngest recognized volcanic formations in the onshore area, and await more datings from the Kanísut Member.

The Kanísut Member is reversely magnetized (Riisager *et al.* 1999) and the magnetic map (Fig. 24) shows that that the dated sample of the Kanísut Member and those from the dikes were all collected in areas with negative magnetic anomalies. This area extends offshore into western Vaigat, but west of Nuussuaq there is a steep transition into an area with high-amplitude normal magnetization. The geological cross-section along Vaigat (Fig. 19) shows that the volcanic rocks dip 15–20° to the west, 10 km west of Nuussuaq. The eastern part of the seismic line (situated in the area with negative magnetic anomalies) corresponds to the part of the seismic line where the seismic units D and E crop out at seabed, whereas seismic units A, B and C are present where there are high-amplitude positive magnetic anomalies, implying that at least unit A, but maybe also units B and C are normally magnetised. Throughout the offshore volcanic area, a coincidence between the area with normal magnetization and the presence of seismic unit A at the sub-sediment surface (Figs 24 and 8), indicates that this seismic unit was emplaced during a normal period.

Seismic unit A is the uppermost volcanic unit interpreted in the offshore volcanic area. In some places its top can be seen to have been slightly eroded, but in most places the rough volcanic surface with volcanic mounds is onlapped non-erosively by sediments, and seismic unit A itself lies non-erosively upon the lower volcanic units. This could indicate that seismic unit A belongs to the magnetic positive chron (C24n) which immediately overlies the onshore recognized dike

and sill systems. From the geomagnetic timescale of Cande & Kent (1995), this implies an age for the youngest offshore volcanic rocks of 52.4–53.6 Ma (Fig. 2).

The offshore well Hellefisk-1, south of the studied area, provides an age determination of the basalt of 57.7 ±1.2 Ma (Williamson *et al.* 2001). This date belongs to the C26n (Cande & Kent 1995), but no magnetic measurements were done on the well samples during or after drilling. Thus a direct determination is not possible. Seismic units B, C and E, which, taking account of the errors reported for the date, means that unit B is at youngest C25 (Fig. 2) but is more likely emplaced during C26. Correspondingly units D and E being reversely magnetised, must belong to either C25r or C26r, and, if the latter, are the offshore equivalents of the onshore Maligât and Vaigat Formations.

Discussion

The combination of the age determinations and the geomagnetic polarity from the onshore volcanic rocks (Storey *et al.* 1998; Riisager & Abrahamsen 1999) together with the dating of the basalt in the Hellefisk-1 well, provide a correlation between the onshore and offshore volcanic rocks. Onshore, most of the exposed volcanic rocks were apparently erupted in two phases, the first between 60.7 and 59.4 Ma and the second between 54.8 Ma to 53.6 Ma, or 52.5 Ma (Fig. 2) (Storey *et al.* 1998; Riisager & Abrahamsen 1999). Offshore the uppermost interpreted seismic horizon, seismic unit A, could be overlying the offshore correlate of the Kanísut Member and therefore erupted during C24n, but could also have been erupted during C26n and C25n, while unit B was erupted during C25 at the latest, and more probably during C26. The dating from Hellefisk-1 at the C26n/C25r boundary gives a dating of the offshore volcanic rocks in the break between the onshore exposures. Thus the clear division of the onshore volcanic rocks into two separate episodes of eruptions cannot be confirmed from the offshore volcanic rocks. The direct correlation between the onshore and offshore volcanic rocks in the western part of Vaigat, and the complexity and unknown thickness of the lowermost interpreted volcanic unit are two very large uncertainties in this estimate. Also the presence, just west of Disko, of the intrusive rocks that have been dated some 25 Ma younger than the volcanic rocks of the Vaigat and Maligât Formations onshore Nuussuaq and Disko, provides another source of uncertainty in this estimate of the eruption periods.

The attempt to determine the base of the volcanic rocks from modelling of the gravity data gives an indication of the thickness of the offshore part of the volcanic rocks. To get a better knowledge of the lowermost structures and the total amounts of the volcanic rocks, more data are needed. A couple of E–W refraction lines and offshore wells to establish the seismic signature of the boundary between the volcanic and the underlying sediments, would be very useful, but would probably not solve the problem in all details, because of the very large changes throughout the volcanic province, e.g. the water depth, the thickness of the overlying sediments, and the thickness of the volcanic rocks themselves. The modelling also shows that the Upper Cretaceous and lower Paleocene sediments known from onshore exposures and the GRO#3 well onshore Nuussuaq (Figs 17 and 19), continue farther out in the offshore basin below the Palaeogene volcanic rocks.

Structures such as volcanic escarpment structures have been used in the determination of the continent-ocean boundary on the Vøring Plateau and the Faeroe-Shetland Ridge (Eldholm *et al.* 1989; Smythe *et al.* 1983). The volcanic escarpment structure described on the Vøring Plateau is probably an earlier boundary between land and sea. The volcanic escarpment described in this paper is almost certainly only of local importance. It cannot be a major structural unit because the seismic unit directly below the escarpment is entirely continuous (Fig. 6). It also faces the wrong way to be a continent-ocean boundary, but it may indicate a lateral change in lithostratigraphic composition as Larsen (1990) interpreted on the East Greenland shelf.

By measuring the height of the escarpment on all four lines that intersect it, a measure for the later subsidence of the area can be estimated. In the middle of the escarpment structure (Fig. 1), where two seismic lines have intersected it a short distance apart, the height of the escarpment is 500 m, and at both the northeastern and the southwestern ends of the escarpment structure its height is 250 m. From this one could conclude that the middle area of the escarpment ridge has been downloaded twice as much as the outer area of the ridge.

It has been observed by Chalmers and Laursen (1995) that the position of the continent-ocean boundary along volcanic margins as the southern and central West Greenland margins often are recognized by the appearance of seaward-dipping reflector sequences. Seaward-dipping reflector sequences are generally indicative of the presence of a spreading axis with extensive subaerial eruption (e.g. Mutter 1985; Talwani *et al.* 1981), but this characteristic has mostly

been described for extensional margins, and not for margins dominated by transform movements as is thought to be the case west of Disko (Chalmers and Pulvertaft in press). Seaward-dipping reflector sequences, as recognized both farther south on the Greenland west coast (Chalmers *et al.* 1993) and in the volcanic area off Baffin Island (Fig 25) have not been identified in this area.

Geoffroy *et al.* (1998) propose that the monoclinal flexure of the basaltic series onshore West Disko represents onshore seaward-dipping reflector sequences derived from a plume-related plate break-up, and infer an ocean-continent boundary close to the west coast of Disko. They based their postulate on their measurements of eastward-dipping deep faults onshore western Disko, with westwards dipping volcanic rocks in the faulted and rotated onshore blocks, which they extend to the offshore area. In 2001 Geoffroy *et al.* dated the main flexing and tectonic stretching in West Greenland as Eocene, i.e. that the crustal flexure is contemporaneous with the earliest stage of development of oceanic crust in Baffin Bay between the North American and Greenland plates. Geoffroy *et al.* (2001) suggested that the hitherto lack of recognition of seaward-dipping reflector sequences in the offshore area is due to too strong a reflectivity of the top of the lavas. However, as shown in this project, internal structures below the top volcanic reflection are easily seen and interpreted, and seaward-dipping reflector sequences have still not been recognized in this area. As already published by Whittaker (1995, 1996), and further stated by Chalmers *et al.* (1999b), the first faults west of Disko throw down to the west. This study, primarily based on 1995 seismic data, with significantly higher resolution than the 1990 seismic data that Whittaker (1995, 1996) had to his disposition, shows that the faults close to the coast of Disko all dip west. The gravity modelling, based on data from the onshore part; the GRO#3 well (Christiansen *et al.* 1999), the onshore seismic line (Chalmers *et al.* 1999a) and the seismic interpretation from the offshore area, further shows that sediments are present below the offshore volcanic rocks as well, implying the presence of continental crust and show that Geoffroy's hypothesis that there is Icelandic-type oceanic crust west of Disko is inconsistent with observations.

Conclusion

The volcanic province in central West Greenland extends 550 km north–south and 200 km east–west, covering 110 000 km^2. The top of the volcanic rocks dips westwards from outcrop at

seabed at water depths of 50–100 m in the near-shore area around Disko and Nuussuaq in the east, and passes below wedges of sediments to depths at 3.5 km in the west.

The presence of different kind of crust in the offshore volcanic area has been tested by gravity modelling. This modelling showed that the presence of oceanic crust in the studied area is inconsistent with observations, whereas continental crust and sediments present below the volcanic rocks fit the models.

By combing the interpretation from the seismic data with the gravity data, it can be shown that the basalts westwards off the coast increase rapidly in thickness to a maximum of 5.5 km in the northern part of the area, and 4 km in the southern. The pre-volcanic sediments may have maximum thicknesses of 7–9 km, but this is displaced ca. 50 km west compared to the maximum thicknesses of the volcanic rocks.

Foresets in the uppermost part of the volcanic rocks prograde east east of a roughly north–south trending line in the middle of the offshore area and to the west west of the line. These observations indicate the position of an eruption zone.

By combining age determinations and geomagnetic records from the onshore volcanic rocks, correlating onshore and offshore volcanic rocks, and combining a magnetic grid to the seismic unit interpretation, an age for the last erupted offshore volcanic rocks can be estimated to C24n, whereas the most of the offshore volcanic rocks appear to have been erupted earlier than C25.

A direct correlation of the first erupted volcanic rocks between the offshore and onshore areas is not possible directly from the data investigated in this study. However indirect correlations suggest that the age for the first erupted volcanic rocks in the offshore area can be the equivalent of the known onshore value of maximum 61.3 Ma.

A continent-ocean boundary cannot be interpreted directly from the seismic data. An interpretation using normal characteristics for continent-ocean boundaries is complicated by the fact that this margin is a transform margin, whereas many previously described continent-ocean boundaries have been recognized on extensional margins by e.g. seaward-dipping reflector sequences which have not been recognized in this area. Here the continent-ocean boundary

might has been compressed and lifted during strike-slip movements, and is thus not as easily recognizable.

References

Barton, A. J. & White, R. S. 1997. Volcanism on the Rockall continental margin. *Journal of the Geological Society of London*, **154**, 531-536.

Bate, K. J. 1995. Pressure indicators from the sedimentary basins of West Greenland. *Grønlands Geologiske Undersøgelse, Open file series*, **95/13**, 1-40.

Berndt, C., Planke, S., Alvestad, E., Tsikalas, F. & Rasmussen, T. 2001. Seismic volcanostratigraphy of the Norwegian Margin: constraints on tectonomagmatic break-up processes. *Journal of the Geological Society, London*, **158**, 413-426.

Bojesen-Koefoed, J. A., Christiansen, F. G., Nytoft, H. P. & Pedersen, A. K. 1999. Oil seepage onshore West Greenland: evidence of multiple source rocks and oil mixing. *In:* Spencer, A.M. (ed.) *Petroleum Geology of Northwest Europe: Proceedings of the 5th Conference.* Geological Society, London, 305-314.

Cande, S. C. & Kent, D. V. 1995. Revised calibration of the geomagnetic polarity timescale for the Late Cretaceous and Cenozoic. *Journal of Geophysical Research*, **100**, 6093-6095.

Chalmers, J. A. 1998. Gravity models in the Disko-Nuussuaq area of central West Greenland *Geological Survey of Denmark and Greenland, Report*, **1998/21**, 1-55.

Chalmers, J. A. and Laursen, K. H. (1995) Labrador Sea: the extent of continental and oceanic crust and the timing of the onset of seafloor spreading, *Marine and Petroleum Geology*, **12**, 205-217.

Chalmers, J. A. & Pulvertaft, T. C. R. in press. Development of the continental margins of the Labrador Sea – a review. In *Geological Society of London, Special Publication.*

Chalmers, J. A., Pulvertaft, T. C. R., Christiansen, F. G., Larsen, H. C., Laursen, K. H. & Ottesen, T. G. 1993. The southern West Greenland continental margin: rifting history, basin development, and petroleum potential. *Petroleum Geology of Northwest Europe, Proceedings of the 4th Conference*, The Geological Society, London, 915-931.

Chalmers, J. A., Pulvertaft, T. C. R., Marcussen, C. & Pedersen, A. K. 1999a. New insight into the structure of the Nuussuaq Basin, central West Greenland. *Marine and Petroleum Geology*, **16**, 197-224.

Chalmers, J. A., Whittaker, R. C., Skaarup, N. & Pulvertaft, T. C. R. 1999b. Discussion on the coastal flexure of Disko (West Greenland), onshore expression of the 'oblique reflectors'. *Journal of Geological Society of London*, **156**, 1051-1055.

Christiansen, F. G. 1993. Disko Bugt Project 1992, West Greenland. *Rapport Grønlands Geologiske Undersøgelse*, **159**, 47-52.

Christiansen, F. G., Bate, K. J., Dam, G., Marcussen, C. & Pulvertaft, T. C. R. 1996. Continued geophysical and petroleum geological activities in West Greenland in 1995 and the start of onshore exploration. *Bulletin Grønlands Geologiske Undersøgelse*, **172**, 15-21.

Christiansen, F. G., Boesen, A., Bojesen-Koefoed, J., Dalhoff, F., Dam, G., Neuhoff, P. S., Pedersen, A. K., Pedersen, G. K., Stannius, L. S. & Zinck-Jørgensen, K.1998. Petroleum geological activities onshore West Greenland in 1997. *Review of Greenland Activities, Bulletin*, 1-9.

Christiansen, F. G., Boesen, A., Bojesen-Koefoed, J. A., Chalmers, J. A., Dalhoff, F., Dam, G., Hjortkjær, B. F., Kristensen, L., Larsen, L. M., Marcussen, C., Mathiesen, A., Nøhr-Hansen, H., Pedersen, A. K., Pedersen, G. K., Pulvertaft, T. C. R., Skaarup, N. & Sønderholm, M. 1999. Petroleum geological activities in West Greenland in 1998. *Geology of Greenland Survey Bulletin*, **183**, 44-56.

Christiansen, F. G., Bojesen-Koefoed, J. A., Chalmers, J. A., Dalhoff, F., Mathiesen, A., Sønderholm, M., Dam, G., Gregersen, U., Marcussen, C., Nøhr-Hansen, H., Piasecki, S., Preuss, T., Pulvertaft, T. C. R., Rasmussen, J. A. and Sheldon, E. (in press) Petroleum geological activities in West Greenland in 2000 *Geology of Greenland Survey Bulletin.*

Christiansen, F. G., Dam, G. & Pedersen, A. K. 1994. Discovery of live oil at Marraat, Nuussuaq: field work, drilling and logging. *Rapport Grønlands Geologiske Undersøgelse*, **160**, 57-63.

Christiansen, F. G., Marcussen, C. & Chalmers, J. A. 1995. Geophysical and petroleum geological activities in the Nuussuaq-Svartenhuk Halvø area 1994: promising results for an onshore exploration potential. *Rapport Grønlands Geologiske Undersøgelse*, **165**, 32-41.

Clarke, D. B. & Pedersen, A. K. 1976. Tertiary volcanic province of West Greenland. *In:* Escher, A. & Watt, W. S (eds) *Geology of Greenland.* Geological Survey of Greenland, 365-385.

Clarke, D. B. & Upton, B. G. J. 1971. Tertiary basalts of Baffin Island: field relations and tectonic setting. *Canadian Journal of Earth Sciences*, **8**, 248-258.

Dam, G. & Sønderholm, M. 1994. Lowstand slope channels of the Itilli succession (Maastrichtian-Lower Paleocene), Nuussuaq, West Greenland. *Sedimentary Geology*, **94**, 49-71.

Eldholm, O., Thiede, J. & Taylor, E. 1989. Evolution of the Voering Volcanic Margin. *Proceedings of the Ocean Drilling Program, Scientific Results*, **104**, 1033-1065.

Geoffroy, L., Gelard, J. P., Lepvrier, C. & Olivier, P. 1998. The coastal flexure of Disko (West Greenland), onshore expression of the 'oblique reflectors'. *Journal of Geological Society of London*, **155**, 463-473.

Geoffroy, L., Callot, J.-P., Scaillet, S., Skuce, A., Gélard, J. P., Ravilly, M., Angelier, J., Bonin, B., Cayet, C., Perrot, K. and Lepvrier, C. 2001. Southeast Baffin volcanic margin and the North American-Greenland plate separation. *Tectonics*, **20**, 566-584

Hald, N. 1977. Lithostratigraphy of the Maligât and Hareøen Formations, West Greenland basalt group, on Hareøen and western Nuussuaq. *Rapport Grønlands Geologiske Undersøgelser*, **79**, 9-16.

Hald, N. & Pedersen, A. K. 1975. Lithostratigraphy of the early Tertiary volcanic rocks of central West Greenland. *Rapport Grønlands Geologiske Undersøgelse*, **69**, 17-24.

Henderson, G. 1973. The geological setting of the West Greenland basin in the Baffin Bay region. Geological Survey of Canada Paper, **71-23**, 521-544.

Henderson, G., Schiener, E. J., Risum, J. B., Croxton, C. A. & Andersen, B. B. 1981. The West Greenland Basin. *In:* Kerr, J. W. & Fergusson, A. J. (eds) *Geology of the North Atlantic Borderlands*. Canadian Society of Petroleum Geologists, Memoirs, **7**, 399-428.

Larsen, H. C. 1990. The East Greenland Shelf. *In:* Grantz, A., Johnson, L. & Sweeney, J. F. (eds) *The Arctic Ocean Region*, Boulder, Colorado, Geological Society of America, **L**, 185-210.

Larsen, J. G. & Pulvertaft, T. C. R. 2000. The structure of the Cretaceous-Palaeogene sedimentary-volcanic area of Svartenhuk Halvø, central West Greenland. *Geology of Greenland Survey Bulletin*, **188**, 40 pp.

Larsen, L. M. & Pedersen, A. K. 1988. Investigations of Tertiary volcanic rocks along the south coast of Nûgssuaq and in Western Disko, 1987. *Rapport Grønlands Geologiske Undersøgelse*, **124**, 28-32.

Larsen, L. M. & Pedersen, A. K. 1992. Volcanic marker horizons in the upper part of the Maligât Formation on eastern Disko and Nuussuaq, Tertiary of West Greenland: syn- to post-volcanic basin movements. *Rapport Grønlands Geologiske Undersøgelse*, **155**, 85-93.

Mutter, J. C. 1985. Seaward dipping reflectors and the continent-ocean boundary at passive continental margins. *Tectonophysics*, **114**, 117-131.

Oakey, G. N. Ekholm, S., Jackson, H. R. & Marcussen, C. in press. Magnetic Anomaly of the Davis Strait Region, Canadian and Greenland Arctic (scale 1:1,500,000). Geological Survey of Canada.

Pedersen, A. K. 1979. A Shale Buchite Xenolith With Al-Armalcolite and Native Iron in a Lava From Asuk, Disko, West Greenland. Contrib. Mineral. Petrol. **69**, 83-94.

Pedersen, A. K. 1981. Armalcolite-Baring Fe-Ti Oxide Assemblages in Graphite-Equilibrated Salic Volcanic Rocks with Native Iron form Disko, Central West Greenland. Contrib. Mineral. Petrol. **77**, 307-324.

Pedersen, A. K. 1985. Lithostratigraphy of the Tertiary Vaigat Formation on Disko, central West Greenland: *Rapport Grønlands Geologiske Undersøgelse*, **124**, 1-30.

Pedersen, A. K., Larsen, L. M. & Dueholm, K. S. 1993. Geological section along the south coast of Nuussuaq, central West Greenland. 1: 20 000. *Coloured geological sheet.* Copenhagen, Denmark, Grønlands Geologiske Undersøgelse.

Pedersen, A. K., Larsen, L. M., Pedersen, G. K. & Dueholm, K. S. 1996. Filling and plugging of a marine basin by volcanic rocks: the Tunoqqu Member of the Lower Tertiary Vaigat Formation on Nuussuaq, central West Greenland. *Bulletin Grønlands geologiske Undersøgelse*, **171**, 5-28.

Pedersen, G. K. & Pulvertaft, T. C. R. 1992. The nonmarine Cretaceous of the West Greenland basin, onshore West Greenland. *Cretaceous Research*, **13**, 263-272.

Pedley, R. C., Busby, J. P. & Dabek, Z. K. 1993. Gravmag vl. 5 user manual - Interactive 2.5D gravity and magnetic modelling. Technical Report WK/93/26/R. Regional Geophysics Series, British Geological Survey, 73 p.

Planke, S. 1994. Geophysical response of flood basalts from analysis of wire line logs: Ocean Drilling Program Site 642, Vøring volcanic margin. *Journal of Geophysical Research*, **99**, 9279-9296.

Planke, S. & Eldholm, O.1994. Seismic response and construction of seaward dipping wedges of flood basalts: Vøring volcanic margin. *Journal of Geophysical Research*, **99**, 9263-9278.

Pujol, J., Fuller, B. N. & Smithson, S. B. 1989. Interpretation of a vertical seismic profile conducted in the Columbia Plateau basalts. *Geophysics*, **54**, 1258-1266.

Riisager, P. & Abrahamsen, N. 1999. Magnetostratigraphy of Paleocene basalts from the Vaigat Formation of West Greenland. *Geophysical Journal International*, **137**, 774-782.

Riisager, J., Riisager, P. & Perrin, M. 1999. Palaeodirectional and Palaeointensity results of Paleocene and Eocene basalts from West Greenland. *Bulletin of the Geological Society of Denmark*, **46**, 69-78.

Rolle, F. 1985. Late Cretaceous – Tertiary sediments offshore central West Greenland: lithostratigraphy, sedimentary evolution, and petroleum potential. *Canadian Journal of Earth Sciences*, **22**, 1001-1019.

Skaarup, N., Chalmers, J. A. and White, D. 2000. An AVO study of a possible new hydrocarbon play, offshore central West Greenland. *AAPG Bulletin*, **84**, 174-182.

Smythe, D. K., Chalmers, J. A., Skuce, A. G., Dobinson, A. & Mould, A. S. 1983. Early opening history of the North Atlantic - I. Structure and origin of the Faeroe-Shetland Escarpment. *Geophysical Journal of the Royal Astronomical Society*, **72**, 373-398.

Storey, M., Duncan, R. A., Pedersen, A. K., Larsen, L. M. & Larsen, H. C. 1998. $^{40}Ar/^{39}Ar$ geochronology of the West Greenland Tertiary volcanic province. *Earth and Planetary Science Letters*, **160**, 569-586.

Talwani, M., Mutter, J. C. & Eldholm, O. 1981. Initiation of opening of the Norwegian Sea. *Oceanologica Acta,* 23-30.

White, R. S. 1992. Magmatism during and after continental break-up. *In*: Storey, B. C., Alabaster, T. & Pankhurst, R. J. (eds) *Magmatism and the causes of Continental Break-up*, Geological Society Special Publication, **68**, 1-16.

Whittaker, R. C. 1995. A preliminary assessment of the structure, basin development and petroleum potential offshore central West Greenland. *Grønlands Geologiske Undersøgelse Open File Series*, **95/9**, 1-43.

Whittaker, R. C. 1996. A preliminary seismic interpretation of an area with extensive Tertiary basalts offshore central West Greenland. *Bulletin Grønlands Geologiske Undersøgelse*, **172**, 28-31.

Whittaker, R. C., Hamann, N. E. & Pulvertaft, T. C. R. 1997. A New Frontier Province Offshore Northwest Greenland: Structure, Basin Development, and Petroleum Potential of the Melville Bay Area. *AAPG Bulletin*, **81**, 978-998.

Williamson, M.-C., Villeneuve, M. E., Larsen, L. M., Jackson, H. R., Oakey, G. N. & MacLean, B.

2001. Age and petrology of offshore basalts from the Southeast Baffin Shelf, Davis Strait, and western Greenland continental margin. St. John's 2001, Abstract Volume **26**, 162.

Figure captions

Fig. 1: Map of the studied area showing the positions of the seismic lines and structures at top volcanic level. Several minor structural features mentioned in the text are also shown. Map east of approximately 55°W from Chalmers *et al.* 1999a.

Fig. 2: Overview of the onshore volcanic succession compared to the seismically-defined volcanic units from the offshore area. The lithostratigraphy and $^{40}Ar/^{39}Ar$ ages are from Storey *et al.* (1998), the $^{40}K/^{40}Ar$ date for the Svartenhuk dikes is from Geoffroy *et al.* (2001), the geomagnetic timescale from Cande & Kent (1995), the measurements of the magnetic chrons and reversals in the Vaigat and Maligât Formations from Riisager & Abrahamsen (1999), the measurements from the Kanísut Member from Riisager *et al.* (1999), the $^{40}Ar/^{39}Ar$ measurement from the offshore Hellefisk-1 well from Williamson *et al.* (2001).

Fig. 3: Part of seismic line GGU/95-12 where the top volcanic reflection is normally seen as a single, sharp positive reflection (to the right), but often shows a more irregular surface with several generations of lava flows or hyaloclastites.

Fig. 4: Part of seismic line GGU/95-08A where seismic unit D with its distinct sigmoidal prograding internal pattern is seen towards WNW, whereas the underlying unit E is here seen as consisting of a high-amplitude parallel to sub-parallel facies. At sp. 8000–8400 the top volcanic surface can be seen to be clearly eroded.

Fig. 5: Part of seismic line GGU/95-11 showing rotated fault blocks between steep, mainly normal faults in the southern part of the studied area. The throws have magnitudes of 100–700 m, and the displacements can be seen reaching up into the overlying sediments, where multi-generation incised channel structures can be observed.

Fig. 6: Part of seismic line GGU/95-12 showing an escarpment structure (marked on Fig. 1). The escarpment structure here could have been formed during rising sea level, where the different generations of volcanic flows can be seen as parallel-bedded reflections. Below, the volcanic units C, D, and E are interpreted, where the base of unit E is interpreted from the gravity modelling. Coincident with the base of unit E is a strong high-amplitude southeast-dipping reflection, which can be followed on the same four seismic lines (12, 10, 14, and 15) as where the escarpment structure is defined at the top volcanic level.

Fig. 7: Part of seismic line GGU/95-13 with the different seismic units interpreted and described in Table 2. Unit A is here seen with a high-amplitude, parallel to sub-parallel internal pattern,

unit B with low-amplitude to almost transparent sub-parallel internal pattern, unit C with a high-amplitude parallel pattern. Unit D is seen with a high-amplitude downlapping internal pattern becoming almost parallel to the SW. Unit E has a parallel to sub-parallel internal pattern becoming chaotic with depth.

Fig. 8: Isopach map of seismic unit A. Unit A has a limited distribution in the northernmost part of the area, and occurs in a rather thin layer of 100-570 m.

Fig. 9: Part of seismic line GGU/95-08A in the northern part of the area, just west of Nuussuaq. Several basin fill structures can be seen. The uppermost seismic unit A is seen here to have a strongly downlapping appearance where the top reflection is seen to pass into eastwards-prograding facies, where the dip decreases from west to east, from 11.3–3.7°. The height of the downlapping units in this offshore basin is 700–800 m, and can be seen as a direct equivalent to what is seen onshore in 700 m deep basins observed in the Vaigat Formation on the south coast of Nuussuaq (Pedersen *et al.* 1993).

Fig. 10: Isopach map of seismic unit B. Unit B is interpreted in most of the studied area, and varies in thickness from 130-1000 m.

Fig. 11: Part of seismic line GGU/95-14 in the westernmost part of the studied area showing an extensional structure, maybe part of a strike-slip system, where the seismic units C, D, and E are interpreted.

Fig. 12: Isopach map of seismic unit C. Unit C is interpreted in most of the studied area, and occurs in a layer of 260-1040 m.

Fig. 13: Isopach map of seismic unit D. Unit D is restricted to the northernmost part of the studied area and occurs in a layer of 310-1430 m.

Fig. 14: Isopach map of seismic unit E. Unit E is interpreted in most of the studied area, and occurs in a layer of 250–4800 m. The base of unit E is derived from the gravity modelling.

Fig. 15: Part of seismic line GGU/95-17. In the middle of the studied area, 50 km west of Disko, a pronounced horst can be seen at top volcanic level. Seismic reflections can be seen in the volcanic rocks in the fault blocks on the flanks of the structure, whereas within the horst structure almost nothing can be seen.

Fig. 16: Part of seismic line GGU/95-11 in the southern part of the studied area showing rotated fault blocks with drags of both the volcanic and sedimentary reflections up along the fault plane. In the eastern part of the figure a drag of the volcanic rocks of the order of 150 m can be seen, whereas more westerly the volcanic rocks are only a little downfaulted and not dragged, maybe reflecting different activity periods.

Fig. 17: Map of the studied area showing position of the seismic lines used in the gravity modelling, and the line extensions to basement at outcrop which (Chalmers *et al.*, 1999a) modelled in their Nuussuaq basin project. Lines of maximum thickness of the volcanic rocks and maximum thickness of the pre-volcanic sediments are also shown. The two lines have almost the same curved outline around Disko, but the line for the pre-volcanic sediments is displaced by 20–50 km towards west compared with that for maximum basalt thickness. In the inset, the eruption zone is shown, interpreted from divergence in the directions of the volcanic foresets in the uppermost part of the volcanic rocks, with the seismic unit indicated. Here the eruption is shown as a continuous line, but more likely it is dissected into several segments en echelon as seen in Iceland.

Fig. 18: Gravity modelling along an onshore line crossing Disko, where basement control can be achieved from the Disko gneiss ridge (Chalmers 1998), and extended westwards where top basalt control is obtained from the offshore seismic line GGU/95-17. a) is a model of "Icelandic warm oceanic crust" where Moho is assumed to be at a depth of 25 km, and the continental crust terminates a short distance offshore. There is a mismatch between modelled and observed gravity of 120–160 mGal in the area of assumed oceanic crust. b is a model for "ordinary cool oceanic crust", where Moho is assumed to be at a depth of 12–13 km. This model shows a difference between calculated and measured gravity data of 250–300 mGal. c shows how Moho has to be modelled to accommodate a margin with thick oceanic crust, but without prevolcanic sediments. Such a downward 'bulge' of the Moho to >50 km is thought to be an unlikely model.

Fig. 19: Line drawing of the eastern part of the Nuussuaq (Pedersen *et al.* 1993) with the interpreted seismic lines below (GGU/95-06; Chalmers *et al.* (1999a) and GGU/95-14). The magnetic reversal C27n/C26r (Riisager & Abrahamsen 1999) was found at Nuusap Qaqqarsua, and the reversely magnetised sample from the Kanísut Member (Riisager *et al.* 1999) was found at the westernmost onshore part of Nuussuaq. The area with the positive magnetic anomalies coincides with the seismic units A, B, and C whereas the easternmost negative anomalies correlate to the seismic units D and E.

Fig. 20: Map of the thickness of the volcanic section showing a curved outline around Disko and Nuussuaq, with the maximum curve at 56°W in the north and 55°30´W in the south, with a local maximum just west of Hareøen at 5–5.5 km.

Fig. 21: Geological model based on seismic line GGU/95-11, in the southern part of the studied area and gravity modelling. The intensely faulted area (sp. 3000–5000) with straight, almost vertical, mostly normal faults is interpreted as a strike-slip basin in the geological model. The basalts display thicknesses to a maximum of 4 km, whereas the pre-basaltic sediments display thicknesses of 7–7.5 km within the fault blocks, 50–80 km.

Fig. 22: Geological model based on seismic line GGU/95-17, in the middle of the studied area, and gravity modelling. The basaltic section display thicknesses of 2.5–4 km, whereas the pre-basaltic sediments show thicknesses up to 6.5 km in the central area 40–75 km. The abrupt fall in the gravity data at 25 km, is partly compensated by the topography of the volcanic surface and by an abrupt increase in the thickness of the pre-basaltic sediments.

Fig. 23: Geological model based on seismic line GGU/95-14, in the northern part of the studied area, with two versions from gravity modelling. In version a the basaltic section displays thicknesses of 3–5 km without any abrupt changes in outline, whereas the pre-basaltic sediments display thicknesses of up to 7 km at their thickest in the central area at 50 km distance. In version b intrusions have been introduced the pre-basaltic sediments and the crust in the nearshore area, thereby raising the density. However that makes little significant difference to the modelling. At the intersection between the two lines, at 0 km, the thickness of the volcanic rocks decreases from 3.5 km to 2.5 km, the thickness of the lower sediments increases from 4 km to 6 km, and the crust/mantle boundary deepens by 2 km, from 25 km to 27 km.

Fig. 24: Magnetic anomaly map of the studied area. The westernmost part of Nuussuaq where the sample of the Kanísut Member has been sampled is seen as a high-amplitude area of negative anomalies. The changes from negative anomalies to high-amplitude positive anomalies west of Nuussuaq can be followed on the line drawing at figure B. The high-amplitude positive is seen to coincide with the presence of seismic unit A (Fig. 8).

Fig. 25: Preliminary map showing where a seaward-dipping reflector sequence has recently been recognized on the Baffin Island margin.

Tables

Table 1: Specifications for the seismic surveys used in this project. The main part of the work for this paper, and especially the interpretation of the seismic units, was done on the GGU/90 and GGU/95 surveys. The GGU/92 survey was used for establishing the tie to the Hellefisk-1 well south of the area. The BUR/BG lines and the ERA/1972 lines are representative of older seismic surveys and were used for control of structures at top volcanic level both to the south and to the north of the studied area.

Table 2: Summary of the stratigraphic division of the offshore volcanic succession, based on seismic interpretation.

Table 3: The densities used for the gravity modelling are partly derived from Chalmers *et al.* (1999a), while the density for the upper sediments is derived from density logs from the five offshore wells further south (Bate 1995; Christiansen *et al.* in press).

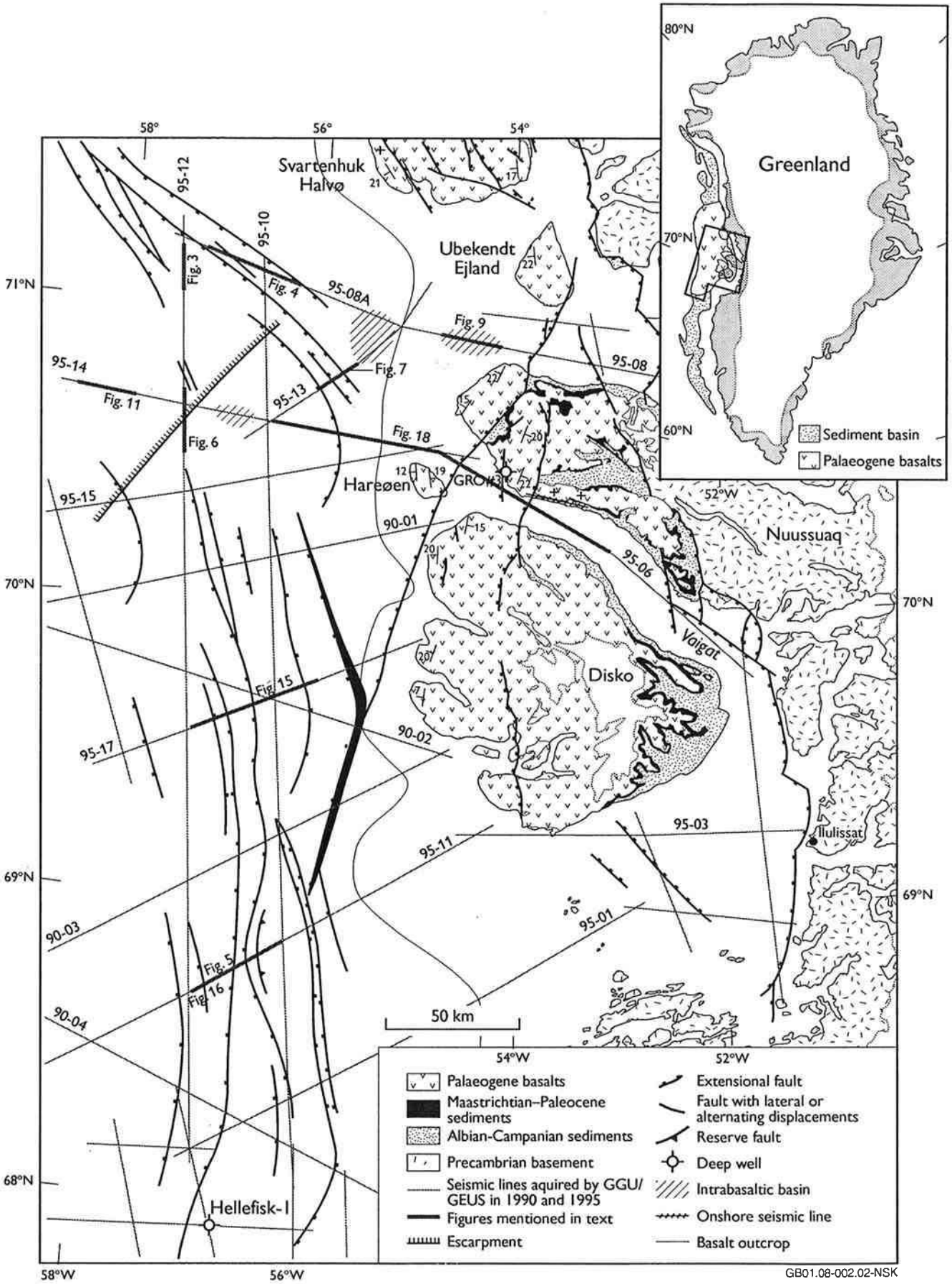
Greenland
80°N
70°N
60°N
Sediment basin
Palaeogene basalts
58°
56°
54°
52°W
Svartenhuk Halvø
Ubekendt Ejland
Hareøen
GRO#3
Nuussuaq
Disko
Vaigat
Ilulissat
Hellefisk-1
71°N
70°N
69°N
68°N
95-12
95-10
95-08A
95-08
95-14
95-13
95-15
95-17
95-06
95-03
95-11
95-01
90-01
90-02
90-03
90-04
Fig. 3
Fig. 4
Fig. 7
Fig. 9
Fig. 11
Fig. 6
Fig. 18
Fig. 15
Fig. 5
Fig. 16
50 km
54°W
52°W
58°W
56°W
Palaeogene basalts
Maastrichtian–Paleocene sediments
Albian-Campanian sediments
Precambrian basement
Seismic lines aquired by GGU/ GEUS in 1990 and 1995
Figures mentioned in text
Escarpment
Extensional fault
Fault with lateral or alternating displacements
Reserve fault
Deep well
Intrabasaltic basin
Onshore seismic line
Basalt outcrop
GB01.08-002.02-NSK

Fig.1

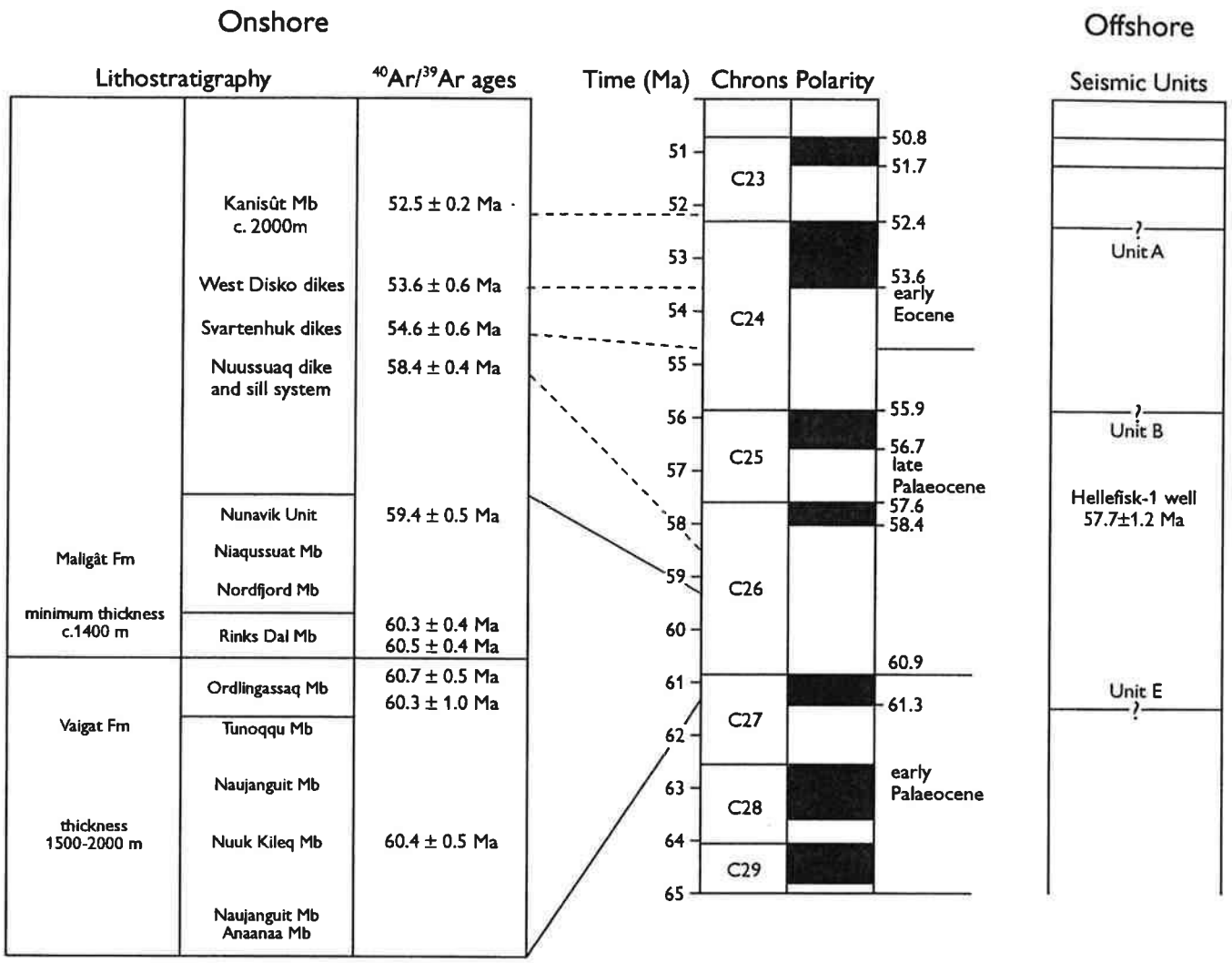

GB04.01-003-NSK

Fig.2

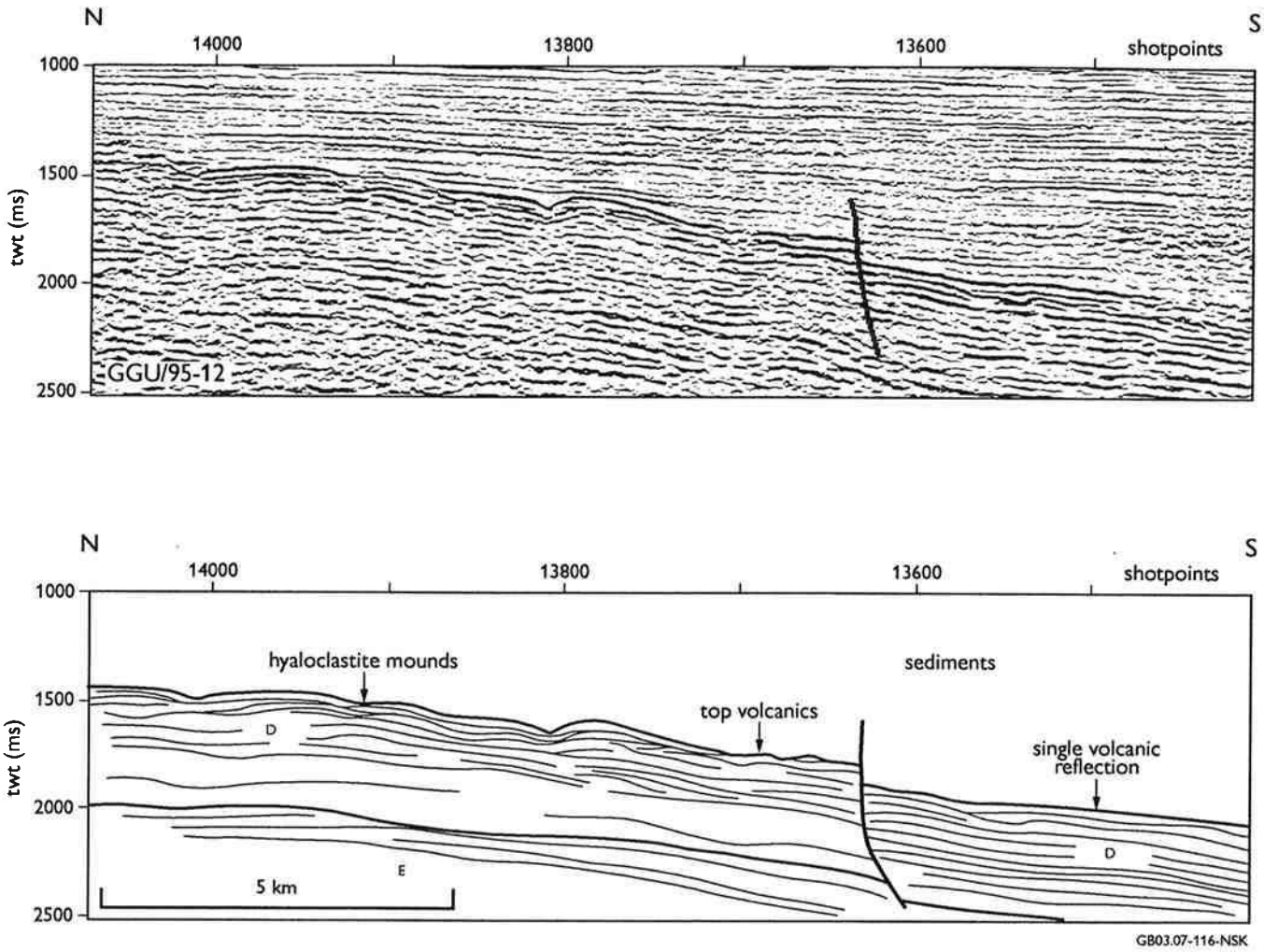
N
S
14000
13800
13600
shotpoints
1000
1500
2000
2500
twt (ms)
GGU/95-12
N
S
14000
13800
13600
shotpoints
1000
1500
2000
2500
twt (ms)
hyaloclastite mounds
sediments
top volcanics
single volcanic reflection
D
D
E
5 km
GB03.07-116-NSK

Fig. 3

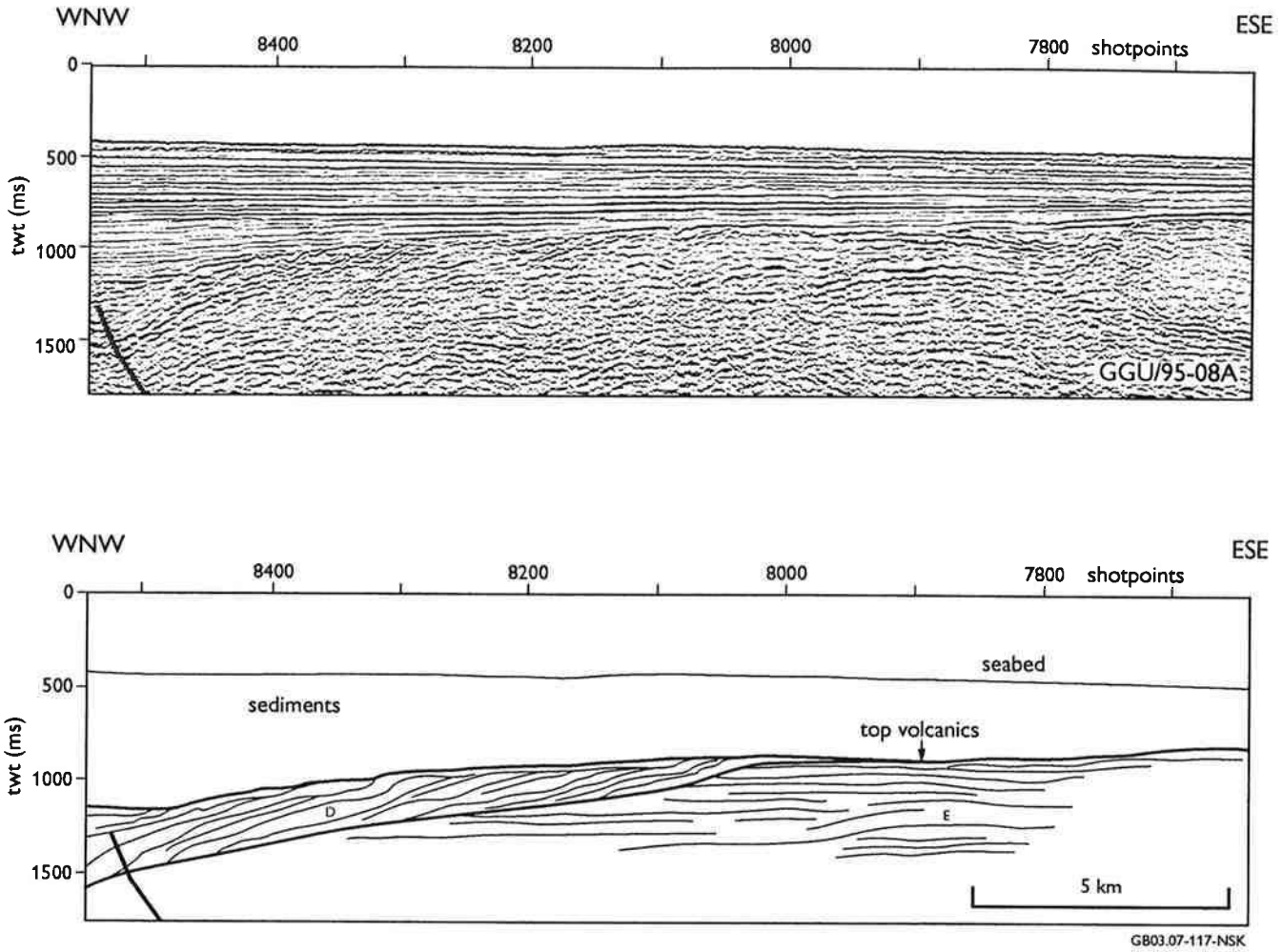
WNW
ESE
8400
8200
8000
7800
shotpoints
0
500
1000
1500
twt (ms)
GGU/95-08A
WNW
ESE
8400
8200
8000
7800
shotpoints
0
500
1000
1500
twt (ms)
seabed
sediments
top volcanics
D
E
5 km
GB03.07-117-NSK

Fig. 4

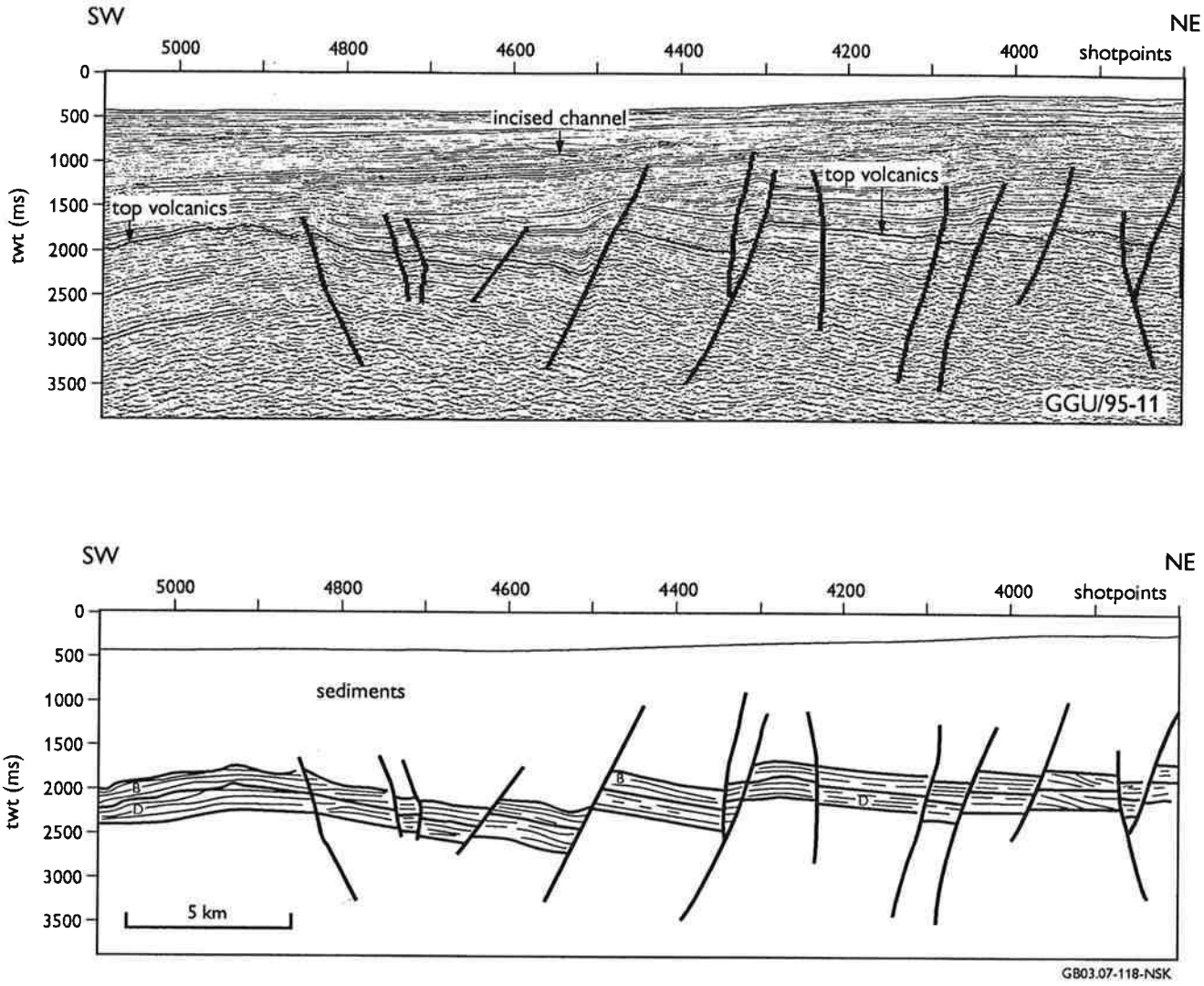
SW
NE
5000
4800
4600
4400
4200
4000
shotpoints
0
500
1000
1500
2000
2500
3000
3500
twt (ms)
incised channel
top volcanics
top volcanics
GGU/95-11
SW
NE
5000
4800
4600
4400
4200
4000
shotpoints
0
500
1000
1500
2000
2500
3000
3500
twt (ms)
sediments
B
D
B
D
5 km
GB03.07-118-NSK

Fig. 5

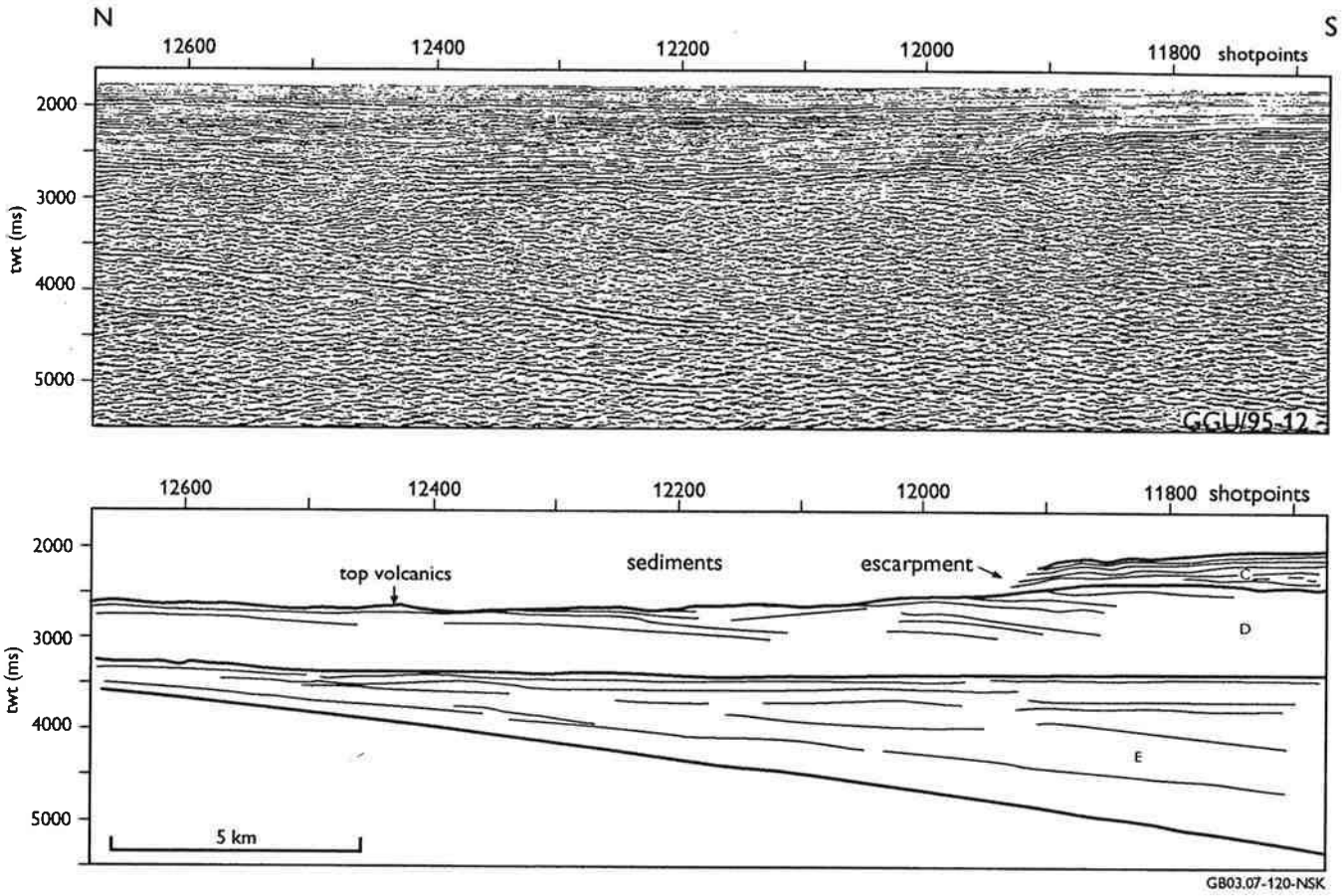
N
S
12600
12400
12200
12000
11800 shotpoints
2000
3000
4000
5000
twt (ms)
GGU/95-12
top volcanics
sediments
escarpment
C
D
E
5 km
GB03.07-120-NSK

Fig. 6

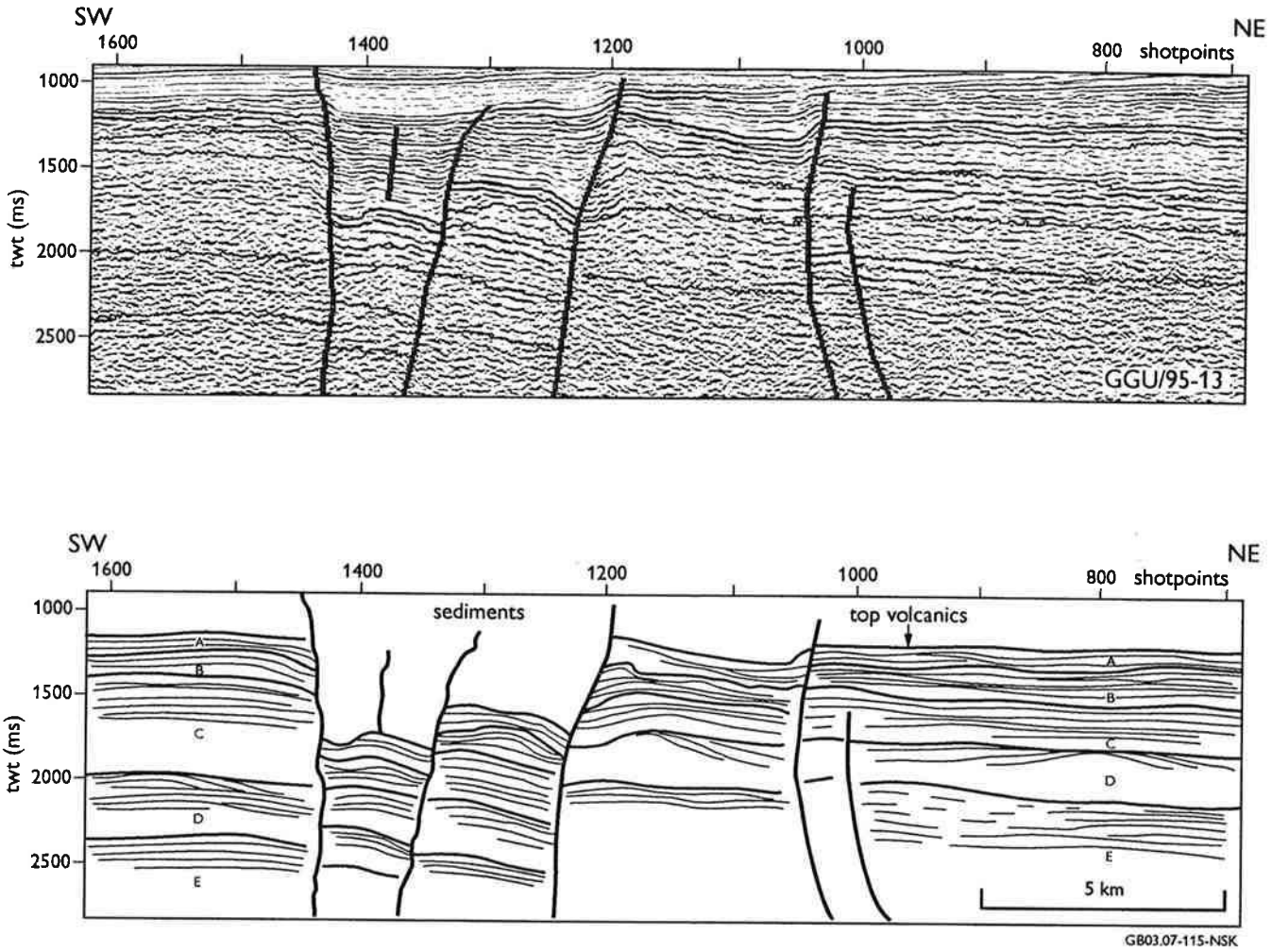
SW
NE
1600
1400
1200
1000
800 shotpoints
1000
1500
2000
2500
twt (ms)
GGU/95-13
SW
NE
1600
1400
1200
1000
800 shotpoints
sediments
top volcanics
A
B
C
D
E
5 km
GB03.07-115-NSK

Fig. 7

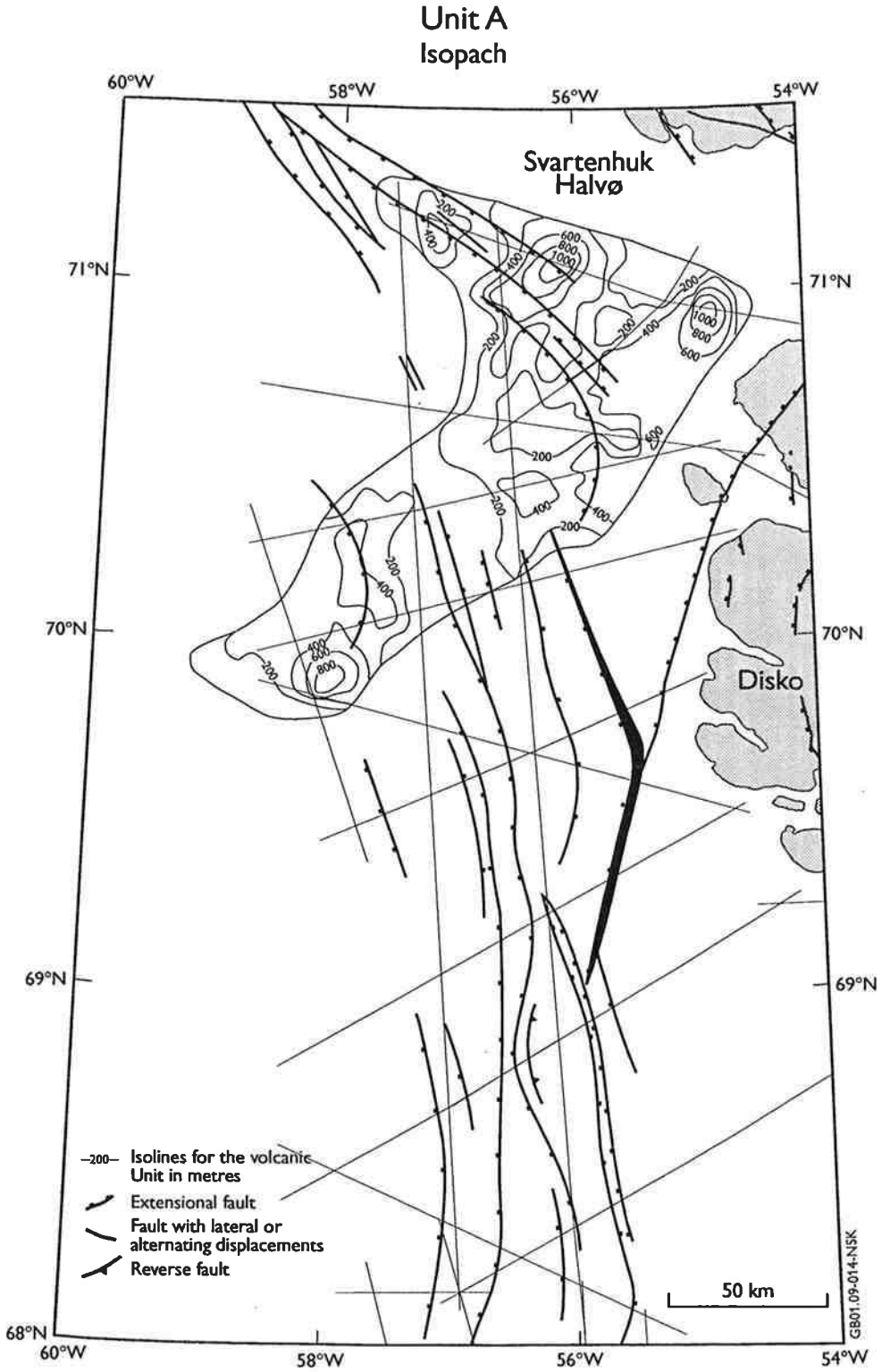
Unit A
Isopach
60°W
58°W
56°W
54°W
71°N
70°N
69°N
68°N
Svartenhuk
Halvø
Disko
200
400
600
800
1000
–200– Isolines for the volcanic Unit in metres
Extensional fault
Fault with lateral or alternating displacements
Reverse fault
50 km
GB01.09-014-NSK

Fig. 8

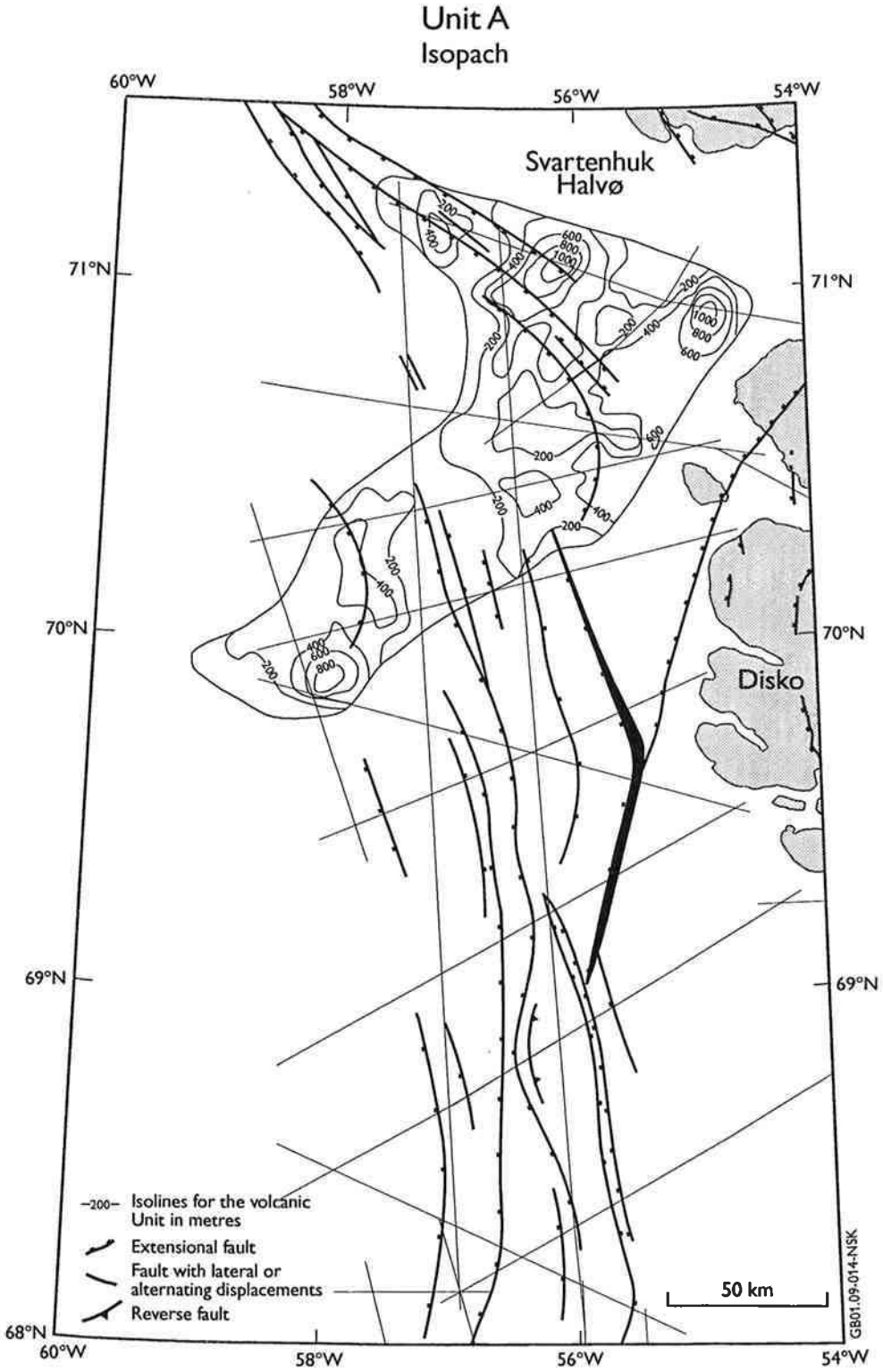
Unit A
Isopach
60°W
58°W
56°W
54°W
71°N
70°N
69°N
68°N
Svartenhuk
Halvø
Disko
-200- Isolines for the volcanic Unit in metres
Extensional fault
Fault with lateral or alternating displacements
Reverse fault
50 km
GB01.09-014-NSK

Fig. 8

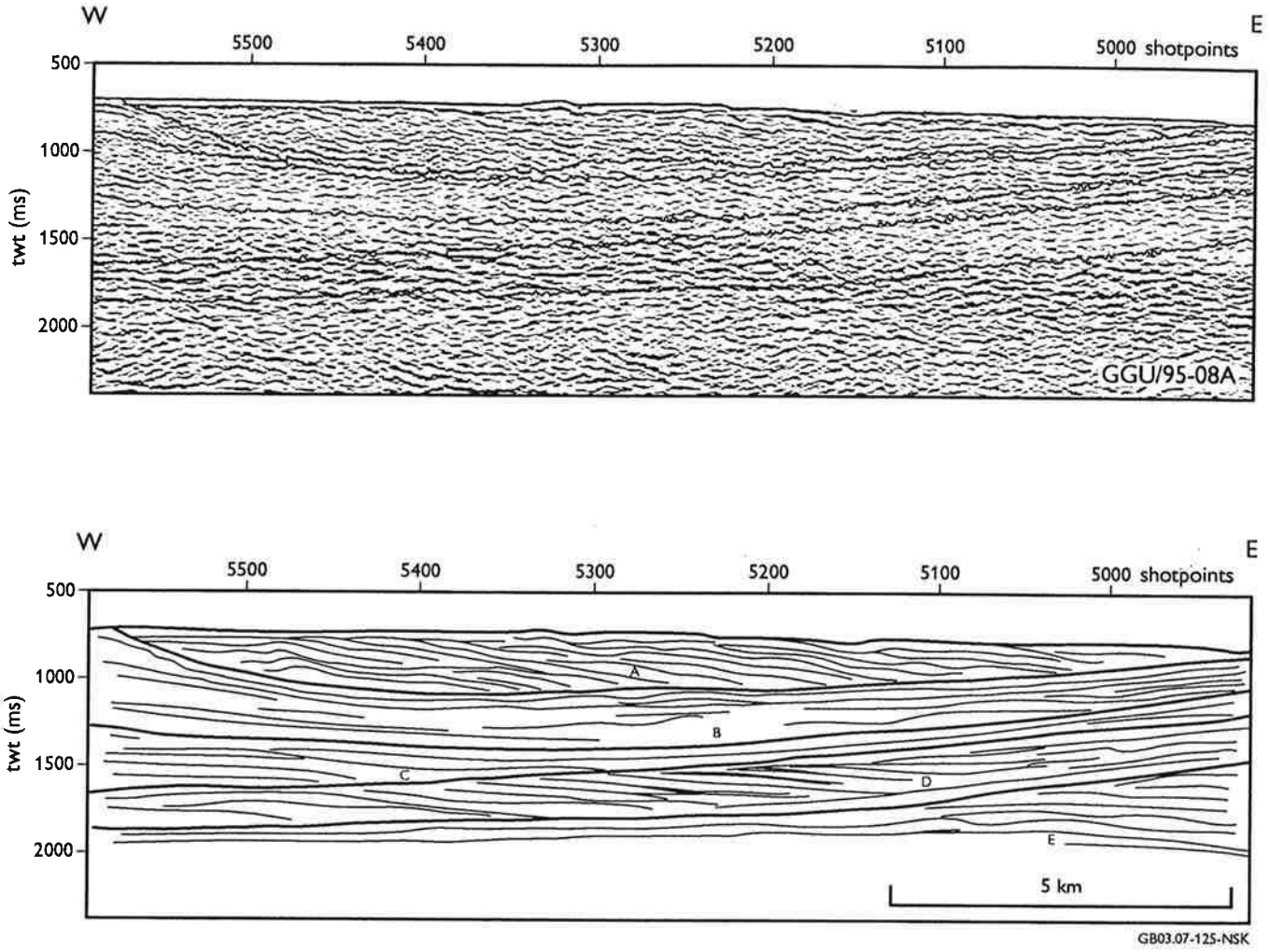
W
E
5500
5400
5300
5200
5100
5000 shotpoints
500
1000
1500
2000
twt (ms)
GGU/95-08A
W
E
5500
5400
5300
5200
5100
5000 shotpoints
500
1000
1500
2000
twt (ms)
A
B
C
D
E
5 km
GB03.07-125-NSK

Fig. 9

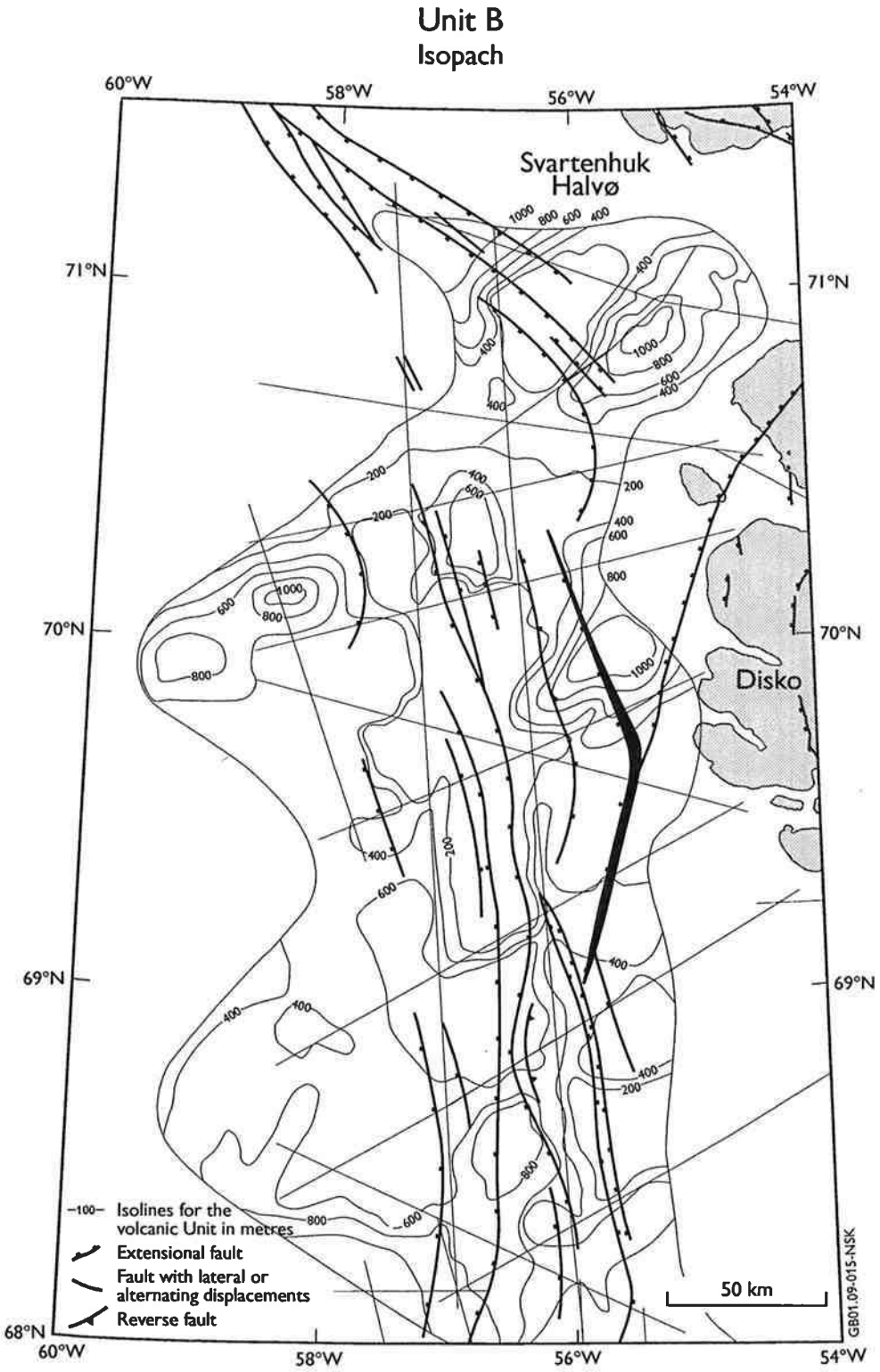
Unit B
Isopach
60°W
58°W
56°W
54°W
71°N
70°N
69°N
68°N
Svartenhuk
Halvø
Disko
-100- Isolines for the volcanic Unit in metres
Extensional fault
Fault with lateral or alternating displacements
Reverse fault
50 km
GB01.09-015-NSK

Fig. 10

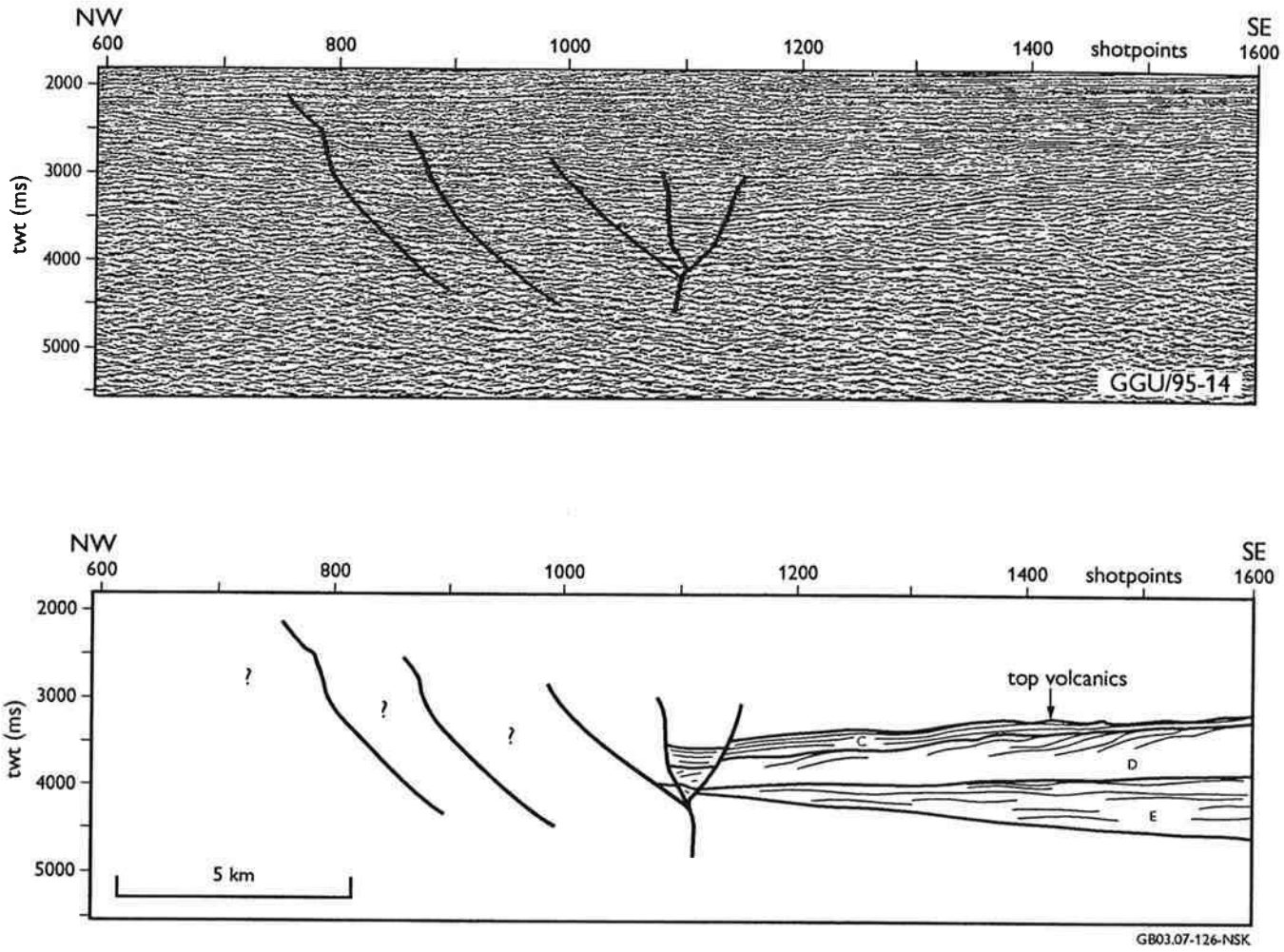
NW
SE
600
800
1000
1200
1400
shotpoints
1600
2000
3000
4000
5000
twt (ms)
GGU/95-14
NW
SE
600
800
1000
1200
1400
shotpoints
1600
2000
3000
4000
5000
twt (ms)
?
?
?
top volcanics
C
D
E
5 km
GB03.07-126-NSK

Fig. 11

Unit C
Isopach

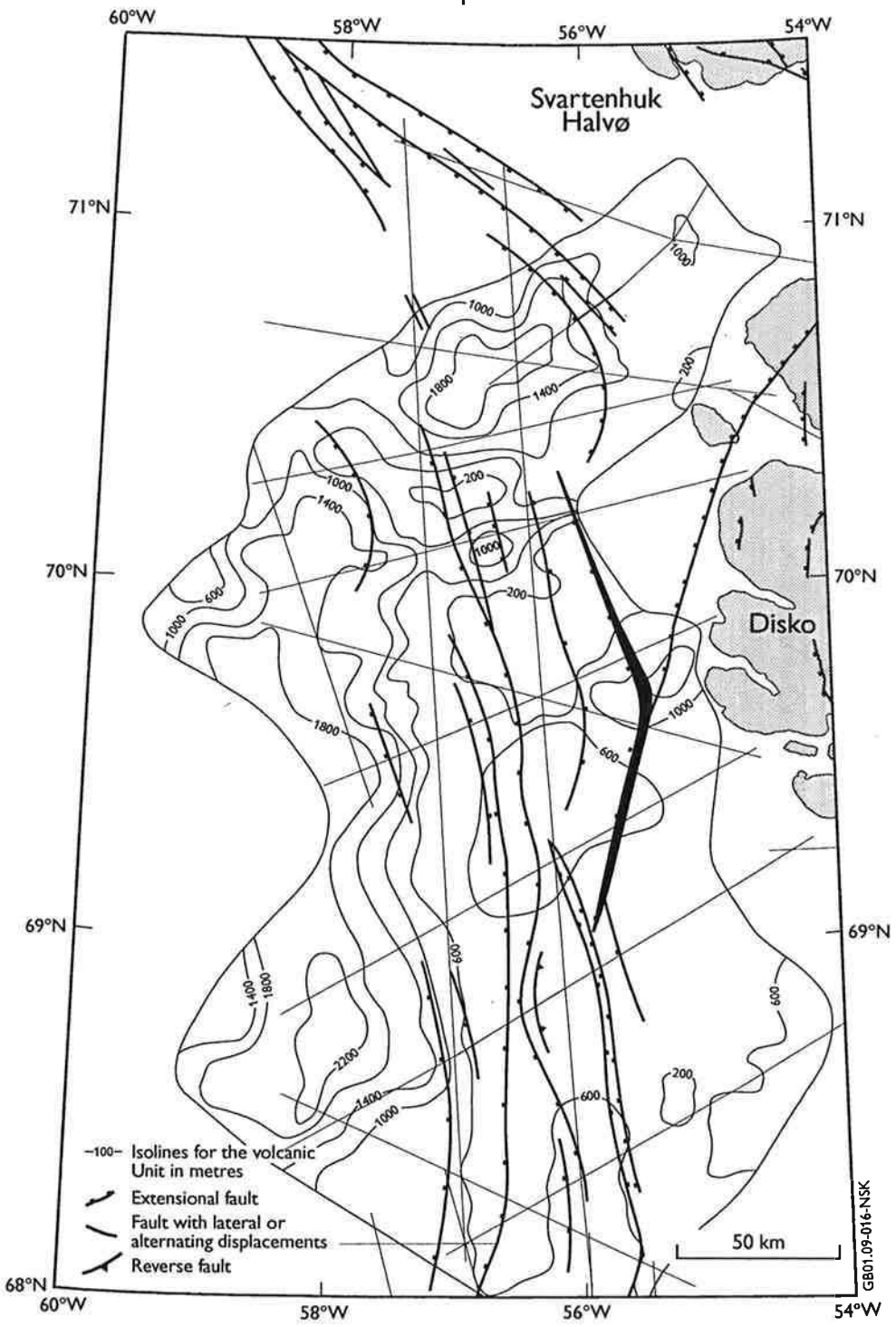

Fig. 12

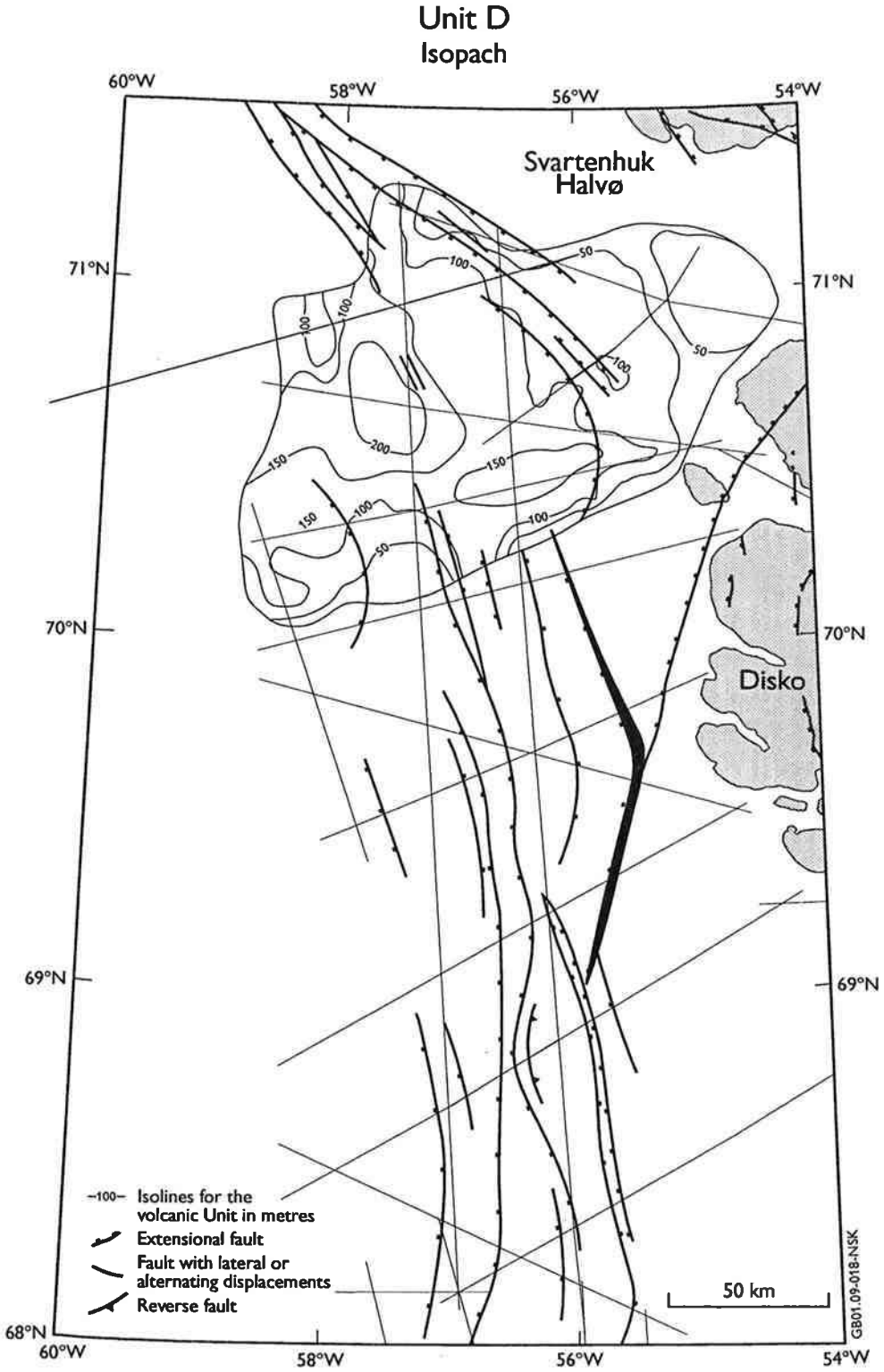
Unit D
Isopach
60°W
58°W
56°W
54°W
71°N
70°N
69°N
68°N
Svartenhuk
Halvø
Disko
50
100
150
200
–100– Isolines for the volcanic Unit in metres
Extensional fault
Fault with lateral or alternating displacements
Reverse fault
50 km
GB01.09-018-NSK

Fig. 13

Unit E
Isopach

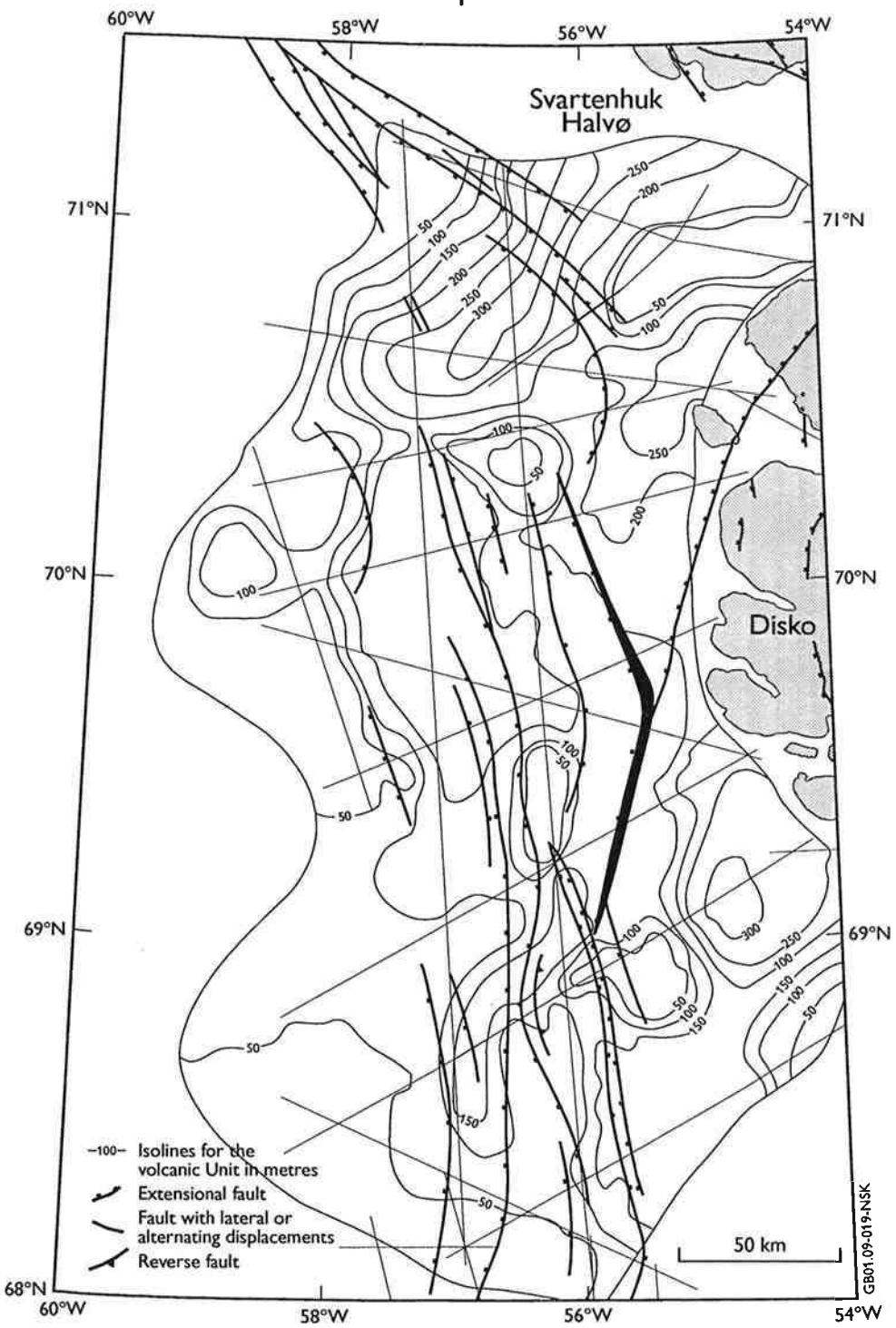

Fig. 14

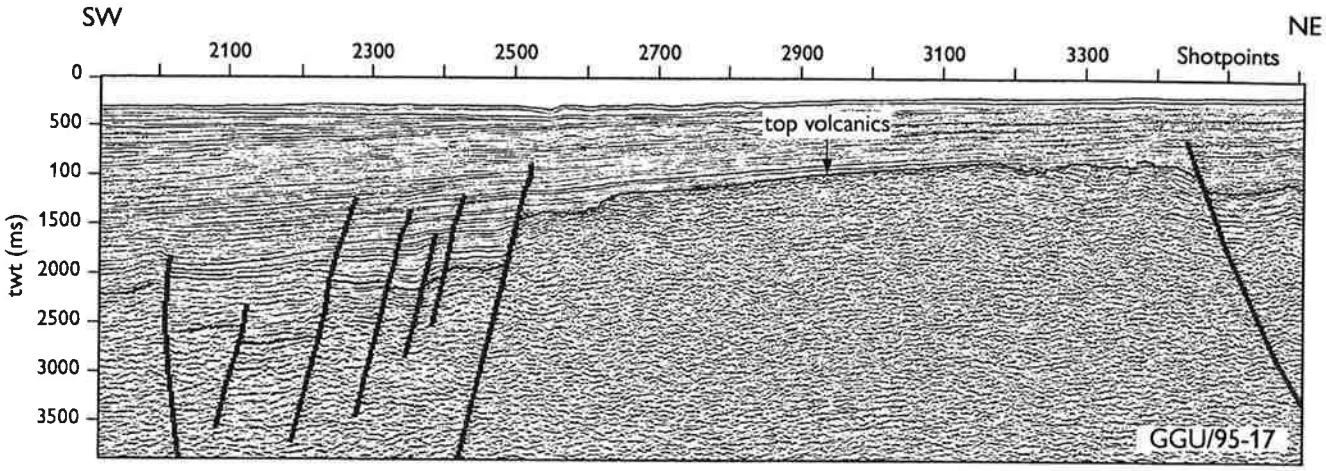
SW
NE
2100
2300
2500
2700
2900
3100
3300
Shotpoints
0
500
100
1500
2000
2500
3000
3500
twt (ms)
top volcanics
GGU/95-17

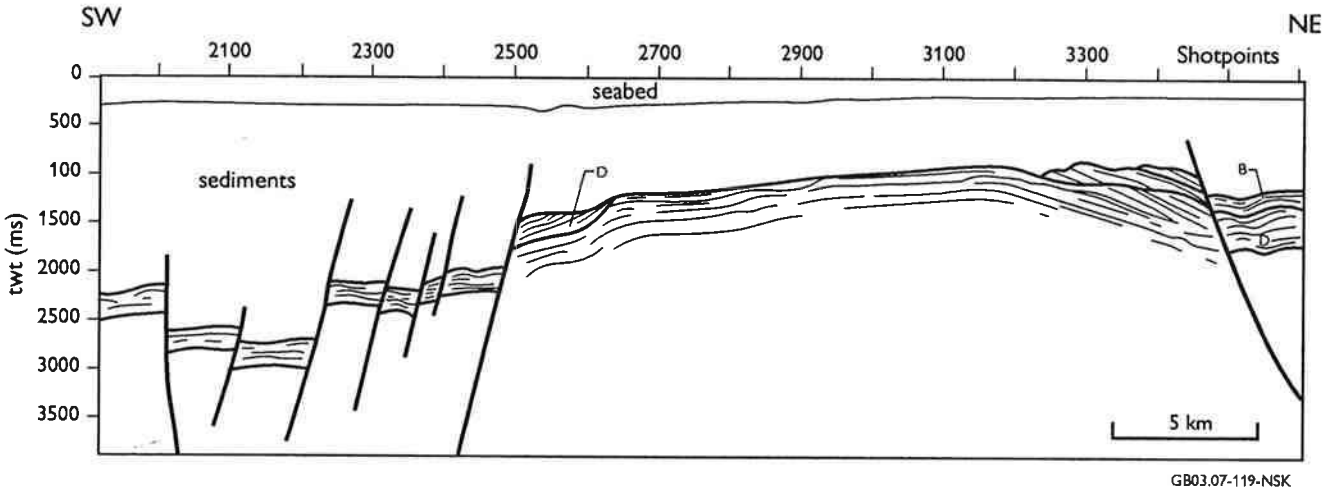
SW
NE
2100
2300
2500
2700
2900
3100
3300
Shotpoints
0
seabed
500
100
sediments
1500
2000
2500
3000
3500
twt (ms)
D
B
D
5 km
GB03.07-119-NSK

Fig. 15

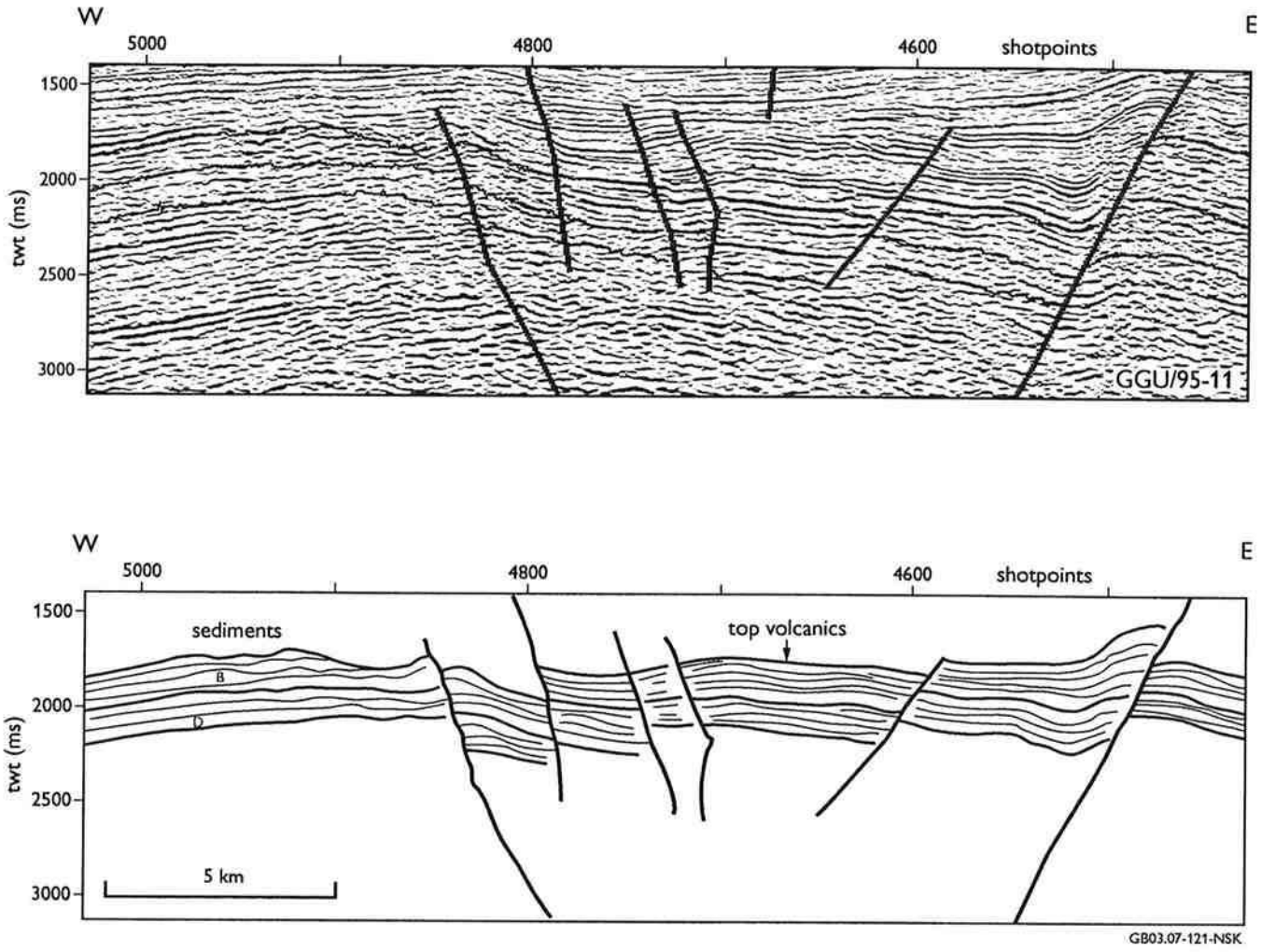
W
E
5000
4800
4600
shotpoints
1500
2000
2500
3000
twt (ms)
GGU/95-11
W
E
5000
4800
4600
shotpoints
1500
2000
2500
3000
twt (ms)
sediments
top volcanics
B
D
5 km
GB03.07-121-NSK

Fig. 16

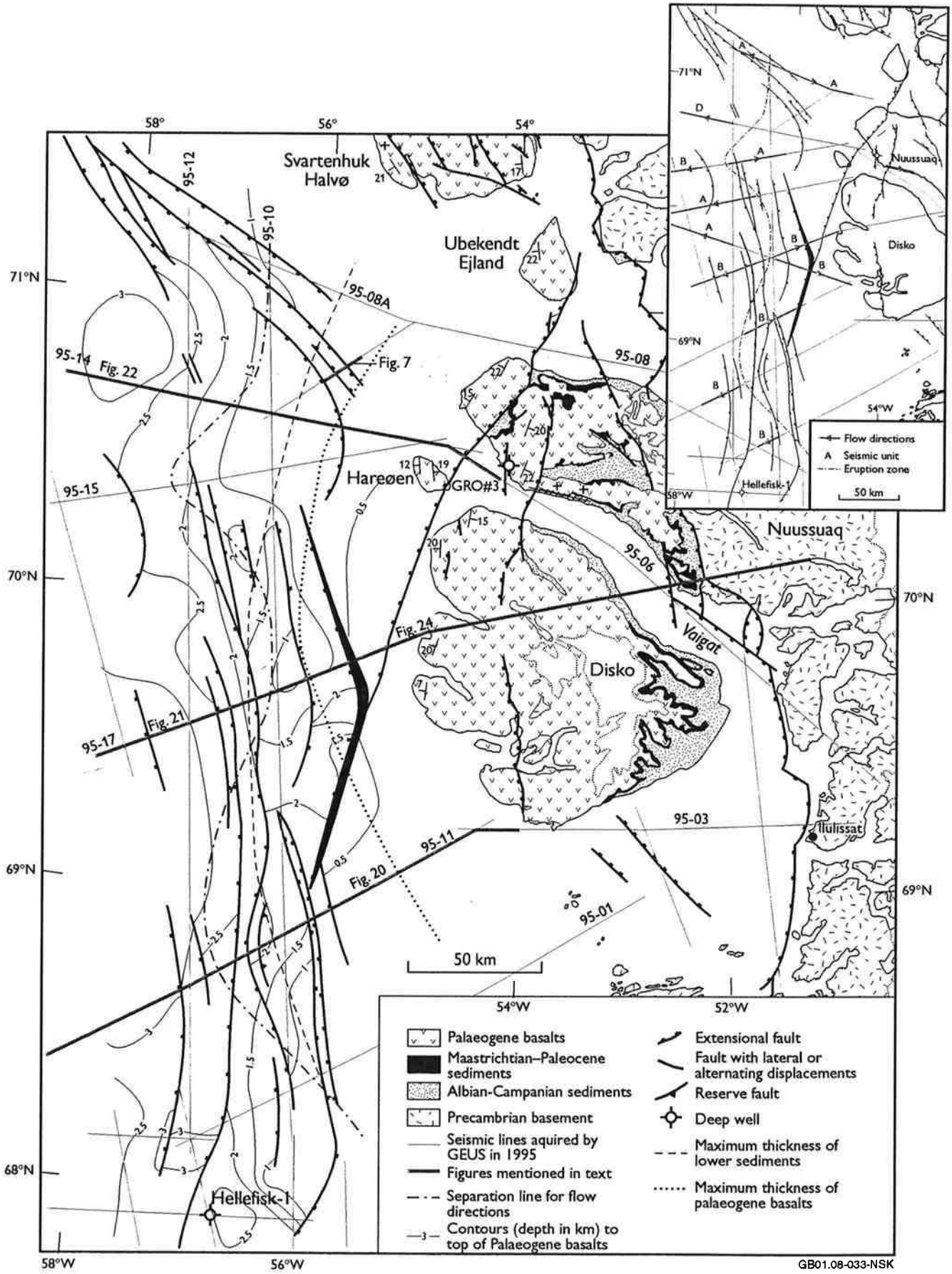
58°
56°
54°
71°N
70°N
69°N
68°N
58°W
56°W
54°W
52°W
Svartenhuk Halvø
Ubekendt Ejland
Hareøen
GRO#3
Hellefisk-1
Nuussuaq
Disko
Vaigat
Ilulissat
95-12
95-10
95-08A
95-08
95-14
95-15
95-17
95-06
95-03
95-11
95-01
Fig. 7
Fig. 22
Fig. 24
Fig. 21
Fig. 20
50 km
Palaeogene basalts
Maastrichtian–Paleocene sediments
Albian-Campanian sediments
Precambrian basement
Seismic lines aquired by GEUS in 1995
Figures mentioned in text
Separation line for flow directions
Contours (depth in km) to top of Palaeogene basalts
Extensional fault
Fault with lateral or alternating displacements
Reserve fault
Deep well
Maximum thickness of lower sediments
Maximum thickness of palaeogene basalts
Flow directions
A Seismic unit
Eruption zone
50 km
GB01.08-033-NSK

Fig. 17

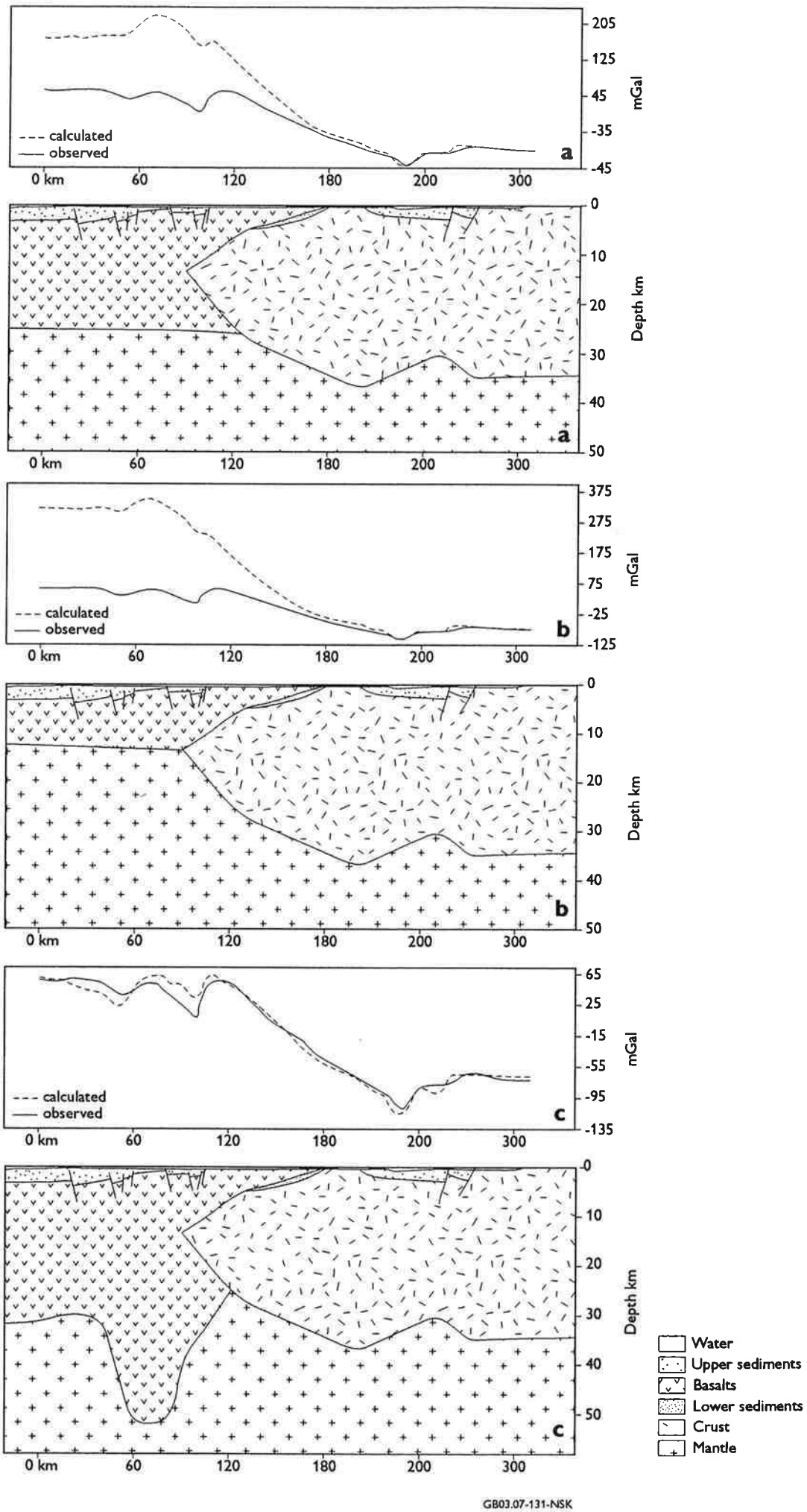
205
125
45
-35
-45
mGal
--- calculated
— observed
a
0 km
60
120
180
200
300
0
10
20
30
40
50
Depth km
375
275
175
75
-25
-125
b
65
25
-15
-55
-95
-135
c
Water
Upper sediments
Basalts
Lower sediments
Crust
Mantle
GB03.07-131-NSK

Fig. 18

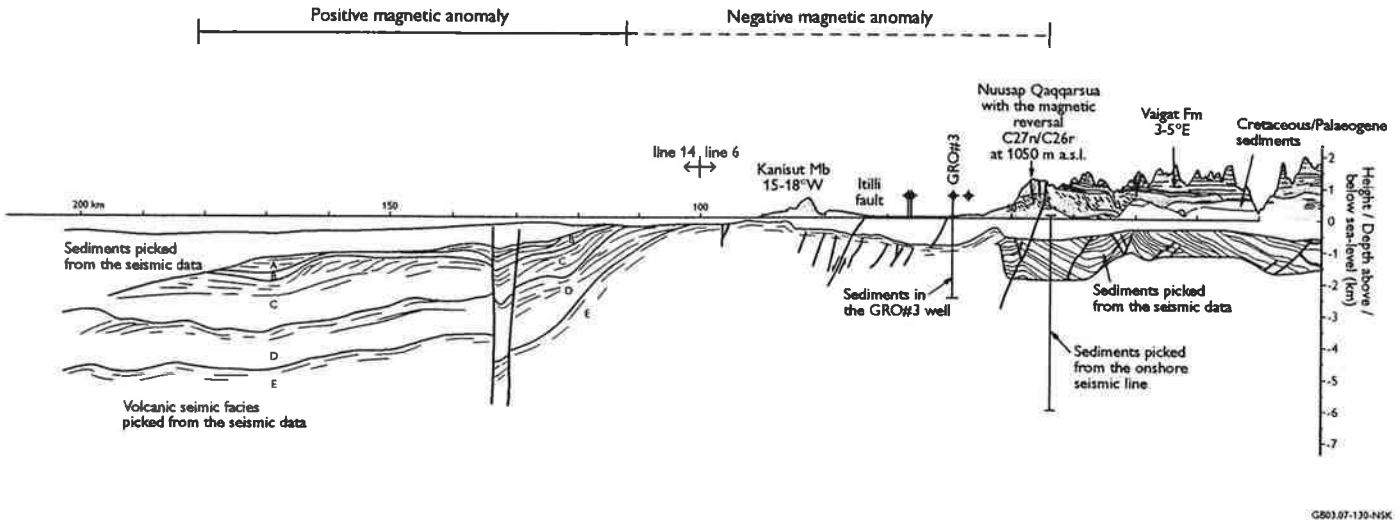
Positive magnetic anomaly
Negative magnetic anomaly
Nuusap Qaqqarsua with the magnetic reversal C27n/C26r at 1050 m a.s.l.
Vaigat Fm 3-5°E
Cretaceous/Palaeogene sediments
line 14, line 6
Kanisut Mb 15-18°W
Itilli fault
GRO#3
200 km
150
100
Heights / Depth above / below sea-level (km)
Sediments picked from the seismic data
A
C
D
E
Volcanic seimic facies picked from the seismic data
Sediments in the GRO#3 well
Sediments picked from the seismic data
Sediments picked from the onshore seismic line
G803.07-130-NSK

Fig. 19

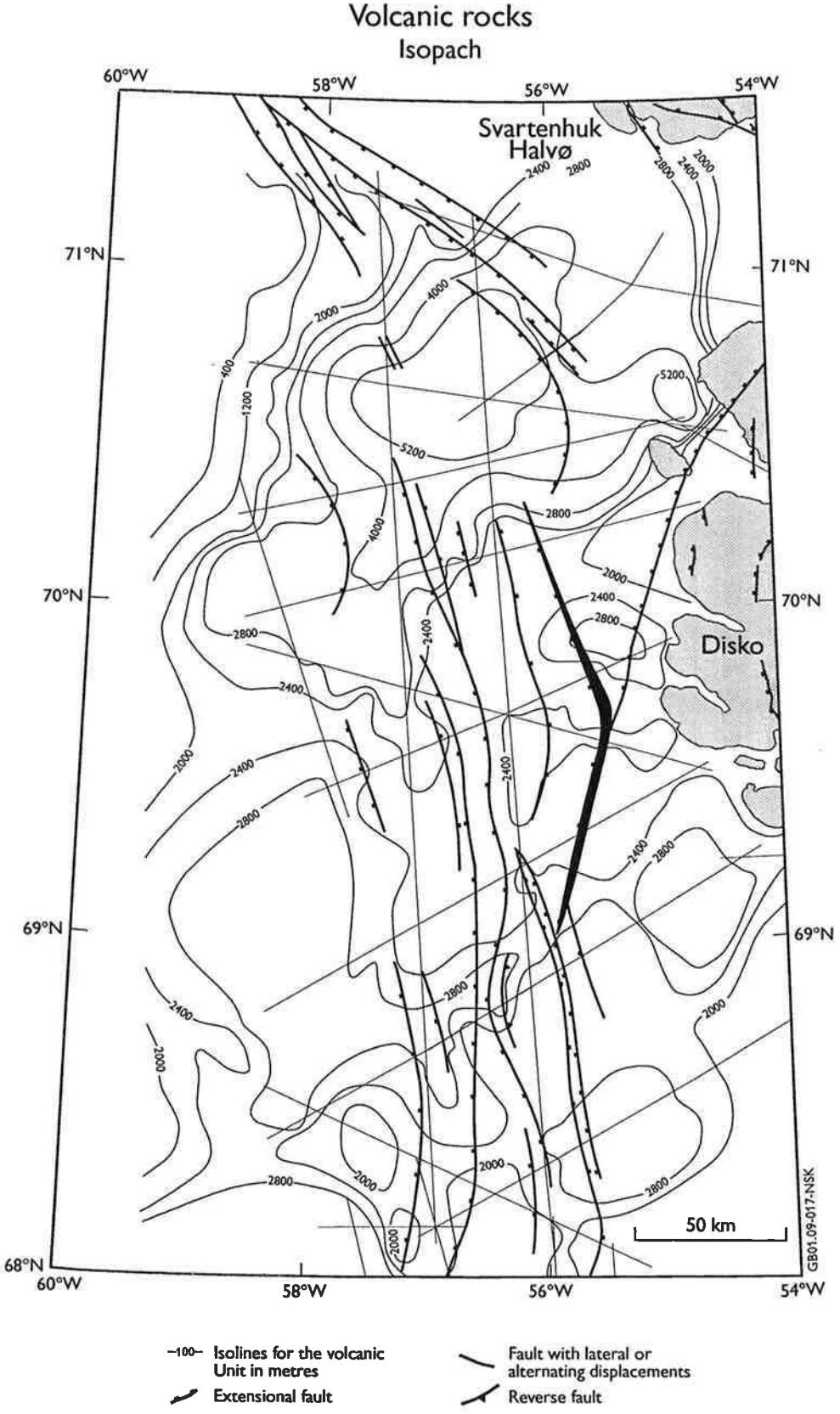
Volcanic rocks
Isopach
60°W
58°W
56°W
54°W
71°N
70°N
69°N
68°N
Svartenhuk Halvø
Disko
50 km
GB01.09-017-NSK
Isolines for the volcanic Unit in metres
Extensional fault
Fault with lateral or alternating displacements
Reverse fault

Fig. 20

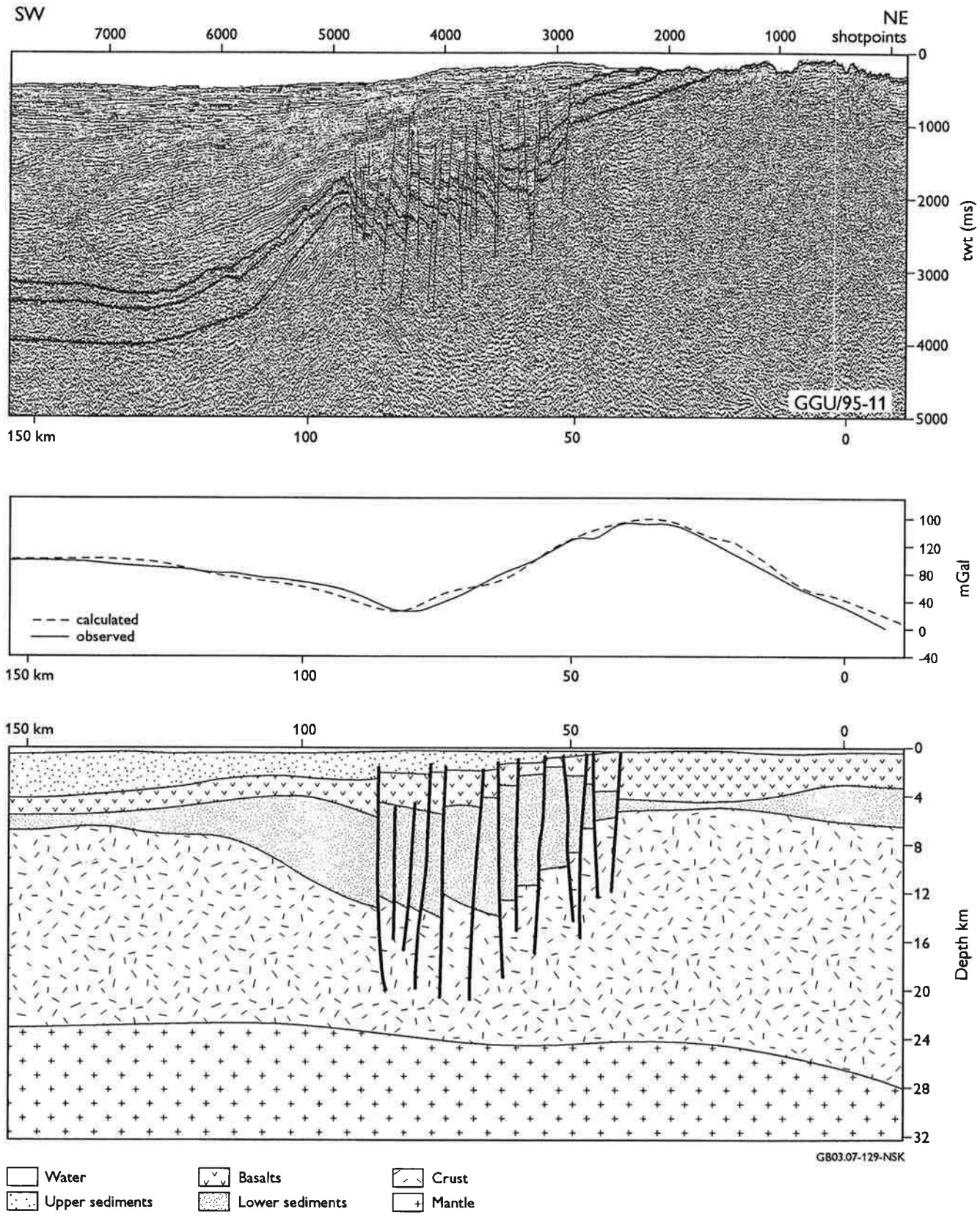
SW
NE
7000
6000
5000
4000
3000
2000
1000
shotpoints
0
1000
2000
3000
4000
5000
twt (ms)
GGU/95-11
150 km
100
50
0
100
120
80
40
0
-40
mGal
calculated
observed
150 km
100
50
0
0
4
8
12
16
20
24
28
32
Depth km
GB03.07-129-NSK
Water
Upper sediments
Basalts
Lower sediments
Crust
Mantle

Fig. 21

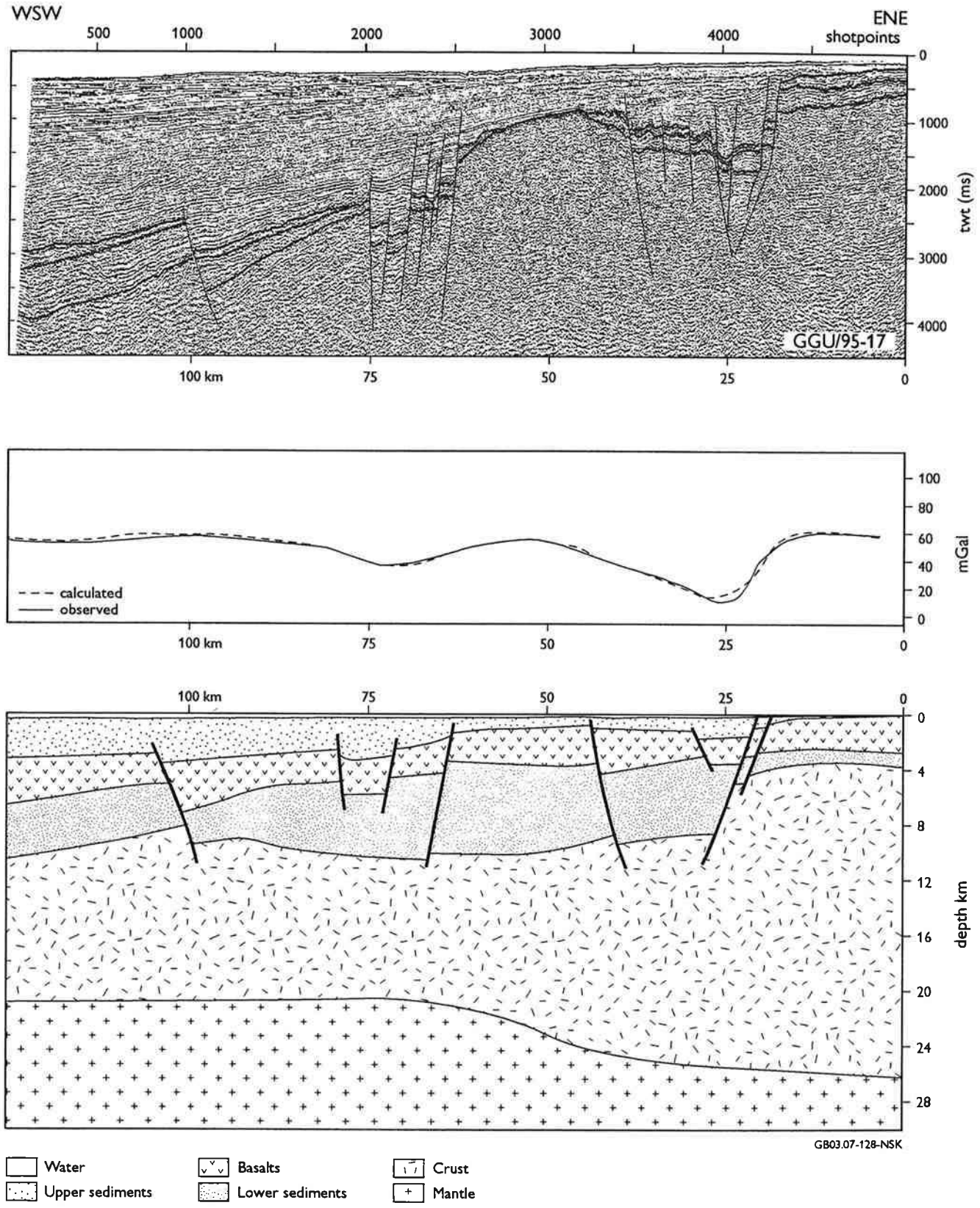
WSW
ENE
500
1000
2000
3000
4000
shotpoints
0
1000
2000
3000
4000
twt (ms)
GGU/95-17
100 km
75
50
25
0
100
80
60
40
20
0
mGal
calculated
observed
depth km
4
8
12
16
20
24
28
GB03.07-128-NSK
Water
Upper sediments
Basalts
Lower sediments
Crust
Mantle

Fig. 22

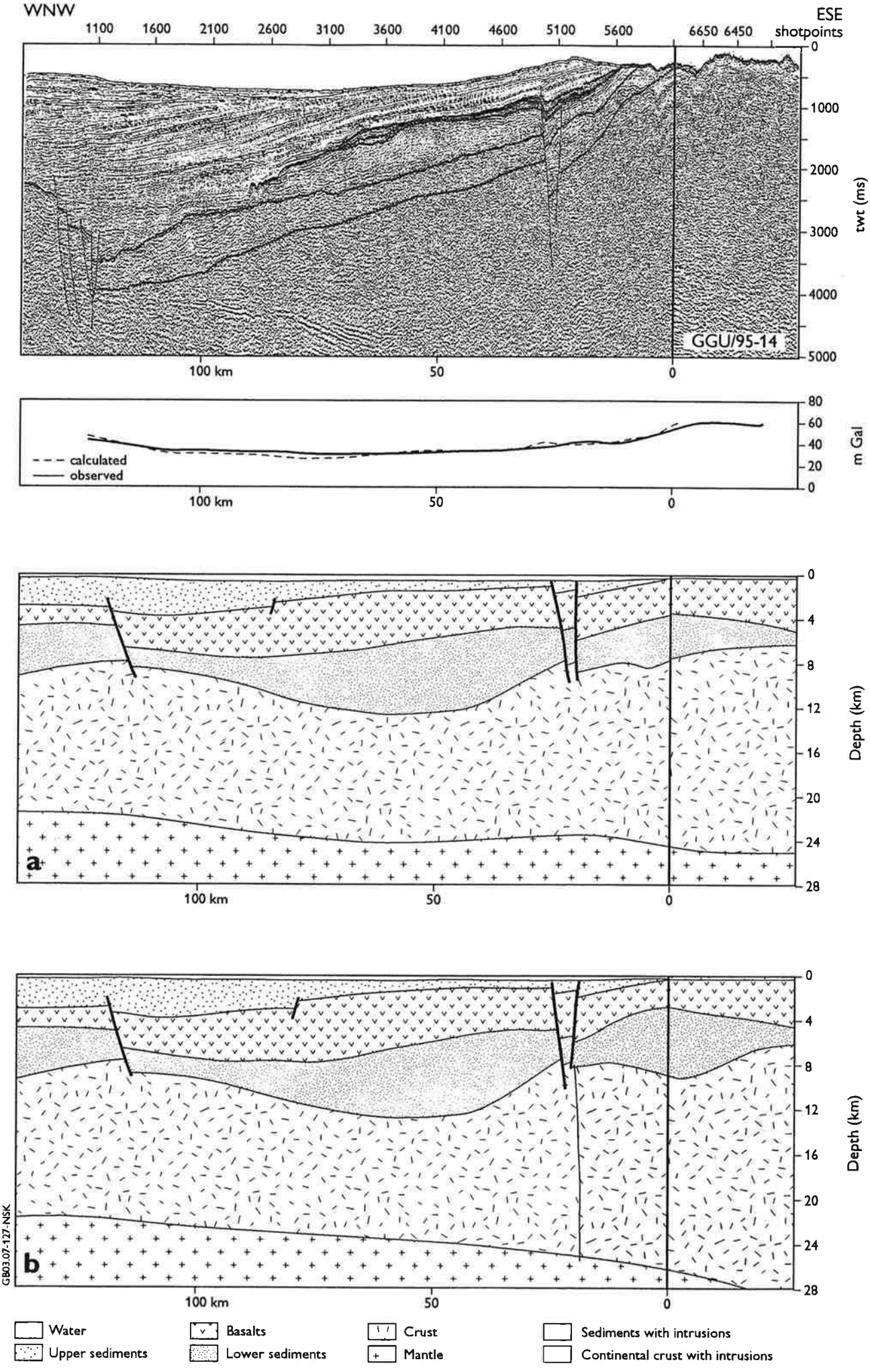
WNW
ESE
1100 1600 2100 2600 3100 3600 4100 4600 5100 5600 6650 6450
shotpoints
0
1000
2000
3000
4000
5000
twt (ms)
GGU/95-14
100 km
50
0
80
60
40
20
0
m Gal
calculated
observed
100 km
50
0
0
4
8
12
16
20
24
28
Depth (km)
a
100 km
50
0
0
4
8
12
16
20
24
28
Depth (km)
b
100 km
50
0
GB03.07-127-NSK
Water
Upper sediments
Basalts
Lower sediments
Crust
Mantle
Sediments with intrusions
Continental crust with intrusions

Fig. 23

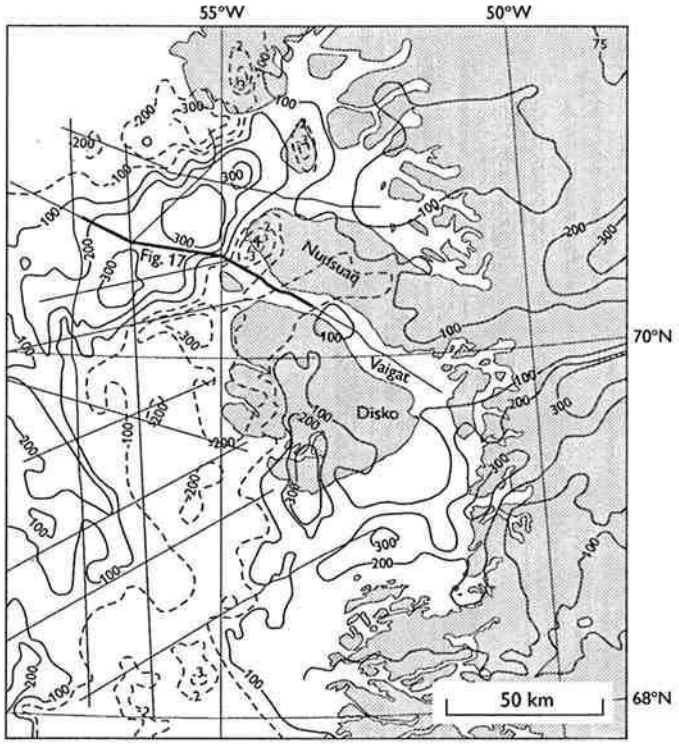
55°W
50°W
70°N
68°N
Fig. 17
Nuussuaq
Vaigat
Disko
50 km
GB01.07-054.NSK

Fig. 24

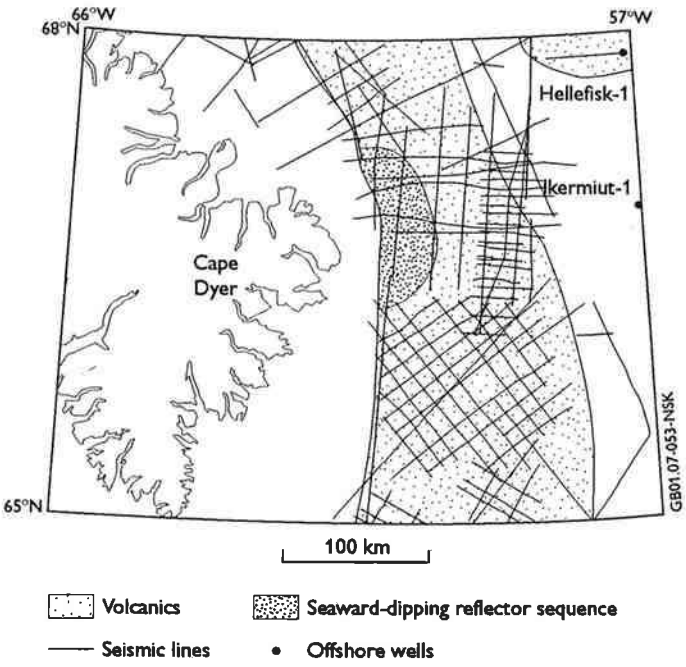
66°W
68°N
57°W
Hellefisk-1
Ikermiut-1
Cape
Dyer
65°N
GB01.07-053-NSK
100 km
Volcanics
Seaward-dipping reflector sequence
Seismic lines
Offshore wells

Fig. 25

	GGU/1990	GGU/1995	GGU/1992	BUR/BG-1971	ERA/1972
Source	3616 cu. in. bolt air gun	4100 cu. in. sleeve air gun	5016 cu. in. air gun	1200 cu. in. air gun	1140 cu. in. air gun
Shotpoint interval	25 m	25 m	25 m	50 m	200 m
Streamer	analogue	Digital	analogue	analogue	analogue
Streamer length	3000 m	4500 m	3000 m	2400 m	2350 m
Fold	60	90	60	24	24

Table 1

	Top	Base	Internal pattern
Unit A	Highly reflective	Well defined, with downlap features	High-amplitude parallel to subparallel; in a few places downlapping events are present
Unit B	Moderate reflective	In places well defined with downlap features, in places just fading into the underlying unit	Low-amplitude to almost transparent parallel to subparallel
Unit C	Highly reflective	In places defined by downlap features	High-amplitude parallel to subparallel passing into hummocky clinoforms
Unit D	Moderately to poorly reflective	Not well defined; sporadic downlap features	High-amplitude parallel to subparallel, in places passing into a sigmoidal pattern
Unit E	Moderately reflective, but sporadically defined	Defined from gravity modelling	Mostly chaotic or indeterminable, in some areas high-amplitude parallel to subparallel

Table 2

	Density
Water	1.0 Mg/m^3
Upper sediments	2.2 Mg/m^3
Volcanic rocks	3.0 Mg/m^3
Lower sediments	2.55 Mg/m^3
Crust	2.8 Mg/m^3
Mantle	3.3 Mg/m^3
Background	3.3 Mg/m^3

Table 3

Paper 4

A seismic reflection and potential field study of Baffin Bay / Davis Strait, eastern Canada: implications for tectonic evolution

To be submitted to Marine and Petroleum Geology

Nina Skaarup, H. Ruth Jackson & Gordon Oakey

A seismic reflection and potential field study of Baffin Bay / Davis Strait, eastern Canada: implications for tectonic evolution

Nina Skaarup
GEUS

H. Ruth Jackson
GSCA

Gordon Oakey
GSCA

Abstract

New regional physiographic, gravity and magnetic maps were compiled for the Baffin Bay, Davis Strait and Labrador Sea area (75°–54°N) with input from Geological Surveys in both Canada and Denmark (Greenland). Industry seismic reflection profiles along the eastern margin of Baffin Island including Davis Strait (60°–72°N) were interpreted in the context of the new potential field data. The interpretations were further constrained by short bedrock cores and industry wells.

Along the continental margin of Baffin Island three distinct areas can be mapped (Fig. 1). In the northernmost area, coast-parallel grabens and continental basement highs are superseded beneath the slope by irregular basement topography. Basement deepens seaward where it is characterized by less relief and a diffracted surface often attributed to oceanic basement. Refraction studies have not detected a high-velocity lower continental crust. This section of the margin is interpreted to be non-volcanic. Offshore Cape Dyer, the seismic data delimit an area of 100 by 130 km containing seaward dipping reflector sequences, and from 150 km to the north of Cape Dyer to 400 km to the south, extensive volcanic rocks are interpreted at and below seabed. The distribution of the volcanic rocks is also revealed by two parallel positive gravity anomalies associated with short-wavelength magnetic anomalies. This is confirmed by volcanic rocks drilled in two wells and by short basalt cores. This section of the margin is postulated to be volcanic. To the south, the depth to basement drops rapidly offshore. A thick prograding sedimentary wedge produces a high-amplitude long-wavelength free-air gravity anomaly that was previously confused with the continent-ocean boundary. This area is conjugate to the well documented non-volcanic Labrador Sea margin and is interpreted to be of similar structure. Segmentation of the margin by transform faults can explain the abrupt transitions from volcanic to non-volcanic margin segments.

Based on the combined potential field and seismic data sets, a continent-ocean boundary (COB) is determined for the North American plate. This plate boundary is used in conjunction with published poles of rotation to reconstruct plate positions during chrons 33 and 27 because both of these chrons have been suggested as the time of the initial opening. The reconstruction during chron 33 shows a slight gap in the plate boundaries in the southernmost region but an extensive overlap to the north. The reconstruction during chron 27 shows the COB in the central and northern areas to be adjacent and the volcanic rocks on either side of Davis Strait overlapping. Our examination of the data indicate that the poles of rotation need to be refined.

Geological and geophysical background

Baffin Bay and Davis Strait are located between Baffin Island and Greenland, to the north of the Labrador Sea (Fig. 1). Baffin Bay is generally believed to be created by the extension to the north of seafloor spreading from the Atlantic Ocean through the Labrador Sea. A review article by Balkwill et al. (1990) discusses the debate on the development of Baffin Bay: One group of proponents suggests that the region formed by seafloor spreading and another that continental crust is present. More recent refraction profiles are consistent with oceanic crust in northern Baffin Bay (Reid and Jackson, 1997). Interpretations of the industry reflection lines from 70°–75°N by Jackson et al. (1992) indicate the position of the continent-ocean boundary and suggested that the structures recorded on the seismic lines are consistent with the plate reconstructions of Roest and Srivastava (1989).

The structures on the Baffin Island margin associated with rifting follow the pre-existing north-northeast and northwest trends of the Precambrian and Paleozoic basement rocks (Tucholke and Fry, 1985). Davis Strait, a physiographic high separating the Labrador Sea and Baffin Bay, is complex with the possibility of both continental and oceanic crust (Balkwill et al. 1990). On both sides of Davis Strait, Palaeogene volcanic rocks (Fig. 2) crop out that belong to a single petrological province (Clark and Upton, 1971). The volcanic rocks are believed to be the first products of the Icelandic mantle plume (Storey et al., 1998). Onshore outcrops occur in a short narrow belt near Cape Dyer on eastern Baffin Island and over a larger region in the Disko-Svartenhuk area of West Greenland. Offshore on the Canadian margin volcanic rocks have been drilled in the Hekja and Gjoa wells and at various sites by a shallow rock drill as well as delineated by high resolution seismic lines and magnetic data (Johnson et al., 1982). East of Cape Dyer, Grant (1975) observed dipping internal reflectors that he interpreted as basalt flows intercalated with sedimentary layers or cross-bedded volcanic breccias. On the West Greenland margin volcanic rocks have been drilled by the Hellefisk-1 and Nukik-2 wells and observed on seismic reflection profiles (Henderson et al., 1981; Rolle 1985; Chalmers et al. 1993; Chalmers and Pulvertaft in press).

Seismic reflection and refraction lines from the conjugate margins of the Labrador Sea, southern Labrador and southern West Greenland, indicate that the margins in this region are non-volcanic (Chian et al., 1995a, b; Chalmers and Pulvertaft in press). The initiation of seafloor spreading in the Labrador Sea has been suggested in the late Cretaceous at chron 33 by Roest and

Srivastava (1989), Srivastava and Roest (1995, 1999) or in the Paleocene at chron 27 by Chalmers and Laursen (1995), Chalmers (1997), Chalmers and Pulvertaft (in press). The first group of authors based their conclusions primarily on identifying linear anomalies on magnetic data and the second on quantitative modelling of magnetic profiles controlled by interpretations of seismic reflection data. In this paper a new compilation of the potential field and bathymetry data are used to constrain the interpretation of 30,000 km of industry seismic reflection data from the margin of Baffin Island, where basement, volcanic rocks, and seaward-dipping reflector sequences are interpreted. We use these data to interpret the margin as volcanic or non-volcanic and discuss the significance for the plate reconstructions.

Description of data, distribution and processing

New compilations of physiographic, magnetic and gravity data for the Baffin Bay and Davis Strait area, were used to control a regional interpretation of seismic reflection data in the area between 60°N and 72°N. Three industry wells, an ODP well and 73 bedrock cores were also used to control the seismic interpretation.

The physiography, magnetic and gravity maps (Oakey et al., 2000a, b, c, d, e, f) are based on integration of a number of data sources in a co-operation between the Geological Survey of Canada, Atlantic (GSCA), the Geological Survey of Denmark and Greenland (GEUS) and National Survey and Cadastre–Denmark (KMS). Data were from both historical archives and recent field programmes. A final grid for each data set was produced in a Lambert Conformal projection with a reference longitude at 55°W, and standard parallels at 65°N and 75°N.

The physiographic grid is a merge of independently assembled topographic and bathymetric compilations. The original data were gridded in the Lambert Conformal projection prior to merging. The final resolution of the physiographic grid is 2 km × 2 km. The topography for Greenland was provided by the National Survey and Cadastre–Denmark (KMS) in a gridded format. The northern region of Greenland (north of 78°N) had an original resolution of 0.005°lat × 0.025°lon (approximately 0.5 km) (Ekholm, 1996). South of 78°N the original grid resolution was 0.02°lat × 0.05°long (approximately 2 km). Topography for Canada was provided by the United States Geological Survey (GTOPO 30). This satellite-derived topography had an original resolution of 30 arcseconds (approximately 1 km). Bathymetry was primarily point observations from Geological Survey of Canada (GSC) marine surveys. In coastal regions of Canada the

density of bathymetric observations was increased using digital data provided by the Canadian Hydrographic Service. Along the Greenland coast, bathymetric contours were used to improve coverage. South of 71°N bathymetric contours (Henderson, 1973) were provided by GEUS. Depths were reduced using a velocity of 1463 m/s and no Matthew's corrections were applied. The 2 km bathymetric grid was interpolated (and extrapolated) using a minimum curvature method (Smith and Wessel, 1990). The extrapolated region was masked using the topographic grid, and depths less than 5 m were erased to eliminate "artificial" land areas.

Gravity data were gridded at 5 km resolution. Data sources included marine ship observations, aerogravity over Greenland, and station data over Baffin Island and Greenland. Bouguer anomalies for land data were reduced by GSC and KMS using a density contrast of 2.67 g/cm^3. Marine data are presented as free-air anomalies.

Magnetic data were combined from various marine surveys, aeromagnetic surveys, and gridded sources. The final grid resolution was 2 km. Ship track data in Davis Strait were readjusted using microlevelling techniques (Oakey et al., 1994) to produce improved versions of gridded data sets. In Baffin Bay, aeromagnetic data from the early 1960's was incorporated. These data had poor navigational accuracy (1-5 km), and were significantly out of level with the IGRF-91 model. Much of this data was still useable, as the density of marine observations was sparse. Onshore Canada, gridded magnetic anomaly data were provided by GSC-Ottawa with an original resolution of 1 km, whereas onshore Greenland, the regional survey data were collected by the American Naval Research Lab with a 10 km track spacing. A detailed coastal survey (64°–69°N) and a regional survey (south of 68°N) were provided by GEUS. The data around Disko came from the DNAG magnetic grid (Verhoef et al., 1996).

The 30,000 km industry seismic reflection data (Fig. 1) used in this project were from 13 different surveys acquired in the 1970's and early 1980's. The energy sources were arrays of airguns with a total volume of 1200 cu. inch at a pressure of 1800 psi. The receivers were hydrophone arrays of 2200-2400 m length. The data were processed to yield 24-fold stacked data, sampled at 4 msec with a record length of 6–8 sec. The interpretation, which was done on paper sections, concentrated on basement and volcanic structures. On most of the seismic lines the basement reflection is seen as the strongest reflection except for the seabed. In some places the basement surface is rough, and in others smooth, often draped by high-amplitude sedimentary horizons. The volcanic reflections are of relatively high amplitude with little energy

penetrating the horizon. In areas where volcanic rocks are exposed at seabed they obscure deeper signals preventing the interpretation of the basement surface.

A total of 73 bedrock samples for lithostratigraphic and biostratigraphic information are available in the area (MacLean, 1978; MacLean and Falconer, 1979; MacLean and Williams, 1983). The samples were retrieved by shallow corehole drilling and to a lesser extent by dredging, and the length of the samples ranges between 4 and 370 cm. On the Northeastern Baffin Shelf in area 1 (Fig. 1) ODP 645 was drilled in 1985 to a depth of 1140 m and penetrated sediments of Pliocene to early Miocene age (Srivastava et al., 1987). In the Saglek basin in area 3 (Fig. 1) the Hekja O-71 well was drilled to 3267 m in 1979 and deepened to 4566 m in 1980. The well penetrated sediments of dominantly nearshore to marine sandstones and shales of Pleistocene to Eocene age and terminated in Paleocene volcanic rocks (Klose et al., 1982). 26 km northeast of Hekja O-71, Raleigh N-18 was drilled in 1982 to a depth of 3858 m, and penetrated non-marine to inner shelf marine sediments of Pleistocene to late Paleocene age. A further 200 km to the northeast, the Gjoa G-37 well was drilled in 1979 to a depth of 3999 m and penetrated mudstones, siltstones, sandstone and coal of Pleistocene to Eocene age, volcanic rocks of late Paleocene age and possibly marine mudstones of Maastrichtian age (Klose et al., 1982). The bedrock samples and the four wells constrain the assigning of rock type to the seismic interpretations.

Interpretation of the geological and structural regimes

Regional setting

The Baffin Island margin (60°–72°N) can be divided into three areas based on the seismic reflection data (Fig. 1). Area 1, the Northeast Baffin Shelf, is characterized by extensive faulting and has a thin cover of sedimentary rocks that makes the basement reflection strong on the seismic data. Area 2, the central area off Cape Dyer, is characterized by volcanic rocks that are either exposed at the seabed or cover the basement in thick sequences, overlain by sediments. Area 3, the Southeast Baffin Shelf and the Saglek Basin, offshore Hudson Strait, is dominated by prograding sedimentary wedges that obscure interpretation of deeper reflections. The structural regime of the entire margin is dominated by elongate normal faults, often as a progression of successively deeper faults all dipping down to the east. The numerous major and minor graben structures and the fault patterns are typical extension features.

The potential field anomalies vary along the Baffin Island margin in a manner consistent with the divisions made on the basis of the seismic data. In area 1 there is a high gravity gradient from Baffin Island to Baffin Bay (Fig. 3), where negative anomalies, associated with the Precambrian rocks shift to positive anomalies seaward of the 500 m contour. Keen et al. (1990) attributed this to the proximity of the mountains on Baffin Island to the coast, the narrow shelf and the rapid transition to oceanic crust. In area 2, offshore Home Bay, there is a prominent local negative-positive pair of circular anomalies. Interpretation of high resolution seismic data in the region show that submarine debris flows have modified the continental slope in the Quaternary (Hiscott and Aksu, 1994). This process can produce paired negative and positive gravity anomalies as is shown further south on the southeastern margin of Canada (Courtney and Piper, 1992). Positive gravity anomalies on the Greenland margin north of 67°N are coincident with volcanic rocks (Escher and Pulvertaft, 1995). Between the margins in Baffin Bay, slightly positive to negative gravity anomalies are observed similar to those in the centre of the Labrador Sea. Offshore of the volcanic rocks on Cape Dyer, a gravity high is displayed. On the shelf, south of Cape Dyer from about 68°–63°N, a pronounced double peaked positive gravity anomaly (80-100 mGal) trending northeast is observed, which is closely associated with the volcanic rocks (Srivastava et al., 1981). In area 3 to the south, seaward of Hudson Strait at 61°N, a 100 km wide positive anomaly has been attributed to a prograding sedimentary wedge.

On the magnetic map (Fig. 4) in area 1, near 71°N, negative anomalies occur over the Scott Graben with positive anomalies on either side. Baffin Bay is dominated by lower amplitude, shorter wavelength anomalies. Seafloor spreading anomalies have been identified on only one survey where a station magnetometer was used to remove the large diurnal variations (Jackson et al., 1979). On the Greenland margin offshore Nuussuaq, a high-amplitude positive anomaly flanked by negatives overlies the region with volcanic rocks shown on the map of Escher and Pulvertaft (1995). In area 2, from Cape Dyer to the mouth of Frobisher Bay, linear, short wavelength magnetic anomalies correlate with the distribution of volcanic rocks (Srivastava et al., 1981). In area 3, south of 62°N, the narrow shelf, with depths of 500 m or less, exhibits a north–south trending linear anomaly that probably has its source in the Precambrian rocks. Further offshore the amplitude of the magnetic anomalies is subdued due to deeper water and a thick prograding sedimentary wedge. The Hekja and possibly Gjoa rises, and the Fylla structural complex (Fig. 1) show a magnetic character similar to that observed on the Precambrian onshore terranes (Oakey et al., 2000e). For example, a linear magnetic anomaly can be traced across the edge of Greenland intersecting the coast at 64°N and followed offshore across the

Fylla structural complex (Fig. 4).

Area 1

The overall structural pattern in area 1 (69°–72°N), is an elongate NW–SE striking fault pattern, almost parallel to the coast (Fig. 5). At the western part of Fig. 6 the basement surface can be seen dipping from onshore exposures in the west to a graben bounded by faults with throws up to 2 sec. Further east a 25–30 km broad basement high can be seen, where the basement surface is seen as a diffracted but clear reflection. The basement high can be followed all along the Northeast Baffin shelf, confirmed by a sample of metamorphic rocks (MacLean, 1978) to the north of line BE-74-51 (Figs 1 and 5). The western side of the basement high is limited by a westward-throwing continuous normal fault striking NW–SE, which can be interpreted from 67°30´–71°30´N sub-parallel to the present coastline at a distance varying between 20 and 40 km. On its eastern side the basement high is limited by synthetic normal faults throwing down to the east. The downfaulted basement (Fig. 6) terminates at one or several basement highs at a depth of 5 sec (4.5 km). These outer basement highs often display a hummocky basement surface, and can be interpreted from 69°30´N to 71°30´N (Fig. 5). At 130–150 km (on Fig. 6) the basement surface dips below 8 sec for 20 km before it rises again to about 5-6 sec becoming relatively flat and smooth.

The gravity profile along line BE-74-51 (Fig. 6) clearly shows the regional trend of negative to positive values. On the gravity map (Fig. 3) the western boundary of the inner graben structure is delimited by negative anomalies, -50 mGal, while over the basement high the gravity anomalies become more positive and decrease slightly on its seaward edge. The downfaulted basement is associated with slightly less negative values, -30 mGal. The western boundary of the hummocky basement is coincident with a transition from negative to positive values, -10 to +10 mGal, and the irregular basement highs (at 85–100 km on Fig. 6) are associated with positive anomalies, +10 mGal. Between the outer basement highs and where basement is observed again in deep water the amplitude of the gravity signature rises and falls with basement.

On the magnetic map (Fig. 4) the inner basement high is delineated as an elongate area with high-amplitude anomalies >200 nT. The easternmost boundary of the basement high on the slope coincides with negative anomalies (-100 to -200 nT) (Fig. 6). The downfaulted basement is associated with magnetic anomalies varying between -200 and +200 nT and the outer basement

highs show a diffuse pattern with both negative and positive anomalies (from -200 to -50 nT and in areas up to +200 nT).

Area 2

Area 2 is characterized by a change in direction of the fault pattern from NW–SE to the north of Cape Dyer, to almost N–S south of Cape Dyer (Fig. 5). Also the longitudinal continuous fault pattern displayed to the north changes to shorter, discontinuous faults. This area has been further subdivided into three sub-areas.

In area 2a, 67°30´–69°N, the margin is still dominated by the along-coast inner basement high seen to the north, while the downfaulted basement slope is less faulted than further north. In the offshore area between the Baffin Island and Greenland margins, a sedimentary cover up to 1.5 km thick overlies up to 4 km of probable volcanic rocks above the basement (Fig. 7). The volcanic rocks are thickest towards Greenland but the total thickness is unknown because strong seabed multiples obscure interpretation of the deeper sections on the seismic data.

The steep gravity gradients, and a magnetic anomaly pattern that is consistent with that to the north in central Baffin Bay could indicate that the offshore basement is oceanic crust (Jackson et al., 1979). The western side of the basement high is not well defined on either the seismic lines or the gravity map (Fig. 3) with slightly to strongly positive anomalies, up to +50 mGal. On the magnetic map (Fig. 4), the western flank of the basement high on the continental shelf in Home Bay is consistent with the edge of the strong negative anomalies, -60 mGal, and the high correlates with slightly magnetized areas, -30 to +20 nT, but the structure is not as clearly delimited on the magnetic data as that further north.

In area 2b, 66°30´–67°30´N, distinct seaward dipping reflections (SDRs) are interpreted (Fig. 8), crossing the margin from the coast near Cape Dyer. The SDRs are seen on 14 seismic lines (9 E–W lines) of relatively high quality where internal reflections can be interpreted and traced from line to line. The SDRs cover an area of approximately 130 km N–S and 100 km E–W. The dip direction of the SDRs changes from northeast in the north, becoming more easterly towards the south. The dip of the individual SDRs varies between 10° and 15°, becoming steeper with depth, up to 20°. Both before and at the end of the SDRs, a depression of the basement surface can be seen on the seismic data (Fig. 8 at 8 and 85 km). These dipping reflections have been previously identified by Grant (1975) and related to the Cape Dyer basalts.

On the gravity map this area is defined by neutral to slightly negative values (Fig. 3).The coastward boundary of the SDRs is delimited by an area with high-amplitude positive anomalies, +50 mGal, that gradually decrease seawards to +20 mGal, while the seaward end of the SDRs is as indistinct on the gravity data as on the seismic records. The volcanic rocks in the deep water show up clearly on the magnetic data (Fig. 4) with high amplitude anomalies ±150 nT similar to but reduced in amplitude and wavelength from the volcanic rocks on the Greenland margin. The coastward start of the SDRs (Fig. 8) is in the middle of large negative magnetic anomalies, -200 nT, whereas they end in an area with positive anomalies, +200 nT. The innermost part of Fig. 8, where volcanic rocks are exposed at seabed (Fig. 4) traverses an area with both high amplitude negative anomalies, -200 nT, and less strongly magnetized areas, -75 nT. Seaward neither the outer basement highs nor the areas with extensive volcanic rocks show up as significant structures on the magnetic map.

In area 2c, 63°–66°30´N, volcanic rocks dominate and in large areas they are exposed at seabed, confirmed by four basalt cores (Figs 1 and 5). Where volcanic rocks are exposed at the seabed, they obscure the interpretation of any deeper structures on the seismic data, so basement has not been mapped in these areas. Outside the areas with intense tectonic activity where volcanic rocks and basement are faulted independently, the volcanic surface imitates the basement relief. In the easternmost part, some badly defined basement highs can be seen, covered smoothly by a thin volcanic layer. The outer limit of the volcanic rocks has been interpreted to strike almost N–S along 58°W, and is bordered on its eastern side by a half graben, with throws up to 1 sec reducing towards the south. The volcanic area is characterized by a shift in direction of the fault pattern. Where the northern part is dominated by NE–SW striking faults, the fault system in the southern part bends more towards NNE–SSW.

The regional gravity low of up to -70 mGal, off Cumberland Sound and Cape Dyer (Fig. 3), is associated with Lower Palaeozoic limestones based on rock samples (MacLean et al., 1977). Seaward of this low, the distribution of volcanic rocks at seabed interpreted from the seismic data correlates with positive gravity anomalies (80 mGal). This is clearly illustrated along seismic line C-73-211 (Fig. 9) where the volcanic rocks at or close to seabed show up with high amplitude values. A basalt sample just south of this line corroborates our interpretation (Fig. 1). In the same area, smaller basement highs have been interpreted, which could indicate a thin volcanic cover and a shallow basement surface. On the gravity map (Fig. 3) two pronounced

gravity highs merge towards the north between 63°–65°N, supporting the presence of basement highs, which also can be seen on Fig. 9. The picture of high-amplitude negative and positive magnetic anomalies are consistent with the distribution of the volcanic rocks (Fig. 4).

Area 3

In the area between 60°–63°N at the western coverage of the seismic data, there is a restricted region with volcanic rocks exposed at seabed (Fig. 3). As in the area off Cape Dyer, the outer limit of the volcanic rocks has been interpreted and is here more curved than in the northern area, located at about 62°W. This region is dominated by westward prograding sedimentary wedges (Fig. 10) thickest at the present shelf break. Because of the thickness of the sediments, minimum 2 km, and the strong seabed multiples, it is only possibly to interpret basement in small discrete areas. Tucholke and Fry (1985) show the sedimentary thickness to be greater than 10 km in the Saglek Basin. This thickness is consistent with the refraction data from Funck and Louden (1999) and Chian et al. (1995b) further south on the Labrador margin. At the eastern end of the seismic data, a basement high has been interpreted on a few lines, but its possible continuation is unresolved. Area 3 shows a weakly defined fault system running almost N–S. The distribution of the volcanic rocks east of 64°W compared to area 2 where volcanic rocks are interpreted between 62° and 58°W, shows a marked displacement, which could indicate the presence of a transform fault striking almost straight E–W. South of 62°30´N the poor quality of the seismic data prohibits interpreting any feature deeper than the thick sedimentary wedges.

On the gravity map (Fig. 3) the prograding sediments show up clearly and conform with high positive gravity values, greater than +80 mGal. The region with volcanic rocks exposed at seabed has strongly positive magnetic anomalies, greater than +150 nT (Fig. 4), and the outer limit of the volcanic rocks is compatible with the edge of a negative anomaly of -100 nT. This area shows slightly negative values, 0 to -75 nT consistent with a deep basement.

Discussion

Interpretation of the volcanic or non-volcanic margin

Most of the margins of eastern Canada are interpreted to be non-volcanic (Louden and Chian, 1999) with the exception of the southwestern portion of the Scotian margin (Keen and Potter, 1995). On the Scotian margin (inset at Fig. 2) the disappearance of the East Coast Magnetic Anomaly and seaward dipping reflector sequences marks a transition from south to north from a

volcanic to a non-volcanic margin. The Newfoundland Basin east of the Grand Banks is largely non-volcanic (Reid, 1994; Todd and Reid, 1989; Srivastava and Roest, 1999); the eastern margin of Flemish Cap, just south of Orphan Basin (Reid and Keen, 1990); and the conjugate margins of Labrador and Southwest Greenland (Chian et al., 1995b; Louden and Chian, 1999) are also interpreted as non-volcanic margins.

Volcanic margins can be characterized by high-velocity lower crust, the presence of SDRs and a magnetic anomaly associated with the high-velocity lower crust (Holbrook and Keleman, 1993). Non-volcanic margins can be characterized by lower seismic velocities in the lower crust than at the volcanic margins, a lack of SDRs, block-faulted basement interpreted as thinned continental crust (Holbrook and Keleman, 1993), and can also be characterized by the presence of serpentinized peridotite both under thinned continental crust and between the continental and oceanic crust (Pickup et al., 1996). Non-volcanic margins are also less elevated than volcanic margins because of the absence of a thick igneous crustal layer (Ruppel, 1995).

The seismic reflection, bathymetry and potential field data we have assembled here enable us to trace block-faulted crust, seaward dipping reflector sequences, and magnetic anomalies along the margin. New reflection and refraction sections are available on the nearby southern West Greenland margin (Chian and Louden, 1992; Chalmers et al., 1993; Chalmers et al., 1995; Chalmers, 1997; Chalmers and Pulvertaft, in press; Louden and Chian, 1999) and wide-angle reflection and refraction data on the northern Labrador margin (Funck and Louden, 1999). Detailed investigations of the continent-ocean boundary are available in the Labrador Sea (Roest and Srivastava, 1989; Chalmers, 1991; Chalmers and Laursen, 1995; Chian et al., 1995a, b; Louden and Chian, 1999).

Off Baffin Island, area 1 is interpreted as a non-volcanic passive margin. The seismic reflection lines show prominent coast-parallel grabens and basement highs (Fig. 1) flanked by a deepening basement with synthetic normal faults down the slope (Fig. 6). There is no evidence for SDRs or a magnetic anomaly associated with the slope. A seismic refraction survey across the margin and into Baffin Bay at 72°N did not detect high-velocity lower crust (Jackson et al., 1979). These observations clearly indicate extension with limited volcanism.

Area 2, the area off Cape Dyer, with exposed volcanic rocks onshore, the presence of SDRs (66°30′–67°30′N) and substantial amounts of volcanic rocks offshore is clearly different from the

non-volcanic margin to the north. The SDRs are indicative of the presence of a spreading axis with extensive subaerial eruption (Mutter, 1985; Talwani et al., 1981; Geotimes, 1982). In the region with the SDRs, the coastline, the fault pattern, and the structures on the magnetic and gravity maps change from a NW–SE direction in the northern part to a N–S direction in the south (Fig. 3). This change in fault directions forms a corner at the junction of the Northeast and Southeast Baffin shelves. The faults and structural features that make this corner are inherited from the prerift geology and suggest major crustal faults. Large scale upper crustal faulting has been suggested by Boutilier and Keen (1994) to control the position and growth of mantle instabilities. Thus the structurally weak corner may have channelled the extensive regional magmatism. On the opposite side of Davis Strait off southwestern Greenland Chalmers and Laursen (1995) interpreted SDRs on the BGR/77-6 seismic line, and interpreted parts of the margin as volcanic. This is south of the region with extensive volcanic rocks on the West Greenland margin and would have been significantly south of Cape Dyer in a plate reconstruction; however, it may indicate that magmatism associated with the rifting and producing the high-velocity lower crust extends over a greater area than previously documented (Henderson, 1973, Henderson et al.,1981; Whittaker 1996; Srivastava et al., 1981; Balkwill et al., 1990). The interpretations on both sides of the Davis Strait of seaward-dipping reflectors and extensive volcanic rocks are consistent with a volcanic margin in the vicinity of Davis Strait.

In area 3 on the southern section of the Southeast Baffin Shelf a major E–W striking transform fault at 63°N is postulated (Fig. 5), based on the interpretation of the volcanic areas compared to the magnetic anomalies. West of the volcanic zone (Fig. 4), two magnetic highs, a strong positive followed seawards by a strong negative, can be seen, and a similar set of magnetic anomalies can be seen for a short distance north of the interpreted transform fault and displaced by 110 km eastwards. Tucholke and Fry (1985) show the offset clearly on their depth to basement map, and Balkwill (1987) calls it the Lady Franklin Arch. If this area is bounded by a transform fault then the distribution of volcanic rocks, extensive to the north and lesser amounts to the south, can be explained by segmentation. For example, large contrasts in geochemical and geophysical properties are separated by transforms in the Southeast Indian Ridge including varying mantle temperatures and melt production rate (Sempéré et al., 1996).

The prograding sedimentary wedges in area 3 conceal the basement on many of the seismic lines. Tucholke and Fry's (1985) sediment thickness map shows a steep nearshore slope with 10 km of sediments in the basin. On the northern (Funck and Louden, 1999) and southern

Labrador (Chian and Louden, 1994) margins an 8-9 km thickness of sediments was measured with the refraction technique. This thickness is consistent with the large sedimentary source from the adjacent mainland and through present day Hudson Strait. The drainage areas include present day Hudson Bay, the southeastern part of the Northwest Territories, all of Alberta including the Cordillera, Saskatchewan, Manitoba, northern Ontario and northwestern Quebec (McMillian, 1973).

On the northern Labrador margin (inset Fig. 2) no high-velocity lower crust was measured beneath the thinned continental crust (Funck and Louden, 1999). No underplated layer was observed on the southern Labrador margin 55°–58°N (Chian and Louden, 1994) based on refraction velocities; instead, a crust typical for non-volcanic margins was documented. Extrapolating northward, we suggest that the southern part of the Southeast Baffin margin adjacent the Saglek Basin is also non-volcanic. The depth to basement is greater than on the margin north of the Lady Franklin arch consistent with Ruppel's (1995) observation that non-volcanic margins are less elevated than volcanic margins.

Determination of the continent-ocean boundary

From studies in adjacent and analogous areas, there is consensus on dividing the seaward edge of passive non-volcanic margins into continental, transitional and oceanic crust. An along-coast basement high and faulted basement blocks down the slope is generally interpreted as continental crust (Chalmers, 1997; Pickup et al., 1996; Beslier et al., 1993). Transitional crust on a non-volcanic margin is characterized by the presence of serpentinized peridotite, both under thinned continental crust and between continental and oceanic crust (Pickup et al., 1996). The transitional crust between the continental and oceanic crust is sometimes dominated by grabens and half-grabens (Chalmers, 1997; Keen et al, 1994) sometimes not (Chian et al., 1995a), whereas the oceanic crust often is characterized by a smoother basement surface (Chalmers, 1997; Keen et al., 1994) with associated linear magnetic anomalies.

In area 1, the coast-parallel graben, basement high and block-faulted slope are interpreted to be underlain by continental crust. This interpretation is supported by magnetic anomalies that mimic the basement highs and graben structures (Fig. 4). The outer edge of the hummocky basement occurs in a region with high gravity gradients from negative to positive values, but no significant magnetic anomalies. Seaward of the outer edge of the hummocky basement, the surface becomes smoother and a little more diffractive. The magnetic anomaly pattern is shorter in

wavelength and smaller in amplitude, which is typical for the deep water region of Baffin Bay where weak lineations associated with seafloor spreading have been identified (Jackson et al., 1979). Thus seaward of the hummocky basement oceanic crust is inferred. This leaves a 30 km wide zone of transitional crust. The inner boundary of the oceanic crust conforms with slightly positive gravity anomalies, 10-20 mGal (Fig. 3), whereas on the magnetic map it is coincident with the landward margin of a strong negative area, -75 nT.

Seaward dipping reflections are generally recognized as lying at the continent-ocean boundary of volcanic margins (Mutter, 1985), so the recognition of the SDRs in this area is an important point in favour of the region being floored by oceanic crust and strengthens the arguments against those who believe Baffin Bay is continental. In area 2 where the volcanic rocks and SDRs dominate, the boundary between continental and oceanic crust is picked at the landward end of the SDRs to be consistent with other volcanic margins (Holbrook and Keleman, 1993). This places the continent-ocean boundary within 50 km of the shoreline. On the gravity map (Fig. 3) this coincides with the seaward limit of a strong positive anomaly, 60 mGal, whereas on the magnetic map (Fig. 4) it follows the seaward limit of a large negative anomaly, greater than -200 nT.

Along the Labrador and southern West Greenland margins a transition zone consisting of highly-stretched continental crust and serpentinized peridotite is interpreted to separate continental and oceanic crust, while along the southeast Baffin Island margin the continent-ocean boundary seems to be a complex transform zone which developed during sea-floor spreading in the late Paleocene and early Eocene (Chalmers & Pulvertaft in press). In area 3, on the Southeast Baffin Shelf, the boundary between continental and transitional crust was predicted on the basis of gravity anomalies. Where the prograding sedimentary strata are responsible for the pronounced gravity high, the anomaly is thought not to be caused by basement structures. The continent-ocean boundary was shifted landward to conform with the seaward limit of a positive gravity anomaly (Fig. 3). On the magnetic map (Fig. 4), the boundary follows an area with highly negative anomalies. Here the continent-ocean boundary is within 40 km of the coast. The linear magnetic anomalies can be traced shoreward beyond the gravity high that was interpreted to be the continent-ocean boundary by Srivastava and Roest (1999). The presence of linear magnetic anomalies in the Saglek Basin suggests oceanic crust. Funck et al. (2000) noted that the gravity anomaly in combination with their tomographic study of northern Labrador suggests a much reduced crustal thickness in NE Ungava Bay and across the northern tip of Labrador that they

attribute to the rifting pattern in the Labrador Sea.

Implications of the plate reconstructions

Storey et al. (1998) suggested that the presence of Palaeogene volcanic rocks on both sides of the Davis Strait is the first product of the Icelandic mantle plume that now forms a submerged large igneous province. The first period of erupted volcanic rocks in West Greenland was dated to between 60.7 ±0.5 and 59.4 ±0.5 Ma (Storey et al., 1998). Within this first period of eruption the C27n/C26r polarity transition was recorded by Riisager and Abrahamsen (1999). A second period of eruption onshore West Greenland, recorded in dike and sill complexes on Nuussuaq and Disko was dated as 54.8 ±0.4 Ma and 53.6 ±0.3 Ma by Storey et al. (1998). Geoffroy et al. (2001) dated five basaltic dikes on the south coast of Svartenhuk Halvø as 54.6 ±0.6 Ma. On the Greenland margin, the offshore Hellefisk-1 well provides an age for the basalt of 57.7 ±1.2 Ma (Williamson *et al.* 2001), which belongs to the C26n magnetic chron (Cande & Kent, 1995). Onshore Baffin Island, the Cape Dyer basalts gave an K/Ar age of 58 ± 2 Ma (Clark and Upton, 1971), and is normally magnetized (Deutsch et al., 1971), so they probably belong to the C27n magnetic chron C27n (Cande and Kent, 1995). On the Canadian margin, in the offshore well Gjoa G-37, two samples from a basaltic flow has been dated to 59.5 ± 1 Ma and 59.2 ± 1.8 Ma (Williamson *et al.* 2001), which according to Cande and Kent (1995) means that they belong to the magnetic chron C26r. Thus it seems from the dates that there have been two pulses of volcanism; one recognized in both West Greenland and eastern Canada, erupted between 60.7 and 57.7 Ma, and a second pulse erupted between 54.8 and 53.6 Ma which until now has only been recognized in West Greenland.

The interpretation of the seismic data presented here has extended the mapped volcanic area on the Canadian side, both in the north–south direction and eastwards towards Greenland. On the West Greenland margin the volcanic province in the Disko–Svartenhuk area is well documented (e.g. Henderson 1973; Clarke and Pedersen, 1976; Whittaker, 1995, 1996; Larsen and Pedersen, 1988; Skaarup et al. 2000; Larsen and Pulvertaft, 2000). South of the mapped volcanic rocks, a seaward dipping reflector sequence observed on a seismic reflection line in this region (Chalmers and Laursen, 1995) and the volcanic rocks drilled in the Nukik-2 well, are evidence of at least limited extrusion. This increases the size of the volcanic province also on the Greenland margin. On the magnetic map (Fig. 4) the volcanic rocks on the Canadian side are characterized by a short-wavelength high-frequency pattern, whereas the Greenland volcanic province is characterized by a longer wavelength high-frequency pattern. This could

imply that there is no direct continuation of the volcanic rocks.

In order to make plate reconstructions, continent-ocean boundaries (COB's) on both sides of the Baffin Bay/Davis Strait have to be determined. In this project, a plate boundary adjacent to Baffin Island on the North American plate has been interpreted. As discussed above, this boundary differs significantly from that of Srivastava & Roest (1999) in area 3 on the southeast Baffin Shelf. On the Greenland plate the continent-ocean boundary has been assembled from three different sources: on the southern West Greenland margin the boundary interpreted by Chalmers & Laursen (1995)has been used. This interpretation was based primarily on modelling of magnetic data controlled by the interpretation of seismic reflection data. The boundary is drawn seaward of the Fylla structural complex, consistent with the striking linear magnetic anomaly that can be traced from Greenland across the complex (Fig. 4). The boundary is also consistent with the results of the Qulleq-1 well (Fig. 1), drilled in the summer of 2000 (Christiansen et al., in press.), where sediments of Santonian age were penetrated. On the central West Greenland margin, the boundary has been drawn outside the area where continental crust has been interpreted from unpublished seismic reflection data and gravity modelling. On the northern West Greenland margin in the Melville Bay the boundary interpreted by Whittaker et al. (1997) has been used. The presence of continental crust has been derived from interpretation of seismic reflection and gravity data.

To examine the consequences with the plate boundaries used here, we have made plate reconstructions to both chron 33 (Roest and Srivastava, 1989) and chron 27 time (Chalmers and Laursen, 1995) because both have been suggested as the initial opening (Fig. 11). The published poles of rotation of Roest and Srivastava (1989) were used to close the intervening ocean.

The rotation with seafloor spreading initiated at anomaly 33 time, proposed by Roest and Srivastava (1989), leaves a gap between the COB's in the Labrador Sea (Fig. 11a) indicating that opening started slightly earlier. This rotation would imply that the area labelled as transitional crust in Fig. 2 was either oceanic or serpentinized mantle similar to that on the Iberia margin (Chian and Louden, 1994; Chalmers, 1997; Louden and Chian, 1999; Dean et al., 2000; Chalmers and Pulvertaft, in press). South of Davis Strait, the two continent-ocean boundaries come nearly adjacent to each other, but there is a serious overlap to the north. If rifting propagated from the North Atlantic through the Labrador Sea and then into Baffin Bay, this

overlap in Baffin Bay would be expected and suggests that oceanic crust was not created in Baffin Bay at this time. The large Melville Bay graben on the West Greenland margin could accommodate the continental stretching. However, between Cape Dyer and the Disko–Svartenhuk region the overlap is a problem (Fig. 11a), and the COB on the North American plate is drawn so close to Cape Dyer that little space for continental stretching is available.

Chalmers and Laursen (1995) proposed that seafloor spreading was initiated at anomaly 27 time. This means that between anomaly 27 and the edge of the continental shelf, in a 100–150 km broad region, the continental crust must have been extensively stretched or serpentinized mantle was unroofed (Chian and Louden, 1994; Chalmers, 1997; Louden and Chian, 1999; Chalmers and Pulvertaft, in press). Since anomaly 27 time, when the large igneous province was extruded (Storey et al., 1998), Greenland has moved 300 km north relative to the North American plate (Fig. 11b). In the Labrador Sea, the rotation reveals a large gap between the two COB's whereas in the Davis Strait an overlap of the volcanic rocks on the shelves is seen and a continuous igneous province is formed. In Baffin Bay the COB's coincide better with the rotation at 27 time, instead of 33 time, but still leaves a minor overlap.

The preliminary results of the plate reconstructions presented here with seafloor spreading initiated at two different times, leaves some problems to be solved. Since the publication of the poles of rotation (Roest and Srivastava, 1989) higher resolution magnetic data for the triple junction to the south of Greenland have been made available. These data need to be evaluated to ensure that the poles of rotation are accurate. A revised set of poles might solve some of the problems with overlap and gaps between the continent-ocean boundaries of the North American and Greenland plate. Revising the poles from Roest and Srivastava (1989) is, however, beyond the scope of this paper.

Conclusion

The two major results of this paper are the division of the Baffin Island margin into non-volcanic and volcanic regions and a reinterpretation of the continent-ocean boundary. The data presented here, in particular, the seaward dipping reflector sequence displayed on the seismic sections, the samples of volcanic rock and the high-frequency magnetic anomalies associated with positive gravity signature indicate extensive magmatism associated with the central portion

of the margin. The Icelandic mantle plume is the probable source for the extensive volcanism in the region. In contrast, the margin segments to north and south of the central areas show no evidence of volcanism based on rock samples, seismic or potential field signature. They are interpreted to be non-volcanic, consistent with the majority of the margins of eastern Canada. Margin segmentation can explain the containment of the magmatism. The seismic data and potential field data are used to determine a continent-ocean boundary that is closer to the coastline of Canada than previously published. This reduces the overlap in published plate reconstructions in the Labrador Sea region and places the volcanic provinces on the conjugate margins adjacent to each other. However, the significant overlap in the Davis Strait regions highlights the need for reviewing the plate reconstruction and for co-operative studies on the conjugate margins of North America and Greenland.

References

Balkwill, H. R. (1987) Labrador Basin: Structural and stratigraphic style, *Canadian Society of Petroleum Geologists Memoir* **12** 17-43

Balkwill, H. R., McMillan, N. J., MacLean, B., Williams, G. L. and Srivastava, S. P (1990) Geology of the Labrador shelf, Baffin Bay and Davis Strait, *Geological Survey of Canada* (Eds. Keen, M. J. and G. L. Williams, Chapter 7 in Geology of the continental margin of eastern Canada, **2** 293-348 (Also *Geological Society of America*, The Geology of North America **I-1**)

Beslier, M.-O., Ask, M. and Boillot, G. (1993) Ocean-continent boundary in the Abyssal Plain from multichannel seismic data, *Tectonophysics* **218** 383-393

Boutilier, R. R. and Keen, C. E. (1994) Geodynamic models of fault-controlled extension, *Tectonics* **13** 439-454

Cande, S. C. & Kent, D. V. 1995. Revised calibration of the geomagnetic polarity timescale for the Late Cretaceous and Cenozoic *Journal of Geophysical Research* **100** 6093-6095

Chalmers, J. A. (1991). New evidence on the structure of the Labrador sea/Greenland continental margin. Journal of the Geological Society, London, 148: 899-908

Chalmers, J. A. (1997) The continental margin off southern Greenland: along-strike transition from an amagmatic to a volcanic margin, *Journal of Geological Society, London* **154** 571-576

Chalmers, J. A., Larsen, L. M. and Pedersen, A. K., 1995. Widespread Palaeocene volcanism around the northern North Atlantic and Labrador Sea: evidence for a large, hot, early plume head. Journal of the Geological Society, London, 152: 965-969

Chalmers, J. A. and Laursen, K. H. (1995) Labrador Sea: the extent of continental and oceanic crust and the timing of the onset of seafloor spreading, *Marine and Petroleum Geology* **12** 205-217

Chalmers, J. A. and Pulvertaft, T. C. R. (in press) Development of the continental margins of the Labrador Sea - a review. submitted to *The Geological Society of London, Special Publication*

Chalmers, J. A., Pulvertaft, T. C. R., Christiansen, F. G., Larsen, H. C., Laursen, K. H. and Ottesen, T. G. (1993) The southern West Greenland continental margin: rifting history, basin development, and petroleum potential: *Petroleum Geology of Northwest Europe*, Proceedings of the 4th Conference, The Geological Society, London 915-931

Chian, D. and Louden, K. E. (1992) The structure of Archean/ketilidian crust along the continental shelf of southwest Greenland from a refraction profile, *Canadian Journal of Earth Sciences* **29** 301-313

Chian, D. and Louden, K. E. (1994) The continent-ocean crustal transition across the southwest Greenland margin *Journal of Geophysical Research* **99** 9117-9135

Chian, D., Keen, C., Reid, I. and Louden, K. E. (1995a) Evolution of the nonvolcanic rifted margins: new results from the conjugate margins of the Labrador Sea, *Geology* **23** 589-592

Chian, D., Louden, K. E. and Reid, I. (1995b) Crustal structure of the Labrador Sea conjugate margin and implications for the formation of nonvolcanic margins, *Journal of Geophysical Research* B12 **100** 24239-24253

Christiansen, F. G., Bojesen-Koefoed, J. A., Chalmers, J. A., Dalhoff, F., Mathiesen, A., Sønderholm, M., Dam, G., Gregersen, U., Marcussen, C., Nøhr-Hansen, H., Piasecki, S., Preuss, T., Pulvertaft, T. C. R., Rasmussen, J. A. and Sheldon, E. (in press) Petroleum geological activities in West Greenland in 2000 *Geology of Greenland Survey Bulletin*

Clarke, D. B. & Pedersen, A. K. (1976) Tertiary volcanic province of West Greenland *in* Escher, A. & Watt, W. S. (eds) Geology of Greenland. *The geological Survey of Greenland*, 365-385.

Clarke, D. B. and Upton, B. G. J. (1971) Tertiary basalts of Baffin Island: Field relationships and Tectonic setting, *Canadian Journal of Earth Sciences* **8** 248-257

Courtney, R. C. and Piper, D. J. W. (1992) The gravity signature of a large Quaternary Depocentre off southeast Canada, *Geographie, physigue et Quaternaire* **48** 349-360

Dean, S. M., Minshull, T. A., Whitmarch, R. B., and Louden, K. E. (2000) Deep crustal structure of the Ocean-continent transition in the southern Iberian Abyssal Plain from seismic refraction profiles: The IAM-9 transect at 40°20' N *Journal of Geophysical Research* **B3** 5859-5885

Deutsch, E. R., Kristjansen, L.G. and May, B. T. (1971) Remanent magnetism of lower Tertiary lavas on Baffin island, *Canadian Journal of Earth Sciences*, **8**, 1542-1552.

Ekholm, S. (1996) A full coverage, high-resolution, topographic model of Greenland computed from a variety of digital elevation data, *Journal of Geophysical Research* **B10** 21961-21972

Esher, J. C. and Pulvertaft, T. C. R. (1995) Geological map of Greenland, 1:2,500,000 Copenhagen, Geological Survey of Greenland

Funck, T. and Louden, K. E. (1999) Wide angle seismic transect across the Torngat Orogen, northern Labrador: Evidence for a Proterozoic crustal root, *Journal of Geophysical Research* **104** 7463-7480

Funck, T. and Louden, K. E., Wardle, R. J., Hall, J., Hobro, J. W., Salisbury, M. H. and Muzzatti, A. (2000) Three-dimensional structure of the Torngat Orogen (NE Canada) from active seismic tomography *Journal of Geophysical Research* **B10** 23,403-23,420

Geoffroy, L., Callot, J.-P., Scaillet, S., Skuce, A., Gélard, J. P., Ravilly, M., Angelier, J., Bonin, B., Cayet, C., Perrot, K. and Lepvrier, C. 2001. Southeast Baffin volcanic margin and the North American-Greenland plate separation. *Tectonics*, **20**, 566-584

Geotimes (1982) Leg 81 drills west margin, Rockall Plateau, *Geotimes* **September** 21-23

Grant, A. C. (1975) Geophysical results from the continental margin off southern Baffin Island, in Canada's continental margins and offshore petroleum exploration (Eds. Yorath, C. J., Parker, E. R. and Glass, D. J.) *Canadian Society of Petroleum Geologists Memoir* **4** 103-131

GTOPO 30 : Global 30 Arc Second Elevation data (1999) United States Geological Survey, National Mapping Division, EROS Data Centre

Henderson, G. 1973. The geological setting of the West Greenland basin in the Baffin Bay region *Geological Survey of Canada Paper*, **71-23**, 521-544

Henderson, G., Schiener, E. J., Risum, J. B., Croxton, C. A. and Andersen, B. B. (1981) The West Greenland Basin in Geology of the North Atlantic Borderlands, *Canadian Society of Petroleum Geologists Memoir* **7** 399-428

Hiscott, R. N. and Aksu, A. E. (1994) Submarine debris flows and continental slope evolution in Front of Quaternary Ice sheets, Baffin Bay, Canadian Arctic, *American Association of Petroleum Bulletin* **78** 445 -459

Holbrook, W. S. and Kelemen, P. B. (1993) Large igneous province on the US Atlantic margin and implications for magnetism during continental breakup, *Nature* **364** 433-436

Jackson, H. R., Keen, C. E., Falconer, R. H. K. and Appleton, K. (1979) New geophysical evidence for seafloor spreading in Baffin Bay, *Canadian Journal of Earth Sciences* **16** 2122-2135

Jackson, H. R., Dickie, K. and Marillier, F. (1992) A seismic reflection study of northern Baffin Bay: implication for tectonic evolution, *Canadian Journal of Earth Sciences* **29** 2353-2369

Johnson, G. L., Srivastava, S. P., Campsie, S. P. and Rasmussen, M. (1982) Volcanic rocks in the Labrador Sea and environs and their relation to the evolution of the Labrador Sea, in: *Current Research, Part B, Geological Survey of Canada* **82-1B** 7-20

Keen, C. E., Loncarevic, B, D., Reid, I., Woodside, J., Haworth, R. T. and Williams, H. (1990) Tectonic and geophysical overview, in: Geology of the continental margins of eastern Canada (Eds. Keen, M. J. and Williams, G. L.) **2** 31-84 (also Geological Society of America, The Geology of North America **I-1**)

Keen, C. E., Potter, P. & Srivastava, S. P. (1994) Deep seismic reflection data across the conjugate margins of the Labrador Sea, *Canadian Journal of Earth Sciences* **31** 192-205

Keen, C. E. and Potter, P. (1995) The transition from a volcanic to a nonvolcanic margin off

eastern Canada, *Tectonics* **14** 359-371

Klose, G. W., Malterre, E., McMillan, N. J. & Zinkan, C. G. (1982) Petroleum exploration offshore southern Baffin Island, Northern Labrador Sea, Canada, in: Arctic geology and geophysics (Eds. Embry, A. F. & Balkwill, H. R.) *Canadian Society of Petroleum Geologists Memoir* **8** 233-244

Larsen, J. G. & Pulvertaft, T. C. R. 2000. The structure of the Cretaceous-Palaeogene sedimentary-volcanic area of Svartenhuk Halvø, central West Greenland. *Geology of Greenland Survey Bulletin*, **188**, 40 pp.

Larsen, L. M. & Pedersen, A. K. (1988) Investigations of Tertiary volcanic rocks along the south coast of Nûgssuaq and in Western Disko, 1987 *Rapport Grønlands Geologiske Undersøgelse* **124** 28-32

Louden, K. E. and Chian, D. (1999) The deep structure of non-volcanic rifted continental margins *Philosophical Transactions of the Royal Society*, London **357** 767-804

MacLean, B. (1978) Marine geological-geophysical investigations in 1977 of the Scott inlet and Cape Dyer - Frobisher Bay areas of the Baffin Island continental shelf, in: *Current Research, Part B, Geological Survey of Canada* **78-1B** 13-20

MacLean, B. & Falconer, R. H. K. (1979) Geological/geophysical studies in Baffin Bay and Scott Inlet-Buchanan Gulf and Cape Dyer-Cumberland Sound areas of the Baffin Island shelf, in: *Current Research, Part B, Geological Survey of Canada* **79-1B** 231-244

MacLean, B., Jansa, L. F., Falconer, R. H. K. and Srivastava, S. P. (1977) Ordovician strata on the southwest Baffin island shelf revealed by shallow drilling, *Canadian Journal of Earth Sciences* **14** 1925-1939

MacLean, B. and Williams, G. L. (1983) Geological investigations of the Baffin Island shelf in 1982, in: *Current Research, Part B, Geological Survey of Canada* **83-1B** 309-315

McMillan, N. J. (1973) Shelves of Labrador Sea and Baffin Bay, Canada, in: The Future Petroleum Provinces of Canada - their geology and potential (McCrossman, R. G.), *Canadian*

Society of Petroleum Geologists, Memoir **1** 473-517

Mutter, J. C. (1985) Seaward dipping reflectors and the continent-ocean boundary at passive continental margins, *Tectonophysics* **114** 117-131

Oakey, G., Kovacs, L. C., Roest, W. R., Macnab, R., Verhoef, J. and Arkani-Hamed, J., (1994) Pre-processing of NRL Aeromagnetic data in the Norwegian and Greenland Seas and the Amerasian Basin, AGU Spring Meeting

Oakey, G., Ekholm, S. and Jackson, H. R. (2000a) Physiography of the Davis Strait Region, Canadian and Greenland Arctic, *Geological Survey of Canada* Open file, scale 1:1,500,000

Oakey, G., Ekholm, S., Jackson, H. R. and Marcussen, C. (2000b) Physiography of the Baffin Bay Region, Canadian and Greenland Arctic, *Geological Survey of Canada* Open file, scale 1:1,500,000

Oakey, G., Forsberg, R. and Jackson, H. R. (2000c) Gravity of the Davis Strait Region, Canadian and Greenland Arctic, *Geological Survey of Canada* Open file, scale 1:1,500,000

Oakey, G. Forsberg, R. and Jackson, H. R. (2000d) Gravity Anomaly of the Baffin Bay Region, Canadian and Greenland Arctic, *Geological Survey of Canada* Open file, scale 1:1,500,000

Oakey, G. and Jackson, H. R. (2000e) Magnetic Anomaly of the Davis Strait Region, Canadian and Greenland Arctic, *Geological Survey of Canada* Open file, scale 1:1,500,000

Oakey, G. and Jackson, H. R. (2000f) Magnetics Anomaly of the Baffin Bay Region, Canadian and Greenland Arctic, *Geological Survey of Canada* Open file, scale 1:1,500,000

Pickup, S. L. B., Whitmarsh, R. B., Fowler, C. M. R. & Reston, T. J. (1996) Insight into the nature of the ocean-continent transition off West Iberia from a deep multichannel seismic reflection profile, *Geology* **24** 1079-1082

Reid, I. (1994) Crustal structure of a nonvolcanic rifted margin east of Newfoundland, *Journal of Geophysical Research* **99** 15161-15180

Reid, I. D. and Keen, C. E. (1990) High seismic velocities associated with reflections from within the lower oceanic crust near the continental margin of eastern Canada, *Earth and Planetary Science Letters* **99** 118-126

Reid, I and Jackson, H. R. (1997) Crustal structure of northern Baffin Bay, seismic refraction results and tectonic implication, *Canadian Journal of Earth Sciences* **102** 523-542

Riisager, P. & Abrahamsen, N. 1999 Magnetostratigraphy of Paleocene basalts from the Vaigat Formation of West Greenland, *Geophysical Journal International* **137** 774-782

Roest, W. R. and Srivastava, S. P. (1989) Sea-floor spreading in the Labrador Sea: A new reconstruction, *Geology* **17** 1000-1003

Ruppel, C. (1995) Extensional processes in continental lithosphere, *Journal of Geophysical Research* B12 **100** 24187-24215

Sempéré, J-C., West, B. P. and Geli, L. (1996) The Southeast Indian Ridge between 127° and 132°40'E: contrasts in segmentation characteristics and implication for crustal accretion, in: Tectonic, Magmatic, hydrothermal and Biological segmentation of the Mid-ocean ridges (Eds. Macleod, C. J., Tyler, P. A. and Walker, C. L. *Geological Society Special Publication* **118** 1-15

Skaarup, N., Chalmers, J. A. and White, D. (2000) An AVO study of a possible new hydrocarbon play, offshore central West Greenland. *AAPG Bulletin* **84** 174-182

Smith W. H. F. and Wessel, P. (1990) Gridding with continuous curvature spines in tension, *Geophysics* **55** 293-305

Srivastava, S. P., Falconer, R. K. H. and MacLean, B. (1981) Labrador Sea, Davis Strait and Baffin Bay: Geology and Geophysics A review, in: Geology of the North Atlantic Borderlands (Eds. Kerr, J. W., Ferguson, A. J. and Machan, L. C.) *Canadian Society of Petroleum Geologists Memoir* **7** 333-398

Srivastava, S. P., Arthur, M., Clement B. et. al. (1987) 4. Site 645, in Proceedings, initial reports,

ODP leg 105 (Eds. Srivastava, S. P., Arthur, M., Clement, B. et. al.) 131-150

Srivastava, S. P and Roest, W. R. (1995) Nature of thin crust across the southwest Greenland margin and its bearing on the location of the ocean-continent boundary, in: *Rifted ocean-continent boundaries* (Eds. Banda et al.) Kluwer Academic Publishers, Netherlands 95-120

Srivastava, S. P. & Roest, W. R. (1999) Extent of oceanic crust in the Labrador Sea, *Marine and Petroleum Geology* **16** 65-84

Storey, M., Duncan, R. A., Pedersen, A. K., Larsen, L. M. and Larsen, H. C. (1998) 40Ar/39Ar geochronology of the West Greenland Tertiary volcanic province, *Earth and Planetary Science Letters* **160** 569-586

Talwani, M, Mutter, J. C. & Eldholm, O. (1981) Initiation of opening of the Norwegian Sea, *Oceanol. Acta. SP* 23-30

Todd, B. J. and Reid, I. (1989) The continent-ocean boundary south of Flemish Cap: constraints from seismic refraction and gravity, *Canadian Journal of Earth Sciences* **25** 744-759

Tucholke, B. E. and Fry, V. A. (1985) Basement structure and sediment distribution in Northwest Atlantic Ocean, *The American Association of Petroleum Geologists Bulletin* **69** 2077-2097

Verhoef, J., Roest, W. R, Macnab, R. Arkhani-Hamed, J., and Members of the Project Team (1996)
Magnetic anomalies of the Arctic and North Atlantic Oceans and adjacent Land Areas, Geological Survey of Canada Open File report 3151, CD-Rom

Whittaker, R. C. (1995) A preliminary assessment of the structure, basin development and petroleum potential offshore central West Greenland *Grønlands Geologiske Undersøgelse Open File Series* **95/9** 1-43

Whittaker, R. C. (1996) A preliminary seismic interpretation of an area with extensive Tertiary basalts offshore central West Greenland *Bulletin Grønlands Geologiske Undersøgelse*, **172**, 28-31

Whittaker, R. C., Hamann, N. E. and Pulvertaft, T. C. R. 1997. A New Frontier Province Offshore Northwest Greenland: Structure, Basin Development, and Petroleum Potential of the Melville Bay Area. *AAPG Bulletin* **81** 978-998

Williamson, M.-C., Villeneuve, M. E., Larsen, L. M., Jackson, H. R., Oakey, G. N. & MacLean, B. (2001) Age and petrology of offshore basalts from the Southeast Baffin Shelf, Davis Strait, and Western Greenland continental margin *St. John's 2001* Conference abstract, **26**, 162

Figure captions:

Figure 1: Newly compiled physiographic map. The solid black lines show the tracks of the industry seismic reflection lines used in this study. The numbered lines locate the seismic lines displayed as figures in the paper. Three industry and one ODP well, and 73 bedrock samples constrain the seismic sections. The green lines are the inner and outer limits of the continent-ocean boundary. The three areas along the left side of the map are the divisions used in the paper to describe the offshore area.

Figure 2: Simplified geological map, where the volcanic rocks on both the Baffin Island and Greenland margin can be seen. The extinct spreading ridges and interpreted magnetic anomalies are from Roest and Srivastava (1989). The inset indicates the location of margins mentioned in the paper: SWG-Southwest Greenland, LAB-Labrador margin, OB- Orphan Basin, FC-Flemish Cap, GB-Grand Banks, Scotian-Scotian margin. The three areas along the left side of the map are the divisions used in the paper to describe the offshore area.

Figure 3: Newly compiled gravity map with interpretation from seismic sections overlain. The highlighted lines are the seismic lines displayed in other figures. The heavy black lines show the inner and outer position of the continent-ocean boundary (COB) based on a combination of the seismic and potential field data. The three areas along the left side of the map are the divisions used in the paper to describe the offshore area.

Figure 4: Newly compiled magnetic map with interpretation from seismic sections overlain. The highlighted lines are the seismic lines displayed in other figures. The heavy black lines show the inner and outer position of the continent-ocean boundary (COB) based on a combination of the seismic and potential field data. The three areas along the left side of the map are the divisions used in the paper to describe the offshore area.

Figure 5: Structural map of the studied area, where the five seismic lines shown in Figs 6–10 are indicated. To the north the structural pattern is dominated by coast-parallel elongate continuous NW–SE striking faults. These faults delimit, from west, a graben structure followed by a pronounced basement high, which on its eastern flank is limited by synthetic normal faults throwing down to the east. The mid area is still dominated by the coast-parallel basement high, but the faulting diminish in size southwards. The mid area with exposed volcanic rocks and seaward-dipping reflectors is characterized by a shift in direction of the fault pattern to a more

NNE–SSW direction. The southernmost area is dominated by thick wedges of sediments, and shows a weakly defined fault system running almost N–S.

Figure 6: Part of seismic profile BE-74-51 across the non-volcanic margin. The location of the profile is shown in Figs 1 and 5. The potential field values are along-track profiles. The basement high on the shelf at 30-50 km range has a peak magnetic anomaly of 800 nT attributed to Precambrian crust consistent with the metamorphic sample recovered in the vicinity (Figs. 1 and 5). The intensity of the magnetic anomaly decreases seaward of the hummocky basement. The gravity profile has a gradient from -50 to 25 mGal from near the shore-line to the deep water.

Figure 7: Part of seismic profile BE-74-45, which crosses from the Baffin Island to the Greenland shelf. The deepening of water depths from ranges of 160 km and greater is due to a problem with the scanning of the seismic section and is an artifact. The location is shown in Figs 1 and 5. Volcanic rocks are interpreted in the entire deep water region. The potential field profiles are synthetic profiles generated from our newly compiled grids. From 20-160 km range regardless of the water depth the range of the magnetic anomalies is similar.

Figure 8: Part of seismic profile 200/75 showing a seaward dipping reflections (SDRs). The location is shown in Figs 1 and 5. At 3 sec depth and 40 km range, a high is imaged apparently separating the SDRs. The potential field data are synthetic profiles generated from our newly compiled grids. The magnetic anomalies increase seaward of the high and the seismic sections below 2 sec shows a character attributed to volcanic rocks.

Figure 9: Part of seismic profile C-73-211 across the margin showing the complex basement topography and overlying volcanic rocks. The location of the line is shown in Figs 1 and 5. The potential field profiles are synthetic profiles generated from our newly compiled grids.

Figure 10: Part of seismic profile C-73-208 showing prograding sedimentary section with a 90 mGal free-air gravity anomaly. The location is shown in Figs 1 and 5. The potential field profiles are synthetic profiles generated from our newly compiled grids. The amplitudes of the magnetic anomaly increases seaward of the prograding sedimentary wedge, where oceanic crust is interpreted.

Figure 11: Plate reconstructions for anomaly 33 (a) and 27 (b) based on rotation poles from Roest and Srivastava (1989). The continent-ocean boundary (COB) for the Baffin Bay margin is from this study and for the Greenland margin from Chalmers and Laursen (1995), Skaarup (in prep.) and Whittaker et al. (1997). The darker gray shading covers the Greenland plate from its COB to the coastline. (a) The chron 33 reconstruction leaves a small gap between the COBs in the Labrador Sea but extensive overlap occurs to the north. (b) At chron 27 time, the COBs are coincident along the Southeast Baffin margin and to the north of the Cape Dyer area. The Greenland COB is located seaward of the mapped volcanic rocks that are dated as having been emplaced during this interval.

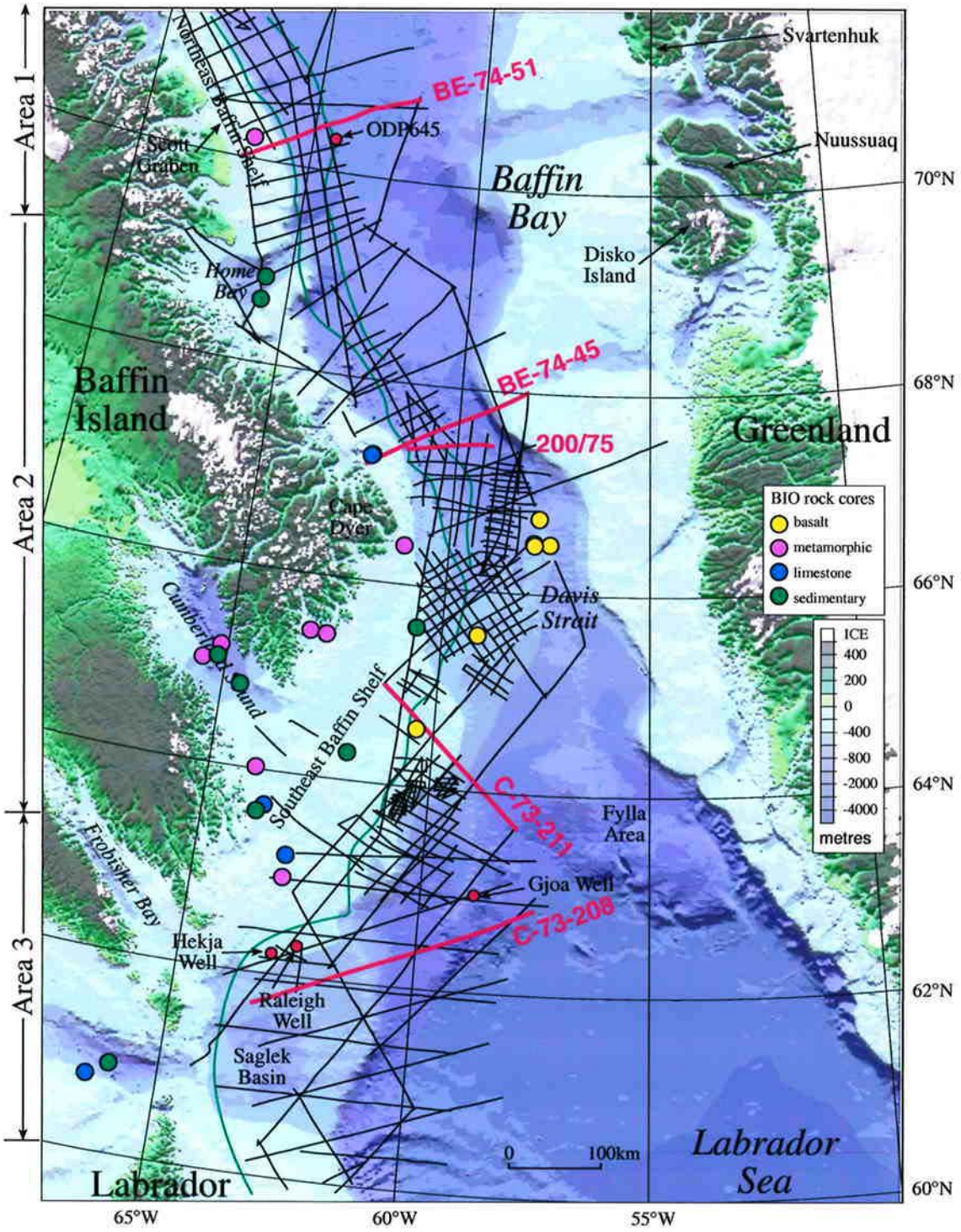
Area 1
Area 2
Area 3
Northeast Baffin Shelf
Scott Graben
BE-74-51
ODP645
Baffin Bay
Svartenhuk
Nuussuaq
Disko Island
70°N
Home Bay
Baffin Island
BE-74-45
200/75
68°N
Greenland
Cape Dyer
BIO rock cores
basalt
metamorphic
limestone
sedimentary
66°N
Davis Strait
Cumberland Sound
Southeast Baffin Shelf
ICE
400
200
0
-400
-800
-2000
-4000
metres
64°N
C-73-211
Fylla Area
Frobisher Bay
Gjoa Well
C-73-208
Hekja Well
62°N
Raleigh Well
Saglek Basin
0
100km
Labrador
Labrador Sea
60°N
65°W
60°W
55°W

Fig. 1

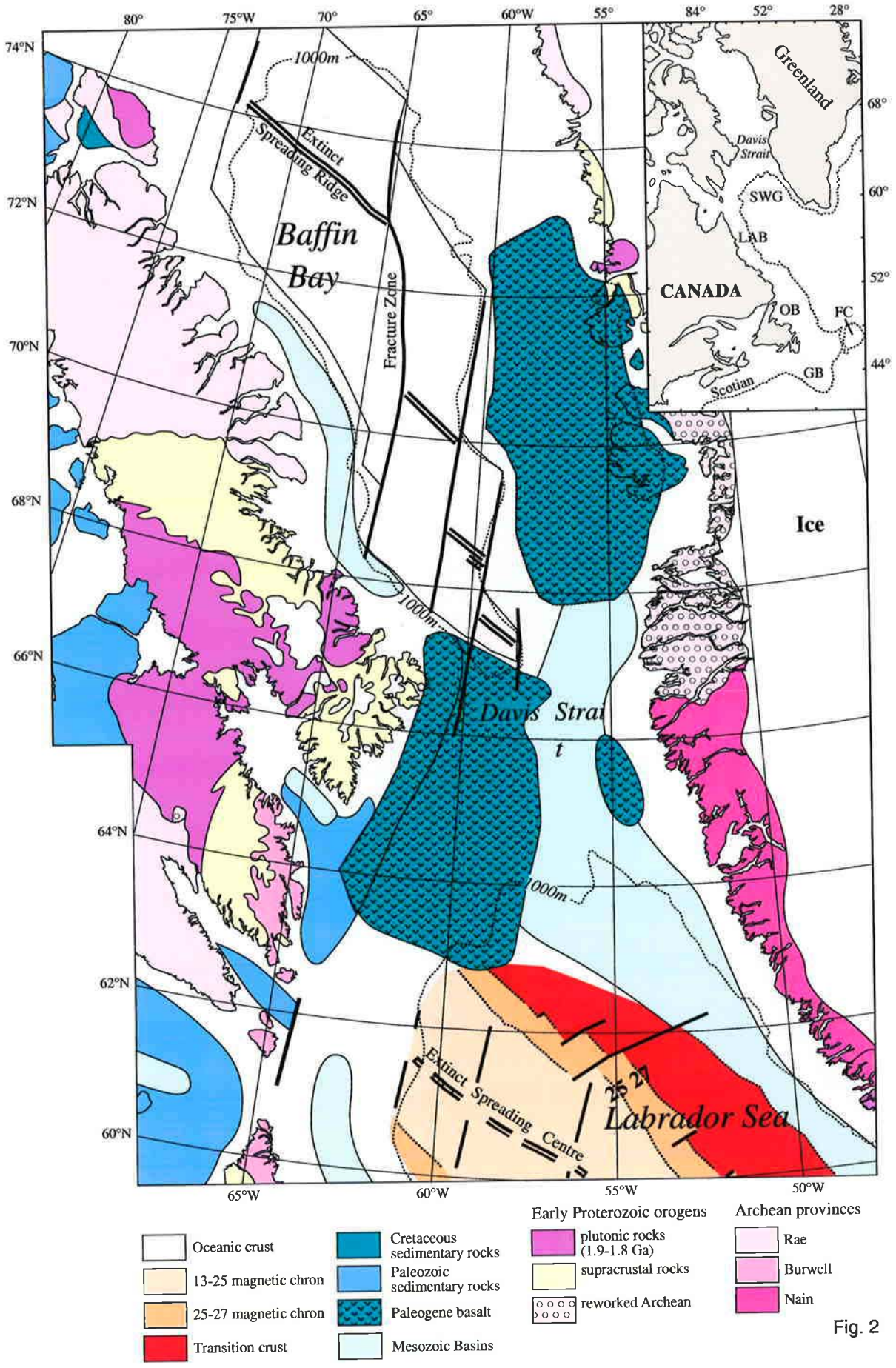
80°
75°W
70°
65°
60°W
55°
74°N
72°N
70°N
68°N
66°N
64°N
62°N
60°N
65°W
60°W
55°W
50°W
1000m
Extinct Spreading Ridge
Baffin Bay
Fracture Zone
Davis Strait
Ice
Extinct Spreading Centre
Labrador Sea
84°
52°
28°
68°
60°
52°
44°
Greenland
Davis Strait
SWG
LAB
CANADA
OB
FC
GB
Scotian
Oceanic crust
13-25 magnetic chron
25-27 magnetic chron
Transition crust
Cretaceous sedimentary rocks
Paleozoic sedimentary rocks
Paleogene basalt
Mesozoic Basins
Early Proterozoic orogens
plutonic rocks (1.9-1.8 Ga)
supracrustal rocks
reworked Archean
Archean provinces
Rae
Burwell
Nain

Fig. 2

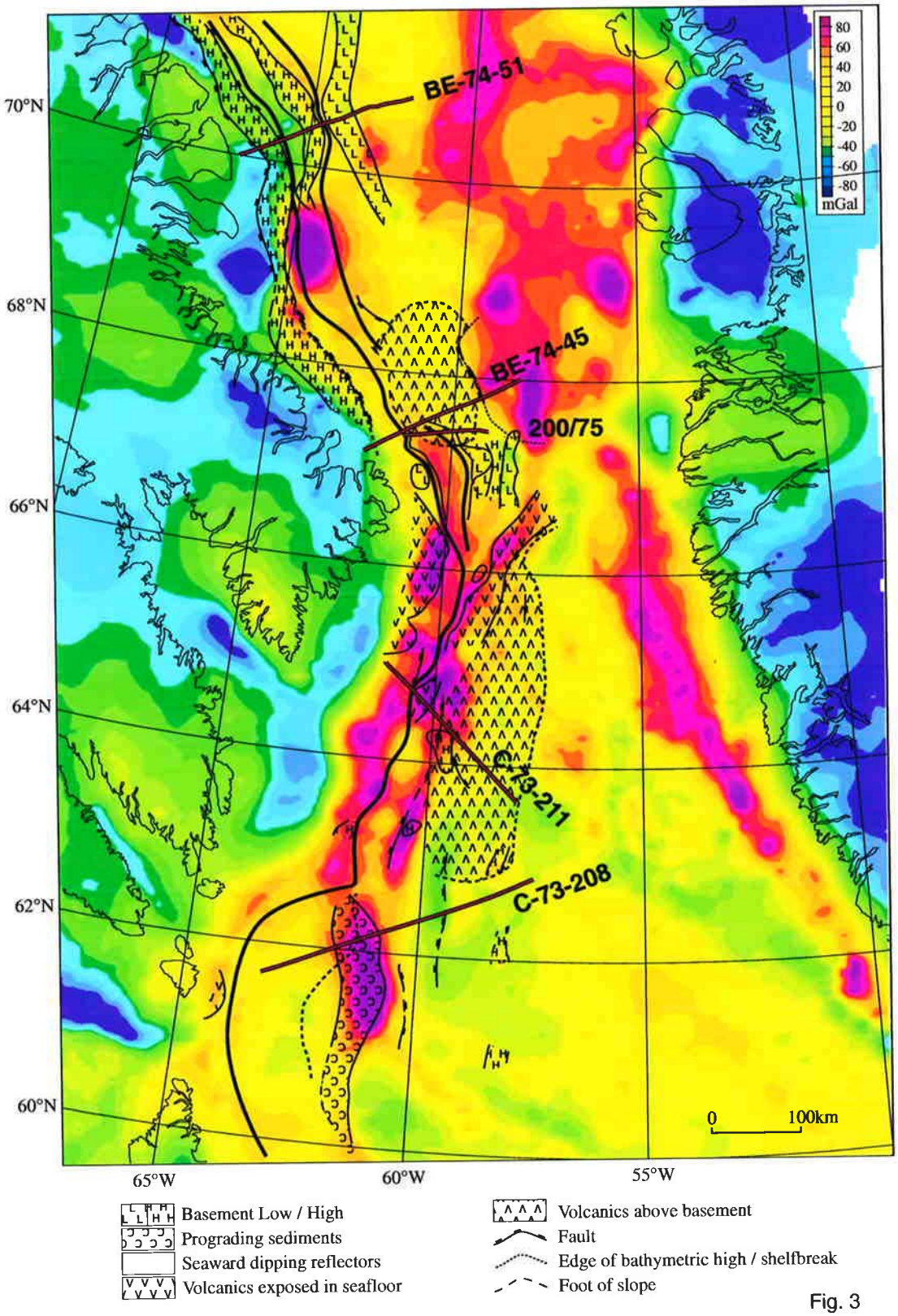
BE-74-51
BE-74-45
200/75
C-73-211
C-73-208
80
60
40
20
0
-20
-40
-60
-80
mGal
70°N
68°N
66°N
64°N
62°N
60°N
65°W
60°W
55°W
0
100km
Basement Low / High
Prograding sediments
Seaward dipping reflectors
Volcanics exposed in seafloor
Volcanics above basement
Fault
Edge of bathymetric high / shelfbreak
Foot of slope

Fig. 3

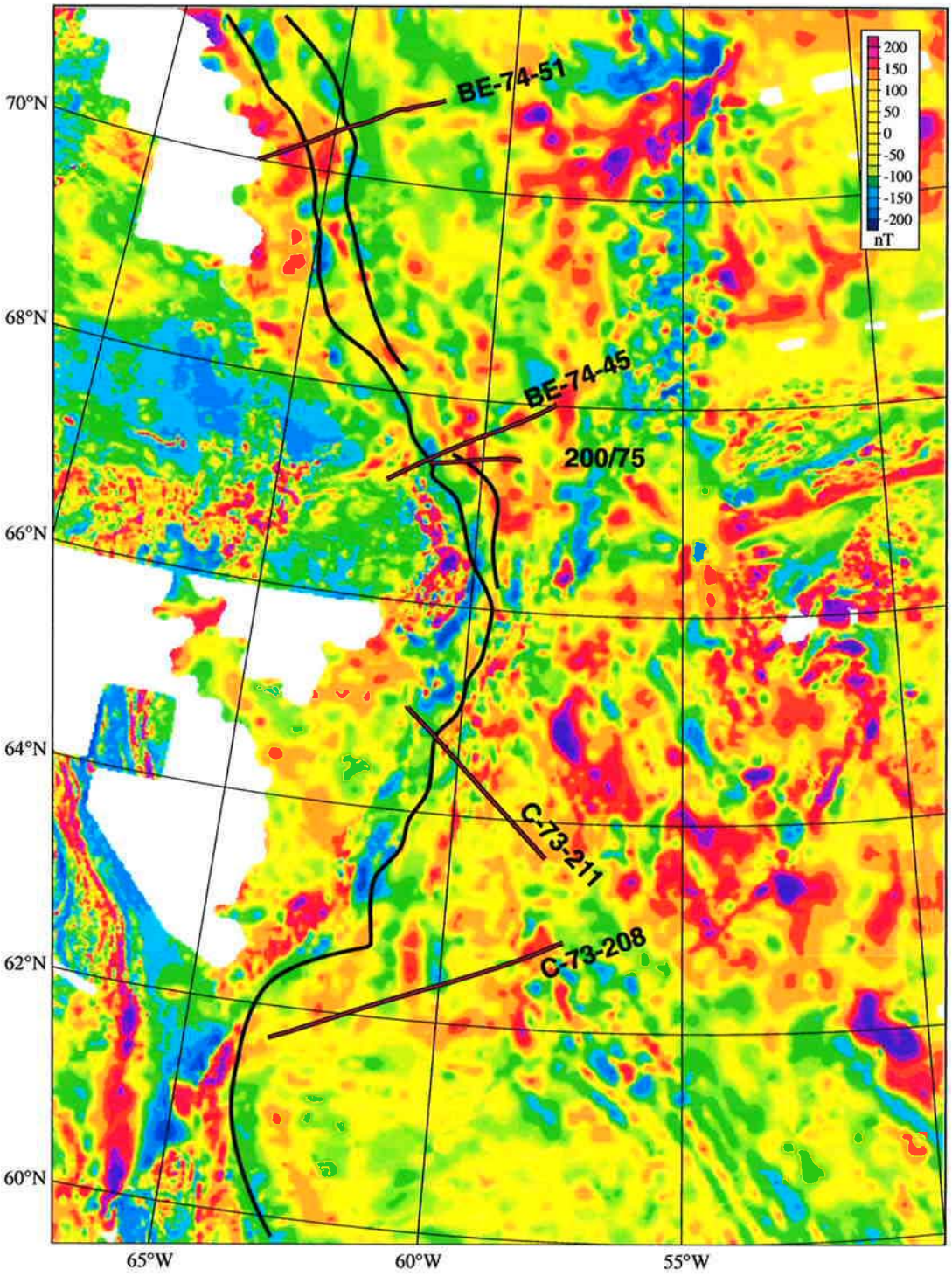
BE-74-51
BE-74-45
200/75
C-73-211
C-73-208
200
150
100
50
0
-50
-100
-150
-200
nT
70°N
68°N
66°N
64°N
62°N
60°N
65°W
60°W
55°W

Fig. 4

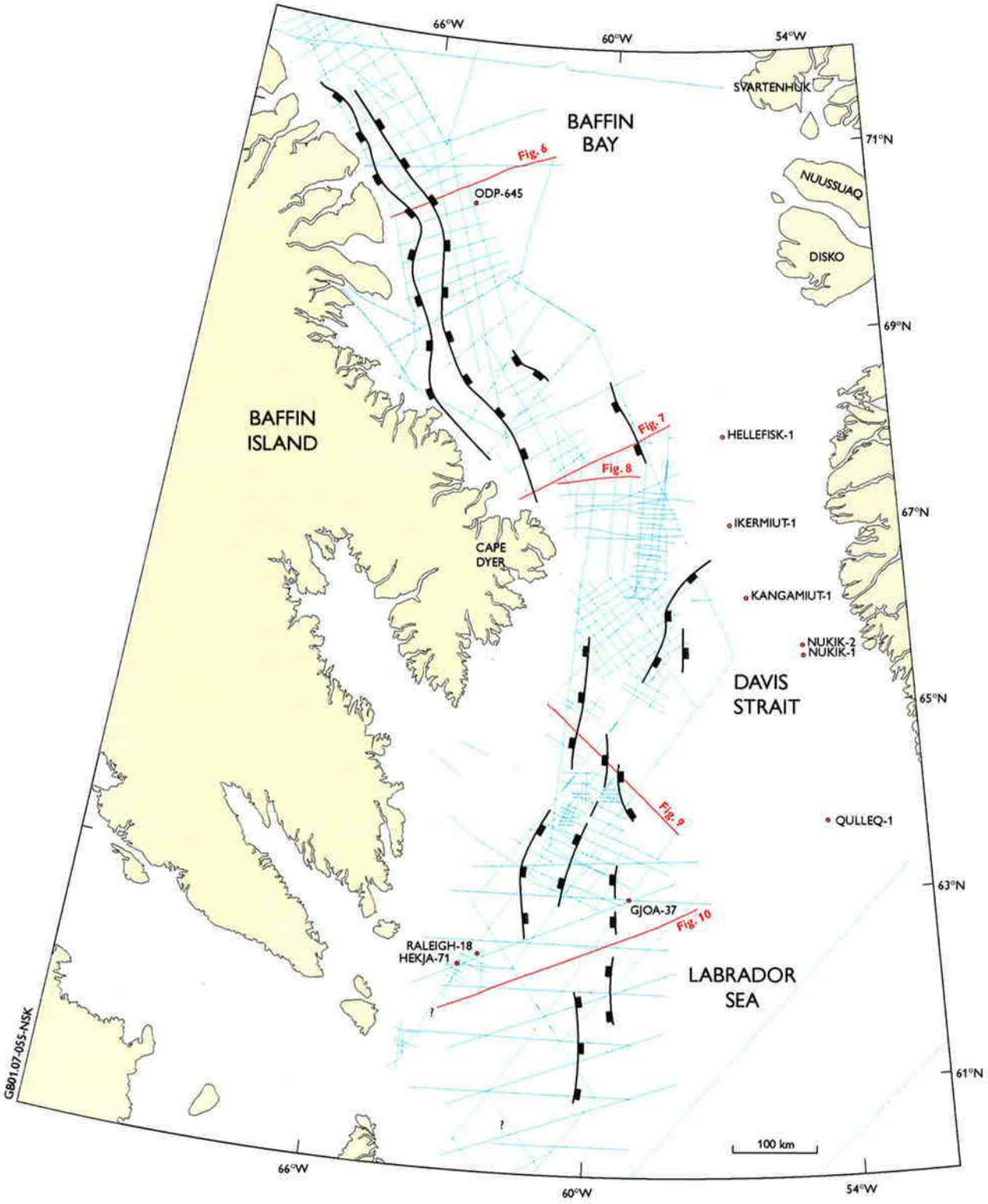
66°W
60°W
54°W
SVARTENHUK
BAFFIN
BAY
71°N
Fig. 6
ODP-645
NUUSSUAQ
DISKO
69°N
BAFFIN
ISLAND
Fig. 7
Fig. 8
HELLEFISK-1
IKERMIUT-1
67°N
CAPE
DYER
KANGAMIUT-1
NUKIK-2
NUKIK-1
DAVIS
STRAIT
65°N
Fig. 9
QULLEQ-1
63°N
GJOA-37
Fig. 10
RALEIGH-18
HEKJA-71
LABRADOR
SEA
61°N
100 km
66°W
60°W
54°W
GB01.07-055-NSK

Fig. 5

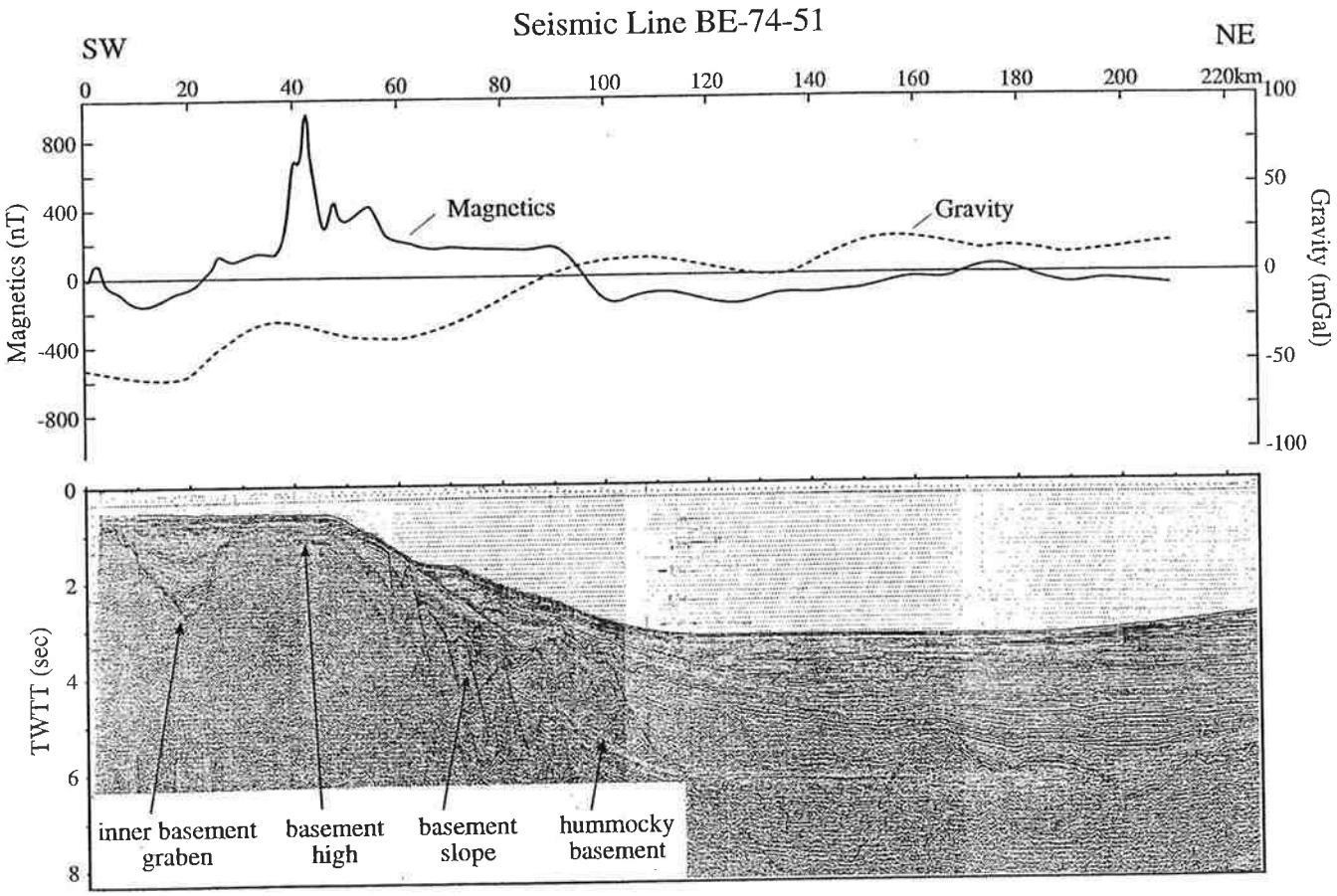
Seismic Line BE-74-51
SW
NE
0
20
40
60
80
100
120
140
160
180
200
220km
800
400
0
-400
-800
Magnetics (nT)
Magnetics
Gravity
100
50
0
-50
-100
Gravity (mGal)
TWTT (sec)
2
4
6
8
inner basement graben
basement high
basement slope
hummocky basement

Fig. 6

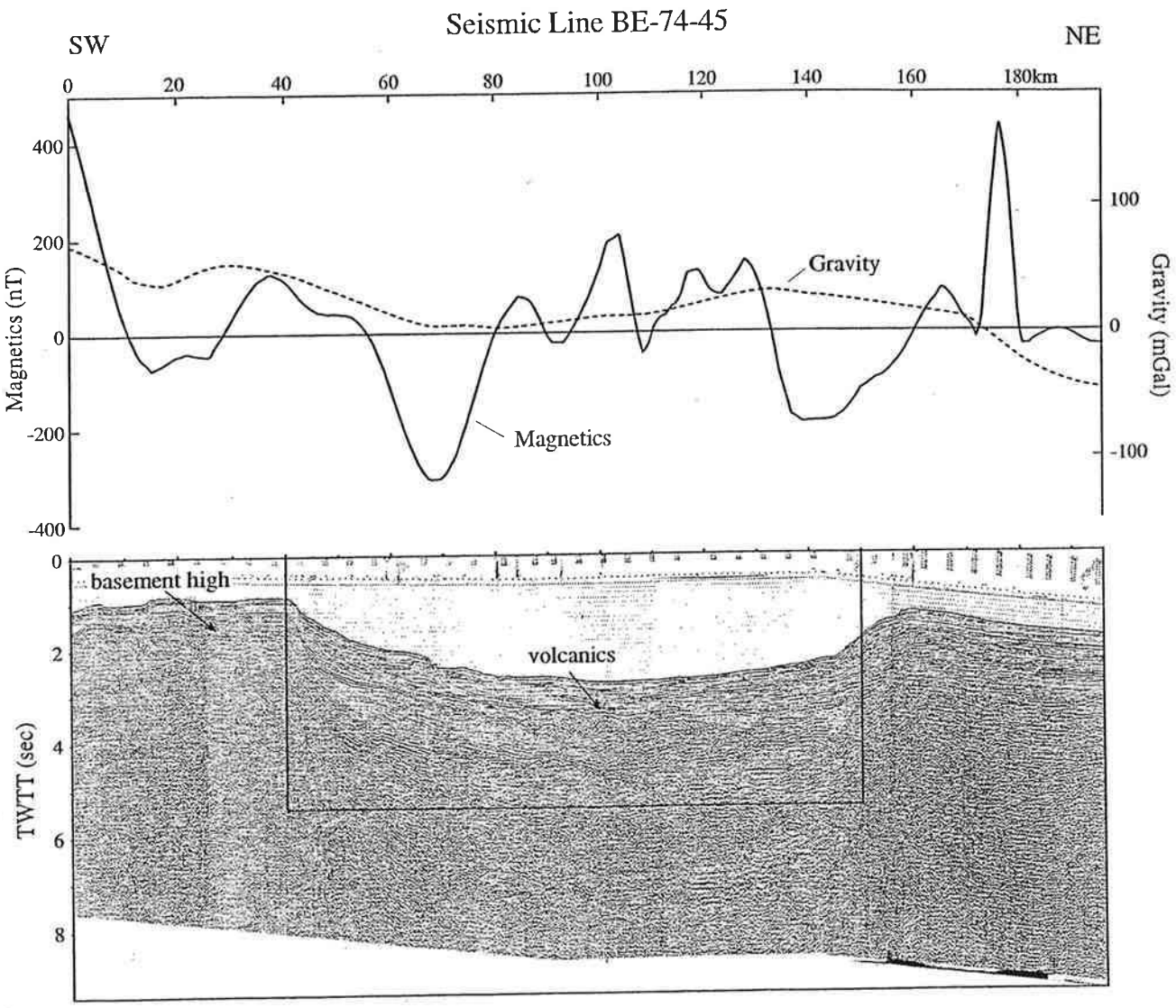
Seismic Line BE-74-45
SW
NE
0
20
40
60
80
100
120
140
160
180km
400
200
0
-200
-400
Magnetics (nT)
100
0
-100
Gravity (mGal)
Gravity
Magnetics
basement high
volcanics
TWTT (sec)
2
4
6
8

Fig. 7

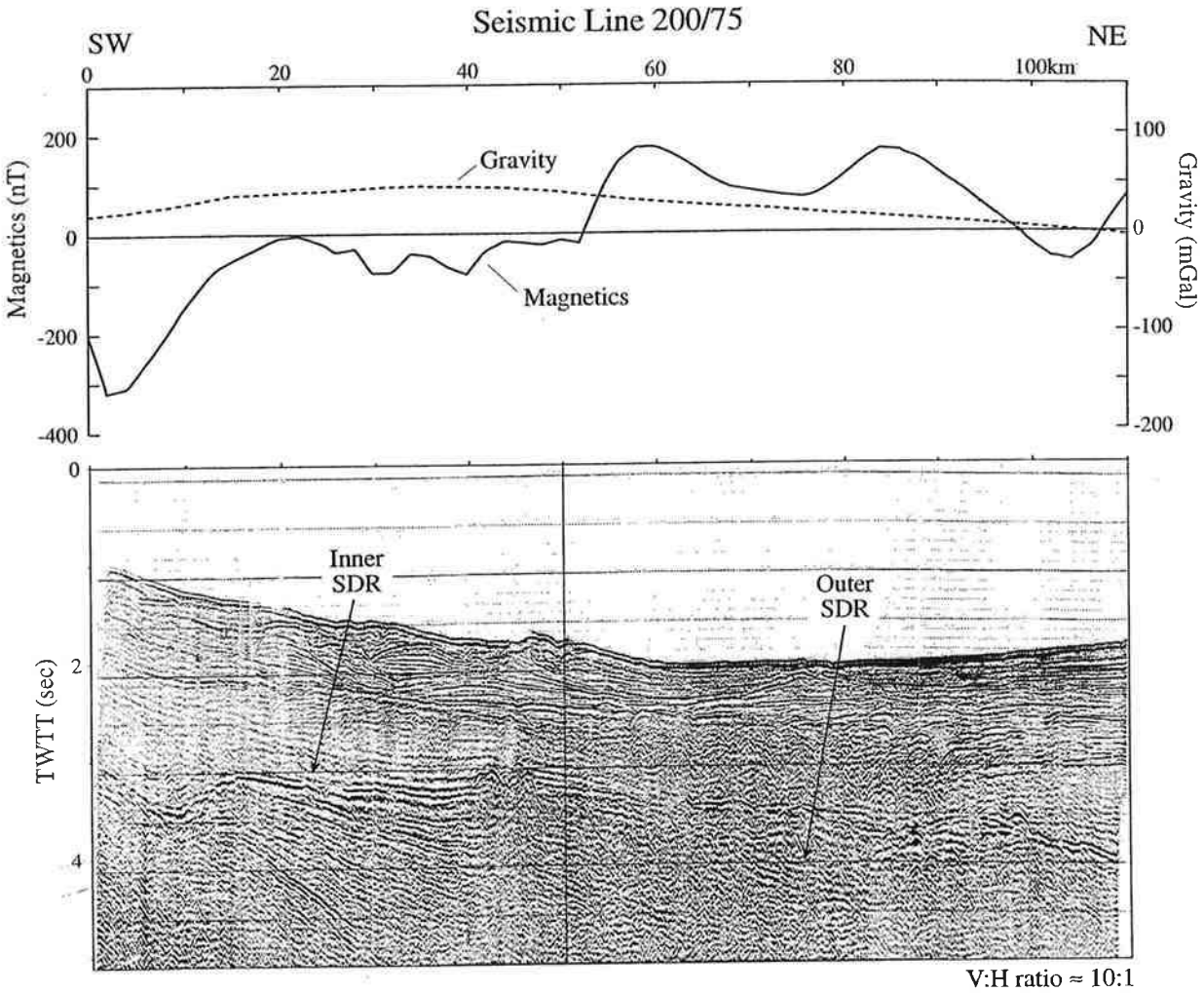
Seismic Line 200/75
SW
NE
0
20
40
60
80
100km
200
0
-200
-400
Magnetics (nT)
Gravity
Magnetics
100
0
-100
-200
Gravity (mGal)
0
2
4
TWTT (sec)
Inner
SDR
Outer
SDR
V:H ratio ≈ 10:1

Fig. 8

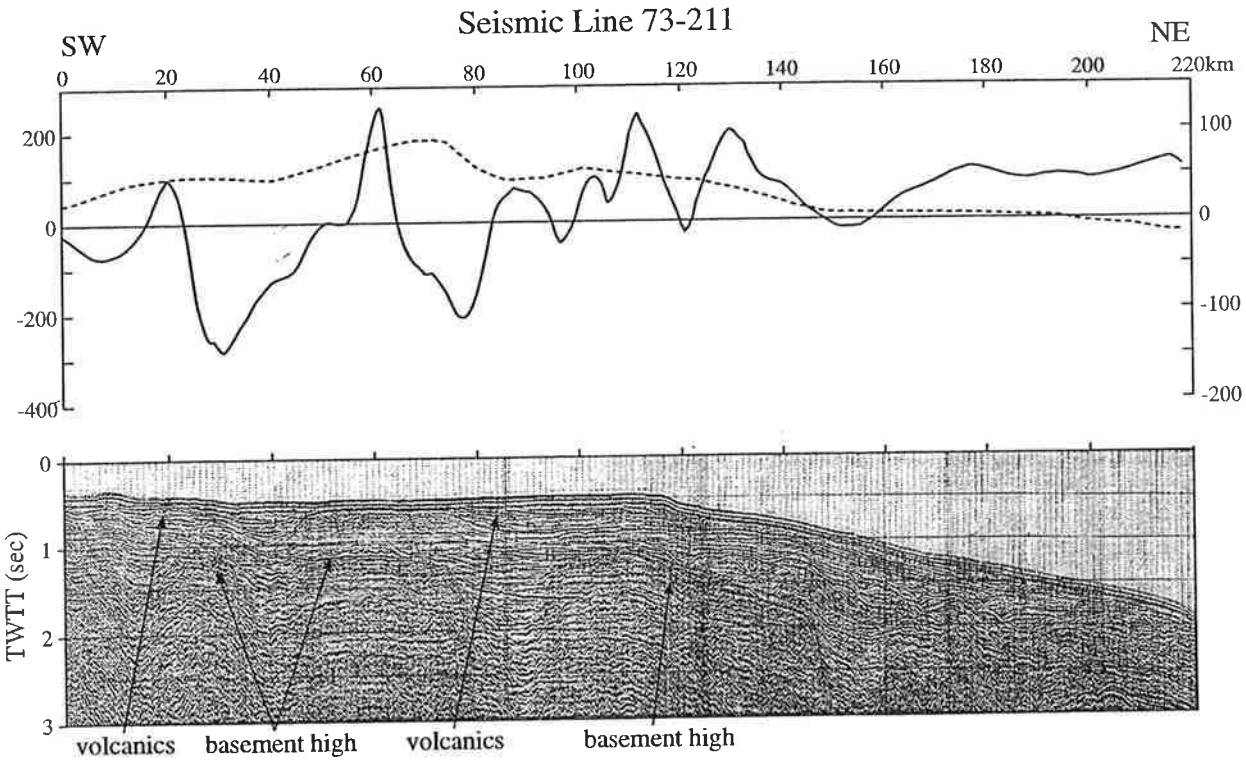
Seismic Line 73-211
SW
NE
0
20
40
60
80
100
120
140
160
180
200
220km
200
0
-200
-400
100
0
-100
-200
TWTT (sec)
1
2
3
volcanics
basement high
volcanics
basement high

Fig. 9

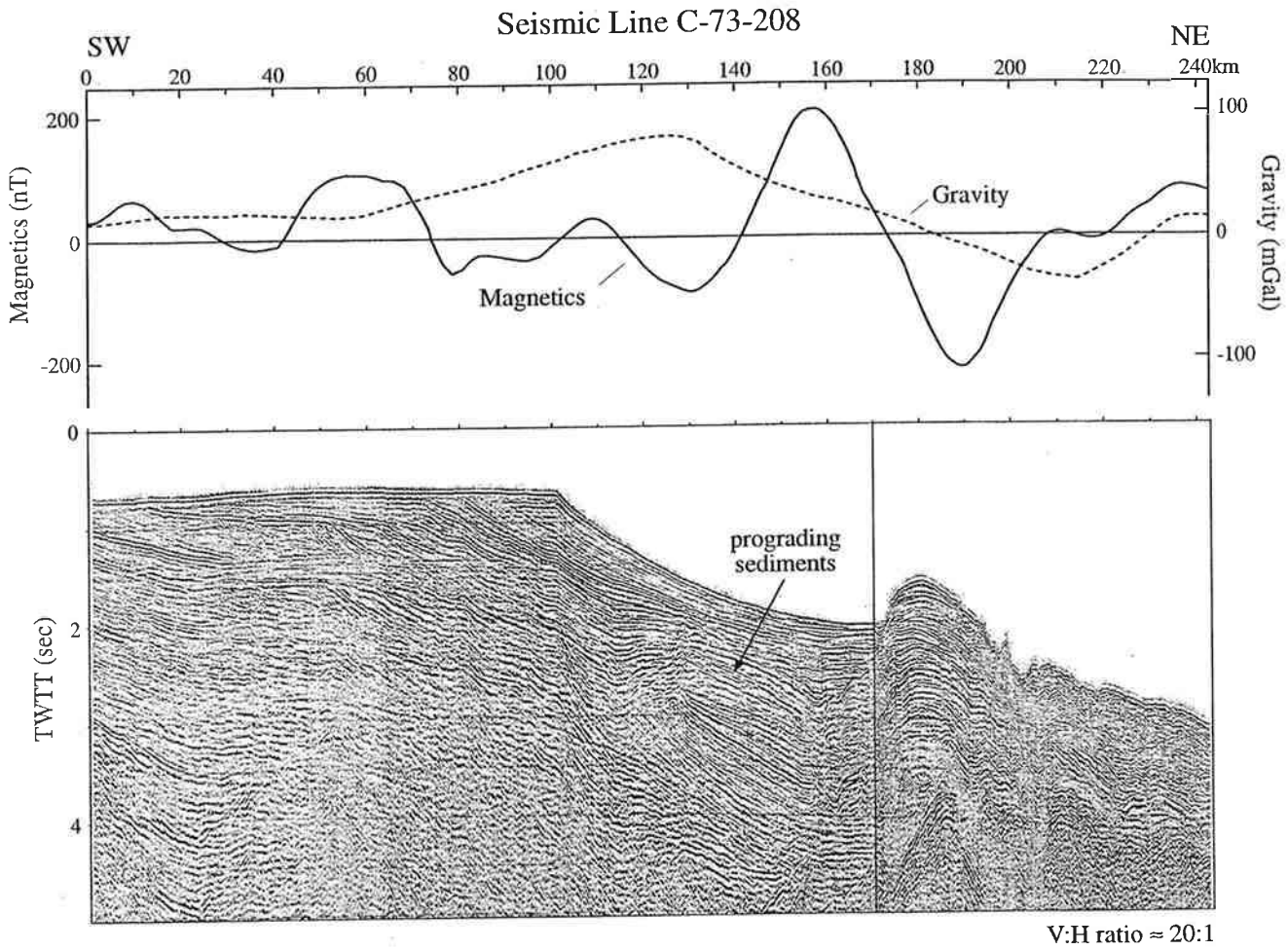
Seismic Line C-73-208
SW
NE
0
20
40
60
80
100
120
140
160
180
200
220
240km
200
0
-200
Magnetics (nT)
100
0
-100
Gravity (mGal)
Gravity
Magnetics
0
2
4
TWTT (sec)
prograding
sediments
V:H ratio ≈ 20:1

Fig. 10

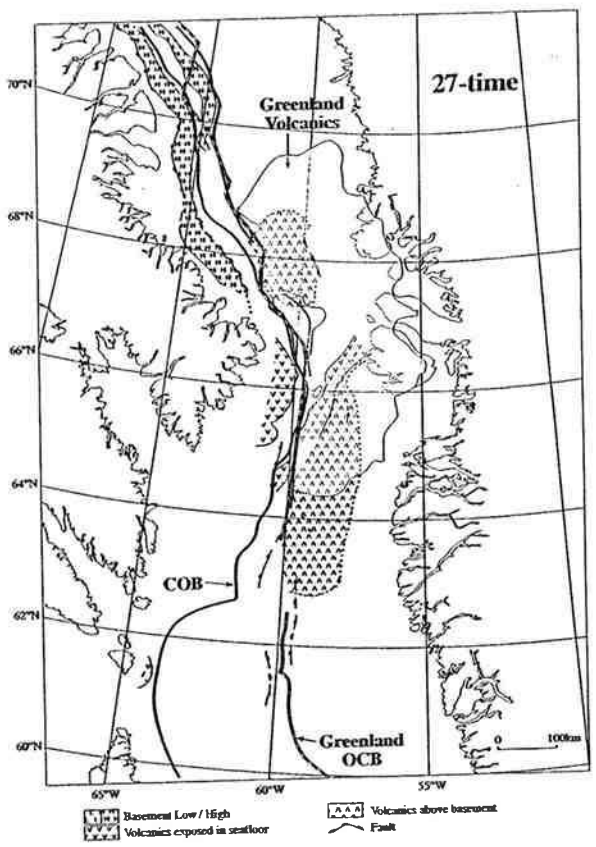
27-time
Greenland Volcanics
COB
Greenland OCB
70°N
68°N
66°N
64°N
62°N
60°N
65°W
60°W
55°W
0
100km
Basement Low / High
Volcanics exposed in seafloor
Volcanics above basement
Fault

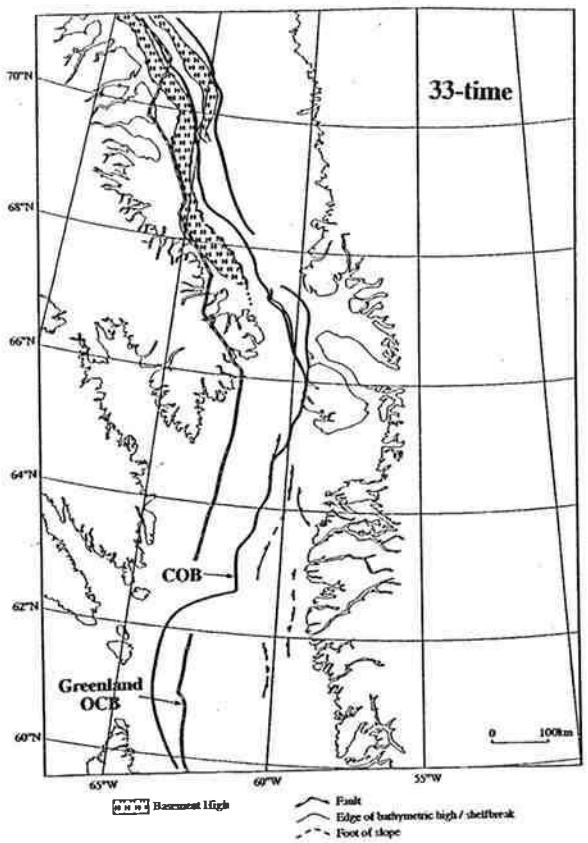
33-time
COB
Greenland OCB
70°N
68°N
66°N
64°N
62°N
60°N
65°W
60°W
55°W
0
100km
Basement High
Fault
Edge of bathymetric high / shelfbreak
Foot of slope

Fig. 11